Bassins de rift à des stades précoces de leur développement: l'exemple du bassin de Makgadikgadi-Okavango-Zambezi, Botswana et du bassin Sud-Tanganyika (Tanzanie et Zambie). Composition géochimique des sédiments: traçeurs des changements climatiques et tectoniques

Philippa Huntsman-Mapila

UNIVERSITE DE BRETAGNE OCCIDENTALE
ECOLE DOCTORALE DES SCIENCES DE LA MER
GEOSCIENCES MARINES

Thèse présentée pour l'obtention du diplôme de :
Docteur de l'université de Bretagne Occidentale
spécialité : Géosciences Marines
par:

Philippa HUNTSMAN-MAPILA

BASSINS DE RIFT À DES STADES PRÉCOCES DE LEUR DÉVELOPPEMENT: L'EXEMPLE DU BASSIN MAKGADIKGADI-OKAVANGO-ZAMBEZI, BOTSWANA ET DU BASSIN SUD-TANGANYIKA (TANZANIE ET ZAMBIE)

Composition géochimique des sédiments: traçeurs des changements climatiques et tectoniques

Jury:

M. Mathieu Benoit	Chargé de recherche CNRS, UBO-Brest	Examinateur
M. François Chabaux	Professeur Université Louis Pasteur-Strasbourg	Rapporteur
M. Christophe Hémond	Maître de Conférence, UBO-Brest	Directeur
Mme Anne-Marie Lézine	Directeur de Recherche CNRS,LSCE-Gif	Rapporteur
Mme Susan Ringrose	Professeur, University of Botswana	Examinateur
M. Michael Talbot	Professeur, University of Bergen	Examinateur
M. Jean-Jacques Tiercelin	Directeur de Recherche CNRS, UBO-Brest	Directeur

BREST, 2006

Remerciements

Je tiens tout d'abord à remercier Jean-Jacques Tiercelin et Christophe Hémond, mes directeurs de thèse. Je leur suis très reconnaissante pour leurs conseils et leur sympathie.

Je remercie beaucoup Mathieu Benoit et Jo Cotten pour la patience qu'ils ont montré lors de la mesure d'échantillons au cours de ma thèse et pour avoir accepté de travailler sur mes échantillons de sédiments.

Mille merci au Professeur Lars Ramberg, directeur de Harry Oppenheimer Okavango Research Centre, Maun pour m'avoir donné le temps de travailler sur ce manuscrit et d'avoir accepté mes absences aux réunions. Grand merci au Professeur Susan Ringrose pour avoir suivi mon travail et pour les discussions fructueuses.

Merci à Mike Talbot pour la datation des carottes du Tanganyika.

Ma reconnaissance va également à Claire Bassoullet et Danièle Hureau-Mazaundier (et Laurence), non seulement pour m'avoir aidé dans le laboratoire mais également pour leur hospitalité inoubliable. C'est grâce à vous, que j'ai reussi à survivre aux absences de ma petite famille. Je remercie Mathieu Schuster pour son aide généreuse dans la rédaction en français. Merci beaucoup à Monica Morrison et Dominique Gac pour leur aide avec la bibliographie et à Sidonie Revillon pour ses commentaires dans la relecture des chapîtres.

Thank you to all my colleagues at HOORC especially Ineelo Mosie, Billy Mogojwa, Wilfred Kaneguba and Thebe Kemosedile for all their field assistance.

Mes plus sincères remerciements vont à mon mari Tlamelo et mes deux filles, Jessica et Elena (née le mois où j'ai commencé la thèse) pour leur soutien permanent. Ils ont supporté mes absences avec courage. Mille-merci à mes parents pour m'avoir toujours encouragé.

Cette thèse est dédiée à mon mentor, Professeur Henri A.B. Kampunzu, qui m'a donné le courage de commencer ce travail. Même après son décès en 2004, c'est lui qui m'a donné l'inspiration pour continuer.

SOMMAIRE

INTRODUCTION (VERSION FRANÇAISE)

0.1 Problématique

Cette thèse concerne l'étude des sédiments lacustres de deux bassins de rift appartenant à un segment du Système de Rift Est-africain décrit comme étant une zone actuellement en cours d'ouverture, connue dans la littérature sous le nom de "*Southern Complex*" ou "*Southwestern Branch*" (Reeves, 1972; Mondeguer et al., 1989; Modisi et al., 2000). Ces deux bassins, considérés comme illustrant deux stades précoces successifs de l'ouverture d'un bassin de rift, sont : 1) Le Bassin de Makgadikgadi-Okavango-Zambèze (MOZ), situé dans la région nord-ouest du Botswana; 2) Le Bassin de Mpulungu, qui constitue l'extrémité sud-est du Bassin du lac Tanganyika (Tanzanie et Zambie) (Figure I-1).

Climat et tectonique, et en particulier les relations qui existent entre le soulèvement de la croûte continentale, induisant le développement de topographies élevées, et les processus d'altération et d'érosion, sont à l'origine des processus qui résultent en la formation de sédiments et la dissolution d'éléments chimiques dans les eaux. En particulier, la composition chimique des eaux joue un grand rôle dans le cycle biogéochimique de la Terre. La composition chimique de la fraction détritique est déterminée pour ses grandes lignes par la composition originelle des roches sources, leur degré d'altération, et les processus qui surviennent au cours de son transport et son accumulation. L'activité tectonique induit la formation des reliefs, qui deviennent les zones sources à la fois des éléments détritiques et solubles. Les conditions climatiques locales à globales (en particulier les paramètres température et précipitations) déterminent elles les paramètres physiques de l'altération et de l'érosion.

Les processus tectoniques possèdent tous une signature géochimique particulière inscrite dans les sédiments qu'ils génèrent, signature qui caractérise : 1) un signal de provenance, et 2) des mécanismes sédimentaires particuliers qui leur sont associés (Rollinson, 1993). Pour des sédiments tels que les grès, les relations existant entre leur composition géochimique, l'origine de ces sédiments et leur contexte tectonique sont des outils efficaces dans l'interprétation de roches et d'environnements anciens mal préservés. L'utilisation des compositions des sédiments en éléments majeurs (Bhatia, 1983; Roser and Korsch, 1986; 1988) et en éléments traces (Bhatia and Crook, 1986) dans des diagrammes d'identification se sont révélés fort efficaces dans la reconnaissance d'environnements tectoniques particuliers.

Afin de vérifier la véracité de certains diagrammes d'identification de contextes tectoniques dans le cas de sédiments anciens, il est possible de comparer les champs géochimiques identifiés à ceux définis pour des sédiments actuels déposés dans des contextes tectoniques

parfaitement identifiés. Ceci a déja été fait (Bhatia, 1983; Bhatia and Crook, 1986; Roser and Korsch, 1986; Roser, 1996) mais de nouvelles données concernant des sédiments bien identifiés dans des contextes tectoniques reconnus afin d'affiner et valider définitivement les critères d'identification. Dans ce travail, nous utilisons des informations concernant des sédiments récents (Pléistocène supérieur à Holocène) dans un environnement tectonique parfaitement bien connu, celui du Système de Rift Est-africain. Dans ce contexte, deux exemples ont été choisis comme correspondant à des stades jeunes de la formation d'un bassin de rift. L'analyse des sédiments associés à ces contextes a permis de d'établir une signature chimique désormais représentative de stades précoces du rifting.

En ce qui concerne les recherches concernant les changements climatiques récents en Afrique, l'attention des chercheurs est essentiellement orientée vers les bio-indicateurs tels les pollens (e.g. Vincens et al., 1993; Vincens et al., 2005) et les diatomées (e.g. Gasse et al., 1989; Gasse et al., 2002), à l'opposé des marqueurs géochimiques. A ce jour, à l'exception de l'utilisation des marqueurs en géochimie organique dans les sédiments lacustres et en ce qui concerne l'Afrique, les recherches sur les lacs Ouest-africains et le lac Malawi (e.g. Schneider et al., 1997; Talbot and Laerdal, 2000; Johnson et al. 2004; Talbot et al., 2006), les marqueurs en géochimie sédimentaire n'ont été que très peu utilisés sur les sédiments récents, alors qu'ils l'ont largement été pour des séries sédimentaires anciennes (e.g. Fedo et al., 1997).

La question posée dans ce travail est : l'étude des compositions chimiques minérales des sédiments quaternaires du Rift Est-africain peut-elle contribuer à la détection des signaux de changement du climat et à l'identification des environnements tectoniques précis des zones de dépôt de ces sédiments?

Pour répondre a cette question, une approche multidisciplinaire à dominante géochimique, avec plusieurs objectifs a été employé :
a) mieux comprendre les processus géochimiques au cours du cycle de genèse des formations sédimentaires (érosion-transport-accumulation) pour des stades précoces de l'évolution d'un bassin de rift ;
b) définir des critères sédimentologiques et géochimiques permettant de discriminer l'activité tectonique et les changements climatiques au cours de l'évolution de ces deux bassins du rift.
c) reconstruire les environnements climatiques et tectoniques caractérisant ces deux régions du Rift Est-africain au cours du Pléistocène et de l'Holocène ;

Le bassin de Makgadikgadi-Okavango-Zambèze (MOZ) est un vaste bassin intracontinental d'âge Plio-Pléistocène dont l'histoire est contrôlée par l'évolution d'un système de failles parallèles de direction NE-SW (Figure I-2). Ces failles délimitent depuis les extrémités sud et nord des bassins des lacs Tanganyika et Malawi un ensemble de fossés à histoire structurale complexe (fossés anciens d'âge Karoo, ou fossés plus récents). Au sein de cette structure

MOZ, le Bassin de l'Okavango est un demi-graben dont la formation est liée à la croissance de trois failles de direction NE-SW, les failles de Gumare, Kunyere et Thamalakane. Le Bassin de l'Okavango est situé dans la zone climatique de l'Afrique du Sud centrale mais son bassin versant s'étend vers le nord-ouest jusqu'aux reliefs de l'Angola situés en zone tropicale.

Le Bassin du lac Tanganyika appartient à la branche ouest du Rift Est-africain, située en zone tropicale. Le Bassin de Mpulungu est le plus méridional des sept sous-bassins qui constituent le Bassin du Tanganyika (Tiercelin and Mondeguer, 1991) (Figure I-3). Sa structure est contrôlée sur son flanc sud-ouest par plusieurs failles de direction N140°, qui s'associent pour former la faille bordière de Mpulungu. Un groupe de failles de direction N30° et N70° intersecte la faille bordière de Mpulungu et contrôle la morphologie des bassins des lacs Mweru et Mweru-Wantipa (Figure I-3). Associés au Bassin de Mpulungu, ces deux bassins sont les plus septentrionaux du «Complexe Sud» (ou Branche sud-ouest) du Rift Est-africain (Mondeguer, 1991). Le Bassin de Mpulungu est le plus récent des sous-bassins du lac Tanganyika. Il s'est formé entre 4 et 2 millions d'années, le segment central du Tanganyika étant lui daté de 12-10 millions d'années (Cohen et al., 2000).

Le Rift Est-africain est célèbre pour les nombreuses découvertes de sites à hominidés anciens, qui ont donné lieu à une littérature fort abondante (Leakey et al., 1964 ; Patterson and Howells, 1967; Johanson and Taieb, 1976; Tattersall, 1993; Prat et al., 2005). La détermination de l'extension spatiale et temporelle des changements d'environnement occasionnés par les variations du climat en Afrique de l'Est et les phénomènes tectoniques liés au développement du rift, a fait l'objet d'études quantitatives afin de mieux comprendre et vérifier les différents scénarios d'évolution proposés pour les diverses populations d'Hominidés **(**Vbra, 1995; deMenocal et al., 2000; Behrensmeyer, 2006).

0.2 Organisation du manuscrit

Tous les chapitres de cette thèse sont rédigés en langue anglaise et, à l'exception du Chapitre I, II et III, ils correspondent soit à des publications parues en 2005 et 2006 dans des revues internationales à comité de lecture soit seront soumises prochainement à de telles revues. Vous trouverez au début des chapitres IV-VIII un résumé en français.

Le Chapitre I présente une description détaillée des deux bassins sédimentaires choisis pour cette étude : Le Bassin Makgadikgadi-Okavango-Zambezi situé dans la région Nord-Ouest du Botswana, et le Bassin de Mpulungu qui forme l'extrémité sud du fossé du lac Tanganyika.

Les caractéristiques essentielles de ces deux bassins, contexte géologique, climatique et hydrologique, sont présentées dans ce chapitre.

Le Chapitre II présente une synthèse des différents travaux en paléoclimatologie pour l'ensemble de la région englobant le Bassin de Mpulungu au Nord et le bassin Makgadikgadi-Okavango-Zambezi au sud.

Le Chapitre III présente une synthèse des différents méthodes géochimiques employées dans cette étude. En plus la justification pour avoir choisi certaine élements et rapports géochimique pour cette étude est donnée.

Le Chapitre IV, intitulé «*Cryptic indicators of provenance from the geochemistry of the Okavango Delta sediments, Botswana*» a été publié dans la revue *Sedimentary Geology* en 2005. Cet article présente l'étude géochimique des sédiments silicoclastiques échantillonnés dans des forages réalisés dans la partie distale du Delta de l'Okavango près de la ville de Maun. La géochimie des élements majeurs, traces et terres rares a été utilisée pour identifier la provenance des sédiments remplissant le Bassin de l'Okavango. Ces sédiments sont composés de deux fractions minérales, l'une d'origine éolienne et l'autre d'origine fluviatile. La fraction éolienne est composée essentiellement de quartz, ce qui provoque un fort effet de dilution des autres éléments. Des modélisations quantitatives utilisant des roches caractéristiques du bassin-versant pouvant être considérées comme sources potentielles ont été réalisées. Les résultats de ces modélisations ont confirmé que ces roches granitoïdes-gabbros Protérozoïques et les complexes volcaniques et ortho-métamorphiques qui sont exposés dans le NW du Botswana et les pays adjacents (Angola et Namibie) constituent bien la source principale des sédiments de l'Okavango.

Le Chapitre V s'intitule «*Sediment geochemistry, provenance and tectonic setting: Application of discrimination diagrams to very early stages of intracontinental rift evolution, with examples from the Okavango and Southern Tanganyika rift basins* ». Il sera soumis au *Journal of African Earth Sciences*. Les cadres tectoniques et les stades d'évolution du Bassin de l'Okavango et du Bassin de Mpulungu (Sud-Tanganyika) dans un contexte de rift continental, sont bien connus (Tiercelin and Mondeguer, 1991; Modisi et al., 2000). Les caractéristiques géochimiques des sédiments de l'Okavango et du Tanganyika sont utilisés ici comme un marqueur des stades d'évolution tectonique de ces deux bassins, par établissement de champs nouveaux à l'intérieur des diagrammes de discrimination conventionnels. Ainsi sont définis par leur signal géochimique 1) un stade de bassin de rift naissant illustré par le bassin de l'Okavango, et 2) un bassin plus mature, représenté par le Bassin de Mpulungu, le plus jeune des sous-bassins constituant l'actuel fossé du lac Tanganyika. Les caractères géochimiques de ces sédiments ont permis en outre de définir la nature des roches dont ils sont issus, et donc de préciser les régions sources à l'intérieur des bassin-versants respectifs.

Le Chapitre VI est intitulé «*Sedimentological and geochemical evidence for palaeo-environmental change in the Makgadikgadi subbasin in relation to the MOZ rift depression, Botswana*». Ce travail a été publié dans la revue *Palaeogeography, Palaeoclimatology and Palaeoecology* en 2005. Ce chapitre représente un travail beaucoup plus pluridisciplinaire que le Chapitre II. Des approches de sédimentologie de terrain et de géomorphologie / morphostratigraphie sont combinées à des études géochimiques et chronologiques (thermoluminescence). Elles contribuent à identifier les marqueurs des changements de paléoenvironments dans le nord du Botswana pendant le Pléistocène. Ce travail représente en particulier une nouvelle approche de l'interprétation de l'environnement paléolacustre du bassin de Makgadikgadi dans le contexte de la dépression du rift de Makgadikgadi-Okavango-Zambezi.

Le Chapitre VII "*Use of the geochemical and biological sedimentary record in establishing palaeo-environments and climate change in the Lake Ngami basin, NW Botswana*" a été publié dans la revue *Quaternary International* en 2006. Cet article présente une étude de reconstruction des paléo-niveaux lacustres du lac Ngami situé dans la région sud-ouest du Bassin de l'Okavango. Deux tranchées réalisées dans le fond du lac asséché ont révélé sur quelques mètres d'épaisseur une succession de faciès lacustres à fluvio-lacustres indiquant d'importantes variations en terme de niveau lacustre et d'hydrologie. L'analyse géochimique des sédiments du Lac Ngami et leur interprétation a été facilitée par le fait que ces sédiments sont caractérisés par une fraction fine (fraction argileuse) beaucoup plus importante que les sédiments silicoclastiques du Delta de l'Okavango au sens strict, très riches en quartz, diminuant ainsi l'effet de dilution des autres minéraux par rapport au quartz. La géochimie des sédiments lacustres renseigne sur les conditions de redox et les environnements de dépôt dans le bassin, résultats supportés par une étude des diatomées. Cette étude renseigne directement sur la qualité de l'eau dans le passé et, couplée à la géochimie des sédiments, permet de mettre en évidence le lien direct entre les fluctuations du niveau du paléolac et le climat pendant le Pléistocène et l'Holocène dans la région du Botswana. En outre, la séquence de Ngami est perturbée par les mouvements tectoniques dans le bassin montré par le dépôt rapide des sables vers 40 ka. Depuis la publication de ce travail, il a été découvert d'autres preuves dans d'autres régions du delta d'un événement tectonique majeur vers 40 ka (Ringrose and Huntsman-Mapila, unpublished data) qui a peut-être influencé la formation du cône alluvial de l'Okavango.

Le Chapitre VIII, «*Major and trace element geochemistry of the Lake Tanganyika sediments: implications for late Quaternary climatic variability*» est destiné à être soumis à la revue *Palaeogeography, Palaeoclimatology, Palaeoecology*. L'enregistrement sédimentaire du Lac Tanganyika (Bassin de Mpulungu) intègre la réponse du bassin à des perturbations externes comme les changements climatiques passés et son étude permet de répondre à des questions

telles que l'impact du Dernier Maximum Glaciaire et du Dryas Récent sur l'environnement de cette région. La séquence sédimentaire récente du Tanganyika est perturbée par des arrivées de cendres volcaniques générées lors d'éruptions du volcan Rungwe situé au sud-est du bassin de Mpulungu. L'identification de ces niveaux pyroclastiques aide à définir les régimes de vents dans cette région d'Afrique, et par là même contribue à l'interprétation de la position de la Zone de Convergence Intertropicale (ZCIT) et à la reconstruction des changements climatiques.

Le papier intitulé «*Characterization of arsenic occurrence in the water and sediments of the Okavango Delta, NW Botswana*», a été publié dans la revue *Applied Geochemistry* en 2006. Ce papier ce trouve dans l'Appendix. Ce travail a été effectué à la suite de l'observation de niveaux élevés en arsenic dans les eaux de plusieurs puits près de Maun, Botswana. Le but de ce travail préliminaire était de caractériser les types de sédiments et les eaux qui révèlent de tels niveaux élevés en arsenic. Les milieux de dépôt des sédiments chargés en arsenic ont été définis, ainsi que les processus de transfert de l'arsenic contenu dans les sédiments dans l'eau souterraine. Ce travail a des applications pratiques immédiates en ce qui concerne la gestion des ressources en eau dans les pays désertiques.

INTRODUCTION (ENGLISH VERSION)

0.1 Statement of the problem

This thesis is a study of fluvio-lacustrine sediments from two basins located within the East African Rift. The zone of interest for this work is known in the literature under the name of the "*Southern Complex*" or "*Southwestern Branch*" (Reeves, 1972; Mondeguer et al., 1989; Modisi et al., 2000). The early initiation stage in the development of a continental rift is characterized by the development of shallow half-graben basins where nascent faults exert a primary control in the deposition, hence modification of catchment drainage. The two basins selected for this study are considered to represent two successive stages in early rift development. They are: 1) the Makgadikgadi-Okavango-Zambezi Basin located in the north-west of Botswana and 2) the Mpulungu sub-basin which constitutes the extreme south western basin of Lake Tanganyika (Tanzania and Zambia) (Figure I-1).

Climate and tectonics, in particular the relationship between the uplift of continental crust and weathering, drives the processes which result in the formation sediment detritus and the ions dissolved in water. The chemical composition of the aqueous component plays a role in the biogeochemical cycling of downstream aquatic systems. The chemical composition of the detrital fraction is determined to a large extent by the composition of the source rocks, the degree of weathering, and the processes which occur during transport and accumulation of sediments. Tectonic activity creates the source area uplift to form relief. It is the regional climatic conditions (temperature and precipitation) which determine physical and chemical weathering regimes of the source area, hence the nature of the sediment pile in the nascent rift basins.

Tectonic processes give a distinctive geochemical signature to sediments in two ways: 1) tectonic settings have characteristic provenance signals and 2) they are characterized by their sedimentary processes (Rollinson, 1993). For sandstones, the relationship between the geochemical composition, the provenance of sediments and the tectonic setting can be a useful tool in elucidating information from ancient rocks. For instance, the use of major (Bhatia, 1983; Roser and Korsch, 1986; 1988). and trace element (Bhatia and Crook, 1986) compositions in diagnostic diagrams has been shown to be useful in determining tectonic settings.

In order to test the accuracy of various diagnostic diagrams to elucidate the tectonic setting of ancient sediments, they should be tested against modern sediments of a known tectonic setting. This has been done in the past (Bhatia, 1983; Bhatia and Crook, 1986; Roser and

Korsch, 1986; Roser, 1996) but more data are required on recent sediments of known tectonic setting to validate and refine these established discrimination criteria. We use data from young (late Pleistocene to Holocene) sediments from a known tectonic setting, the East African Rift System (EARS), an early stage rifted basin, to establish how well discriminant diagrams and bivariate plots of tectonic settings categorize these sediments, thereby shedding light on their tectonic history.

With respect to climate change work conducted on lake sediments in Africa, the focus to date has been more on bio-indicators of climate such as pollen series (e.g. Vincens et al., 1993; Vincens et al., 2005) and diatom assemblages (e.g. Gasse et al., 1989; Gasse et al., 2002) as opposed to geochemical methods. To date, with the exception of organic geochemistry methods of lake sediments (e.g. Talbot and Laerdal, 2000; Talbot et al., 2006), and work conducted in West Africa and Lake Malawi (e.g. Schneider et al., 1997; Johnson et al. 2004) sedimentary geochemistry has been a tool primarily used on ancient sedimentary suites in Africa (e.g. Fedo et al., 1997).

Hypothesis: Can the interpretation of sedimentary inorganic geochemistry of Quaternary sediments from the East African Rift contribute both to the detection of climate change signals and to the understanding of tectonic evolution of the Southern Complex?

In order to assess the hypothesis, a multidisciplinary approach was used with an emphasis on geochemical methods, based on the following primary objectives:
a) to enhance our understanding of geochemical processes which occur during the formation of sedimentary sequences (erosion – transport - accumulation) accumulating during the early stage development in rift evolution;
b) to define sedimenatry and geochemical criteria which allow for the discrimination of tectonic activity and climate changes throughout the evolution of these rift basins
c) reconstruct the tectonic and climatic environments which characterised these two regions of the East African Rift throughout the late Pleistocene and Holocene.

The Makgadikgadi-Okavango-Zambezi (MOZ) Basin is an extensive intracontinental basin of Plio-Pleistocene age. The evolution of this basin is controlled by a system of parallel faults in the NE-SW direction (Figure I-2). Located within the larger MOZ basin is the Okavango Basin which is a half-graben whose formation is linked to the development of NE-SW trending faults, in particular the Gumare, Kunyere and Thamalakane faults. The Okavango Delta is located within the central southern Africa climate zone however the catchment area extends into the north-west of Angola, in the tropical climate zone.

The Lake Tanganyika Basin belongs to the western branch of the East African Rift and is located within the tropics. The Mpulungu sub-basin is the most southerly of the seven sub-basins which constitute the Tanganyika Basin (Tiercelin and Mondeguer, 1991) (Figure I-3). The Mpulungu sub-basin is the most recent of the sub-basins of Lake Tanganyika. It was formed between 4 and 2 million years ago, whereas the central segment of Tanganyika is believed to have formed between 12 – 10 million years ago (Cohen et al., 2000). The Mpulungu sub-basin and the associated Mweru and Mweru-Wantipa Lakes represent the most northerly extent of basins within the "Southern Complex" of the East African Rift.

The East African Rift is famous for its numerous discoveries of fossil homonid sites which has given rise to abundant literature on the region and the sites (Leakey et al., 1964 ; Patterson and Howells, 1967; Johanson and Taieb, 1976; Tattersall, 1993; Prat et al., 2005). The determination of the spatial and temporal extent of environmental changes brought about by climatic variations and tectonic events linked to the development of the rift has become a key issue in palaeo-anthropology today. These issues are crucial in order to better understand and verify the different scenarios of evolution and migrations for different groups of Hominids **(**Vbra, 1995; deMenocal et al., 2000; Behrensmeyer, 2006).

0.2 Organisation of the manuscript

All chapters in this thesis are written in English, and with the exception of Chapters I, II and III, represent work already published in international journals or manuscripts in preparation for submission to journals. At the beginning of Chapters IV – VIII a summary written in French is presented.

Chapter I gives a detailed description of the two sites chosen for this study: the Makgadikgadi-Okavango-Zambezi Basin located in north-west Botswana and the Mpulungu sub-basin of Lake Tanganyika. In this chapter a description of the geological, climatic and hydrological characteristics of each site is given.

Chapter II presents a review of published work on palaeo-climate for the region encompassing the Mpulungu sub-basin to the north and the Makgadikgadi-Okavango-Zambezi Basin to the south.

Chapter III presents an overview of the major geochemical methods employed in this work. In addition, it provides the scientific justification behind choosing certain geochemical indicators in this study.

Chapter IV entitled «*Cryptic indicators of provenance from the geochemistry of the Okavango Delta sediments, Botswana*» was published in the journal *Sedimentary Geology* in 2005. This article presents the results of a geochemical study conducted on siliciclastic sediments sampled from boreholes drilled in the distal Okavango Delta, near Maun (Figure IV-1). The geochemistry of major, trace and rare earth elements was used to identify provenance of the sediments which currently fill the Okavango Delta alluvial fan. These sediments are composed primarily of two fractions, one aeolian and one fluvial component. The aeolian fraction is composed essentially of quartz which results in a strong dilution of the other geochemical elements in the sediments. Quantitative modelling using representative rocks from the catchment as potential source rocks was carried out. The results confirm that Proterozoic granitoid–gabbro and related volcanic and ortho-metamorphic rock complexes exposed in NW Botswana and adjacent Angola and Namibia are the source rocks of the sediment component which was mixed with aeolian sand and interacted with a variable proportion of diagenetic carbonates to produce the Okavango sediments.

Chapter V entitled «*Sediment geochemistry, provenance and tectonic setting: Application of discrimination diagrams to very early stages of intracontinental rift evolution, with examples from the Okavango and Southern Tanganyika rift basins* ». This mansucript is being prepared for submission to the *Journal of African Earth Sciences*. The tectonic setting and the stages of evolution of the MOZ basin and the Mpulungu sub-basin within the context of a continental rift has been investigated in earlier work (Tiercelin and Mondeguer, 1991; Modisi et al., 2000; Ringrose et al., 2005). The geochemical characterisitcs of the Okavango and Mpulungu sediments are used in this mansucript as markers in the stages of tectonic evolution of these two rift basins. In this work, two new fields within the classical discrimination diagrams for tectonic setting are proposed. One field represents the nascent stages of early rift development illustrated by the Okavango Delta alluvial fan and the second stage represents and successive, more mature stage, represented by the Mpulungu lacustrine basin. The significance of this work is in the possible future use of these diagrams to elucidate the stage of rifting in ancient sediments.

Chapter VI is entitled «*Sedimentological and geochemical evidence for palaeo-environmental change in the Makgadikgadi subbasin in relation to the MOZ rift depression, Botswana*». This work was published in the journal *Palaeogeography, Palaeoclimatology and Palaeoecology* in 2005. This chapter represents the result of a multidisciplinary study including field sedimentology and geomorphological techniques combined with geochemical methods and dating to help constrain palaeo-climatic events. This work contributes to the identification of palaeoenvironmental markers in north west Botswana during the Pleistocene. This work represents a new approach to the interpretation of palaeoenvironments in the Makgadikgadi basin within the context of the larger MOZ rift depression

Chapter VII "*Use of the geochemical and biological sedimentary record in establishing palaeo-environments and climate change in the Lake Ngami basin, NW Botswana*" was published in the journal *Quaternary International* en 2006. This article presents the results of a study to reconstruct palaeoenvironments and lake levels in the Lake Ngami basin, located to the south-west of the Okavango Delta. Two trenches dug into the dry lake bed revealed over several meters of thickness, a succession of lacustrine to fluvio-lacustrine facies which demonstrate important variations in terms of lake levels and hydrological input to the sub-basin. The geochemical analysis of the Lake Ngami sediments and the subsequent interpretation was facilitated by the fact that the Lake Ngami sediments are characterised by a fine fraction (clay fraction) as a result of being a drainage terminus, much more significant than the through-flow fluvial siliciclastic sediments of the Okavango Delta. The geochemistry of the lacustrine sediments therefore provides more detailed evidence of palaeo-redox conditions which when combined with a study of the diatoms, contribute significant information on water quality and lake levels during the late Pleistocene and Holocene in the Lake Ngami Basin.

Chapter VIII, «*Major and trace element geochemistry of the Lake Tanganyika sediments: implications for late Quaternary climatic variability*» is being prepared for submission to *Palaeogeography, Palaeoclimatology, Palaeoecology*. The sedimentary record of Lake Tanganyika (Mpulungu Basin) records the response of the basin to external perturbations such as climate change and the study of this record enhances our understanding of the impact of climatic events such as the Last Glacial Maximum and the Younger Dryas on the environment of the region. The sedimentary sequence of Lake Tanganyika is interrupted by the input of volcanic ash generated from eruptions of the Rungwe volcanoes located to the south-east of the Mpulungu Basin. The identification of the pyroclastic layers in the sedimentary sequence helps in the reconstruction of wind regimes in the region which in turn is related to the position of the ITCZ and the reconstruction of past climate.

The paper entitled «*Characterization of arsenic occurrence in the water and sediments of the Okavango Delta, NW Botswana*», was published in the journal *Applied Geochemistry* in 2006. This paper is located in Appendix 1. This work was conducted following a preliminary investigation of water quality in the Okavango Delta which revealed the presence of elevated arsenic in some of the boreholes located around Maun. The aim of this work was to characterize the types of sediments and waters which contain elevated arsenic. The sedimentary environment under which sediments with elevated arsenic were discussed as well as the process of the transfer of arsenic from the sediments into the groundwater. This work has important practical outcomes related to water resource management in a semi-arid country, such as Botswana.

References

Behrensmeyer, A.K., 2006. Climate change and human evolution. Science 311, 476-478.
Bhatia, M.R., 1983. Plate tectonics and geochemical composition of sandstones. Journal of Geology 91, 611-627.
Bhatia, M.R., Crook, K.A.W., 1986. Trace element characteristics of graywackes and tectonic setting discrimination of sedimentary basins. Contributions to Mineralogy and Petrology 92, 181-193.
Cohen, A.S., Scholz, C.A., Johnson T.C., 2000. The international decade of East African Lakes (IDEAL) drilling initiative for the African Great Lakes, Journal of Paleolimnology, 24 (2), 231-235.
deMenocal, P., Ortiz, J., Guilderson, T., Adkins, J., Sarnthein, M., Baker, L., Yarusinsky, M., 2000. Abrupt onset and termination of the African humid period: rapid climate responses to gradual insolation forcing. Quaternary Science Reviews 19, 347-361.
Fedo, C.M., Eriksson, K.A., Krogstad, E.J., 1996. Geochemistry of shales from the Archaean (~3.0 Ga) Buhwa Greenstone Belt, Zimbabwe: implications for provenance and source-area weathering. Geochim. Cosmochim. Acta 60, 1751–1763.
Gasse, F., Lédée, V., Massault, M., Fontes, J.Ch., 1989. Water-level fluctuations of Lake Tanganyika in phase with oceanic changes during the last glaciation and deglaciation. Nature 342, 57-69.
Gasse , F., Barker, P., Johnson,T.C., 2002. A 24,000 yr diatom record from the northern basin of Lake Malawi. In: Odada E.O., and Olago, D.O. (eds), The East African Great lakes: Limnology, Palaeolimnology and Biodiversity. Dordrecht, Kluwer, pp. 393-414.
Johanson, D.C., Taieb, M., 1976. Plio-Pleistocene hominid discoveries in Hadar, Ethiopia. Nature 260, 293-297.
Leakey, L.S.B., Tobias, P.V., Napier, J.R., 1964. A new species of the genus *Homo* from Olduvai Gorge. Nature 202, 7-9.
Modisi, M.P., Atekwana, E.A., Kampunzu, A.B., Ngwisanyi, T.H., 2000. Rift kinematics during the incipient stages of continental extension: evidence from nascent Okavango rift basin, northwest Botswana. Geology 28, 939– 942.
Mondeguer, A., Ravenne, C., Masse, P., Tiercelin, J-J., 1989. Sedimentary basins in an extension and strike-slip background: the South Tanganyika Trough complex, East African rift. Bull. Soc. Geol. France 8 (3), 501-522.
Mondeguer, A., 1991. Bassin sedimentaires en contexte extensive et decrochant: L'example du "Complexe des fosses sud-Tanganyika", Rift Est- Africain. Morphostructure et sedimentation. PhD thesis. L'Universite de Bretagne Occidentale.
Partridge, T.C., Scott, L., Hamilton, J.E., 1999. Synthetic reconstructions of southern African environments during the Last Glacial Maximum (21-18 kyr) and the Holocene Altithermal, (8-6 kyr). Quaternary International 57/58, 207-214.
Patterson, B., Howells, W.W., 1967. Hominid humeral fragment from Early Pleistocene of Northwestern Kenya. Science 156, 64-66.
Prat, S., Brugal, J-P., Tiercelin, J-J., Barrat, J-A., Bohn, M., Delagnes, A., Harmand, S., Kimeu K., Kibunjia, M., Texier, P-J., Roche, H., 2005. First occurrence of early Homo in the Nachukui Formation (West Turkana, Kenya) at 2.3-2.4 Myr. Journal of Human Evolution 49, 230-240.
Reeves, C.V., 1972. Rifting in the Kalahari? Nature 237, 95-96.
Ringrose, S., Huntsman-Mapila, P., Kampunzu, H.,Downey, W.D. Coetzee S., Vink, B., Matheson W, Vanderpost, C., 2005. Geomorphological and geochemical evidence for palaeo-environmental change in the Makgadikgadi sub-basin, in relation to the MOZ rift depression, Botswana. *Palaeogeography, Palaeoclimatology and Palaeoecology* 217, 265-287.
Roser, B.P., Korsch, R.J., 1986. Determination of tectonic setting of sandstone-mudstone suites using SiO_2 content and K_2O/Na_2O ratio. Journal of Geology 94, 75-83.
Roser, B.P., Korsch, R.J., 1988. Provenance signatures of sandstone-mudstone suites determined using discriminant function analysis of major-element data. Chemical Geology 67, 119-139.
Schneider, R.R., Price, B., Muller, P.J., Kroon, D., Alexander, I., 1997. Monsoon related variations in Zaire (Congo) sediment load and influence of fluvial silicate supply on marine productivity in the east equatorial Atlantic during the last 200,000 years. Paleoceanography 12 (3) 463-481.

Talbot, M.R., Jensen, N.B., Laerdal, T., Filippi, M.L., 2006. Geochemical responses to a major transgression in giant African lakes. Journal of Paleolimnology. 35 (3), 467-489.

Talbot, M.R., Laerdal, T., 2000. The Late Pleistocene-Holocene palaeolimnology of Lake Victoria, East Africa, based upon elemental and isotopic analyses of sedimentary organic matter. Journal of Paleolimnology 23, 141-164.

Tattersall, I., 1993. The Human Odyssey: Four Million Years of Human Evolution. Prentice Hall, New York, 191 pp.

Tiercelin, J-J, Mondeguer, A., 1991. The geology of the Tanganyika Trough. In: Coulter G.W. (ed), Lake Tanganyika and its life. Oxford University Press, Oxford, pp. 7-48.

Tyson, P.D., Preston-Whyte, R.A., 2000. The weather and climate of Southern Africa. Oxford University Press, Cape Town, 396 pp.

Vrba, E.S., 1995. In: Paleoclimate and evolution with emphasis on human origins. E.S. Vrba, G.H. Denton, T.C. Partridge, L.H. Burckle (eds), Yale University Press, New Haven, CT, pp.24-25.

Vincens, A., Chalié, F., Bonnefille, R., Guiot, Tiercelin, J-J., 1993. Pollen-derived rainfall and temperature estimates from lake Tanganyika and their implications for late Pleistocene water levels. Quaternary Research 40, 343-350.

Vincens, A., Buchet, G., Williamson, D., Taieb, M., 2005. A 23,000 yr pollen record from Lake Rukwa (8^{o}S, SW Tanzania): New data on vegetation dynamics and climate in Central Eastern Africa. Review of Palaeobotany and Palynology 137, 147-162.

I. STUDY SITE

The East African Rift System (EARS) is a vast Cenozoic structure with a length of more than 4500 km, extending from Afar in the north to the south of the African continent (Botswana, Mozambique) (Figure I-1). It is a major intracontinental extension zone, with two main branches characterized by N-S to NNE-SSW oriented deep troughs, which are mainly half-grabens.

The Eastern Branch, with a length of 1800 km, extends from the Afar Depression to the Kenya Rift and the North Tanzanian Divergence. The early phases of rifting characterizing this branch are dated from Eocene - Lower Oligocene and resulted in major fissural volcanic activity and half-graben development in northern Kenya and southern Ethiopia (Morley et al., 1992; Ebinger and Ibrahim, 1994; Ebinger et al., 2000; Tiercelin et al., 2004).

The Western Branch, with a length of 2500 km, is more complex in structure and includes the Lake Tanganyika and Lake Malawi Troughs, which are the two largest and deepest structures of the EARS. Compared to the Eastern Branch, the Western Branch is marked by having only a few volcanic provinces which are: Ruwenzori, Virunga, Kivu and Rungwe (Figure I-1). Initial volcanic activity occurred in these regions at about 8 Ma (Ebinger et al., 1989). Two major NW-SE-trending transcurrent fault zones, the Aswa Fault Zone and the TRM (Tanganyika-Rukwa-Malawi) Fault Zone, act as links between the Eastern and Western Branches, and between segments of the Western Branch, respectively. These transverse structures are recognized as Late Precambrian features reactivated during the Cenozoic rifting phases (McConnell, 1980).

To the southwest, a suite of half-graben basins extend from the southern Tanganyika-northern Malawi region in a NE-SW direction, forming the “Southern Complex” (Mondeguer et al., 1989; Tiercelin and Mondeguer, 1991) (Figure I-1). This Southern Complex, which includes the Makgadikgadi-Okavango-Zambezi (MOZ) basin, differs from the two other branches of the EARS as it is much younger than the other segments and has no record of volcanic activity during the Cenozoic.

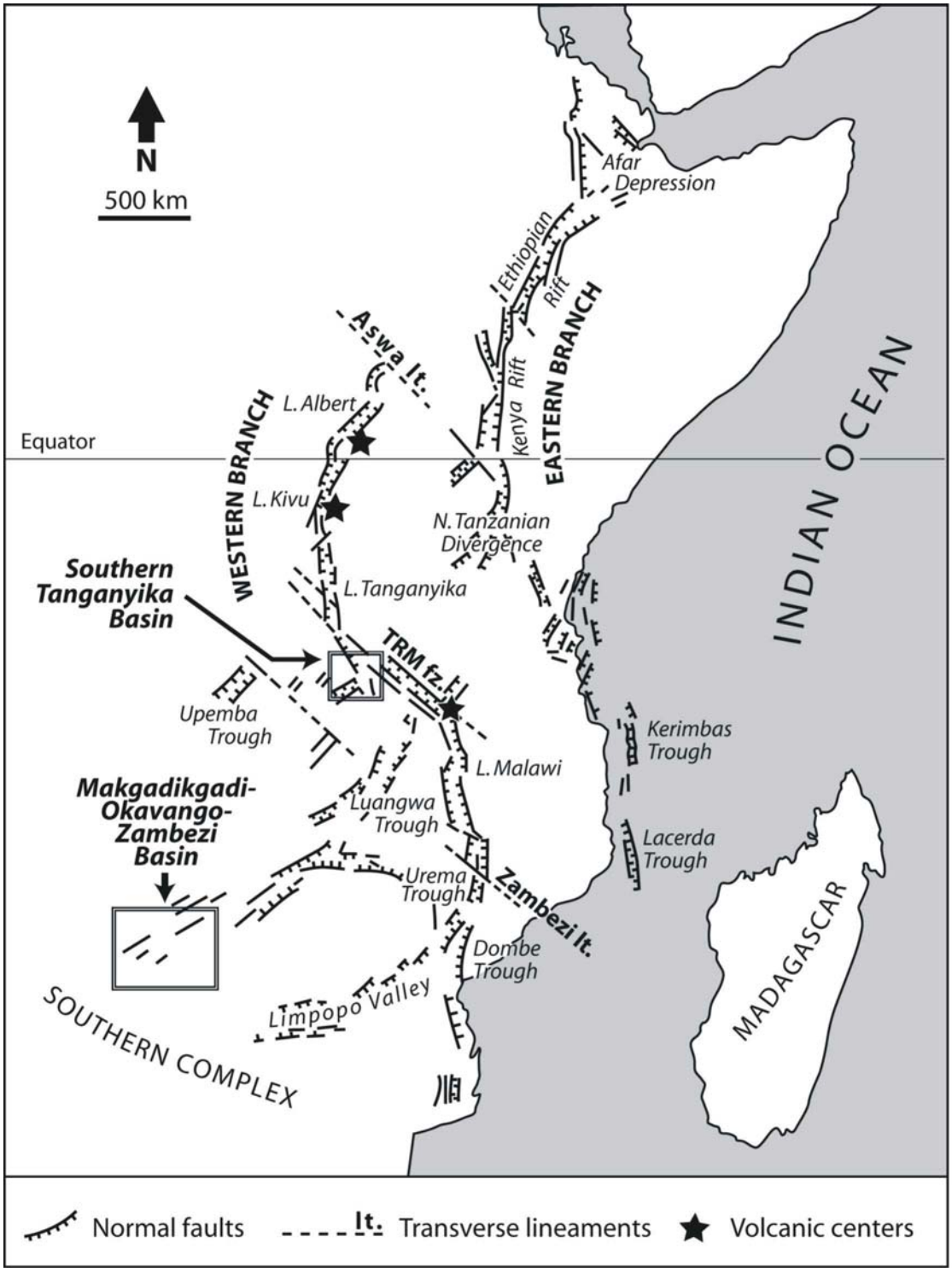

Figure I 1. Map of East African Rift System showing the Western and Eastern Branches and the Southern Complex. Study areas are located within boxes.

The early initiation stage in the development of a continental rift is characterized by the development of shallow half-graben basins where nascent faults exert a primary control in the evolution of drainage catchment formation (Gawthorpe and Leeder, 2000). This stage is illustrated by the present Okavango alluvial fan, located within the larger MOZ basin. The Okavango Delta is a broad subsiding half-graben occupied by an alluvial fan, strongly controlled by fault growth (Modisi, 2000). The immediate successive stage concerns the development of deeper basins where swamps and shallow lacustrine environments (<50 m water depth) occur, as the result of fault growth and propagation, and initiation of basin subsidence, represented by the larger MOZ basin. A more mature stage concerns the development of well-defined, actively subsiding half-graben basins, where propagation and interaction between fault segments lead to basin linkage and strong control of drainage. Wider and deeper lacustrine environments characterize this stage, which is illustrated by the southern Mpulungu sub-basin of Lake Tanganyika.

Samples for this study were obtained from northern Botswana, within the Makgadikgadi-Okavango-Zambezi depression and from the Mpulungu sub-basin in Lake Tanganyika. Both sites are described in detail below.

I.1 The Makgadikgadi-Okavango-Zambezi Basin

Fluvio-lacustrine deposition in northern Botswana has mainly taken place within a large structural depression considered as a southwesterly propagating extension of the EARS (Figure 1-1). This rift depression was drained and filled by southeasterly flowing rivers on a number of occasions during the Tertiary and Pleistocene as the area was faulted and half grabens developed (Cooke, 1980; Mallick et al., 1981; Modisi et al., 2000). The MOZ (Makgadikgadi–Okavango–Zambezi) depression (Figure I-2) is controlled by a series of NE–SW normal faults related to rifting which reactivated Proterozoic and Karoo structures (Baillieul, 1979; Smith, 1984; Modisi et al., 2000). Tectonic activity along the same trend resulted in uplift along the Zimbabwe–Kalahari axis possibly during the late Pliocene (Partridge and Maud, 2000; Moore and Larkin, 2001) causing the impoundment of proto Okavango, Kwando and upper Zambezi drainage and the development of the Makgadikgadi (MSB), Ngami and Mababe subbasins (Cooke, 1980; Ringrose et al., 2002).

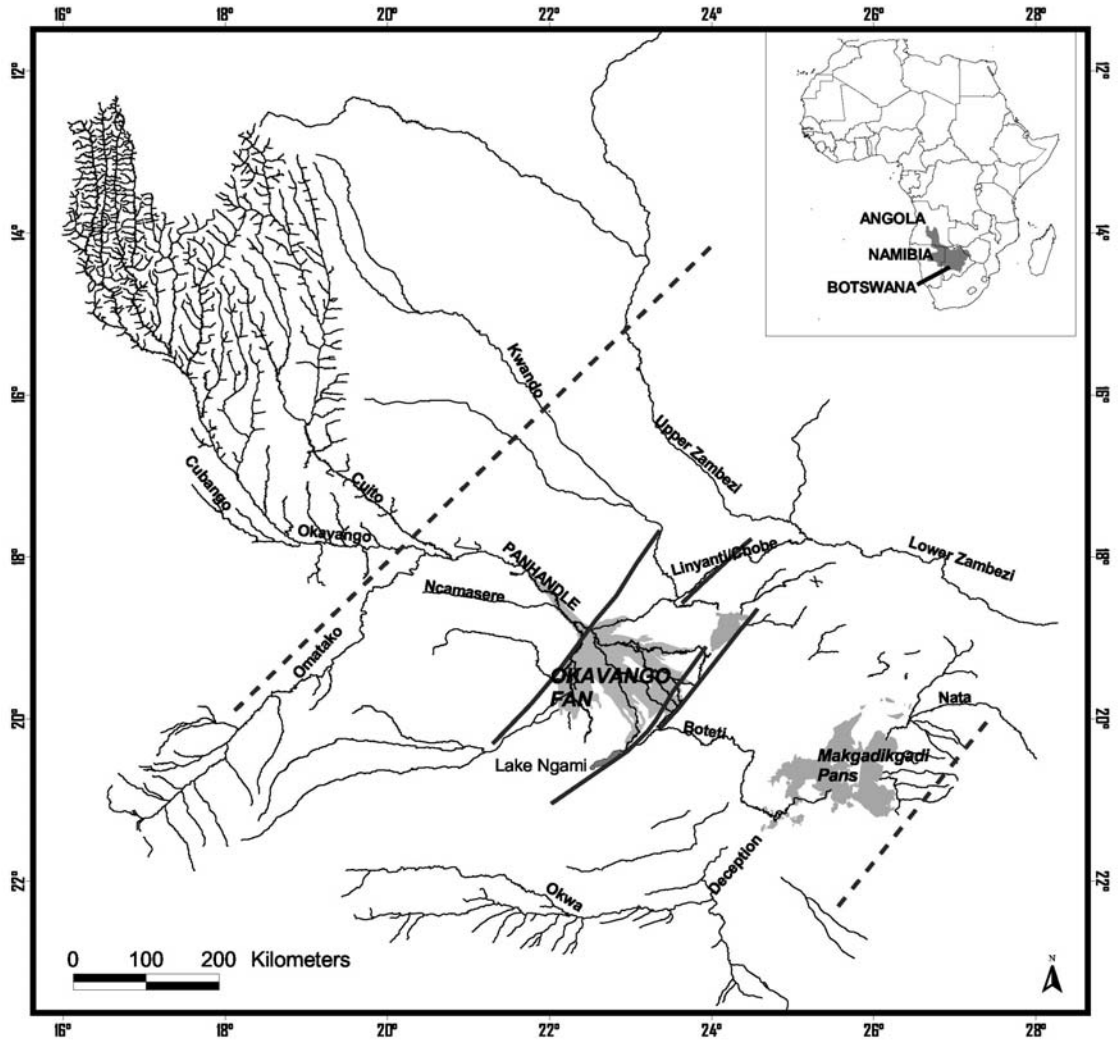

Figure I 2. The Okavango Delta within the MOZ rift depression. Extent of rift depression is shown by the dashed lines.

The nascent Okavango Delta alluvial fan is located within the Kalahari Basin, which is a shallow intracontinental basin. Aeromagnetic and seismic refraction studies suggest that the maximum thickness of sediment, in excess of 300 m, occurs in northern Namibia and in the Okavango graben in Botswana (Reeves, 1978; Modisi et al., 2000). The major part of the catchment area is covered by unconsolidated to loosely consolidated, chiefly reworked aeolian sand of the presently active Kalahari Basin. The Okavango Delta sediments represent the youngest (Quaternary) stratigraphic unit of the Kalahari sedimentary basin. Potential sources of the Okavango Delta sediments are mainly Proterozoic granitoids, gabbros and related volcanic and orthometamorphic rocks exposed in the catchment area in Angola, northern Namibia and northern Botswana.

Samples for the Makgadikgadi-Okavango-Zambezi study include sediment and water samples from boreholes drilled in the distal Okavango Delta, calcrete samples from the shorelines of palaeo-lake Makgadikgadi, and sediment samples from an excavation pit dug in Lake Ngami.

I.2 Lake Tanganyika

The Lake Tanganyika Trough (3° 30'-8° 50' S, 29°-31°20' E) is the largest structure of the Western Branch of the EARS (Figure I-1). It is structurally divided into two main basins, the northern basin orientated N0^{o}, and the southern basin oriented in the N150^{o} direction, separated by N130-150°-trending horst block called the Kalemie-Mahali shoal (Mondeguer, 1991) (Figure I-3). These two basins are occupied by Lake Tanganyika, which is 650 km long and the deepest of the African rift lakes at 1470 m.

The basin geometry and stratigraphy of the Tanganyika Basin were recorded by the seismic reflection studies of Projects PROBE and GEORIFT (Rosendahl et al., 1986, 1988; Tiercelin and Mondeguer, 1991; Lezzar et al., 1996). The central part of the basin is known to contain a > 5 km thick sequence of rift-related sediments (Rosendahl et al., 1986; Morley, 1988). Age estimates by Cohen et al. (1993) suggest that the central segment of the Tanganyika Basin began to form between 9 and 12 Ma, whereas the northern basin, characterized by a 4-km-thick sequence of sediments (Rosendahl et al., 1986; Ebinger, 1989), formed more recently, at 7-8 Ma. The southern end of the basin, known as the Mpulungu sub-basin (Mondeguer, 1991), contains a 2.5 km thick pile of rift sediments with an estimated age of 4-2 Ma.

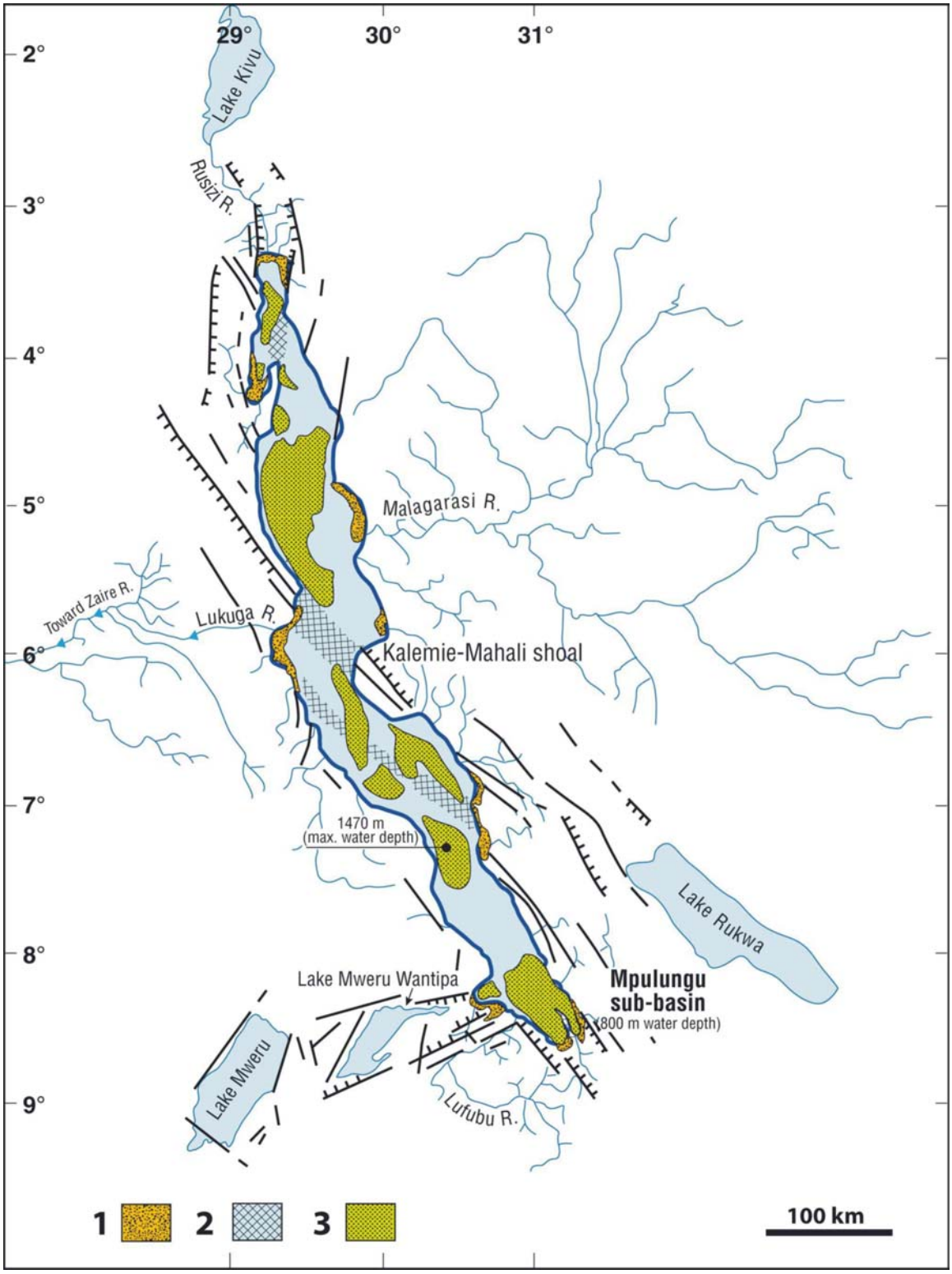

Figure I 3. The structure and hydrology of Lake Tanganyika Basin. Key 1-littoral platforms; 2-transverse shoals; 3-sub-basin deep zones (after Tiercelin and Mondeguer, 1991).

The Mpulungu sub-basin is 100 km long, 25 km wide with up to 800 m water depth (Figure I-3) The sub-basin is delineated by three groups of faults: a main group trending N150° forming the Mpulungu Border Fault characterized by an important vertical throw of at least 2000 m, a second group of faults oriented N70^{o} that developed on the western flank of the Mpulungu Basin, and a minor group of faults oriented N30°, respectively. The two main groups of faults deeply intersect the Upper Precambrian tabular terrains of the northern side of the Zambian craton (also known as Bangweulu Block) (Unrug, 1984). The craton is of Middle Proterozoic age (around 1820 Ma (Brewer et al., 1979)), and mainly composed of granites, granitoides and metavolcanites; 2) the Mporokoso Group formed of conglomerates, sandstones, quartzites and shales; and 3) the Katanga super-group, that include conglomeratic and quartzitic series overlain by carbonate series (Daly and Unrug, 1983). To the south-east of the Mpulungu sub-basin is the Rungwe volcanic province (Figure VI-3 a), which is the most southern eruptive centre in the EARS western branch. Volcanic activity in the Rungwe started in the Late Miocene (~ 8 Ma) and remained active during the late Pleistocene and Holocene with major pyroclastics eruptions (Harkin, 1960; Ebinger et al., 1989; Williams et al., 1993).

Lake Tanganyika sediments were recovered from the Mpulungu sub-basin duirng the GEORIFT Project of Elf-Aquitaine. Several Kullenberg piston cores were collected in December 1985 in the central part of the Mpulungu sub-basin and on the platform/slope of Cameron Bay (Mondeguer, 1991). Sediments from two cores have been considered for this study: the MPU-10 core, 8.09 m long, was collected from a water depth of 422 m in the central part of the basin, and the 11.19 m long MPU-3 core was collected from a water depth of 140 m at the limit of the slope between Cameron Bay and the Mpulungu sub-basin.

I.3 Regional climate

Rainfall in tropical Africa is strongly influenced by the seasonal migration of the Intertropical Convergence Zone (ITCZ) to the north and south of the equator (Figure I-4). During austral winter, the ITCZ migrates northwards and during this dry season, south-eastern Africa is dominated by SE winds (Lindesay, 1998). In the austral summer, when the ITCZ migrates to its southward position, north winds bring moisture to this region. In south-western Africa, the wet ITCZ and the dry high-pressure system over the South Atlantic are the two major systems that control today's climate. When the ITCZ moves to its southward position in the austral summer,

the moist north winds replace the dry westerly wind system. The strength of African monsoon and variations of the mean ITCZ position over tropical Africa are mainly driven by the earths 23 kyr precessional cycle which results in changes in the amount of solar radiation received at low latitudes (deMenocal et al., 2000; Tyson and Preston-Whyte, 2000; Baker et al., 2001).

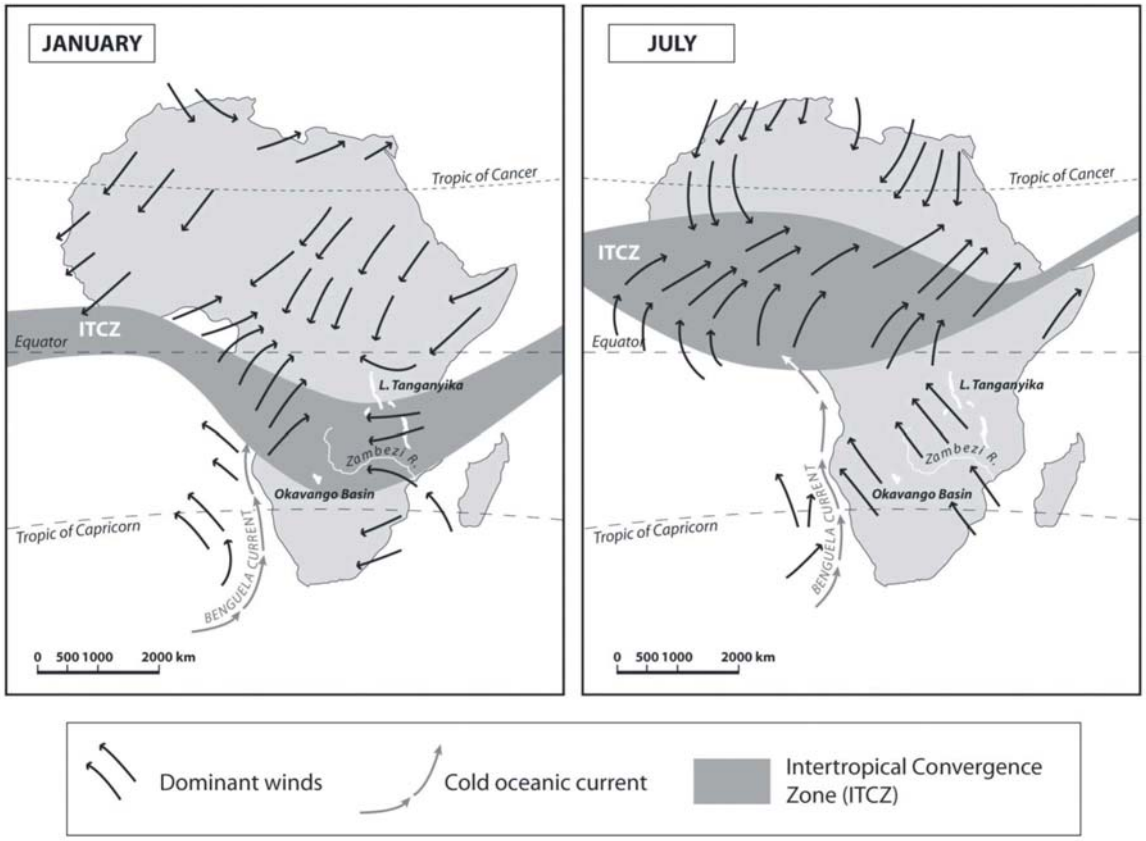

Figure I 4. Present ITCZ seasonal migration over Africa shown as dark grey band. Predominant wind directions are represented as black arrows. Figure from Grand Atlas du Continent Africain (1973).

Flooding in the Okavango Delta is influenced by both local rainfall and in-flow from the catchment in the Angolan highlands. Under the current climatic conditions, local rainfall over the Okavango Delta is influenced by the anticyclonic conditions that dominate the interior of southern Africa and rainfall patterns are subject to an 18 year oscillation pattern (McCarthy et al., 2000). The Angolan catchment climate is currently strongly influenced by the ITCZ and the South Atlantic high pressure systems (Figure I-4). The Okavango River derives its water from two major tributaries, the Cubango River in the west and the Cuito River in the east. Rainfall over

the Cubango catchment shows an 18-year rainfall oscillation which is out of phase with that of central southern Africa (McCarthy et al., 2000).

In Lake Tanganyika, there is a single rainy season in the catchment area from November to April with a mean annual rainfall of 1000-1100mm (Vincens, 1991). South easterly winds predominate during the dry season, resulting in seasonal upwelling of deep water at the southern end of Lake Tanganyika (Vincens, 1991). During the rainy season, solar heating forces air to rise through convection, resulting in the African monsoon.

References

Baillieul, T.A., 1979. A reconnaisance survey of the cover sands in the Republic of Botswana. Journal of Sedimentary Petrology 45,494-503.

Baker, P.A., Rigsby, C.A., Seltzer, G.O., Fritz, S.C., Lowenstein, T.K., Bacher, N.P., Veliz, C., 2001. Tropical climate changes at millennial and orbital timescales on the Bolivian Altiplano. Nature 409, 698-701.

Brewer, M.S., Halsam, H.W., Darbyshire, P.F.P., Davis, A.E., 1979. Rb/Sr age determinations in the Bangweulu Block, Luapula Provnice, Zambia. Inst. Geol. Sci. London 79 (5), 11 pp.

Carney, J.N., Aldiss, D.T., Lock, N.P., 1994. The geology of Botswana. Geol. Surv. Dep., Lobatse, Botswana, p. 113.

Cohen, A.S., Soreghan, M.J., Scholz, C.A., 1993. Estimating the age of formation of lakes: an example from Lake Tanganyika, East African Rift system. Geology 21, 511-514.

Cooke, H.J., 1980. Landform evolution in the context of climatic changes and neotectonics in the middle Kalahari of north-central Botswana. Trans. Inst. Brit. Geog., NS 5, 80-99.

Daly, M.C., Unrug, R. 1983. The Muva Supergroup of northern Zambia: a craton to mobile belt sedimentary sequence. Transaction of the Geological Society of South Africa 85, 155-165.

deMenocal, P., Ortiz, J., Guilderson, T., Adkins, J., Sarnthein, M., Baker, L., Yarusinsky, M., 2000. Abrupt onset and termination of the African humid Period: rapid climate responses to gradual insolation forcing. Quaternary Science Reviews 19, 347-361.

Ebinger, C.J., 1989. Tectonic development of the western branch of the East African Rift system. Bulletin of the Geological Society of America 101, 885-903.

Ebinger, C.J., Deino, A.L., Drake, R.E., Tesha, A.L., 1989. Chronology of volcanism and rift basin propogation: Rungwe volcani province, East Africa: Journal of Geophysical Research 94, 15785-15803.

Ebinger, C.J., Ibrahim, A., 1994. Multiple episodes of rifting in Central and East Africa: A re-evaluation of gravity data. Geological Rundschau 83, 689-702.

Ebinger, C.J., Yemane, T., Harding, D.J., Tesfaye, S., Kelley, S., Rex, D.C., 2000. Rift deflection, migration, and propagation: Linkage of the Ethiopian and eastern rifts, Africa. Bulletin of the Geological Socciety of America 112, 163-176.

Gawthorpe, R.L., Leeder, R., 2000. Tectono-sedimentary evolution of active extensional basins. Basin Research 12, 195-218.

Harkin, D.A., 1960. The Rungwe volcanics at the northern end of Lake Nyasa. Mem. Geol. Surv. Tanganyika, II: 172pp.

Kampunzu, A.B., Bonhomme, M.G., Kanika, M., 1998. Geochronology of volcanic rocks and evolution of the Cenozoic Western branch of the East African rift system. Journal of African Earth Sciences 26, 441–461.
Kampunzu, A.B., Armstrong, M.P., Modisi, M.P., Mapeo, R.B., 1999. The Kibaran belt in southwest Africa: ion microprobe U– Pb zircon data and definition of the Kibaran Ngami belt in Botswana, Namibia and Angola. Gondwana Res. 2, 571–572.
Kampunzu, A.B., Armstrong, R.A., Modisi, M.P., Mapeo, R.B.M., 2000. Ion microprobe U–Pb ages on single detrital zircon grains from Ghanzi Group: implications for the identification of a Kibaran-age crust in northwestern Botswana. Journal of African Earth Sciences 30, 579–587.
Le Gall, B., Tshoso, G., Jourdan, F., Fe´raud, G., Bertrand, H., Tiercelin, J.J., Kampunzu, A.B., Modisi, M., Dyment, J., Maia, M., 2002. Ar–Ar geochronology and structural data from the Okavango giant mafic dike swarm, Karoo large igneous province, N Botswana. Earth Planetary Science Letters 202, 595–606.
Lezzar, K.E., Tiercelin, J.J., De Batist, M., Cohen, A.S., Bandora, T., van Rensbergen, P., Le Turdu, C., Wafula, M., Klerk, J., 1996. New seismic stratigraphy and Late Tertiary history of the North Tanganyika Basin, East African Rift system, deduced from multifold reflection and high resolution seismic data and piston core evidence: Basin Research 8, 1-28.
Lindesay, J.A., 1998. Present climates of Southern Africa. In: Hobbs, J.E., Lindesay, J.A., and Bridgeman, H.A., (eds), Climates of the Southern Continents: Present, Past and Future. John Wiley and Sons, New York, pp. 5-62.
Mallick, D.I.J, Habgood F, Skinner AC. 1981. A geological interpretation of Landsat imagery and air photography of Botswana. Overseas Geological and Mineral Resources, London, 56, 1-36.
Mapeo, R.B.M., Armstrong, R.A., Kampunzu, A.B., 2000. Ages of detrital zircon grains from Neoproterozoic siliciclastic rocks in Shakawe area: implications for the evolution of the Proterozoic crust in northern Botswana. South African Journal of Geology 103, 156–161.
Mapeo, R.B.M., Armstrong, R.A., 2001. Ion microprobe U–Pb zircon geochronology of gneisses from the Gweta borehole, NE Botswana: implications for the Paleoproterozoic Magondi belt in southern Africa. Geological Magazine 138, 299–308.
McCarthy, T.S., Cooper, G.R.J., Tyson, P.D., Ellery, W.N., 2000. Seasonal flooding in the Okavango Delta, Botswana—recent history and future prospects. South African Journal of Science 96, 25–33.
McConnell, R.B., 1980. A resurgent taphrogenic lineament of Precambrian origin in eastern Africa. Journal of the Geological Society of London 137, 483-489.
Modisi, M.P., 2000. Fault system of the southeastern boundary of the Okavango Rift, Botswana. Journal of African Earth Sciences 30, 569– 578.
Modisi, M.P., Atekwana, E.A., Kampunzu, A.B., Ngwisanyi, T.H., 2000. Rift kinematics during the incipient stages of continental extension: evidence from nascent Okavango rift basin, northwest Botswana. Geology 28, 939– 942.
Mondeguer, A., Ravenne, C., Masse, P., Tiercelin, J.J., 1989. Sedimentary basin in an extension and strike-slip background : the South Tanganyika troughs complex, East African Rift. Bull. Soc. Geol. Fr., 8 (3), 501-522.
Mondeguer, A., 1991. Bassin sedimentaires en contexte extensive et decrochant: L'example du "Complexe des fosses sud-Tanganyika", Rift Est- Africain. Morphostructure et sedimentation. PhD thesis. L'Universite de Bretagne Occidentale.
Moore A. E., Larkin, P. 2001. Drainage evolution in south-central Africa since the breakup of Gondwana. South African Journal of Geology, 104, 47-68.
Morley, C.K., 1988. Variable extension in Lake Tanganyika. Tectonics 7, 785-801.

Morley, C.K., Wescott, W.A., Stone, D.M., Harper, R.M., Wigger, S.T., Karanja, F.M., 1992. Tectonic evolution of the northern Kenyan Rift. Journal of the Geological Society of London 149, 333-348.

Partridge, T.C., Maud, R.R., 2000. The Cenozoic of southern Africa. New York: Oxford University Press, 406 pp.

Reeves, C.V., 1978. The gravity survey of Ngamiland: 1970–71. Geol. Surv. Botsw., Bull. 11, 84 pp.

Ringrose, S., Huntsman-Mapila, P., Kampunzu, A.R., Matheson, W., Downey, W.S., Vink, B., 2002. Geomorphological evidence for MOZ palaeo-wetlands in northern Botswana; implications for wetland change. Presentation to Monitoring of Tropical and Sub-tropical Wetlands Conference, December 2002, Maun, Botswana, Published by HOORC and the University of Florida, Centre for Wetlands.

Rosendahl, B.R., Reynolds, D.J., Lorber, P.M., Burgess, C.F., McGill, J., Scott, D., Lambiase, J.J., Derksen, S.J., 1986. Structural expressions of rifting. Lessons from lake Tanganyika, Africa. In: Sedimentation in the African Rifts (eds) Frostick, L.E., Renaut, R.W., Reid, I., Tiercelin, J-J.) Geol. Soc. London Spec. Publ. 25, 127-139.

Rosendahl, B.R., Versfelt, J.W., Scholz, C.A., Buck, J.E., Woods, L.D., 1988. Seismic atlas of Lake Tanganyika, East Africa: Project PROBE Geophysical Atlas Series, Folio 1, Durham, Duke University.

Smith, R.A., 1984, Lithostratigraphy of the Karoo stratigraphy in Botswana, Botswana Geological Survey Bulletin, Lobatse, Botswana, 26, 34pp.

Tiercelin, J-J, Mondeguer, A., 1991. The geology of the Tanganyika Trough. In: Coulter G.W. (ed), Lake Tanganyika and its life. Oxford University Press, Oxford, pp. 7-48.

Tiercelin, J-J., Potdevin, J-L., Morley, C.K., Talbot, M.R., Bellon, H., Rio, A., Le Gall, B., Vetel, W., 2004. Hydrocarbon potential of the Meso-Cenzoic Turkana Depression, northern Kenya. I. Reservoirs: depositional environments, diagenetic characteristics, and source rock-reservoir relationships. Marine and Petroleum Geology 21, 41-62.

Tyson, P.D., Preston-Whyte, R.A., 2000. The weather and climate of Southern Africa. Oxford University Press, Cape Town, 396pp.

Unrug, R., 1984. The mid-proterozoic Mporokoso group of northern Zambia: Stratigraphy, sedimentation and regional position. Precambrian Research 24, 99-121.

Vincens, A., 1991. Late Quaternary vegetation history of the South-Tanganyika Basin. Climatic implications in South Central Africa. Palaeogeography, Palaeoclimatology, Palaeoecology 86, 207-226.

Williams, T.M., Henney, P.J., Owen, R.B., 1993. Recent eruptice episodes of the Rungwe Volcanic Field (Tanzania) recorded in the lacustrine sediments of the Northern Malawi Rift. Journal of African Earth Sciences, 17, 33-39.

II. SYNTHESIS OF PALEOCLIMATIC DATA FOR THE REGION

This chapter provides an overview of the important climatic and environmental changes in the late Quaternary for the region encompassing southern Lake Tanganyika and the Okavango Delta.

Tectonic uplift of the subcontinent occurring during the Tertiary and Early Quaternary had palaeoclimatic consequences as surface temperatures decreased by approximately 0.6 – 0.7^{o}C. In addition, a major climatic shift took place across the Mio-Pliocene boundary, with the west coast becoming drier and the tropical conditions developing in the eastern subcontinent (Tyson and Preston-Whyte, 2000). During the Quaternary, oxygen isotope stages are assigned to successive alternating interglacial and glacial periods. The Quaternary is generally characterized by relatively short successions of glacials and interglacial (Tyson and Preston-Whyte, 2000). The period from 125 ka to around 16 ka BP in the southern hemisphere was characterized by a series of rapid warming stages followed by slow declines to progressively lower minima. The deuterium isotopic record from the Antarctic Vostok ice core illustrates this sequence, with the last minimum occurring at the Last Glacial Maximum (LGM) at around 20 ka BP. Orbit-related parameters such as eccentricity, obliquity and precession constitute the major forcing of the climatic periodicities. High lake levels at 135 ka , 110 ka, 90 ka and 66 ka BP in Lake Naivasha, East Africa coincide with the precessional cycles (Trauth et al., 2001). Marine core data off the coast of KwaZulu-Natal, South Africa reflect the 100 kyr Milankovitch forcing events (Prell et al., 1979). The impact on climate of the precessional cycle have been determined from sediments of the Tswaing impact crater lake in the northern part of South Africa (Partridge et al., 1997; Kirst et al. 1999; Tyson et al., 2002). Evidence from the MOZ (Makgadikgadi-Okavango-Zambezi) basin in northern Botswana also indicates some co-incidence with the last 120 kyr wet cycles as suggested by recent TL dates (Ringrose et al., 2002, 2005).

II.1 Last Glacial Maximum

The hydrological record reconstructed from sediments from tropical African lakes has shown that most of the East African lakes from the ITCZ region were at a low level (Beuning et al., 1997; Gasse et al., 1989; Gasse et al., 2002; Barker and Gasse, 2003, Scholz et al., 2003; Talbot et al., 2006) during the cooler and drier Last Glacial Maximum (LGM). During the LGM (23-18 ka BP) generally dry conditions prevailed in both hemispheres associated with lower tropical land and

sea surface temperatures. Sedimentological studies from Tswaing Crater indicate that whilst enhanced summer rainfall is predicted due to orbital forcing during the LGM, grain-size (Partridge et al., 1997) and diatom data (Metcalfe, 1999) indicate increased aridity. High resolution seismic profiles in Lake Tanganyika indicate a LGM low stand ca. 250-300m below current lake levels (Tiercelin and Mondeguer, 1991). This is supported by a multi-proxy study of a core from central Lake Tanganyika where Scholz et al. (2003), from abundances of benthic diatoms, infer that the lake was about 350 m lower than present during the LGM. South east African lakes Malawi and Rukwa indicate from diatom records, a negative water balance during the LGM (Johnson et al., 2004; Barker et al., 2002). Pollen records from Lake Rukwa spanning the last 23 kyr indicate that between 23 and 20 kyr cal BP vegetation indicates cooler and probably drier climatic conditions than today (Vincens et al., 2005). Pollen records from cores in the Mpulungu sub-basin suggest a mean temperature decrease of about 4.2^{o}C and mean annual precipitation decrease of about 180 mm/yr (Vincens et al., 1993). The LGM was a period of increased aridity and cooler conditions in the Kalahari region (Partridge et al., 1999; Lancaster, 1989; Thomas and Shaw, 2002), with a minimum of 60% less rainfall than present. Pollen and microfossil data from a marine core off southwest Africa suggest the temperatures were 4-6ºC lower than today and that the winter rainfall regime shifted northwards at this time (Shi et al., 2000).

However, during the LGM, summer insolation, which is under the control of orbital precession (Berger, 1978), was at a maximum in the southern tropics, and might normally have been expected to strengthen the summer African monsoon (Kutzbach and Liu., 1997), resulting in higher rainfall inland. Recent studies from Lake Masoko have suggested water levels in this crater basin were higher, reflecting a moister climate locally at this time (Garcin et al., 2006b). In addition, work conducted at Lake Ngami, situated in NW Botswana has suggested that this basin, which receives inflow from Angola, was at a highstand during the LGM (Huntsman-Mapila et al., 2006). Reconstructions of the equatorial river discharge, on the other hand, indicate significantly lower discharge and dry conditions in the Congo basin during the LGM (Adegbie et al., 2003; Schefuss et al., 2005).

II. 2 Deglacial period

In equatorial Africa, significantly wetter conditions followed the LGM which led to a rise in water levels in many of the lakes. This is thought to have been triggered by insolation changes which reached 4.2% higher than modern values (Berger and Loutre, 1991). Most equatorial lakes rose substantially at ca. 15 ka although in some lakes an earlier humid phase is apparent. The rapid refilling of Lake Victoria commenced at ca. 15 ka BP (Talbot and Laerdal, 2000) and flow from Lake Victoria via Lake Albert into the Nile was re-established no later than 14.5 ka (Williams et al., 2006). Talbot et al., 2006 report major changes in organic matter (OM) composition in Mpulungu cores (Lake Tanganyika) during and following the period of lake level change. Diatom records from Lake Rukwa indicate that deep water conditions were reached by 13.5 ka BP (Barker et al., 2002). In Lake Malawi, a reported warming trend is also reported for this period (Powers et al., 2005). Geomorphological and pollen studies, as well as stable isotope analysis of stalagmites in southern Africa suggest a rapid increase starting between 18 ka and 17.5 ka BP (Thomas and Shaw, 2002; Dupont and Behling, 2006). Sea surface temperatures of the northern Benguela System off the coast of southwestern Africa began to increase about 17 ka BP (Shi et al., 2000; Dupont et al., 2004) which corresponded with changes in the vegetation cover, reflecting a higher rainfall/ moisture adapted vegetation, in southern Africa detected from pollen records (Scott and Thackeray 1987).

II.3 The Younger Dryas Event

During the Younger Dryas (YD), event, dry climatic conditions with increased northerly trade winds prevailed over much of Africa. This resulted in the failure of the African monsoon which in turn led to lower lake levels in a number of East African lakes at ca. 12.5 – 11.5 ka cal BP (Street-Perrott and Perrott, 1990: deMenocal et al., 2000; Gasse, 2000; Peck et al., 2004). The failure of the African monsoon during the Younger Dryas, was then followed by a return to more humid climatic conditions leading into the generally more humid Holocene period (Barker et al., 2004; Johnson et al., 2004; Schefuss et al., 2005). During the YD (13.8 ka BP) temperatures in Lake Malawi dropped by 2ºC (Powers et al., 2005). The YD event is recorded in other climate records, for example, the mollusc stable isotope data for the Atlantic Ocean (Cohen et al. 1992), the Wonderkrater pollen record from South Africa (Scott and Thackeray 1987; Thackeray 1988), and minimum SSTs from an Atlantic Ocean core (12.4-11.8 ka BP) (Dupont et al., 2004). Following the Younger Dryas event, temperatures rose over much of the subcontinent.

II.4 The Early Holocene

Diatom records from Lake Rukwa show that between 11.8 and 6.7 ka cal BP the lake was deep and fresh (Barker et al., 2002) and may have overflowed into Lake Tanganyika (Haberyan, 1987). Based on sedimentologic and geochemical analyses of cores from Lake Edward, Russell et al. (2003) propose a well-mixed, deep waterbody between 11 and approximately 9 ka BP. From 12.1 to 5.5 ka cal BP more humid conditions in Lake Rukwa are confirmed from the pollen record (Vincens et al., 2005).

In southern Africa, arid conditions are thought to have predominated in the early Holocene (Shaw, 1986). These conditions contrast with the more humid conditions prevalent at this time in the sub-tropical region. The inverse relationship between the humid intertropical and the more arid subtropical southern climate during the early Holocene may have been a response to precessional forcing which led to a northward migration of the ITCZ and a general reduction in precipitation in southern Africa region (Shi et al., 2000). The arid conditions, including the SW Kalahari dune system (Lancaster, 1989), prevailed in the early Holocene and generally persisted in southern Africa till about 6.8 ka BP, when, according to Shaw, 1986, the region experienced a return to more humid conditions. The vegetation cover in southern Africa began to reflect more high rainfall/moisture adapted vegetation by 7 ka BP (Scott and Thackeray, 1987).

II.5 The Late Holocene

Barker et al. (2002) report saline conditions from the diatom record of Lake Rukwa after 5.5 ka cal BP and Russell et al. (2003) report the onset of drier conditions in Lake Edward from about 5.2 ka BP based on the occurrence of authigenic calcite. From 5.5 ka cal BP drier conditions are also indicated from the pollen record of Lake Rukwa, which intensify ca. 3.5 ka cal BP towards modern conditions (Barker et al., 2002).An abrupt rise in biogenic silica mass accumulation rates at 4.5 ka BP in northern Lake Malawi is attributed either to stronger northerly winds or a shift to wetter conditions (Johnson et al., 2004). Data from northwest Botswana (Nash et al., 1997) from palaeo-lake levels indicates more humidity in the northern and central Kalahari at this time. Lake levels at Lake Ngami increased at 4 ka BP. This apparent increase in humidity in northern and central Kalahari at 4 ka BP may be more a reflection of increased rainfall in the Angolan catchment as opposed to localized rainfall (Huntsman-Mapila et al., 2006).

References

Adegbie, A.T., Schneider, R.R., Röhl, U., Wefer, G., 2003. Glacial millennial-scale fluctuations in central African precipitation recorded in terrigenous sediment supply and freshwater signals offshore Cameroon. Palaeogeography, Palaeoclimatology Palaeoecology 197, 323-333.

Aucour, A., Hillaire-Marcel, C., Bonnefille, R., 1993. A 30, 000 yr record of $d^{13}C$ and $d^{18}O$ changes in organic matter from an equatorial peatbog. *Climate change in continental isotopic records. Geophys. Monogr. American Geophysical Union* 78, 343 - 351.

Aucour, A., Hillaire-Marcel, C. and Bonnefille, R., 1994. Late Quaternary biomass changes from ^{13}C measurements in highland peatbog from equatorial Africa (Burundi). *Quart. Res.* 41, 225-233.

Barker, P., Telford, R., Gasse, F., Thevenon, F., 2002. Late Pleistocene and Holocene palaeohydrology of lake Rukwa, Tanzania, inferred from diatom analysis. Palaeogeography, Palaeoclimatology, Palaeoecology 187, 295-305.

Barker, P., Gasse, F., 2003. New evidence for a reduced water balance in East Africa during the Last Glacial Maximum; implication for model-data comparison. Quaternary Science Reviews 22, 823-837.

Barker, P., Talbot, M.R., Street-Perrot, A., Marret, F., Scourse, J., Odada, E., 2004. Late Quaternary climatic variability in intertropical Africa. *In* "Past Climate Variability Through Europe and Africa." (R. W. Batterbee, Gasse, F., Stickley, C.E., Ed.), pp. 118-138. Developments in Palaeoenvironmental Research. Springer, Dordrecht.

Berger, A., 1978. Long-term variations of caloric insolation resulting from the earth's orbital elements. Quaternary Research 9, 139-167.

Beuning, K.R.M., Talbot, M.R., Kelts, K., 1997. A revised 30,000-year paleoclimatic and paleohydrologic history of Lake Albert, East Africa. Palaeogeography, Palaeoclimatolgy, Palaeoecology 136, 259-279.

Cohen, A. L., Parkington, J.E., Brundritt, G.B., Merwe, N.J. van der., 1992. A Holocene marine climate record in mollusk shells from the southwest African coast. *Journal of Quaternary Research* 38, 379-385.

deMenocal, P., Ortiz, J., Guilderson, T., Adkins, J., Sarnthein, M., Baker, K., Yarusinsky, M., 2000. Abrupt onset and termination of the African Humid Period: rapid climate responses to gradual insolation forcing. *Quaternary Science Reviews* 19, 347-361.

Dupont, L., Behling, H., 2006. Land-sea linkages during deglaciation: High-resolution records from the eastern Atlantic off the coast of Namibia and Angola (ODP site 1078). *Quaternary International* 148, 19-28.

Dupont, L. M., Kim, J-H, Schneider, R.R., Shi, N., 2004. Southwest African climate independent of Atlantic sea surface temperatures during the Younger Dryas. *Quaternary Research* 61, 318-324.

Haberyan, K.A., Hecky, R.E., 1987. The late Pleistocene and Holocene stratigraphy and paleolimnology of lakes Kivu and Tanganyika. Palaeogeography, Palaeoclimatology, Palaeoecology 61, 169-197.

Garcin, Y., Williamson, D., Taieb, M., Vincens, A., Mathe, P., Majule, A., 2006b. Centennial to millennial changes in lake deposition during the last 45,000 years in Tropical Southern Africa (Lake Masoko, Tanzania). Palaeogeography, Palaeoclimatology, Palaeoecology 239 (3-4), 334-354.

Gasse, F., Lédée, V., Massault, M., Fontes, J.Ch., 1989. Water-level fluctuations of Lake Tanganyika in phase with oceanic changes during the last glaciation and deglaciation. Nature 342, 57-69.

Gasse , F., Barker, P., Johnson,T.C., 2002. A 24,000 yr diatom record from the northern basin of Lake Malawi. In: Odada E.O., and Olago, D.O. (eds), The East African Great lakes: Limnology, Palaeolimnology and Biodiversity. Dordrecht, Kluwer, pp. 393-414.

Gasse, F., 2000. Hydrological changes in the African tropics since the Last Glacial maximum. *Quaternary Science Reviews* 19, 189 - 211.

Heine, K., 1982. The main stages of late Quaternary evolution of the Kalahari region, southern Africa. *Palaeoecology of Africa* 15, 53-76.

Huntsman-Mapila, P., Ringrose, S., Mackay, A.W., Downey, W.S., Modisi, M., Coetzee, S.H, Tiercelin, J-J., Kampunzu, A.B., Vanderpost C., 2006. Use of the geochemical and biological sedimentary record in establishing palaeo-environments and climate change in the Lake Ngami basin, NW Botswana. *Quaternary International* 148, 51-64.

Johnson, T. C., Brown, E.T., McManus, J., 2004. Diatom productivity in Northern Lake Malawi during the past 25,000 years: implictions for the position of the intertropical convergence zone at millennial and shorter time scales. *In* "Past Climate Variability Through Europe and Africa." (R. W. Batterbee, Gasse, F., Stickley, C.E., Ed.), pp. 93-116. Developments in Palaeoenvironmental Research. Springer, Drodrecht.

Kirst, G. J., Schneider, R.R., Muller, P.J., Storch, I. von, Wefer, G., 1999. Late Quaternary temperature variability in the Benguela Current system derived from alkenones. *Quaternary Research* 52, 92-103.

Kutzbach, J.E. , Liu, Z., 1997. Response of the African monsoon to orbital forcing and ocean feedbacks in the middle Holocene. Science 278: 440-443.

Lancaster, N. (1989). Late Quaternary palaeoenvironments of the southwestern Kalahari. *Palaeogeography, Palaeoclimatology, Palaeoecology* 70, 367-376.

Metcalfe, S.E., 1999. Diatoms from the Pretoria Salt Pan- a record of lake evolution and environmental change. In: Partridge, T.C. (ed.), Investigations into the origin, age and palaeoenvrionments of the Pretoria Saltpan. Geological Survey of South Africa. pp. 192-192.

Nash, D. J., Meadows, M.E., Shaw, P.A., Baxter, A.J., Gieske, A., 1997. Geomorphological and chronostratigraphic evidence for late Holocene environmental change in the Ncamasere Valley, Okavango Delta, Botswana: preliminary results. *South African Geographical Journal* Special edition, 93-100.

Olago, D. O., 2001. Vegetation changes over palaeo - time scales in Africa. *Climate Research* 17, 105 -121.

Partridge, T. C., deMenocal, P.B., Lorentz, S.A., Paiker, M.J., Vogel, J.C., 1997. Orbital forcing of climate over South Africa: a 200,000 year rainfall record from the Pretoria Saltpan. *Quaternary Science Reviews* 16, 1125-1133.

Partridge, T. C., Scott, L., Hamilton, J.E., 1999. Synthetic reconstructions of southern African environments during the Last Glacial Maximum (21-28 kyr) and the Holocene Altithermal, (8-6 kyr). *Quaternary International* 57/58, 207-214.

Peck, J.A., Green, R.R., Shanahan, T., King, J.W., Overpeck, J.T., Scholz, C.A., 2004. A magnetic mineral record of Late Quaternary tropical climate variability from Lake Bosumtwi, Ghana. Palaeogeography, Palaeoclimatology, Palaeoecology 215, 37-57.

Powers, L. A., Johnson, T.C., Werne, J.P., Castaneda, S., Hopmans, E.C., Sinninghe Damste, J.S., Schouten, S. (2005). Large temperature variability in the southern African tropics since the Last Glacial Maximum. *Geophysical Research Letters* 32, L08706, doi:10.1029/2004GL022014.

Prell, W. L., 1984. Monsoonal climate of the Arabian sea during the late Quarternary: a response o changing solar radiation. *In* "Milankovitch and climate, Part 1. NATO ASI Series C: Mathematical and Physical sciences Vol. 126 D." (A. Berger, Imbrie, J., Hays, J. Kukla, G., Saltzman, B., Ed.), pp. 349 - 366. Reidel Publishers, Dordrecht.

Ringrose, S., Kampunzu, A.B., Vink, B., Matheson, W., Downey, W.S., 2002. Origin and palaeo-environments of calcareous sediments in the Moshaweng dry valley, southeast Botswana. *Earth Surface Processes and Landforms* 27, 591-611.

Ringrose, S., Huntsman-Mapila, P., Kampunzu, H.,Downey, W.D. Coetzee S., Vink, B., Matheson W, Vanderpost, C., 2005. Geomorphological and geochemical evidence for palaeo-environmental change in the Makgadikgadi sub-basin, in relation to the MOZ rift depression, Botswana. *Palaeogeography, Palaeoclimatology and Palaeoecology* 217, 265-287.

Scholz, C.A., King, J.W., Ellis, G.S., Swart, P.K., Stager, J.C., Colman, S.M., 2003. Paleolimnology of Lake Tanganyika, East Africa over the past 100 k yr. Jounral of Paleolimnology 30, 139-150.

Schefuss, E., Schouten, S., Schneider, R.R., 2005. Climatic controls on central African hydrology during the past 20, 000 years. Nature 437, 1003-1006.

Shaw, R. P., 1986. The palaeohydrology of the Okavango delta-some preliminary results. *Palaeocology Africa* 17, 51 - 58.

Shi N., D., L.M., Beug, H., Schneider, R., 2000. Correlation between vegetation in Southwestern Africa and oceanic upwelling in the past 21, 000 years. *Quartenary Research* 54, 72 - 80.

Scott, L., Thakeray, J.F., 1987. Multivariate analysis of late Pleisocene and Holocene pollen spectra from Wonderkrater, Transvaal, South Africa. *South African Journal of Science* 83, 93-98.

Scott, L., Anderson, H.M., Anderson, J.M., 1997. Vegetation history. *In* "Vegetation of souhern Africa." (R. M. Cowling, Richardson, D.M., Pierce, S.M., Ed.), pp. 62 - 84. Cambridge University Press, Cambridge.

Street-Perrott, F. A., Perrott, R.A..,1990. Abrupt climatic fluctuations in the tropics - the influence of Atlantic Ocean circulation. *Nature* 343, 607 - 612.

Street-Perrott, F. A., Perrott, R.A. 1993. Holocene vegetation, lake levels and climate of Africa. *In* "Global Climates since the Last Glacial Maximum." (H. E. Wright, Kutzbatch, J.E., Webb III, T., Ruddiman, W.F., Street-Perrott, F.A., Bartlein, P.J., Ed.), pp. 318 - 356. University of Minnesota Press, Minneapolis.

Talbot, M.R., Jensen, N.B., Laerdal, T., Filippi, M.L., 2006. Geochemical responses to a major transgression in giant African lakes. Journal of Paleolimnology. 35 (3), 467-489.

Talbot, M.R., Laerdal, T., 2000. The Late Pleistocene-Holocene palaeolimnology of Lake Victoria, East Africa, based upon elemental and isotopic analyses of sedimentary organic matter. Journal of Paleolimnology 23, 141-164.

Taylor, D. M., 1990. Late Quaternary pollen records from two Ugandan mires: evidence for environmental change in the Rukiga Highlands of southwest Uganda. *Palaeogeograhy, Palaeoclimatology Palaeocology* 80, 283 - 300.

Thackeray, J. F., 1988. Quantification of climatic change during the late Quaternary in southern Africa. *Palaeocology of Africa* 19, 317 - 326.

Thomas, D. S. G., Shaw, P.A., 2002. Late Quaternary environmental change in central southern Africa: new data, synthesis, issues and prospects. *Quaternary Science Reviews* 21, 783-797.

Tiercelin, J-J, Mondeguer, A., 1991. The geology of the Tanganyika Trough. In: Coulter G.W. (ed), Lake Tanganyika and its life. Oxford University Press, Oxford, pp. 7-48.

Trauth, M. H., Deino, A.L., Strecker, M.R., 2001. Response of the East African climate to orbital forcing during the last interglacial (130-117 ka) and the early last glacial (117-60 ka). *Geology* 29, 499-502.

Tyson, P. D., Preston-Whyte, R.A., 2000. "The Weather and Climate of Southern Africa." Oxford University Press, Cape Town.

Tyson, P. D., Fuchs, R., Fu, C., Lebel, L., Mitra, A.P., Odada, E., Perry, J., Steffen, W., Virji, H. 2002. Global-Regional Linkages in the Earth System. *In* "Global Change - The IGBP Series." pp. 198. Springer, Berlin.

Vincens, A., Chalié, F., Bonnefille, R., Guiot, Tiercelin, J-J., 1993. Pollen-derived rainfall and temperature estimates from lake Tanganyika and their implications for late Pleistocene water levels. Quaternary Research 40, 343-350.

Vincens, A., Buchet, G., Williamson, D., Taieb, M., 2005. A 23,000 yr pollen record from Lake Rukwa (8°S, SW Tanzania): New data on vegetation dynamics and climate in Central Eastern Africa. Review of Palaeobotany and Palynology 137, 147-162.

III. SUMMARY OF GEOCHEMICAL ANALYTICAL PROCEDURES

This chapter presents an overview of the geochemical analytical procedures followed in this thesis and in addition gives an explanation of why certain elements were selected to be used as indicators of either climatic and tectonic change or both.

Major elements are the elements which predominate in any rock analysis. They include Si, Ti, Al, Fe, Mn, Mg, Ca, Na, K and P and their concentrations are expressed as a weight per cent (wt. %) of the oxide. Major elements for this work were measured by inductively coupled plasma-atomic emission spectrometry (ICP-AES) after employing standard silicate dissolution methods with HF (see Chapter V and VIII for more details). ICP-AES uses a plasma which is an electrical conducting gaseous mixture containing a significant concentration of cations and electrons, capable of reaching a temperature in the range of 6000 – 10 000 K. The sample solution is passed as an aerosol from a nebulizer into an argon plasma where the sample dissociates and a large number of atomic and ionic spectral lines are excited. The spectral lines are detected by a range of photomultipliers, compared with calibration lines, and their intensities are converted into concentrations (Rollinson, 1993).

In this work, major elements were used to determine the degree of chemical weathering using for example the chemical index of alteration (CIA) of Nesbitt and Young (1982) and also the CaO + Na2O-Al2O3-K2O triangular plots of Nesbitt and Young (1984, 1989). Since feldspar makes up in excess of 50% of the upper crust (with quartz comprising an additional 20%), the CIA effectively measures the degree of alteration of feldspars to clay minerals during weathering. Major elements are also used, in particular the ratios of SiO_2/Al_2O_3 to reflect the relative abundance of quartz and the clay and feldspar content (Potter, 1978) while the Na_2O/K_2O ratio reflects the feldspar content (Pettijohn et al., 1972), as indicators of the degree of chemical maturity of the sediments. Major element composition of sediments was used in determining the tectonic settings of the depositional basins. Useful discriminating parameters of tectonic setting for major elements include Fe_2O_3 + MgO%, TiO_2% and the Al_2O_3/SiO_2, K_2O/Na_2O and $Al_2O_3/(CaO+Na_2O)$ ratios. The $Al_2O_3/(CaO+Na_2O)$ is a ratio of the relatively immobile to the more mobile elements. In general, as the tectonic setting changes from oceanic island arc to continental island arc to active continental margins to the passive margin type, there is a detectable decrease in Fe_2O_3+MgO, TiO_2, Al_2O_3/SiO_2 and an increase in K_2O/Na_2O and

$Al_2O_3/(CaO+Na_2O)$ (Bhatia, 1983; Roser and Korsch, 1986; 1988). Passive margin sandstones are generally enriched in SiO_2 and depleted in Na_2O, CaO and TiO_2. They also usually exhibit a large variation in their K_2O/Na_2O and $Al_2O_3/(CaO+Na_2O)$ compositions and have a low Fe_2O_3+MgO content. This is a reflection of the recycled nature of passive margin sediments with an enrichment of quartz and depletion of chemically unstable grains, for example, feldspars (Bhatia, 1983; Roser and Korsch, 1986; 1988). Relative tectonic stability which results in enhanced weathering leads to the maturity of the sediments of this setting (Bhatia, 1983)

Trace elements are defined as those which are present in a sample in concentrations of less than 0.1 wt. % or less than 1000 ppm. Trace element measurements were conducted using inductively coupled plasma-mass spectrometry (ICP-MS) after silicate dissolution of the sediment samples (see Chapter V and VIII for more details). ICP-MS is widely used as a tool for trace element analysis due to its very low detection limits and good accuracy and precision (Rollinson, 1993). Mass spectrometry is based on the separation of ions on the basis of their mass-to-charge ratio. With ICP-MS, ions are extracted from the plasma into a vacuum system and focused with an ion lens into a mass spectrometer. In the mass spectrometer, an ion beam is fired along a curved tube with an electromagnet which separates the atoms according to their mass. A mass spectrum is produced in which the lighter ions are deflected with a smaller radius of curvature than the heavier ions (Rollinson, 1993).

Trace element concentrations in sediments result from a number of factors including provenance, weathering, diagenesis, sediment sorting and the aqueous geochemistry of the particular element hence may be used to infer past climatic conditions. Generally the highest concentrations of trace elements are found in clay-rich sediments. The trace elements used to identify sedimentary provenance have included the REE, Th and Sc. This is due to the fact that these are relatively insoluble in water are transferred almost quantitatively into terrigenous clastic material. Cullers et al., 1988 showed that the immobile elements La and Th are more abundant in felsic than in basic rocks, but that the opposite is true for Sc and Co. Ratios such as La/Sc, Th/Sc, Th/Co and La/Co allow a distinction to be made between a felsic or mafic source.

Studies have indicated that high pH water show enrichments in heavy REEs (HREE) and the degree of enrichment appears to increase with increasing alkalinity (Moller and Bau, 1993; Johannesson et al., 1994). For the high pH alkaline waters, speciation modelling (Johannesson et al., 1994) indicates that REE dicarbonate complexes are the only important form of dissolved

REE. The HREE are more strongly complexed in alkaline solution leading to enrichment of the HREEs over light REEs (LREE) in the water. This implies that certain sediments should be the site of preferential accumulation of LREE. Normalization of Ce abundances to those of its neighbouring REE, measured in various biogenic and authigenic components has been used to deduce redox conditions of the water column at the time of REE uptake by these phases. Unlike the other REE, cerium can undergo oxidation from soluble Ce(III) to highly insoluble Ce (IV). Its fixation in particulate matter, including organics is thought to be responsible for distinctive depletion of Ce in well oxygenated seawater (Wright et al., 1987; Liu et al., 1988; Bellanca et al., 1997).

Other elements, such as the transition metals are more soluble and redox sensitive and therefore good indicators of wet and dry conditions in sedimentary basins. Metals that occur as minor and trace elements in clastic sediments may become concentrated by precipitation under appropriate redox conditions and thus have redox-proxy potential. These include Cu, Fe, Mo, U, Pb, Co, Zn, Ni, V and Cr (Sageman et al., 2003). The redox state of a depositional system regulates various organic and inorganic reactions which results in dissolved constituents being precipitated as preservable minerals. This allows for reconstructions of past redox states which have been used in this thesis for the climate change component of the work.

In most instances in this work, we look at the variations in the geochemical composition of sediments which are due to surface processes such as weathering or redox conditions. However trace elements vary in their behaviour in melts and this variation is largely due to the charge/size ratio of the elements. Trace elements whose preference is the mineral phase are described as compatible whereas elements whose preference is the melt are described as incompatible. In Chapter VIII we use the Nb/Ti ratio of the Lake Tanganyika sediments as an indicator of volcaniclastic sediments in the basin. Niobium is an incompatible element which becomes concentrated in magma but not in silicate minerals. Elevated Nb concentrations are found in the volcanic ash from eruptions and within weathered ash.

References

Bellanca, A., Masetti, D., Neri, R., 1997. Rare earth elements in limestone/marlstone couplets from the Albian-Cenomanian Cismon section (Venetian region, northern Italy): assessing REE sensitivity to environmental changes. Chemical Geology 141, 141-152.

Cullers, R.L., Barrett, T., Carlson, R., Robinson, B., 1987. Rare earth element and mineralogical changes in Holocene soil and stream sediment: a case study in the Wet Mountains, Colorado, USA. Chemical Geology 63, 275-297.

Johannesson, K.H., Lyons, W.B., Bird, D.A., 1994. Rare earth element concentration and speciation in alkaline lakes from the western USA. Geophysical Research Letters 21, 773-776.

Liu, Y.G., Miah, M.R.U., Schmitt, R.A., 1988. Cerium: a chemical tracer for paleo-oceanic redox conditions. Geochimica Cosmochimica Acta 52, 1361-1371.

Moller, P., Bau, M., 1993. Rare earth patterns with positive cerium anomaly in alkaline waters from Lake Van Turkey. Earth Planetary Science Letters 117, 671-676.

Nesbitt, H.W., Young, G.M., 1982. Early Proterozoic climates and plate motions inferred from major element chemistry of lutites. Nature 299, 715– 717.

Nesbitt, H.W., Young, G.M., 1984. Prediction of some weathering trends of plutonic and volcanic rocks based on thermodynamic and kinetic considerations. Geochim. Cosmochim. Acta 48, 1523– 1534.

Nesbitt, H.W., Young, G.M., 1989. Formation and diagenesis of weathering profiles. J. Geol. 97, 129– 147.

Pettijohn, F.J., Potter, P.E., Siever, R., 1972. Sand and sandstones. Springer-Verlag, New York.

Potter, P.E., 1978. Petrology and chemistry of modern big riber sands. J. Geol. 86, 423-449.

Rollinson, H., 1993. Using geochemical data: Evaluation, Presentation, Interpretation. Longman Scientific and Technical, New York, 352 pp.

Sageman, B.B., Murphy, A.E., Werne, J.P., Ver Straeten, C.A., Hollander, D.J., Lyons, T.W., 2003. A tale of shales: the relative role of production, decomposition, and dilution in the accumulation of organic-rich strata, Middle-Upper Devonian, Appalachian Basin. Chemical Geology 195, 229-273.

Wright, J., Schrader, H., Holser, W.T., 1987. Paleoredox variations in ancient oceans recorded by rare earth elements in fossil apatite. Geochimica Cosmochimica Acta 51, 631-644.

IV. CRYPTIC INDICATORS OF PROVENANCE FROM THE GEOCHEMISTRY OF THE OKAVANGO DELTA SEDIMENTS, BOTSWANA

IV.1. La géochimie des sédiments de l'Okavango comme indicateur de provenance

Résumé de l'article

Les sédiments siliceux du Delta de l'Okavango au nord-ouest du Boswana ont une composition modale d'arène quartzeuse et une histoire complexe qui inclut le transport fluvial et le dépôt dans un bassin de rift naissant. L'Okavango est situé dans le désert du Kalahari, qui alimente le système en sables éoliens remaniés. La composition géochimique des sédiments du Delta de l'Okavango a été déterminée pour contraindre l'altération à la source et la composition des roches de la source. Les concentrations et rapports d'éléments chimiques montrent une large gamme de compositions qui sont proches du PAAS. L'indice chimique d'altération et le diagramme A-CN-K montrent une évolution qui peut être interprétée en utilisant un modèle de mélange entre une fraction très altérée correspondant à la fraction sédimentaire transportée par la fleuve Okavango et une fraction moins altérée correspondant aux apports de sables éoliens. Les données géologiques de terrain, appuyées par les rapports géochimiques tels que Th/Cr, Th/Sc, La/Sc, La/Co et Eu/Eu* indiquent une source a affinité mafique-ultramafique et felsique avec ou sans les termes intermédiaires. Les relations entre certains éléments (Cr-Ni, Na_2O-Al_2O_3, K_2O-Al_2O_3) améliorent l'interprétation en montrant l'existence d'au moins trois types de roches sources, comprenant des roches felsiques, riches en pyroxène et mafiques-ultramafiques riches en olivine. Les granitoïdes-gabbros Protérozoïques et les complexes volcaniques et ortho-métamorphiques qui sont exposés dans le NW du Botswana et les pays adjacents (Angola et Namibie) sont proportiennelement les sources des sédiments, à laquelle s'ajoute une contribution des sables éoliens et une proportion de carbonates diagénétiques. Tous ces differents termes ont contribué à l'édification du bassin sédimentaire de l'Okavango.

IV.2. Cryptic indicators of provenance from the geochemistry of the Okavango Delta sediments, Botswana

P. Huntsman-Mapila[a,b*], A.B. Kampunzu[c], B. Vink[c], S. Ringrose[a]

a Harry Oppenheimer Okavango Research Centre, University of Botswana, P/Bag 285, Maun, Botswana
b UBO-CNRS UMR 6538, Institut Universitaire Européen de la Mer, 29280 Plouzané, France
c Geology Department, University of Botswana, P/Bag 0022, Gaborone, Botswana
** Corresponding author email: pmapila@orc.ub.bw*

Article published by Sedimentary Geology 174 (2005) 123-148

Abstract

The siliciclastic sediments of the Okavango inland Delta of northwest Botswana have a modal composition of quartz arenites and result from a complex history, including transport by river and deposition in a nascent rift basin located in a desert environment with input of aeolian sands. The geochemical composition of sediments from the Okavango Delta was determined in order to constrain the role of weathering at the source and the composition of the source rocks. The chemical analyses and the interelement ratios show a broad compositional range usually encompassing the PAAS composition. The chemical index of alteration (CIA) values and the A–CN–K diagram define an evolution trend which can be interpreted using a mixing model involving a strongly weathered component which corresponds to the sedimentary fraction transported by the Okavango River and a relatively immature component which corresponds to the aeolian sand component of the Okavango sediments. Field geological data supported by geochemical ratios involving elements with affinity for mafic–ultramafic and felsic rocks such as Th/Cr, Th/Sc, La/Sc, La/Co and Eu/Eu* support a source area including mafic–ultramafic and felsic rocks, with or without intermediate rocks. The relationships between certain elements (Cr–Ni, Na_2O–Al_2O_3, K_2O–Al_2O_3) refine the interpretation by pointing to the existence of at least three source rock end-members, including a felsic rock source and pyroxene-rich and olivine-rich mafic–ultramafic source rocks. Proterozoic granitoid–gabbro and related volcanic and ortho-metamorphic rock complexes exposed in NW Botswana and adjacent Angola and Namibia are the source rocks of the sediment component which was mixed with aeolian sand and interacted with a variable proportion of diagenetic carbonates to produce the Okavango sediments.

IV.2.1. Introduction

The geochemical composition of siliciclastic sedimentary rocks is a sensitive indicator of provenance and weathering at the source of sediments (Taylor and McLennan, 1985; Roser and Korsch, 1988; Hassan et al., 1999; Cullers, 2000). Concentrations of major,trace and rare earth elements (REE) of sediments are well suited to constrain provenance and source rock composition. The REE are transferred with minimal fractionation from the source material into sediments (Taylor and McLennan, 1985). The negative Eu anomaly commonly recorded in felsic igneous rocks is usually detected in clastic sedimentary rocks originating from a source made of felsic rocks (Gao and Wedepohl, 1995). Elemental ratios, e.g., La/Sc, La/Co, are usually good discriminators between mafic and felsic source rocks because La, Th and Zr are more concentrated in felsic igneous rocks whereas Co, Sc and Cr have higher concentrations in mafic rocks (e.g., Wronkiewicz and Condie, 1987). The Okavango siliciclastic sediments, which are the focus of this study, are particularly important because they occur in a large alluvial fan with a wetland which is the largest Ramsar site on earth. The sediments result from a complex history including erosion from a relatively wet hinterland in Angola, transport by river and deposition in a basin located in a semiarid environment and direct input of aeolian sands from reworked dunes in the Kalahari desert. In this paper, the term aeolian sand refers to both direct input of fresh aeolian sand and reworked aeolian sand transported into the basin by the Okavango River. The objectives of this paper are (1) to present new chemical analyses of Quaternary siliciclastic sediments from the Okavango inland Delta; (2) to constrain the role of weathering at the source of the Okavango sediments and the composition of the source rocks for the Okavango Delta sediments excluding the aeolian sand input.

IV.2.2. Geological setting

The Okavango Delta overlies Precambrian igneous –metamorphic rocks that include the following main units (Figure IV-1): (1) Paleoproterozoic ~2.05 Ga augen gneiss, granites and amphibolites exposed in the Qangwa area (Kampunzu and Mapeo, unpublished data) and 2.03 Ga granulites exposed in the Gweta area (Mapeo and Armstrong, 2001); (2) Mesoproterozoic 1.2–1.0 Ga gabbros, granites, metarhyolites and metabasalts (Kampunzu et al., 1998a, 1999); (3) Neoproterozoic siliciclastic and carbonate sedimentary rocks forming a blanket above older

Proterozoic rocks (Kampunzu et al., 2000; Mapeo et al., 2000); (4) Karoo Supergroup (not shown in Figure IV-1), including mainly siliciclastic sedimentary rocks deposited during the Permo-Carboniferous and mafic lavas and dolerites emplaced between ca. 181–179 Ma (Carney et al., 1994; Le Gall et al., 2002). The Okavango Basin is a Quaternary half-graben (McCarthy et al., 1993; Modisi, 2000; Modisi et al., 2000) which represents the southwestern extension of the East African rift system (Kampunzu et al., 1998b). It is located within the Kalahari Basin, which is a shallow intracontinental basin. Aeromagnetic and seismic refraction studies suggest that the maximum thickness of sediment, in excess of 300 m, occurs in northern Namibia and in the Okavango graben in Botswana (Reeves, 1978; Modisi et al., 2000). Mineralogical studies of Kalahari sands suggest that it represents an accumulation of in situ weathering products of pre-Kalahari lithologies, in addition to material transported into the basin. (Thomas and Shaw, 1991). The major part of the catchment area comprises loosely consolidated, chiefly aeolian sand of the presently active Kalahari Basin. The Okavango Delta sediments studied in this paper represent the youngest (Quaternary) stratigraphic unit of the Kalahari sedimentary basin. Potential source rocks of the Okavango Delta sediments are mainly Proterozoic granitoids, gabbros and related volcanic and orthometamorphic rocks exposed in the catchment area in Angola, northern Namibia and northern Botswana.

IV.2.3. Local setting

The Okavango River enters the Makgadikgadi–Okavango–Zambezi (MOZ) rift depression (Ringrose et al., 2005) through a narrow NW–SE-trending swamp called the Panhandle (Figure IV-2) before extending into a large (>12,000 km^2) inland alluvial fan (McCarthy et al., 2000). The Okavango Delta represents the terminus of a fluvial system which drains from the central highlands of Angola where annual inflow is estimated at $1.01x10^{10}$ m^3 measured at the apex of the Panhandle (McCarthy et al., 2000). The present fan can be divided into distinct geo- morphic regions: (1) the Panhandle where the Okavango River is confined; (2) the permanent swamps; (3) the seasonal floodplains and (4) occasional (or intermittent) floodplains of the distal reaches of the Delta. Sedimentological and geochemical evidence suggests that the wetlands of the MOZ basin have expanded and contracted over the past 400,000 years and may have been subject to extensive flooding approximately 120,000 years ago (Ringrose et al., 2005). The latest phase of contraction appears to have commenced ca. 7000 years BP (the Holocence Altithermal) and is continuing to the present day. The distal reaches of the Okavango Delta are presently a site of

significant subsurface chemical precipitation of calcite and silica (McCarthy and Metcalfe, 1990). The Okavango Delta sediments contain a high proportion of sand of aeolian origin, and the floodwater constitutes the major source of the fine sediments. Airborne dust could account for the presence of clays on islands, but because the content of clay rich fines in floodplain sediments is greater than on islands, floodwater is believed to be the major source (McCarthy and Ellery, 1995). Few clastic sediments are currently introduced onto the distal reaches of the fan because of the very low gradient, dense vegetation and low suspended load of the Okavango River (McCarthy et al., 1991). Throughout the Okavango system, the current chemical sedimentation volumetrically exceeds the amount of clastic sediment being brought into the fan (McCarthy and Metcalfe, 1990).

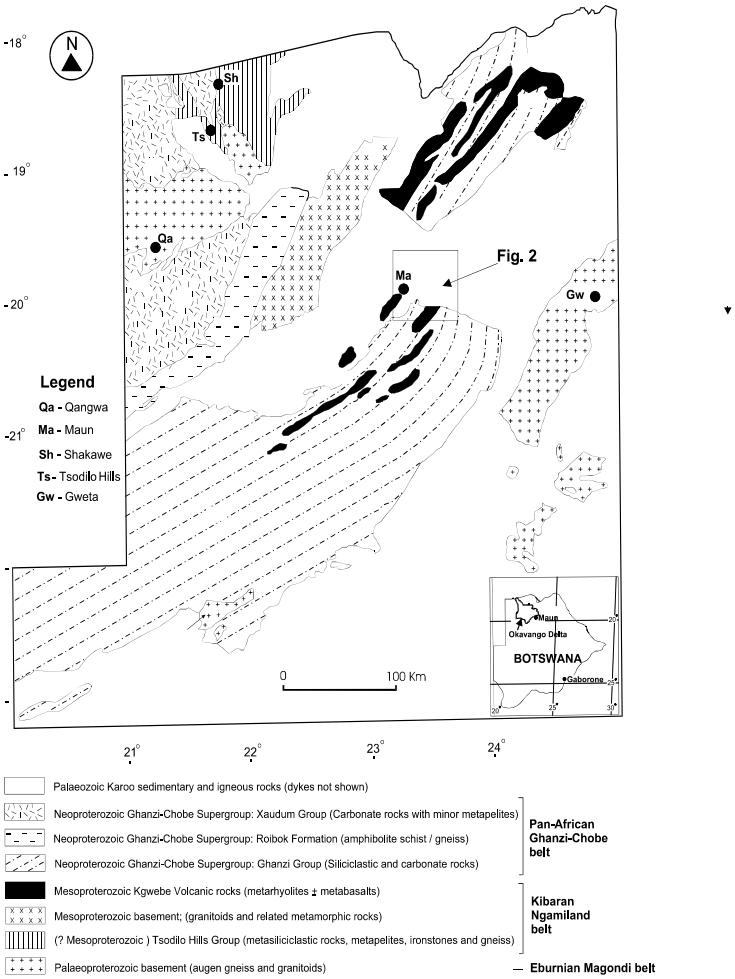

Figure IV. 1. Precambrian geology map of NW Botswana (Kampunzu et al., 2000). Box: location of Figure IV..2 in northwestern Botswana. Inset: location of the Okavango Delta in Botswana

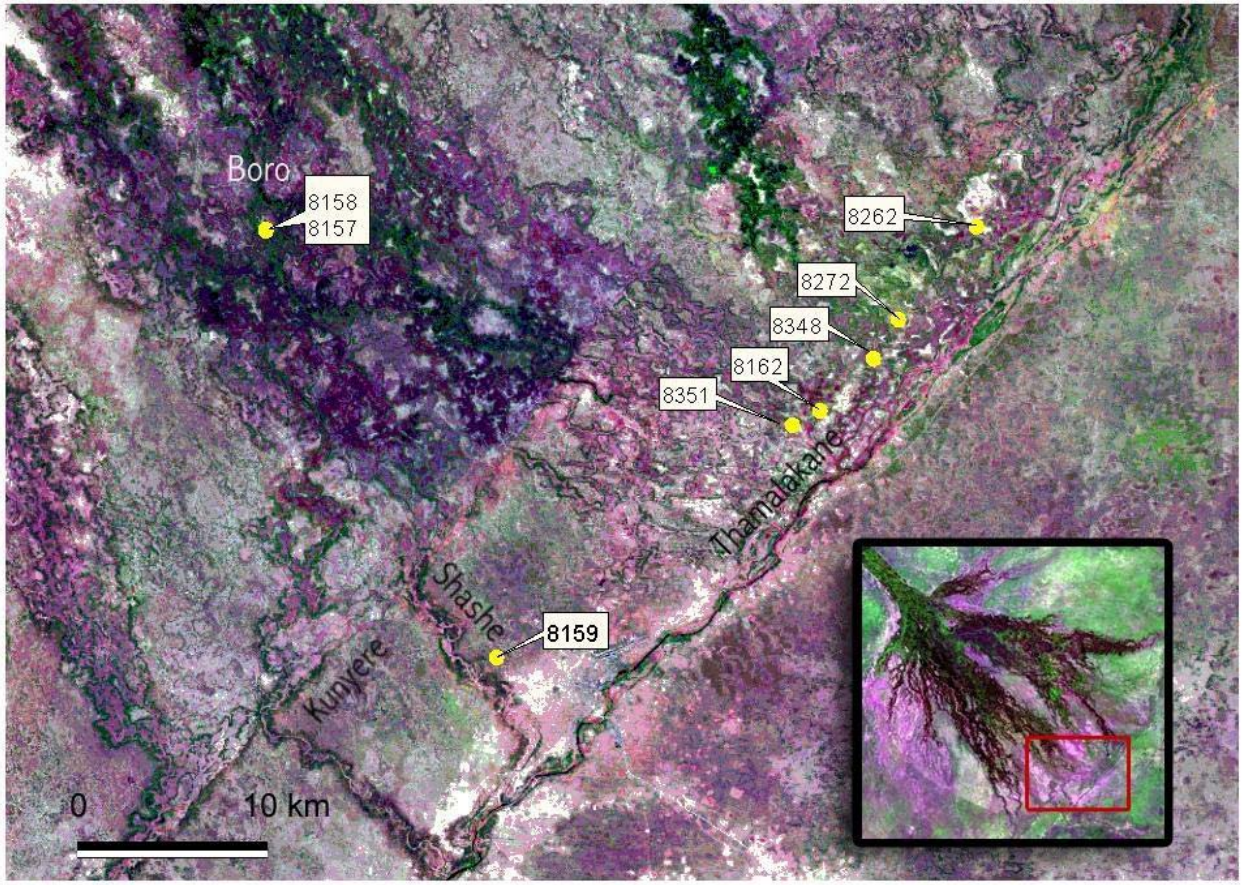

Figure IV 2. Satellite image of the Okavango region showing the location of sampled boreholes. Fault zones related to the Okavango rift are prominent on this image. Insert: Okavango Delta alluvial fan morphology (courtesy of SAFARI 2000). Red rectangle: position of the main image.

IV.2.4. Sampling and analytical procedures

Fifty-eight samples from boreholes sunk in the study area were selected for grain size (sieving) analysis performed as part of the Maun Groundwater Development Project (DWA (Department of Water Affairs), 1997). In addition, during the course of this study, grain size was determined on 42 samples taken from shallow (3 m) holes sunk in the study area (see data in Table IV-1). Thirteen representative samples were selected for microscope investigations conducted on a Zeiss Axioskop 40 microscope fitted with a Zeiss AxioCam MRc digital camera. Twelve representative samples were selected for X-ray diffraction analyses using a Philips PW 3710 X-ray Diffraction unit, operated at 45kV and 40 mA, employing Cu-Kα radiation and a graphite monochromator. The samples were scanned from 3o to 70o for 2θand their diffractograms were digitally recorded.

Table IV 1. Petrographic characteristics of the Okavango sediments

Grain size data

Location	Depth	No. of samples	Mean (phi)	Sorting
Shashe[1]	40-65m	32	1.66	0.56
Thamalakane[1]	12-38m	8	1.89	0.56
Thamalakane[1]	42-70m	9	1.94	0.66
Boro[1,2]	38-65m	3	2.18	0.57
Boro[1,2]	45-57m	6	2.07	0.77
Shallow depth holes[3]	0-3m	42	2.40	0.69
Shallow depth holes[4]	2-3m		2.20	well sorted

Microscopic and XRD data

Sample nr	Quartz	Calcite	Dolomite	Kaolinite	K-feldspar	Muscovite	Clay[5]
8157a	96	-	-	2	2		-
8157f	100	-	-	-	-		-
8159g	93	5	-	-	Trace	2	-
8159j	28	65	7	-	-		-
8159n[6]	44	10	43	-	3		-
8159o	30	23	45	-	2		-
8159t	82	5	13	-	-		-
8262c	100	-	-	-	-		-
8162e	90	-	-	3	4		3
8162o	98	-	-	-	-		2
8348d	100	-	-	-	-		-
8348j	95	-	-	3	2		-

1) DWA (1997)
2) Split spoon sample analysis
3) This study
4) McCarthy and Ellery, 1995
5) clay minerals other than kaolinite
6) possibly some heulandite

Ninety samples were collected from seven boreholes (Figure IV-2) drilled during the Maun Groundwater Development Project (DWA (Department of Water Affairs), 1997) for whole rock geochemical analyses. Two boreholes (BH8157 and BH8158) are located on the lower reaches of the Boro channel, a major tributary of the Delta that has active flow throughout most of the year. This channel abuts on the distal Kunyere and Thamalakane faults which are major normal faults bounding the Okavango half-graben to the southeast (Figure IV-2). The boreholes BH8351, BH8162, BH8262 and BH8348 are located along the Thamalakane River valley, and BH8159 is located in the Shashe valley, which has been dry since the early 1990s. Representative samples were obtained at 3-m intervals up to depths of between 69–147 m. The chemical analyses of sediments were performed at Chemex Laboratories in Canada. Major elements were determined using ICP-AES. Trace and rare earth elements were analysed using ICP-MS (detection limits generally between 0.1 and 0.5 ppm) with the exception of Li, Cr, Ni and Pb that were determined by flame AAS (detection limits 1 ppm). The analyses of standards run at the same time as the studied samples are shown in Table IV-2. The precisions are <1% and <10% for major and trace elements, respectively. Inorganic CO2 was determined using a Leco-Gasometric and Leco-IR detector with detection limits of 0.2%.

Table IV 2. Representative samples and sumary of the range of chemical compositions of the Okavango Delta sediments

Sample	8157A	8157F	8158A	8158F	8158H	8159A	8159E	8159G	8159I	8159J	8159M
Depth (m)	3	54	6	60	90	6	45	60	69	81	99
SiO_2 (wt.%)	89.97	96.11	83.17	97.79	96.43	98.18	68.72	68.07	68.17	58.39	48.45
TiO_2	0.23	0.10	0.29	0.07	0.09	0.02	0.23	0.14	0.23	0.27	0.23
Al_2O_3	4.99	1.77	5.47	0.65	1.31	0.34	3.90	1.96	3.11	4.52	4.57
Fe_2O_3	1.27	0.38	1.40	0.22	0.31	0.40	1.27	0.71	1.17	1.82	1.83
MnO	0.01	0.01	0.01	0.01	0.01	0.01	0.06	0.03	0.04	0.04	0.04
MgO	0.36	0.09	0.34	0.13	0.06	0.03	1.95	4.53	3.21	2.79	5.49
CaO	0.68	0.27	1.83	0.04	0.05	0.10	11.43	9.62	10.07	13.51	15.29
Na_2O	0.16	0.06	0.13	0.02	0.09	0.03	0.15	0.24	0.37	0.71	0.99
K_2O	0.49	0.21	0.50	0.13	0.22	0.10	0.59	0.72	1.08	1.68	2.46
P_2O_5	<0.01	<0.01	<0.01	0.01	<0.01	0.01	0.01	0.01	0.03	0.08	0.10
CO_2	<0.2	<0.2	<0.2	<0.2	<0.2	<0.2	6.4	9.8	7.6	10.2	14.8
LOI	-	1.47	5.86	0.75	1.11	0.76	11.19	14.09	13.04	16.94	20.73
Total	98.30	100.50	99.16	99.83	99.70	99.23	99.64	100.20	100.65	100.95	100.40
Cr (ppm)	60	11	29	6	9	4	71	1300	4	55	39
Ni	4.8	4.0	13.4	2.0	3.0	2.0	3.8	440	2.0	3.6	17
Co	40.0	46	25	45	54	64	21	21	16	15	14
Sc	30	<5	5	<5	<5	5	20	750	5	70	5
V	75	20	90	5	15	<5	45	30	45	60	85
Cu	10	5	10	5	5	5	10	5	5	15	15
Pb	6.5	3.0	8.5	1.5	2.5	1.0	44	236	1.0	3.0	5.5
Zn	20	5	15	5	20	25	25	5	20	25	25
Rb	26.4	9.4	27.4	11.4	8.4	3.0	24.8	23.4	32.0	47.8	53.6
Cs	1.3	0.4	1.5	29.0	0.3	-	0.8	0.9	0.9	1.4	1.5
Ba	261	94	270	52	107	38	316	1120	1110	653	759
Sr	35.6	14.2	50.4	4.5	9.7	6.0	213	559	397	357	824
Li	14	6	15	4	6	4	17	10	12	15	31
Ta	11	13	5	15	18	22	5	5	4	2	2
Nb	8	5	6	5	7	7	6	4	5	5	4
Hf	3	1	9	3	1	-	3	1	3	1	1
Zr	143	97	443	166	113	29	146	104	149	78	69
Y	9	5	15	3	4	2	10	7	10	11	9
Ga	6	2	7	1	<1	1	5	1	3	5	5
Th	3	1	5	<1	<1	<1	4	1	3	4	4
U	1.0	0.5	2.0	0.5	0.5	0.5	1.5	5.5	5.0	5.0	10.0
La	13.0	6.0	18.5	3.0	5.0	2.0	12.5	7.5	10.5	13.5	12.5
Ce	21.5	12.0	34.5	6.5	10.0	3.0	25.5	16.0	21.5	26.0	24.0
Pr	2.8	1.5	4.3	0.7	1.1	0.3	2.8	1.8	2.5	3.2	3.0
Nd	9.0	5.0	14.5	2.0	3.5	1.5	9.5	6.5	9.0	11.5	10.5
Sm	1.6	1.0	2.7	0.4	0.8	0.3	1.8	1.1	1.6	2.1	2.0
Eu	0.4	0.1	0.6	<0.1	0.1	0.1	0.4	0.3	0.5	0.5	0.4
Gd	1.9	0.8	3.0	0.5	0.6	0.1	1.7	1.1	1.7	2.0	1.7
Tb	0.2	0.1	0.4	0.1	0.1	0.1	0.3	0.1	0.3	0.3	0.3
Dy	1.5	0.6	2.2	0.3	0.4	0.1	1.6	0.9	1.5	1.5	1.5
Ho	0.3	0.1	0.4	0.1	0.1	0.1	0.3	0.1	0.3	0.4	0.3
Er	0.9	0.5	1.3	0.2	0.2	0.1	1.0	0.7	0.8	1.0	0.8
Tm	0.1	<0.1	0.1	<0.1	<0.1	<0.1	0.1	0.1	0.1	0.1	<0.1
Yb	0.8	0.5	1.4	0.3	0.4	0.1	1.0	0.7	1.0	0.8	0.6
Lu	<0.1	<0.1	<0.1	<0.1	<0.1	<0.1	<0.1	<0.1	<0.1	<0.1	<0.1

*All the samples are BH series boreholes shown in Fig. 2. The four digits in the sample numbers Correspond to the numbers of these BH boreholes.

1. UCC values from Taylor and McLennan (1995) except for TiO_2, Nb, Cs, Tb and Ta from Plank and Langmuir (1998)

2. PAAS composition from Taylor and McLennan (1985)

3. NASC composition from Gromet et al. (1984)

Table IV-2
continued

Sample Nr	8159N	8159O	8159T	8162D	8162E	8162J	8162K	8162L	81620	8262A	8262B
Depth (m)	102	114	147	15	24	45	51	54	63	3	12
SiO_2 (wt.%)	53.82	44.07	89.28	89.46	87.09	80.17	93.97	88.55	90.32	83.28	76.75
TiO_2	0.14	0.09	0.05	0.13	0.23	0.22	0.08	0.09	0.15	0.56	0.62
Al_2O_3	2.67	1.28	0.54	2.41	4.77	3.37	0.90	1.15	2.72	9.49	11.76
Fe_2O_3	1.33	0.78	0.49	1.01	2.03	1.34	0.39	0.49	1.39	1.73	2.21
MnO	0.04	0.03	0.01	0.01	0.01	0.02	0.01	0.02	0.01	0.03	0.02
MgO	6.65	7.54	1.52	0.32	0.37	1.36	0.81	1.50	0.63	0.39	0.45
CaO	14.60	19.63	3.53	0.10	0.54	4.97	1.20	3.29	0.18	0.39	0.39
Na_2O	0.48	0.26	0.14	0.06	0.10	0.31	0.08	0.10	0.09	0.18	0.17
K_2O	1.67	0.86	0.27	0.30	0.42	1.16	0.34	0.53	0.69	0.90	0.87
P_2O_5	0.05	0.04	<0.01	-	0.03	<0.01	-	0.01	0.01	0.01	0.01
CO_2	16.4	22.2	4.2	<0.2	0.2	3.6	1.0	3.8	0.8	0.8	0.4
LOI	19.21	23.69	4.54	-	4.34	7.27	2.49	4.80	2.69	-	-
Total	100.80	98.36	100.40	94.55	100.15	100.35	100.30	100.60	99.03	97.15	93.50
Cr (ppm)	27	22	10	45	28	26	12	80	18	52	74
Ni	27	11	9.0	<2.8	1.6	2.6	0.6	3.0	10.8	17	25
Co	16	10	42	16	25	27	31	41	26	22	21
Sc	<5	<5	<5	70	15	15	10	10	5	40	40
V	55	50	10	15	55	60	40	10	35	105	145
Cu	15	20	5	5	5	5	5	5	5	20	20
Pb	4.5	1.5	2.5	7.0	3.0	2.5	2.0	7.0	5.0	12	30
Zn	25	15	15	15	15	10	5	10	15	95	30
Rb	31.0	18.8	6.0	8.0	26.0	38.8	10.0	15.0	29.8	53.0	55.0
Cs	0.7	0.4	0.1	0.3	1.1	1.1	0.1	0.3	0.7	2.4	2.8
Ba	927	388	174	47	204	788	151	212	219	341	364
Sr	871	1910	215	7.0	35.2	199	101	251	16.6	44.8	50
Li	22	16	6	6	12	13	5	5	9	21	25
Ta	2	2	14	4	6	8	11	14	9	5	4
Nb	2	1	4	1	6	6	4	5	5	11	12
Hf	<1	<1	<1	-	1	3	3	1	5	6	7
Zr	44	37	54	32	83	136	145	109	223	272	281
Y	7	6	3	2	8	9	4	6	10	19	22
Ga	2	<1	1	1	5	2	1	1	2	11	15
Th	2	2	<1	1	4	3	1	1	2	8	10
U	9.0	12.0	1.5	0.5	1.5	2.0	1.0	1.5	0.5	2.0	4.0
La	8.5	6.5	3.5	3.5	11.0	11.5	6.5	5.5	9.0	25.0	28.5
Ce	16.5	13.0	6.0	6.0	19.5	20.0	9.0	11.0	18.5	61.0	54.5
Pr	2.0	1.4	0.8	0.8	2.6	2.6	1.3	1.3	2.0	5.9	6.7
Nd	7.0	5.0	3.0	3.0	8.5	9.0	4.0	4.5	8.0	20.5	22.5
Sm	1.2	1.0	0.7	0.5	1.5	1.9	0.7	0.7	1.8	3.9	4.7
Eu	0.4	0.2	0.1	0.1	0.4	0.4	0.1	0.1	0.4	0.9	1.0
Gd	1.6	0.9	0.5	0.7	1.6	1.7	0.6	0.9	1.7	3.9	4.1
Tb	0.1	0.1	0.1	0.1	0.2	0.3	0.1	0.1	0.2	0.6	0.6
Dy	1.2	0.9	0.4	0.3	1.2	1.3	0.4	0.9	1.4	2.9	3.6
Ho	0.2	0.1	0.1	0.1	0.2	0.2	0.1	0.1	0.3	0.6	0.7
Er	0.7	0.5	0.2	0.2	0.7	0.8	0.3	0.6	0.9	1.9	1.9
Tm	<0.1	<0.1	<0.1	<0.1	<0.1	0.1	0.1	0.1	0.1	0.3	0.3
Yb	0.8	0.4	0.2	0.1	0.8	0.9	0.3	0.5	0.8	1.7	2.3
Lu	<0.1	0.1	<0.1	<0.1	<0.1	<0.1	<0.1	<0.1	<0.1	0.3	0.3

TableIV- 2 continued

Sample Nr	8262C	8262D	8262F	8348A	8348B	8348C	8348D	8348E	8348F	8348G	8348H
Depth (m)	21	24	42	6	12	24	33	39	42	45	54
SiO_2 (wt.%)	93.15	98.32	92.13	97.42	97.51	98.54	99.04	98.25	91.81	93.73	81.90
TiO_2	0.15	0.09	0.14	0.05	0.08	0.04	0.07	0.06	0.16	0.14	0.34
Al_2O_3	2.70	0.95	2.47	0.57	0.88	0.40	0.65	0.57	2.73	2.53	6.91
Fe_2O_3	1.01	0.27	0.94	0.16	0.22	0.13	0.31	0.24	1.21	0.81	2.15
MnO	0.01	0.01	0.01	0.01	0.01	0.01	0.01	0.01	0.01	0.01	0.01
MgO	0.25	0.07	0.21	0.04	0.05	0.03	0.06	0.05	0.25	0.27	0.73
CaO	0.14	0.04	0.09	0.01	0.01	<0.01	0.06	0.03	0.41	0.11	0.28
Na_2O	0.05	0.05	0.12	0.02	0.04	0.05	0.07	0.05	0.11	0.11	0.38
K_2O	0.32	0.18	0.37	0.10	0.14	0.09	0.13	0.1	0.32	0.36	1.14
P_2O_5	-	-	<0.01	0.01	0.02	<0.01	-	0.01	0.01	0.01	0.03
CO_2	<0.2	<0.2	<0.2	<0.2	0.2	<0.2	<0.2	<0.2	0.2	0.6	<0.2
LOI	2.94	0.88	2.57	0.71	0.89	0.66	-	0.72	3.26	2.21	5.84
Total	97.78	100.90	99.14	99.10	99.87	99.95	100.45	99.37	100.3	100.35	99.95
Cr (ppm)	44	28	15	6	7	5	10	6	20	22	33
Ni	24	32	5.6	4.0	3.0	2.2	1.0	3.0	1.4	1.4	12.4
Co	23	131	33	110	101	98	251	108	71	49	46
Sc	55	40	5	5	5	5	10	5	10	15	5
V	40	10	35	10	15	5	10	5	35	20	130
Cu	5	5	5	<5	<5	<5	<5	<5	<5	5	35
Pb	12	28	4.5	3.0	2.5	1.5	1.0	1.5	3.0	3.5	11
Zn	5	5	10	5	5	15	5	5	15	75	70
Rb	21.0	7.0	19.0	4.0	5.8	3.2	5.0	4.0	17.4	15.6	93.4
Cs	0.6	0.2	0.5	-	0.1	<0.1	0.1	0.1	0.6	0.4	3.0
Ba	132	77	124	37	62	38	86	57	210	179	708
Sr	20.0	8.0	17.4	5.0	6.3	3.0	7.0	6.0	18.0	11.0	79.4
Li	7	3	7	3	4	3	3	4	7	7	18
Ta	6	46	11	39	37	38	81	40	24	16	11
Nb	4	14	6	12	12	11	24	12	10	6	14
Hf	3	1	2	-	1	<1	-	1	1	1	5
Zr	124	92	117	55	87	48	71	69	90	67	227
Y	6	3	6	2	3	2	3	3	9	4	20
Ga	1	1	1	<1	<1	<1	<1	<1	1	1	18
Th	2	1	1	<1	<1	<1	<1	<1	3	1	10
U	0.5	0.5	0.5	<0.5	<0.5	<0.5	<0.5	<0.5	2	0.5	2.5
La	8.0	4.0	8.5	2.5	4.5	4.0	5.0	4.5	14.5	7.0	33.5
Ce	15.0	7.5	16.0	4.0	7.0	5.0	9.5	8.5	31.5	13.5	65.0
Pr	1.8	0.9	1.9	0.5	0.9	0.6	1.2	1	3.6	1.7	8.2
Nd	5.5	3.0	7.0	1.5	3.0	2.0	3.5	3.5	12	5.5	26.0
Sm	1.2	0.5	1.4	0.3	0.5	0.3	0.8	0.7	2.6	0.9	5.0
Eu	0.1	0.1	0.3	0.1	0.1	0.1	0.1	0.1	0.6	0.2	1.3
Gd	1.0	0.5	1.2	0.1	0.3	0.2	0.6	0.7	2.2	0.9	4.0
Tb	0.1	0.1	0.1	<0.1	<0.1	<0.1	<0.1	<0.1	0.3	0.1	0.7
Dy	0.8	0.5	0.8	0.1	0.2	0.1	0.4	0.4	1.6	0.7	3.9
Ho	0.1	0.1	0.1	0.1	0.1	0.1	0.1	0.1	0.3	0.1	0.7
Er	0.6	0.3	0.5	0.1	0.1	0.1	0.4	0.3	1	0.3	2.2
Tm	0.1	0.1	0.1	<0.1	<0.1	<0.1	<0.1	<0.1	<0.1	0.1	0.3
Yb	0.6	0.3	0.6	0.1	0.3	0.1	0.2	0.3	0.7	0.3	1.6
Lu	<0.1	<0.1	0.1	<0.1	0.1	0.1	<0.1	<0.1	<0.1	<0.1	0.3

Table IV-2
continued

Sample Nr	8351C	8351F	8351I	range	mean	standard	UCC	PAAS	NASC
Depth (m)	24	51	74	n=90	n=90	deviation	(1)	(2)	(3)
SiO_2 (wt.%)	95.78	89.40	67.78	44.07-99.04	85.34	12.23	65.92	62.8	64.8
TiO_2	0.08	0.21	0.25	0.02-0.62	0.18	0.11	0.76	1.0	0.78
Al_2O_3	0.87	3.50	3.75	0.34-11.76	3.01	2.12	15.19	18.9	16.9
Fe_2O_3	0.29	1.22	1.40	0.13-2.96	1.00	0.69	4.1	5.8	5.1
MnO	0.01	0.01	0.03	<0.01-0.06	0.01	0.01	0.08	0.11	0.06
MgO	0.07	0.32	2.24	0.03-7.54	1.06	1.53	2.2	2.2	2.85
CaO	0.02	0.17	10.32	<0.01-19.63	2.96	4.65	6.89	1.3	3.56
Na_2O	0.06	0.09	0.29	0.02-0.99	0.19	0.18	3.89	1.2	1.15
K_2O	0.21	0.48	1.31	0.09-2.46	0.59	0.45	3.37	3.7	3.99
P_2O_5	0.01	0.01	0.01	<0.01-0.10	0.01	0.02			
CO_2	<0.2	<0.2	8.4	<0.2-22.2	2.6	4.4			
LOI	0.90	2.87	12.51	0.66-23.69	5.55	5.09			
Total	98.32	98.41	100.05						
Cr (ppm)	7	19	24	4-1300	38.33	139.33	35	110	125
Ni	6.8	13	25	1-440	12.39	47.40	20	55	58
Co	91	32	38	10-251	43.57	34.35	10	23	26
Sc	5	5	5	<5-750	21.29	79.63	11	16	15
V	10	35	45	<5-145	42.62	29.59	60	150	
Cu	5	5	200	<5-200	15.36	26.55		50	
Pb	5	12	12	<0.5-236	9.39	26.01			
Zn	25	170	15	<5-170	21.44	26.49		85	
Rb	7.8	23.6	45.2	3.2-93.4	23.21	16.10	112	160	125
Cs	0.2	0.7	1.1	<0.1-29	1.09	3.12		15	
Ba	84	173	491	36.5-1120	291.06	250.07	550	650	636
Sr	6.9	17.1	408	3-1910	163.54	305.87	350	200	142
Li	4	11	14	3-31	10.11	5.59		75	
Ta	35	9	11	1.5-80.5	13.37	12.14			
Nb	11	6	7	1-24	6.77	3.38	13.7	19	
Hf	1	5	10	<1-10	2.25	1.87	6	5.0	
Zr	91	248	467	28.5-467	127.2	71.86	190	210	
Y	3	8	13	1.5-21.5	7.44	4.35	22	27	
Ga	1	3	3	<1-18	4.11	3.37		20	
Th	1	3	4	<1-10	2.92	2.14	10.7	14.6	12.3
U	0.5	1.0	3.0	<0.5-12	2.01	2.15	2.8	3.1	2.7
La	4.0	11.0	15.0	2-33.5	9.91	5.81	30	38	32
Ce	8.0	22.0	29.5	3-65	19.15	11.95	64	80	73
Pr	0.9	2.7	3.6	0.3-8.2	2.32	1.41	7.1	8.9	7.9
Nd	3.5	9.0	12.0	1.5-26	7.95	4.82	26	32	33
Sm	0.5	1.6	2.1	0.3-5	1.54	0.97	4.5	5.6	5.7
Eu	0.1	0.4	0.5	<.1-1.3	0.35	0.25	0.9	1.1	1.2
Gd	0.6	1.3	2.3	0.1-4.1	1.45	0.90	3.8	4.7	5.2
Tb	0.1	0.2	0.3	<0.1-0.7	0.2	0.14	0.64	0.77	
Dy	0.4	1.2	1.8	0.1-3.9	1.15	0.76	3.5	4.4	
Ho	0.1	0.2	0.4	<0.1-0.7	0.24	0.17	1	1.0	
Er	0.4	0.6	0.9	0.1-2.2	0.71	0.42	2.3	2.9	3.4
Tm	0.1	0.1	0.1	<0.1-0.3	0.11	0.04		0.40	
Yb	0.4	0.6	1.2	0.1-2.3	0.71	0.41	2.2	2.8	3.1
Lu	<0.1	<0.1	<0.1	<0.1-0.3	0.11	0.04		0.43	

Table IV-2 continued

Sample Nr Depth (m)	Accepted value for standard	laboratory obtained	laboratory obtained	Accepted value for standard	laboratory obtained	laboratory obtained
SiO_2 (wt.%)	59.99	61.51	60.15	49.90	49.83	51.05
TiO_2	0.71	0.67	0.71	0.29	0.28	0.29
Al_2O_3	14.41	13.78	14.27	20.69	19.28	19.95
Fe_2O_3	7.38	7.20	7.57	6.21	5.90	6.04
MnO	0.11	0.14	0.15	0.11	0.11	0.10
MgO	1.69	1.72	1.82	0.54	0.50	0.51
CaO	3.07	3.09	3.23	8.05	7.79	7.94
Na_2O	1.11	1.20	1.28	7.10	7.03	7.13
K_2O	2.37	2.14	2.25	1.66	1.57	1.61
P_2O_5				0.13	0.11	0.10
CO_2				1.8	1.8	2.0
LOI				8.37	8.63	8.57
Total						
Cr (ppm)	74	116	115	74	113	117
Ni	286.0	292	291	286	305	284
Co	18	24	23	3	3	3
Sc	12	10	10	12	10	10
V	170	180	175	5	5	5
Cu	175	190	185	5	5	5
Pb	670	623	638	670	611	601
Zn	165	210	180	95	90	90
Rb	84.5	86.0	88.2	55	54	51
Cs	4.7	4.7	4.5	2	2	1
Ba	1210	1190	1240	340	341	285
Sr	238.0	228.0	254	1190	1120	1175
Li	29	28	29	29	29	28
Ta	1	1	1	0.9	1.0	0.5
Nb	8	8	8	13	12	10
Hf	4	3	3	11	9	9
Zr	138	145	143	517	547	479
Y	24	22	23	119.0	120.0	124.5
Ga	18	17	17	35	38	38
Th	10	7	7	1	1	1
U	11.1	10.5	11.5	0.8	0.5	0.5
La	23.0	22.0	22.0	58.0	54.5	56.5
Ce	45.0	44.5	45.5	122.0	118.5	120.0
Pr	5.2	5.3	5.4	15.0	14.3	14.4
Nd	21.0	19.5	19.5	57.0	51.5	50.5
Sm	4.5	3.9	4.0	12.7	11.7	11.8
Eu	1.0	0.9	1.0	2.0	1.9	1.9
Gd	4.2	4.0	4.0	14.0	13.8	13.4
Tb	0.7	0.7	0.7	2.6	2.7	2.4
Dy	3.8	3.6	3.8	18.2	16.8	16.3
Ho	0.8	0.7	0.7	4.3	4.0	3.9
Er	2.4	2.3	2.2	14.2	13.8	12.9
Tm	0.4	0.3	0.3	2.3	2.0	2.0
Yb	2.3	2.1	2.3	14.8	13.3	13.6
Lu	0.3	0.3	0.3	2.1	1.9	1.8

IV.2.5 Petrography

Table IV-1 provides a summary of the grain size data from both drilling and split spoon samples from boreholes investigated. These data indicate an average grain size of between 1.7 and 2.2 φ, with a sorting between 0.56 and 0.77 for the different boreholes. Furthermore, the average grain size of the 42 shallow depth samples collected during this study was 2.40 φ (range 2.13–2.70), with an average sorting of 0.69. All these data are consistent with previously published grain size data of McCarthy and Ellery (1995) who pointed out that sediments from the lower Boro region of the Okavango Delta are dominated by well sorted sand of 2.2 φ average grain size.

Microscopic and X-ray diffraction data (Figure IV-3 and Table IV-1) indicate that the studied samples contain the following minerals: quartz (28–100 vol.%), calcite (0–65 vol.%), dolomite (0–45 vol.%), K-feldspar (0–4vol.%), kaolinite (0–3 vol.%), traces of muscovite and other clays (0–3 vol.%). XRD analysis of the sample 8159G indicates that it containsV-muscovite, in addition to the minerals reported in other Okavango sediments. Important to stress is that (1) no detrital muscovite has been observed under the microscope in this sample; (2) submicroscopic muscovite recorded in young sediments by XRD analyses is usually muscovite–smectite mixed layers (e.g., Deer et al., 1992). The existence of traces of heulandite in the sample 8159N (XRD data) is not yet well constrained. The presence of a micritic carbonate cement around quartz grains can be seen in Figure IV-3c. There are no lithic fragments in the samples documented. The samples with the lowest quartz modal content (<85 vol.%) are rich in carbonates (>15 vol.%). Recalculating the modal composition in terms of quartz (Q), feldspars (F) and lithic fragments (L) result in Q≥94, F≤6% and L=0. In the Q–F–L diagram (Figure IV-4); the data indicate that these sediments have the modal composition of very mature quartz arenites of continental cratonic provenance (e.g., Dickinson and Suczec, 1979). However, it is important to keep in mind that this modal composition is mainly controlled by the aeolian sand component and is not representative of the other sediment components discussed later.

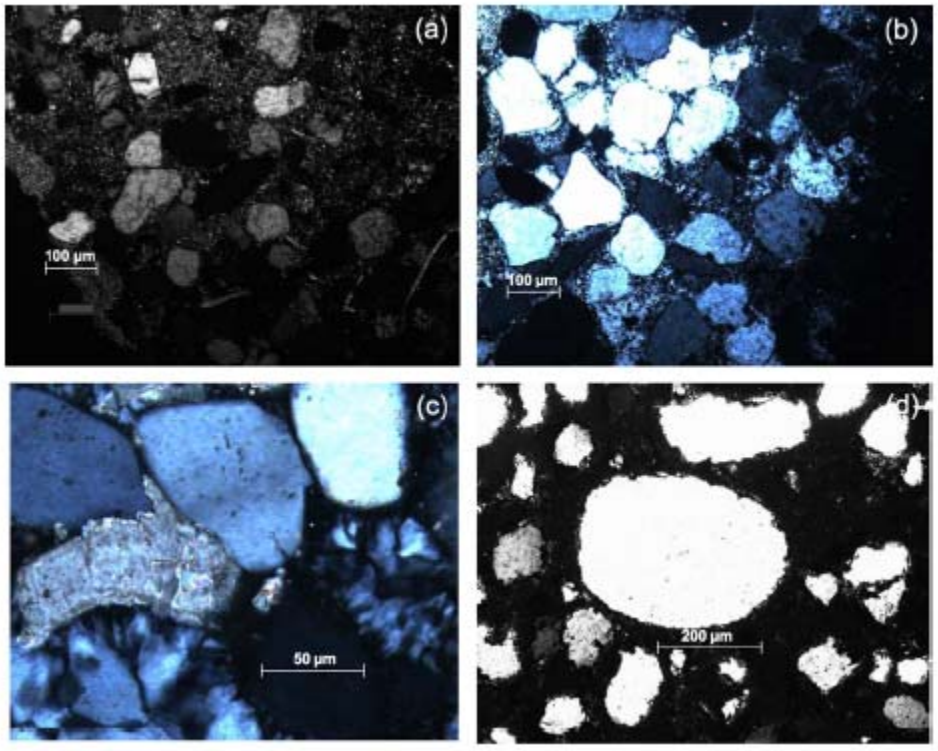

Figure IV 3. Representative thin sections of Okavango sediments. (a) sand grains (some fractured) within a carbonate cement. (b) Sand grains within a minor diagenetic silica overgrowth. (c) Micritic calcrete forming between the sand grains. (d) sand grains showing considerable weathering on the surface.

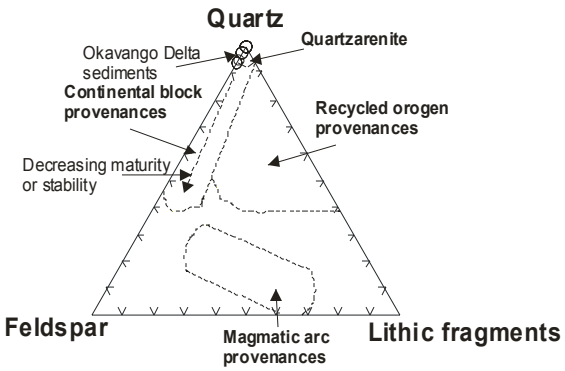

Figure IV 4. Q-F-L diagram for the Okavango sediments (after Dickinson and Suczec, 1979)

IV.2.6 Major element composition

The SiO_2 content of the Okavango siliciclastic sediments ranges from 53.82 to 99.04 wt.%. Two samples, BH8159O and BH8159M, have lower SiO_2 contents (TableIV-2). These two samples are also marked by high concentrations of CaO, MgO and CO_2. There is a strong negative correlation between SiO_2 and Al_2O_3 when carbonate-bearing (CO_2>0.2 wt.%) samples are discarded (Figure IV-5a). Al_2O_3 shows a strong positive correlation with TiO_2 (Figure IV-5b) and total Fe_2O_3 (Figure IV-5c). In carbonate-free samples (CO_2<0.2 wt.%), Al_2O_3 shows a positive correlation with MgO (Figure IV-5d) and LOI (Figure IV-5h). There is a weak positive correlation between Al_2O_3 and K_2O (Figure IV-5e) and Na_2O (Figure IV-5f). In the Al_2O_3–K_2O diagram (Figure IV-5e), the analyses are distributed between the lines K_2O/Al_2O_3=0.09 and 0.67. Similarly, the samples plot between the lines Na_2O/Al_2O_3=0.02 and 0.22 in the Al_2O_3–Na_2O diagram (Figure IV-5f). The average K_2O/Al_2O_3 ratios of the Okavango Delta sediments is close to K_2O/Al_2O_3 ratios in the upper continental crust average composition (UCC), Post-Archaean Australian shales average composition (PAAS) and North American shale composite average value (NASC; Table IV-3).

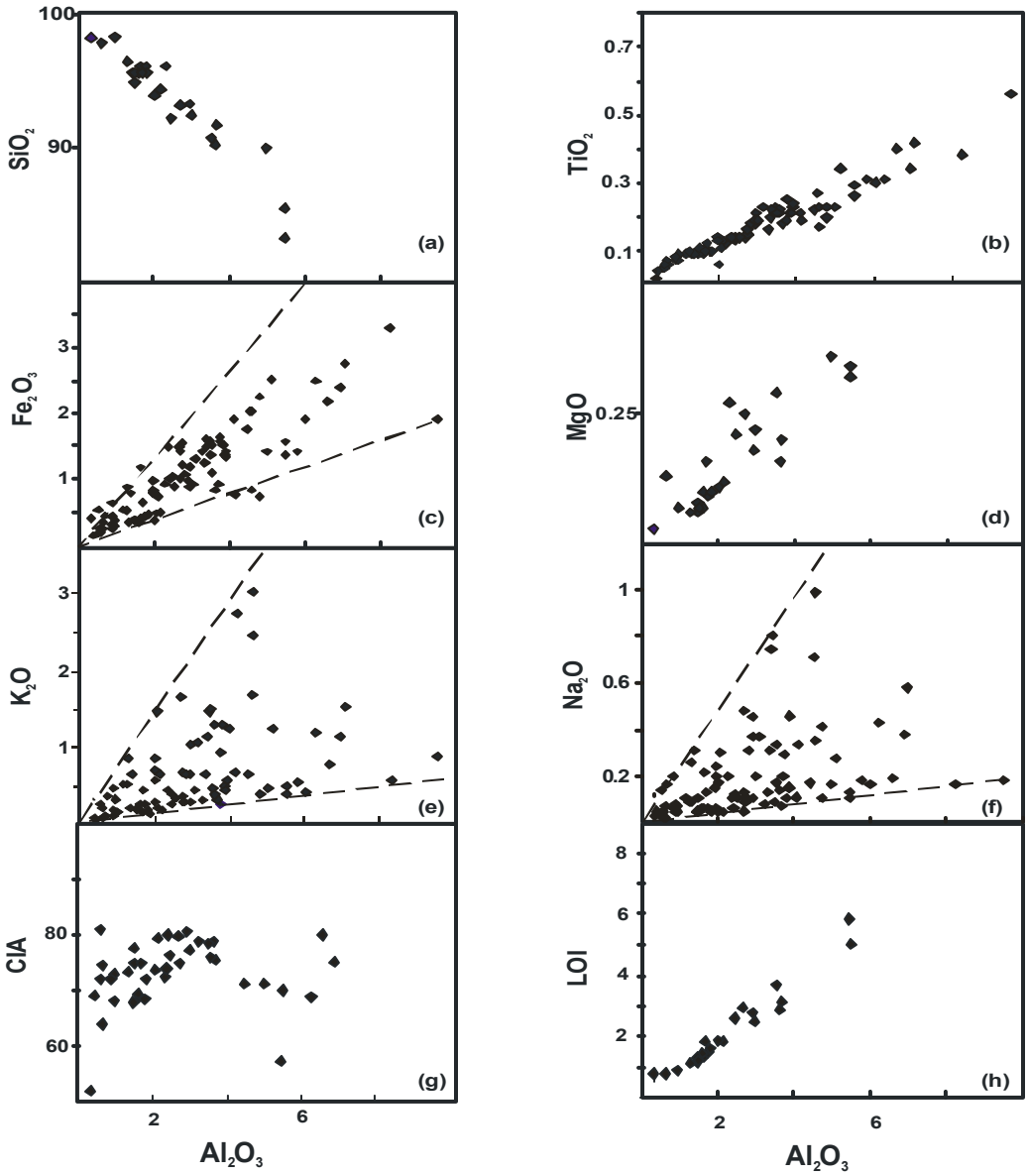

Figure IV 5. Binary diagrams for Okavango Delta sediment: major elements compositions in wt.%

Table IV 3. Representative samples and summary of the range of inter-element ratios for the Okavango Delta sediments

Sample Nr	8157A	8157F	8158A	8158F	8158H	8159A	8159E	8159G	8159I	8159J	8159M
Depth (m)	3	54	6	60	90	6	45	60	69	81	99
Al_2O_3/SiO_2	0.06	0.02	0.07	0.01	0.01	<0.01	0.06	0.03	0.05	0.08	0.09
K_2O/Al_2O_3	0.10	0.12	0.09	0.20	0.17	0.29	0.15	0.37	0.35	0.37	0.54
CIA	71.1	68.4	57.3	74.5	73.3	51.8	-	-	-	-	-
Cr/Ni	13	2.8	2.2	3.0	3.0	2.0	19	3.0	2.5	15	2.2
Cr/V	0.8	0.6	0.3	1.2	0.6	0.8	1.6	43.3	0.3	0.9	0.5
Ni/Co	0.12	0.09	0.54	0.04	0.06	0.03	0.19	21.5	0.1	0.25	1.2
V/Ni	16	5.0	6.7	2.5	5.0	2.5	12	0.07	28.1	17	4.9
K/Rb	154	185	151	95	217	244	197	255	278	292	381
Rb/Sr	0.74	0.67	0.54	2.53	0.87	0.54	0.12	0.04	0.08	0.13	0.07
Ti/Zr	9.6	6.2	3.9	2.5	4.8	4.2	9.5	8.1	9.3	21	20
Cr/Zr	0.42	0.11	0.07	0.04	0.08	0.14	0.49	12.50	0.03	0.71	0.57
Y/Ni	1.9	1.1	1.1	1.3	1.2	0.8	2.6	0.02	5.9	3.1	0.52
Th/U	3.0	2.0	2.5	2.0	2.0	2.0	2.7	0.2	0.6	0.8	0.4
Th/Cr	0.05	0.09	0.17	0.17	0.11	0.25	0.06	<0.001	0.75	0.07	0.10
Th/Sc	0.10	0.2	1.0	0.2	0.2	0.2	0.2	<0.001	0.60	0.1	0.8
La_N/Yb_N	11.0	8.1	8.9	6.8	8.4	13.5	8.4	7.2	7.1	11.4	14.1
La_N/Sm_N	5.1	3.8	4.3	4.7	3.9	4.2	4.4	4.3	4.1	4.0	3.9
Gd_N/Yb_N	1.9	1.3	1.7	1.4	1.2	0.8	1.4	1.3	1.4	2.0	2.3
Eu/Eu*	0.70	0.34	0.64	0.60	0.44	-	0.70	0.83	0.92	0.75	0.66
Ce/Ce*	0.89	1.02	0.97	1.19	1.08	0.79	1.07	1.07	1.03	0.97	0.97
La/Sc	0.43	1.20	3.70	0.60	1.00	0.40	0.63	0.01	2.10	0.19	2.50
La/Co	0.33	0.13	0.74	0.07	0.09	0.33	0.61	0.37	0.66	0.93	0.89

1. UCC values from Taylor and McLennan (1995) except for TiO_2, Nb, Cs, Tb and Ta values from Plank and Langmuir (1998)

2. PAAS composition from Taylor and McLennan (1985)

3. NASC composition from Gromet et al. (1984)

Table IV-3 continued

Sample Nr	8159N	8159O	8159T	8162D	8162E	8162J	8162K	8162L	8162O	8262A	8262B
Depth (m)	102	114	147	15	24	45	51	54	63	3	12
Al_2O_3/SiO_2	0.05	0.03	0.01	0.03	0.05	0.04	0.01	0.01	0.03	0.11	0.15
K_2O/Al_2O_3	0.63	0.67	0.50	0.12	0.09	0.34	0.38	0.46	0.25	0.09	0.07
CIA	-	-	-	79.9	-	-	-	-	-	-	-
Cr/Ni	1.0	2.1	1.1	16	14	10	12	27	1.7	3.1	3.0
Cr/V	0.5	0.4	1.0	3	0.5	0.4	0.3	8.0	0.5	0.5	0.5
Ni/Co	1.8	1.1	0.21	0.18	0.07	0.10	0.02	0.07	0.42	0.77	1.22
V/Ni	2.0	4.7	1.1	5.4	28	20	67	3	3.2	6.2	5.8
K/Rb	447	380	374	311	134	248	294	297	192	141	131
Rb/Sr	0.04	0.01	0.03	1.20	0.74	0.20	0.10	0.06	1.80	1.20	1.10
Ti/Zr	19	15	5.6	24.3	16.7	9.7	3.3	5.0	4.0	12.3	13.2
Cr/Zr	0.62	0.60	0.19	1.4	0.34	0.19	0.08	0.73	0.08	0.19	0.26
Y/Ni	0.26	0.57	0.33	0.71	4.0	3.3	4.0	5.8	0.9	1.1	0.86
Th/U	0.2	0.2	0.7	2	2.7	1.5	1.0	0.7	4.0	4.0	2.5
Th/Cr	0.07	0.09	0.10	0.02	0.14	0.12	0.08	0.01	0.11	0.15	0.14
Th/Sc	0.1	0.4	0.2	0.01	0.3	0.2	0.1	0.1	0.4	0.2	0.3
La_N/Yb_N	7.2	11.0	11.8	23.6	9.3	8.6	14.6	7.4	7.6	9.9	8.4
La_N/Sm_N	4.5	4.1	3.1	4.4	4.6	3.8	5.8	4.9	3.1	4.0	3.8
Gd_N/Yb_N	1.6	1.8	2.0	5.7	1.6	1.5	1.6	1.5	1.7	1.9	1.4
Eu/Eu*	0.88	0.64	0.52	0.51	0.79	0.68	0.47	0.39	0.70	0.71	0.70
Ce/Ce*	0.99	1.04	0.86	0.86	0.92	0.90	0.78	1.02	1.02	1.25	0.99
La/Sc	1.70	1.30	0.70	0.05	0.73	0.77	0.65	0.55	1.80	0.63	0.71
La/Co	0.55	0.65	0.08	0.23	0.45	0.43	0.21	0.14	0.35	1.14	1.39

Table IV-3 continued

Sample Nr	8262C	8262D	8262F	8348A	8348B	8348C	8348D	8348E	8348F	8348G	8348H
Depth (m)	21	24	42	6	12	24	33	39	42	45	54
Al_2O_3/SiO_2	0.03	0.01	0.03	0.01	0.01	<0.01	0.01	0.01	0.03	0.03	0.08
K_2O/Al_2O_3	0.12	0.19	0.15	0.18	0.16	0.23	0.20	0.17	0.12	0.14	0.16
CIA	79.8	73.1	76.4	80.8	-	69.0	64.0	72.1	-	-	75.1
Cr/Ni	1.8	0.9	2.7	1.7	2.3	2.3	10.0	2.0	14.2	15.7	2.7
Cr/V	1.1	2.8	0.4	0.6	0.5	0.4	1.0	1.2	0.6	1.1	0.3
Ni/Co	1.07	0.25	0.17	0.03	0.03	0.02	<0.01	0.03	0.02	0.03	0.27
V/Ni	1.7	0.3	6.3	2.8	5.0	8.0	10.0	1.7	25	14.3	10.5
K/Rb	128	207	162	218	200	233	224	207	153	191	101
Rb/Sr	1.00	0.86	1.10	0.73	0.92	1.10	0.69	0.71	0.97	1.40	1.20
Ti/Zr	7.3	5.9	7.2	5.5	5.5	5.0	6.0	5.3	10.7	12.6	9.0
Cr/Zr	0.35	0.30	0.13	0.11	0.08	0.11	0.14	0.09	0.22	0.33	0.15
Y/Ni	0.23	0.09	1.07	0.56	0.83	0.68	3.00	0.83	6.4	2.86	1.61
Th/U	4.0	2.0	2.0	2.0	2.0	6.0	2.0	2.0	1.5	2.0	4.0
Th/Cr	0.05	0.04	0.07	0.14	0.09	0.19	0.10	0.16	0.15	0.05	0.30
Th/Sc	0.04	0.03	0.2	0.2	0.2	0.2	0.1	0.2	0.3	0.07	2.0
La_N/Yb_N	9.0	9.0	9.6	16.9	10.1	27.0	16.9	10.1	14.0	15.8	14.1
La_N/Sm_N	4.2	5.0	3.8	5.2	5.7	8.4	3.9	4.0	3.5	4.9	4.2
Gd_N/Yb_N	1.4	1.4	1.6	0.8	0.8	1.6	2.4	1.9	2.6	2.4	2.0
Eu/Eu*	0.28	-	0.71	-	-	-	0.44	-	0.77	0.68	0.89
Ce/Ce*	1.02	0.99	0.96	0.91	0.85	0.75	1.02	0.98	1.11	1.00	1.01
La/Sc	0.14	0.10	0.24	0.50	0.30	0.80	0.20	0.90	1.45	0.47	6.7
La/Co	0.36	0.03	0.26	0.02	0.04	0.04	0.02	0.04	0.20	0.14	0.73

Table IV-3 continued

Sample Nr	8351C	8351F	8351I	range	mean	standard	UCC (1)	PAAS (2)	NASC (3)
Depth (m)	24	51	74	n=90	n=90	deviation			
Al_2O_3/SiO_2	0.01	0.04	0.06	<0.01-0.15	0.04	0.03	0.23	0.30	0.26
K_2O/Al_2O_3	0.24	0.14	0.35	0.07-0.67	0.23	0.14	0.22	0.20	0.24
CIA	71.6	78.6	-	52-81	73	6.0			
Cr/Ni	1.0	1.4	1.0	0.88-27	5.68	6.09	1.8	2.0	2.2
Cr/V	0.7	0.5	0.5	0.3-43	1.28	4.66	0.6	0.7	
Ni/Co	0.08	0.42	0.66	<0.01-22	0.51	2.32	2.0	2.4	2.2
V/Ni	1.5	2.7	1.8	0.07-67	9.37	10.13	3.00	2.7	
K/Rb	224	169	241	95-447	215	75.28	250	171	
Rb/Sr	1.10	1.40	0.11	0.01-2.53	0.92	0.5	0.32	0.80	0.88
Ti/Zr	5.3	5.1	3.2	2.5-24.3	8.82	4.43	23.9	28.5	
Cr/Zr	0.08	0.08	0.05	0.04-12.50	0.36	1.31	0.18	0.52	
Y/Ni	0.44	0.57	0.50	0.02-6.4	1.65	1.68	1.1	0.49	
Th/U	2.0	4.0	1.3	0.2-6	2.2	1.36	3.8	4.7	
Th/Cr	0.40	0.16	0.17	<0.001-0.75	0.12	0.08	0.31	0.13	0.10
Th/Sc	0.2	0.7	0.8	<0.001-2	0.3	0.32	0.97	0.91	0.82
La_N/Yb_N	6.8	12.4	8.4	6.8-27	10.3	3.48	9.2	9.2	7.0
La_N/Sm_N	5.0	4.3	4.5	3-8.4	4.22	0.75	4.2	4.3	3.5
Gd_N/Yb_N	1.2	1.8	1.6	0.8-5.7	1.74	0.64	1.4	1.4	1.4
Eu/Eu*	0.56	0.85	0.70	0.3-0.9	0.62	0.15	0.67	0.66	0.67
Ce/Ce*	1.00	1.02	1.01	0.75-1.3	0.98	0.08	1.1	1.1	1.1
La/Sc	0.80	3.0	3.0	0.01-6.7	1.39	1.27	2.7	2.4	2.1
La/Co	0.04	0.35	0.39	0.03-1.39	0.34	0.27	3.0	1.7	1.2

The degree of chemical weathering of the source material of sedimentary siliciclastic rocks can be constrained by calculating the chemical index of alteration (CIA) of Nesbitt and Young (1982), where CIA=molar [$Al_2O_3/(Al_2O_3+CaO^*+Na_2O+K_2O)$], CaO* being the amount of CaO in silicate minerals only (i.e., excluding carbonates and apatite). The CIA values vary from about 50 for unweathered upper crust to about 100 for highly weathered residual soils. The Okavango sediments contain variable amounts of carbonate minerals and this is reflected by variable CO2 contents. Calcite and dolomite coexist in these rocks, and there are no microprobe data available on these minerals. Therefore, it is unrealistic to attempt correcting the carbonate-effect on the total content of CaO and MgO in the Okavango sediments. To avoid the diagenetic carbonate-effect, only samples devoid of carbonate minerals and marked by CO_2<0.2 wt.% are used in the calculation of CIA and in geochemical diagrams requiring the utilisation of CaO or MgO content in silicate minerals. The Okavango siliciclastic sediments with CO_2 <0.2 wt.% were corrected for apatite-effect using P_2O_5 values of the samples (Table IV-2) and yielded CIA values (Table IV-3) in the range 52–81 (average 73). Nesbitt and Young (1982) indicate that the influence of weathering processes at the source on the composition of clastic sediments can also be detected using the A–CN–K diagram [=molar (Al_2O_3–(CaO^*+Na_2O)–K_2O)] where CaO* represents the amount of CaO entering into the structure of silicate minerals. Figure IV-6 shows the distribution of the carbonate-free Okavango sediments in the A–CN–K diagram. For comparison, the compositions of UCC, PAAS and NASC are also plotted in the diagram along with the predicted weathering trend for the average upper continental crust (Taylor and McLennan, 1985). This trend encompasses the majority of the Okavango samples.

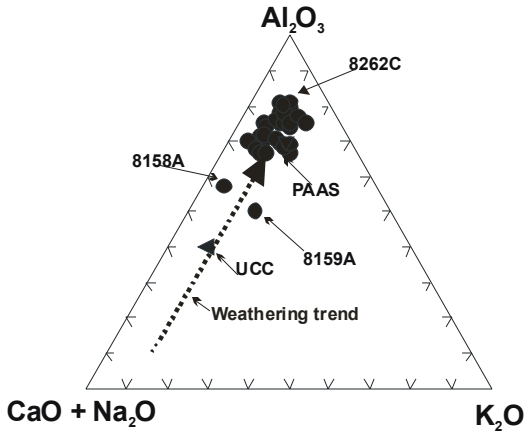

Figure IV 6. A-CN-K diagram (molecular proportions) for the Okavango sediments

IV.2.7. Trace element compositions

IV.2.7.1. Transition metals

The concentration of Ni in the Okavango sediments is between 1 and 32 ppm with a higher value of 440 ppm in the sample BH8159G. The Okavango sediments are marked by a large variation of cobalt, vanadium and chromium concentrations. Cr and V show positive correlations with TiO_2 and Ni (Figure IV-7a–d). Ni and Cr show a positive correlation with MgO in carbonate-free samples and a weak negative correlation with SiO2 (Figure IV-7e–h). The sample BH8159G is characterised by a high concentration of Cr (1300 ppm) and high Cr/V and Ni/ Co ratios (Tables IV-2 and IV-3). In contrast, it is marked by a lower V/Ni ratio. Elevated Cr and Ni abundances, as seen in sample BH8159G, were suggested by Garver et al. (1996) to reflect ultramafic rocks in the source area of sediments.

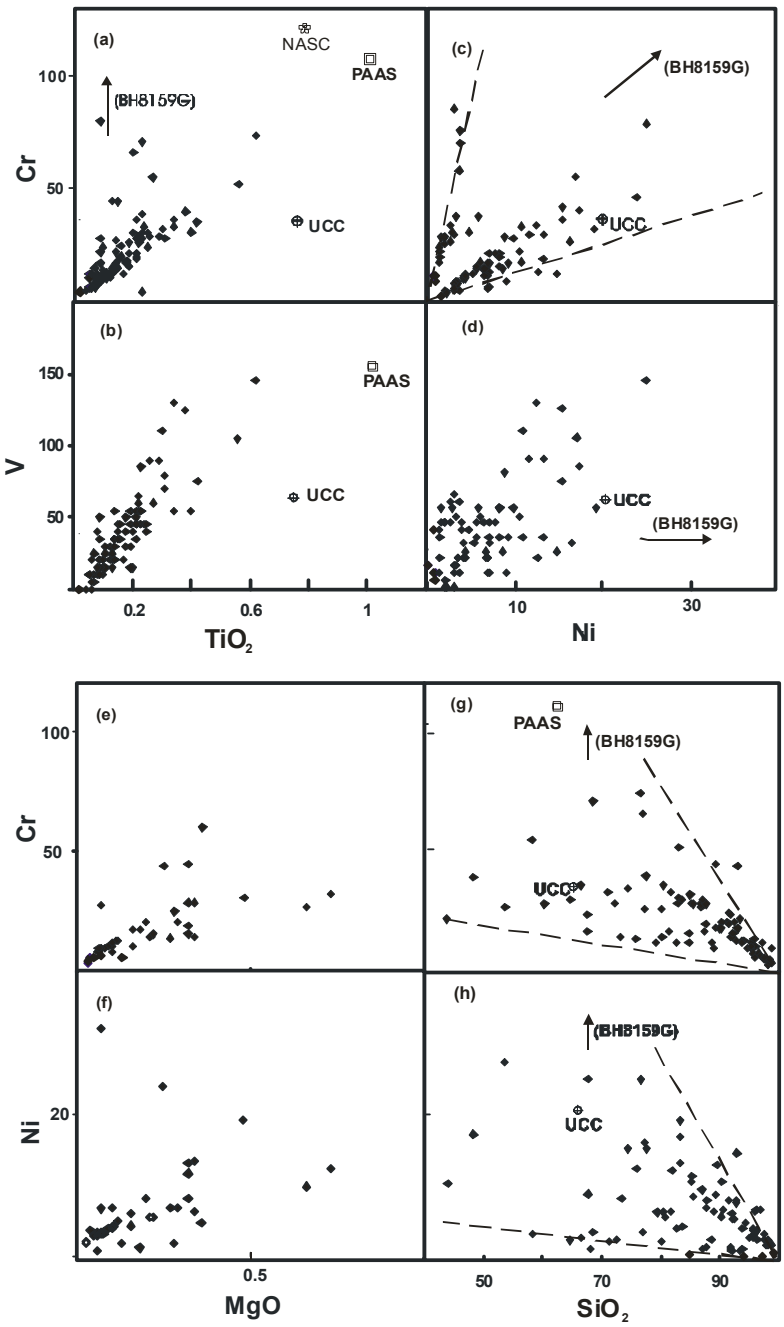

Figure IV. 7. Transition metal characteristics of the Okavango sediments in the plots Cr and V vs. TiO_2 (a,b); Cr and V vs. Ni (c,d); Cr and Ni vs. MgO (e,f) and Cr and Ni vs. SiO_2

IV.2.7.2. Alkalis and alkali-earth elements

A strong positive correlation exists between K_2O and Rb (Figure IV-8a). Sr shows a large range and a positive correlation with CO_2 (Figure IV-8b). Rb/Sr range of carbonate-free samples encompasses the Rb/Sr ratio for PAAS. The sample BH8158F is marked by a high Cs concentration. Rb shows a strong positive correlation with Cs in carbonate-free samples (Figure IV-8c). There is also a positive correlation between K_2O and Ba in carbonate-free samples (Figure IV-8d), showing relative Ba enrichment or K_2O depletion of the Okavango sediments relative to the variation trendline in Archaean siliciclastic sedimentary rocks (e.g., Lahtinen, 2000).

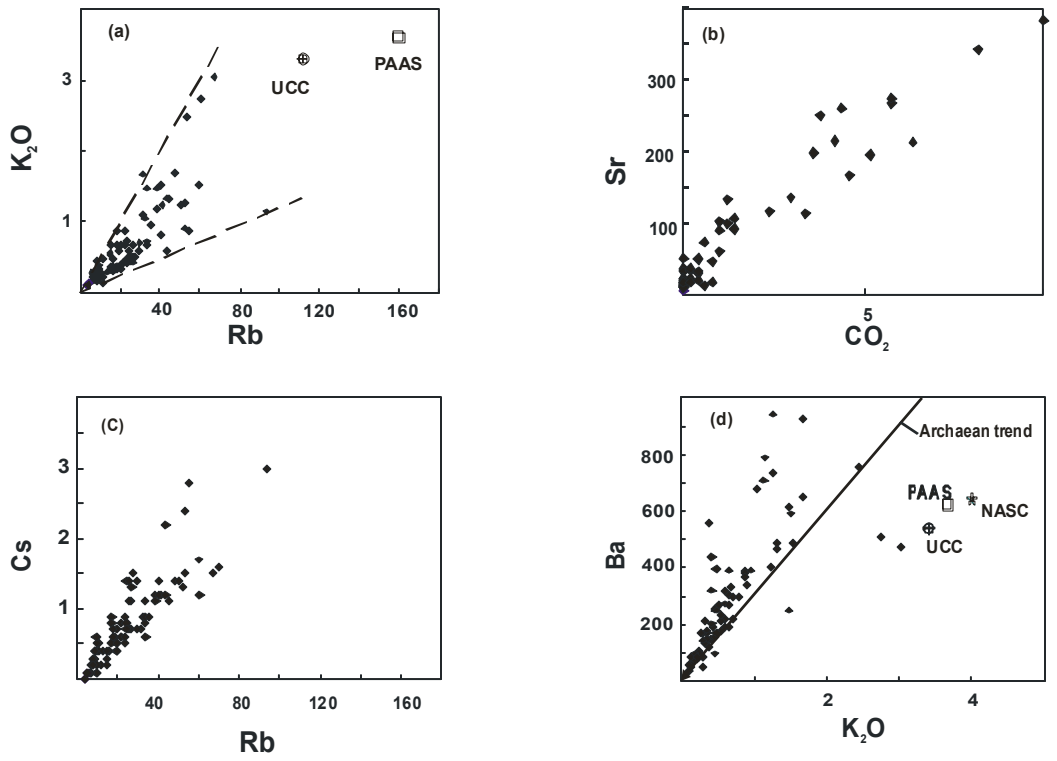

Figure IV. 8. Geochemical characteristics of the Okavango sediments in the binary diagrams: (a) K_2O vs. Rb; (b) Sr vs. CO_2; (c) Cs vs. Rb and (d) Ba vs. K_2O. The Archaean trend for panel (d) is from data from Lahtinen (2000)

IV..2.7.3. High-field-strength-elements (HFSE), Th and U

Average Zr concentration in the Okavango sediments (Table IV-2) is 120 ppm, and fine-grained clastic sedimentary rocks are characterised by an average Zr concentration of 200F100 ppm (Taylor and McLennan, 1985). Two Okavango samples (BH8158A and BH8351I) have higher Zr concentrations between ~440 and 470 ppm (Table IV-2). The average Zr/Hf ratio of the Okavango sediments deduced from the Zr–Hf correlation curve is ~38 (Figure IV-9). This value is similar to chondritic values and to Zr/Hf ratios in Archaean and Proterozoic sedimentary rocks in Southern Africa (Wronkiewicz and Condie, 1987; Toulkeridis et al., 1999; David et al., 2000).

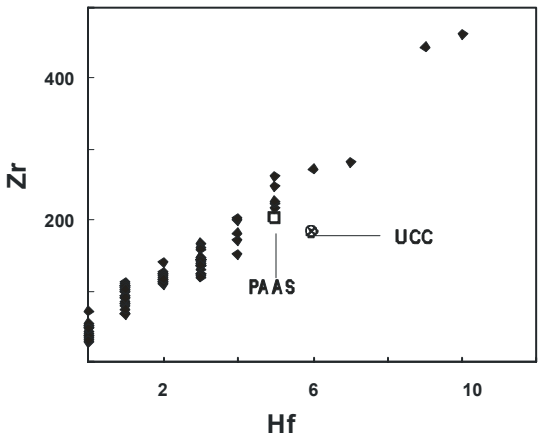

Figure IV. 9. Binary diagram Zr vs. Hf for the Okavango sediments

Ti/Zr ratios for the Okavango sediments (Table IV-3) are lower than values commonly recorded in mafic igneous rocks (usually>>50), whereas felsic igneous rocks are characterised by lower values of <20. Cr/Zr and Y/Ni ratios for the Okavango samples overlap the range of values reported in both mafic and felsic igneous rocks. Cr/Zr in igneous rocks is usually >1 for mafic and <0.5 for felsic rocks. The ratio Y/Ni is lower in mafic igneous rocks (<1) than in felsic igneous rocks (>10 except in some extensional granites/rhyolites). The Nb concentrations are high in sample BH8348D (Table IV-2). The Th concentrations are lower in the Okavango sediments compared to average values in UCC, PAAS and NASC. The range of U and Th/U values in the Okavango sediments encompasses the values obtained from UCC, PAAS and NASC. With the exception of sample BH8159G, which is marked by an extremely low Th/Cr ratio, the Th/Cr ratios for the Okavango sediments overlap values recorded in fine sands/sandstones originating from both felsic and mafic sources (Table IV-4). Archaean pelites

from the Kaapvaal craton in southern Africa are characterised by Th/Cr≤0.02 (e.g., Condie and Wronkiewicz, 1990; Jahn and Condie, 1995), whereas Proterozoic pelites are marked by higher values, similar to those in the Okavango clastic sediments. With the exception of sample 8159G, the Th/Sc ratios for the Okavango sediments overlap the range of ratios obtained for sediments from felsic and mafic source rocks (Table IV-4).

IV.2.7.4. Rare earth elements

The Okavango clastic sediments show a strong positive correlation between individual REE and Al_2O_3 contents (Figure IV-10). The rare earth element compositions of these sediments (Table IV-2) are shown in chondrite-normalized diagrams (Figure IV-11). The chondrite-normalized REE pattern of PAAS is also shown in the diagrams for comparison. The REE patterns of the Okavango sediments are characterized by: (1) chondrite-normalized REE values (La_N up to Yb_N) greater than one. The REE patterns show that the Okavango sediments are less enriched in REE than the PAAS; (2) substantial fractionation of light rare earth elements (LREE); (3) flat to slightly fractionated heavy rare earth element (HREE) patterns; (4) a variable Eu-negative anomaly. The sample 8159G displays REE contents similar to values in Okavango sediments with the same SiO_2 content (Table IV-2). The range of Eu/Eu* for the Okavango sediments overlaps the ranges recorded in clastic sediments from felsic and mafic source rocks (Table IV-4); (5) a weak to strong negative Ce anomaly in some samples with the majority of samples characterised by Ce/Ce* in the range 0.9–1.2.

Table IV. 4.The range of elemental ratios in fine sandstones derived from felsic and maifc rocks and comparison with the range for the Okavango sediments. Potential source rocks from NW Botswana also included (CKP suite).

Ratio	Fine sandstone		Okavango sediments	CKP11220	CKP10926B	CKP11277	CKP10A299	CKP samples	CKP samples
	Range for sediments from felsic source[1]	Range for sediments from mafic sources[1]	Range	Felsic	Felsic	Mafic	Ultra-mafic	Felsic n= 46	Mafic n= 30
Th/Cr	0.13-2.7	0.018-0.046	<0.001-0.75	0.17	0.58	0.01	0.01	0.07-14.50	<0.01-0.50
Th/Sc	0.84-20.5	0.05-0.22	<0.001-2						
Eu/Eu*	0.4-0.94	0.71-0.95	0.3-0.9	0.64	1.23	1.18	0.94	0.28-1.23	0.55-1.22
La/Sc	2.5-16.3	0.43-0.86	0.01-6.7						
La/Co	1.8-13.8	0.14-0.38	0.03-1.39	2.03	1.09	0.21	0.48	0.42-15.18	0.10-1.58

1) Cullers (2000)

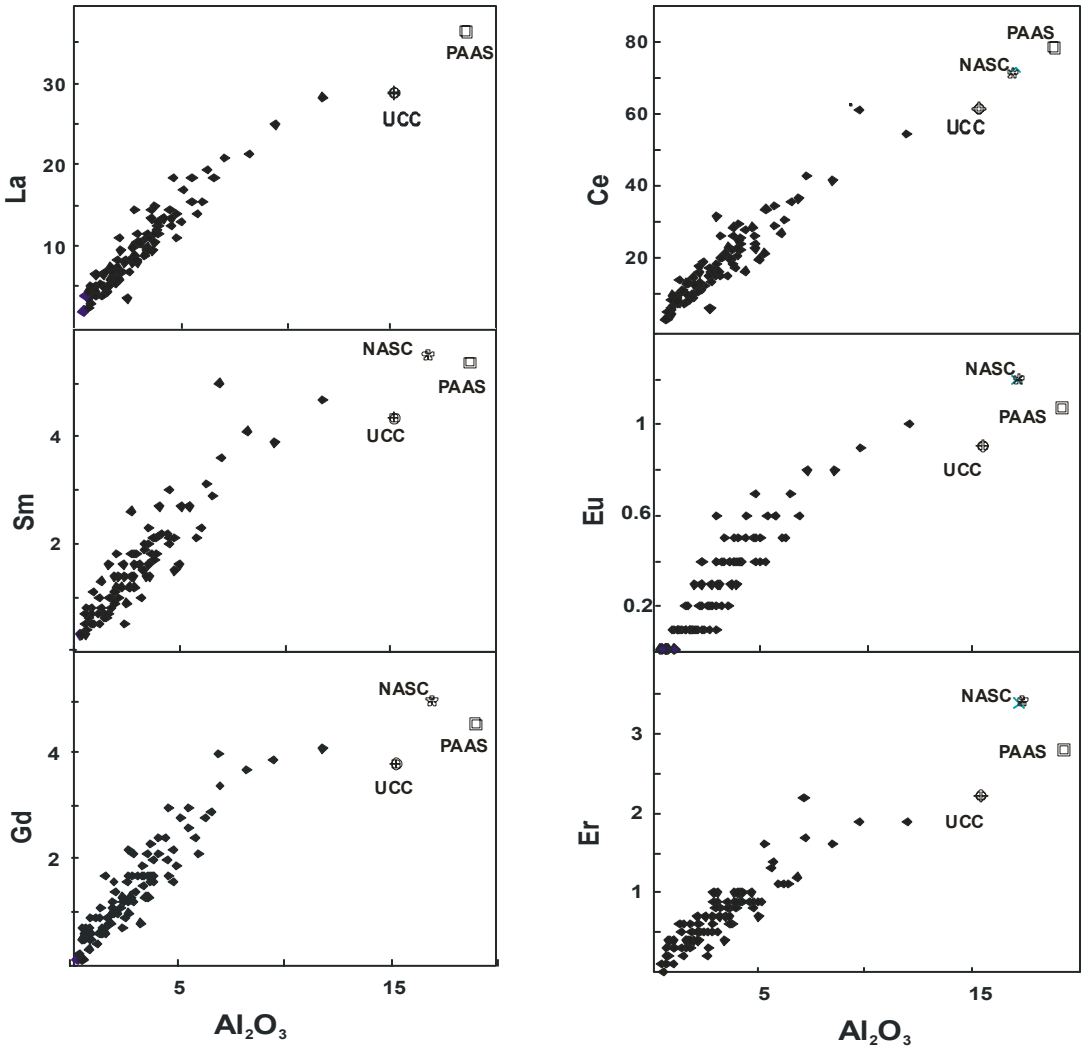

Figure IV. 10. REE vs. Al_2O_3 diagrams for the Okavango sediments

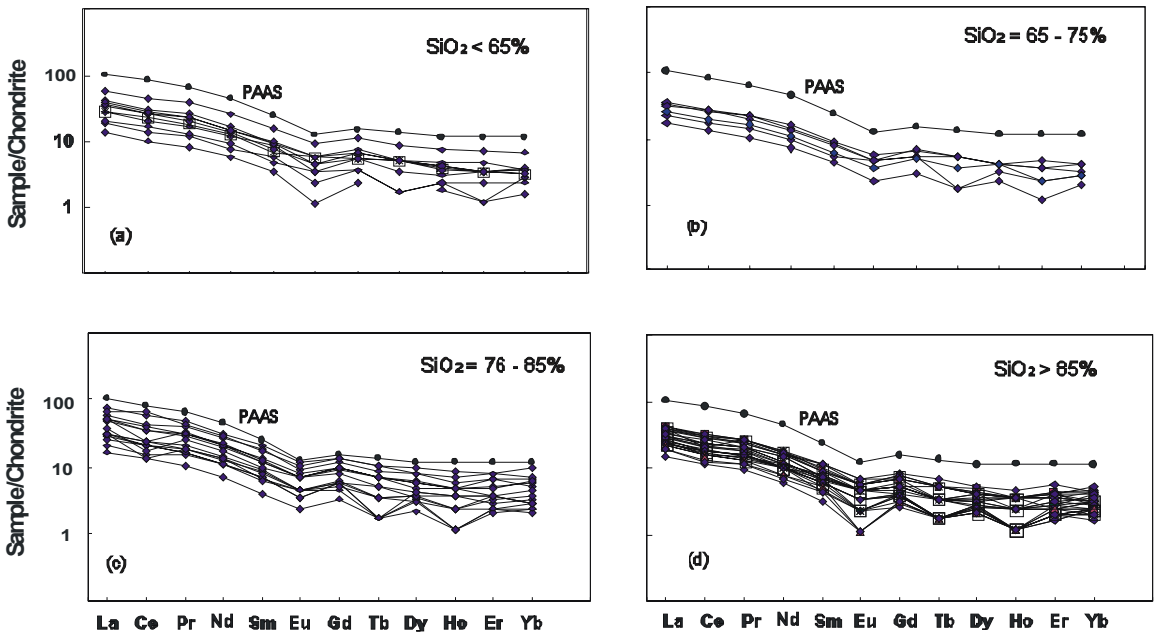

Figure IV. 11. Chondrite normalized REE plots of the Okavango sediments. PAAS plotted as reference

The La/Sc ratios of the Okavango sediments overlap the ratios recorded in sediments originating from felsic and mafic source rocks (Table IV-4). La/Co ratios for the Okavango sediments include low values similar to those recorded in sediments from mafic sources and higher values (up to 1.39 in sample 8262B) requiring either an intermediate composition source or a contribution from both mafic and felsic source rocks.

Wronkiewicz and Condie (1987) indicated that the source rock lithology (mafic, intermediate or felsic) strongly influences the concentrations of Th, Sc, La, Zr, Hf and Co in the siliciclastic sedimentary rocks. The relationships between these elements were used to devise ternary diagrams for the identification of the nature of the source rocks of siliciclastic sedimentary rocks. In the diagrams La–Th–Sc (Figure IV-12a), Th–Sc–Zr (Figure IV-12b) and Th–Hf–Co (Figure IV-12c), the Okavango sediments define evolutionary trends or a field extending from mafic to felsic source rock endmembers. Since these elements do not enter in the structure of quartz, these trends/fields exclude the aeolian sand component of the sediments. The samples BH8158A and BH8351I plot outside that evolution trend in the Th–Sc–Zr diagram, being displaced towards the Zr apex.

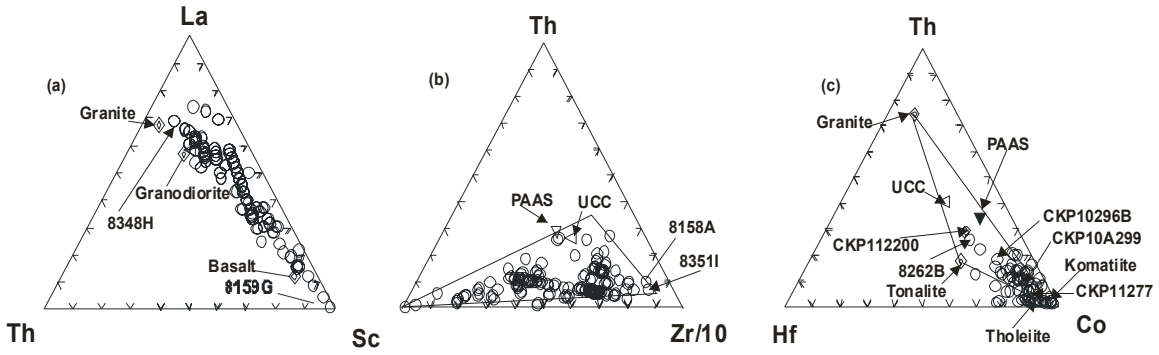

Figure IV. 12. Geochemical characteristics of the Okavango sediments in the ternary diagrams: (a) La-Th-Sc showing a single evolution trend; (b) Th-Sc-Zr/10 and (c) Th-Hf-Co. Note that the Okavango sediment sample BH8262B overlaps with the composition of the Proterozoic granitoids sample CKP11220 from NW Botswana suggesting that these granitoids could be the source of this sediment

IV.2.8. Discussion

IV.2.8.1. Introduction

Several factors control the chemical composition of elements in siliciclastic sedimentary rocks. The most commonly documented are diagenesis, metamorphism, grain-size and density-controlled hydraulic sorting, petrological composition of the source rocks, degree of weathering of the source area and the tectonic setting (e.g., Nesbitt and Young, 1982; McLennan et al., 1983; Wronkiewicz and Condie, 1987; Roser and Korsch, 1988; Camire´ et al., 1993; Cullers, 1994a; Fedo et al., 1996; Bock et al., 1998). Metamorphic remobilisation is excluded for the studied samples because the Okavango sediments are unconsolidated. The first major geochemical complexity of the Okavango sediments is that they show variable content of CO_2, reflecting variable amounts of diagenetic carbonate minerals and organic matter (organic C in the range ~0–1.64 wt.%; authors, unpublished data). Carbonates induce a variable dilution on the clastic component of the studied sediments. However, this study places emphasis on major, trace and ratios of elements hosted in silicate minerals because when processing or plotting the chemical composition of elements involved in the structure of carbonates (e.g., CaO and MgO), emphasis was on carbonate-free samples. The second major geochemical complexity of the Okavango sediments is that they contain a variable but important amount of quartz that induces a drastic variation of SiO_2 contents. This silica dilution effect induces strong variation on all trace element

contents (expressed in ppm). To overcome this complexity, this paper places emphasis on interelement ratios and ternary diagrams involving elements that do not enter into the structure of quartz. Most of the discussion below concentrates on unravelling the complex factors controlling the geochemical characteristics of the Okavango sediments in terms of provenance excluding the aeolian sand component.

The Okavango alluvial fan is a nascent (Quaternary) rift, and the half-graben is amagmatic (Modisi et al., 2000). Thus, there is no input of young, weakly weathered volcanoclastic material in the Okavango sediments. Therefore, this paper focuses on the remaining four main factors discussed below.

IV.2.8.2. Grain-size and density-controlled sorting

The Okavango Delta sediments, including all the samples studied, are well sorted fine to mediumgrained sands, with variable amounts of carbonates and minor silt and clay (Table IV-1 and DWA (Department of Water Affairs), 1997). The Okavango River water constitutes the major source of the fine fraction of the sediments (McCarthy and Ellery, 1995). A number of studies comparing the chemical composition of fine and coarse clastic sediments from the same source showed that fine sediments are particularly rich in clay minerals and preferentially concentrate elements entering in the structure of mafic minerals in igneous rocks (e.g., Cullers, 1994a,b). Coarser sediments contain a higher proportion of quartz and alkali feldspars. In the Okavango sediments, quartz induces a dilution that is shown by the decrease of all elements with the increase of silica in carbonate-free sediments (e.g., Figs. IV-5a and IV-7g,h). As stated above, the quartz dilution effect explains the large variation of the concentration of the individual trace elements (e.g., 25-fold for Co). Note that the variation of interelement ratios is smaller if samples with abnormal contents for some elements (e.g., 8159G) are excluded. More complex compositional variation occurs in clastic sediments when heavy minerals such as zircon, apatite, monazite and titanite are concentrated in some stratigraphic units due to density-controlled hydraulic sorting. Such units will be enriched in some elements entering in the structure of those heavy minerals. In the Okavango sediments, the two samples showing a relatively high content of Zr (BH8158A and BH8351I) are also marked by high Hf and HREE (e.g., Yb) abundances, indicating a minor hydraulic concentration of zircon. In the ternary diagram Th–Sc–Zr (Figure IV-12b), these samples are displaced towards the Zr-apex, indicating a higher amount of zircon compared to other Okavango sediment samples. Monazite is characterised by high abundances of

LREE correlated with high contents of P_2O_5. This mineral and related geochemical trend has not been found in the Okavango sediments. Chemical analyses of bulk-suspended solids led Sawula et al. (1992) to suggest that TiO_2-rich phases (e.g., titanite) were probably among the solid phases transported by the Okavango floodwater. However, our microscopic and XRD data and a detailed scanning electron microscope (SEM) investigation of Okavango sediments conducted by McCarthy and Ellery (1995) did not record TiO_2-rich phases. The excellent correlation between Al_2O_3 and TiO_2 (Figure IV-3b) suggests that both elements are hosted within clay minerals, as previously pointed out by McCarthy and Ellery (1995). Thus, concentration of heavy minerals is not the main factor controlling the chemical variation of the Okavango sediment composition, although zircon concentration does occur in a few samples.

IV.2.8.3. Source area weathering and diagenetic processes

K-feldspar is the only feldspar detected in five out of 11 samples examined for XRD. The apparent absence of plagioclase may be due to its somewhat lower resistance during transport and weathering. The occurrence of both kaolinite and K-feldspar suggests an advanced weathering source. This is supported by the absence of any mafic minerals, which are generally less resistant to weathering. Calcite and dolomite cements are diagenetic. McCarthy and Metcalfe (1990) estimated that 113,000 t· a^{-1} of CaCO3 and 135,000 t. a^{-1} of SiO_2 are accumulating in the Okavango Delta as a result of subsurface precipitation, as opposed to 40,000 t. a^{-1} of clastic sediment. Thus, chemical precipitation is currently a major depositional process in the Okavango basin.

Investigations of siliciclastic sedimentary rocks in several regions of the world show that their chemical composition is largely inherited from the composition of the weathering profiles at the source of sediments (Nesbitt and Young, 1982, 1984, 1989; Nesbitt et al., 1996). Nesbitt and Young (1982) devised the chemical index of alteration (CIA) which provides a good measure of the degree of alteration of the sediments' source rocks. CIA value in the main rock-forming minerals (quartz, plagioclase, alkali feldspars, pyroxene and olivine) is ≤55. Clay minerals yield higher CIA values (usually ≥75), with the highest value (~100) recorded in kaolinite. Shales are characterized by CIA values ~70–75, which reflect the predominance of clay minerals in their composition. The Okavango sediments are marked by a large range of CIA values (52–81) and a negative correlation of SiO2–Al2O3 (Figure IV-5a). These trends reflect a substantial quartz±feldspar dilution-effect.. Petrographic studies (Figure IV-3 and Table IV-1) support this

observation since the Okavango sediments are predominantly made of quartz sand. CIA values ≥80 in sedimentary rocks are indication of a source severely affected by chemical weathering. The Okavango sediments contain kaolinite as the dominant clay mineral, and McCarthy and Ellery (1995) suggest that illuviation of fines, including clays, from the floodwater, into preexisiting aeolian sand occurs beneath frequently flooded areas in the lower Delta.

In the A–CN–K diagram (Figure IV-6), the Okavango sediments define an evolution trend similar to soils developing above igneous bedrocks. However, in the case of the Okavango sediments, this trend should be interpreted with caution, especially when the origin of sediments is considered. The data in Figure IV-6 can be interpreted using a mixing model involving two components: (1) a strongly weathered component plotting close to the A-apex (e.g., sample BH8262C). Kaolinite, which is the most abundant clay in the Okavango sediments (Table IV-1), plots at this apex; (2) a relatively immature component which predominates in the sediments plotting closer to the igneous trend line (e.g., sample BH8159A and BH8158A). Important to keep in mind is that none of the studied samples is a pristine end-member since all the Okavango Delta sediments contain a large proportion of sand but both end-members defined above should be located along the mixing line shown in Figure IV-6. The component marking a source area severely affected by chemical weathering corresponds to the sedimentary fraction transported by the river from the Angolan hinterlands to the Okavango basin. The component from a weakly weathered source area corresponds to the currently active aeolian component of the Okavango sediments. An important observation from these data is that the geochemical trend in the A–CN–K diagram (Figure IV-6) does not, in this case, reflect a progressive unroofing of a weathering profile as is commonly the case in sedimentary rocks (e.g., Nesbitt and Young, 1984, 1989). Therefore, caution should be exercised when interpreting the source area paleoweathering process, using geochemical data from sedimentary packages containing an aeolian input. In such cases, CIA values, evolution trends in A–CN–K diagrams and various other geochemical indicators could underestimate the importance of chemical weathering at the source for the component of the sediment transported by rivers from wetter regions and entering in a sedimentary basin located in a semiarid region.

The range of negative Ce anomalies reported in the Okavango sediment samples may have been associated with the process of soil formation at the source. Changing pH and oxidation state within the weathering profile allows fractionation of REE, leading to the formation of a range of Ce/Ce* (e.g., Duddy, 1980; Braun et al., 1990).

IV.2.8.4. Source rock lithology

The combination of aeolian and fluviatile processes in the Okavango sedimentary records implies a diversity of potential source rock components. Several workers showed that a number of chemical elements are not fractionated by exogene processes and therefore could be used for the identification of sediments source rock lithologies (e.g., Taylor and McLennan, 1985; McLennan et al., 1990). The most important among these elements are REE, HFSE and some transition metals (e.g., Cr, Co and Ni). However, Duddy (1980) and Condie et al. (1995) showed that REE are in some cases redistributed in weathering profiles. Redox-dependent Ce-negative anomalies observed in the Okavango sediments are also an indication of fractionation of this element during weathering, fluvial transportation and/or deposition in the basin. Dupre´ et al. (1996) documented the composition of suspended and dissolved loads and bedloads of the Congo River and showed complex variation trends for REE. For example, there is an inverse correlation between river-dissolved REE with pH (especially at pH>6.5), and a similar correlation has been reported worldwide (e.g., Goldstein and Jacobsen, 1987; Elderfield et al., 1990). However, REE, HFSE and the above transition metals are usually immobile elements concentrated in weathering minerals formed in soils after removal of mobile elements such as the alkali earths. Therefore, these immobile elements are transferred mainly as suspended sediments to the depositional site of sediments. This is supported by the fact that REE, HFSE and transition metal concentrations are up to 10,000 times higher in the suspended load compared to the dissolved load in the major rivers of the world (Goldstein and Jacobsen, 1988; Dupre´ et al., 1996). Therefore, the concentrations of these elements in sedimentary rocks are mainly controlled by their abundances in the clay fraction of suspended sediments. This is supported by the composition of the Okavango sediments showing excellent correlations between REE and Al_2O_3 (Figure IV-10), indicating that the REE is hosted in clay minerals. In this paper, the relationship between immobile elements (REE, HFSE and the transition metals Cr, Co, Ni and V) is used to constrain the source rock lithologies.

V, Cr, Co and Ni are compatible elements during igneous fractionation processes and are generally “depleted” in felsic rocks and “enriched” in mafic–ultramafic rocks. Cr and Ni levels in the Okavango samples are generally lower than in PAAS (cf. silica dilution effect in the Okavango sediments), with the exception of one sample, BH8159G, containing extremely high concentrations of transition metals and MgO (4.5 wt.%), requiring either an ultramafic source or

strong adsorption of transition elements on clays or organic matter during deposition or both. XRD data indicated that this sample contains "V-muscovite". As stressed above, submicroscopic muscovite sensu stricto is rather uncommon in sedimentary rocks, and much of the fine-grained "micaceous" material in sediments is made of muscovite–smectite mixed layers (Deer et al., 1992). Furthermore, it is known that lateritic horizons above ultramafic rocks contain smectites (e.g., Trescases, 1997), and presumably, muscovite–smectite mixed layers as inferred to occur in sample 8159G could accommodate high Cr and Ni contents. The concentration of Al_2O_3 in this sample is relatively low (<2 wt.%), indicating that adsorption on clays is unlikely. The authors' unpublished organic carbon analysis of sample BH8159G (1.02 wt.%) indicates that the high-transition metal content of this sample is not related to an abnormally high abundance of organic carbon. Thus, the most likely interpretation is that the source area lithologies of the Okavango sediments include ultramafic rocks. Cr and Ni show strong positive correlation with MgO and a negative correlation with SiO2 in the Okavango sediments. These trends support the presence of ultramafic–mafic rocks at the source of the sediments. The contribution of felsic source rocks is required by the presence of quartz and kaolinite (after feldspars) in the sediments and by the high content of silica in several samples (Table IV-1). The plot of Cr vs. Ni (Figure IV-7c) and several other binary plots (e.g., Figures IV-5c,e,f, IV-7g,h and IV-8a) show two distinct trendlines, indicating three distinct source end-member compositions. One of these three components is the felsic end-member marked by Cr and Ni concentrations clustered close to the origin of the axes in Figure IV-7c. The other endmembers are two distinct mafic–ultramafic source rocks, one marked by higher Cr content (pyroxene-rich component) and the other marked by higher Ni abundances (olivine-rich component).

The relative contribution of felsic and ultramafic–mafic rock sources should be reflected in the distribution of Zr and Cr–Ni, as these elements monitor zircon from felsic rocks and chromite/pyroxene/olivine from mafic–ultramafic rocks (e.g., Wronkiewicz and Condie, 1987). Co, Ni and Ti abundances are higher in mafic to intermediate rocks, whereas Y and Zr are higher in felsic rocks (e.g., Ishiga and Dozen, 1997). The Cr/Zr ratio is expected to decrease if zircons are concentrated by hydraulic sorting in the sedimentary process. The Cr/Zr ratios in the Okavango sediments (Table IV-3) show a large range, from low values, 0.04 (e.g., sample BH8158F), identical to values in sediments originating from a felsic source rock, up to high values, ~1.4 (sample BH8162D), reflecting a predominantly mafic source rock. The high Cr/Zr value of ~13 in sample BH8159G indicates ultramafic source rocks. Most Okavango sediments have Cr/Zr between these two end-members, indicating a source made of bimodal felsic/mafic

rocks and/ or intermediate rocks. A similar conclusion is reached using Y/Ni ratios that are identical to values in sediments from felsic sources for sample BH8348F and from an ultramafic–mafic source for sample BH8159G. The Okavango sediments are commonly marked by values intermediate between these two end-members.

The ternary plots La–Th–Sc, Th–Sc–Zr and Th–Hf–Co (Figure IV-12) have been used to deduce the composition of sediments source rocks (Bhatia, 1983; Taylor and McLennan, 1985; Bhatia and Crook, 1986; Camire´ et al., 1993; Jahn and Condie, 1995). Th is typically concentrated in felsic rocks, whilst Sc, although a member of the same group (III) of the periodic table, is more concentrated in mafic rocks. This is due to the much smaller size of the Sc ion, allowing it to enter early crystallizing pyroxenes (Taylor and McLennan, 1985). The Okavango sediments define a single evolutionary trend in the La–Th–Sc, supporting a bimodal ultramafic–mafic and felsic source rock association. The nonquartz component of sample BH8159G, marked by extremely high Sc, Cr and Ni, represents a sedimentary material produced almost exclusively from ultramafic–mafic rocks, whereas that in the sample BH8348H corresponds to a sedimentary material originating almost exclusively from felsic rocks. The range of Eu/Eu* values for sands/sandstones derived from felsic and mafic sources partly overlaps, and the Eu/Eu* ratios for samples BH8159G and BH8348H (Table IV-3) fall in the common field to sediments from mafic and felsic source rocks. In addition, the range of Eu/Eu* in Okavango Delta sediments (Table IV-3) also requires both felsic and ultramafic–mafic source rocks. Important to note is that, in Figure IV-12c, the composition of the sample BH8262B overlaps with that of the sample CKP11220, which represents Proterozoic granitoids exposed in NW Botswana and in adjacent countries (Angola and Namibia). These granitoids represent a potential felsic end-member source rock lithology for the Okavango sediments.

The distribution of analyses in the diagrams Th–Sc–Zr (Figure IV-12b) and Th–Hf–Co (Figure IV-12c) supports the involvement of at least three distinct source rocks for the Okavango sediments. Quantitative modelling (Table IV-5) was performed using analyses of potential source rocks from the catchment area (Kampunzu, unpublished data) represented by CKP11220 and CKP10926B (granite), CKP11277 (gabbro) and CKP10A299 (ultramafic rock). In this quantification, quartz (SiO_2) was used as one additional mixing component to accommodate the aeolian input, and carbonates (CaO–MgO) were used to accommodate diagenetic calcite/dolomite components. In sediments containing substantial diagenetic carbonates where CaO–MgO were added during quantification, higher least square values were obtained probably because the CO_2

content of carbonates was not taken into consideration. Otherwise, the results from the mixing calculations in carbonate-poor samples yield calculated compositions (Table IV-5) matching the compositions of Okavango Delta sediments, as shown by least square values of <1. This indicates that the CKP samples listed above represent realistic potential source rocks for the Okavango sediments.

Table IV 5. Results from quantitative modelling using major and REEs

Sample	Composition	Least squares
8157f	15% CKP 11220	0.99
	4% CKP 10296B	
	81% SiO2	
8158f	9% CKP 11220	0.42
	91% SiO2	
8159g	18% CKP 11277	7.8
Without	15% CKP 10A299	
Al2O3	11% CKP 10296B	
	45% SiO2	
	3% MgO	
	8% CaO	
8158h	11% CKP 11220	0.83
	1% CKP 10A299	
	3% CKP 10296B	
	85% SiO2	
8162k	12% CKP 11220	1.8
	2% CKP 11277	
	7% CKP 10296B	
	78% SiO2	
	1% CaO	
8159t	4% CKP 11220	1.7
	5% CKP 11277	
	4% CKP 10A299	
	1% CKP 10296B	
	82% SiO2	
	1% MgO	
	3% CaO	

IV.2.9. Conclusions

The Okavango sediments are mainly sands, with variable proportions of silt, clays and carbonates and show a large variation of most elements. The chemical index of alteration displays a continuous trend and a large range from low CIA values (52) marking minimal chemical weathering corresponding to the currently active aeolian component of the Okavango sediments up to high CIA values (81) indicating severe chemical weathering corresponding to a sedimentary fraction transported by the river from the Angolan hinterlands to the Okavango basin.

Elemental compositions, binary diagrams (e.g.,Cr–Ni, V–Ni, Ni–SiO_2, Cr–SiO_2, K_2O–Al_2O_3 and Na_2O–Al_2O_3), interelements ratios (e.g., Cr/Zr, Y/Ni, Th/Cr, Th/Sc, Eu/Eu*, La/Sc and La/Co) and source-rock discrimination diagrams (e.g., Th–Sc–Zr and Th–Hf–Co), supported by quantitative modelling, indicate that the Okavango sediments originate from the mixing of aeolian quartz, diagenetic carbonates and a component derived from three distinct source rock groups, including ultramafic–mafic and felsic source rock association, with or without input of intermediate source rocks. Proterozoic granitoids and mafic–ultramafic rocks exposed in NW Botswana and in adjacent countries (Angola and Namibia) represent source rocks for the Okavango sediments.

Acknowledgements

This research project was funded by the University of Botswana Research and Publication Fund (RP 680-063). The Botswana Geological Survey is acknowledged for allowing us to sample the boreholes used for this study. Water Resources Consultants is acknowledged for assistance with grain size data. A. Jellema is acknowledged for assistance with Figure IV-2 and J. J. Tiercelin and D. Kolokose for assistance with the thin sections. This is a contribution to SAFARI 2000 Research Project. The satellite image used in this paper was acquired through that project. This paper benefited significantly from comprehensive reviews by R. Cullers, K. Condie, A. Morton and the Chief-Editor K.A.W. Crook, to whom we extend our thanks.

This paper is dedicated to the memory of Prof. A.B. Kampunzu, a friend, colleague, and mentor, whose profound knowledge, enthusiasm, and desire to help others will continue to be an inspiration to all.

References

Bhatia, M.R., 1983. Plate tectonics and geochemical composition of sandstones. J. Geol. 91, 611 – 627.

Bhatia, M.R., Crook, K.A.W., 1986. Trace element characteristics of graywackes and tectonic setting discrimination of sedimentary basins. Contrib. Mineral. Petrol. 92, 181–193.

Bock, B., McLennan, S.M., Hanson, G.N., 1998. Geochemistry and provenance of the Middle Ordovician Austin Glen Member (Normanskill Formation) and the Taconian Orogeny in New England. Sedimentology 45, 635– 655.

Braun, J.J., Pagel, M., Muller, J.P., Bilong, P., Michard, A., Guillet, B., 1990. Cerium anomalies in laterite profiles. Geochim. Cosmochim. Acta 54, 791–795.

Camire´, G.E., Lafle`che, M.R., Ludden, J.N., 1993. Archaean metasedimentary rocks from the northwestern pontiac subprovince of the Canadian shield; chemical characterization, weathering and modelling of the source areas. Precambrian Res. 62, 285– 305.

Carney, J.N., Aldiss, D.T., Lock, N.P., 1994. The geology of Botswana. Geol. Surv. Dep., Lobatse, Botswana, p. 113.

Condie, K.C.,Wronkiewicz, D.J., 1990. A new look at the Archean– Proterozoic boundary: sediments and the tectonic setting constraint.In: Naqvi, S.M. (Ed.), Precambrian Continental Crust and its Economic Resources. Elsevier, Amsterdam, pp. 61– 84.

Condie, K.C., Dengate, J., Cullers, R.L., 1995. Behaviour of rare earth elements in a paleoweathering profile on granodiorite in the Front Range, Colorado, USA. Geochim. Cosmochim. Acta 59, 279–294.

Cullers, R.L., 1994a. The controls on the major and trace element variations of shales, siltstones, and sandstones of Pennsylvanian –Permian age from uplifted continental blocks in Colorado to platform sediment in Kansas, USA. Geochim. Cosmochim. Acta 58, 4955–4972.

Cullers, R.L., 1994b. The chemical signature of source rocks in size fractions of Holocene stream sediment derived from metamorphic rocks in the Wet Mountains region, USA. Chem. Geol. 113, 327– 343.

Cullers, R.L., 2000. The geochemistry of shales, siltstones and sandstones of Pennsylvanian–Permian age, Colorado, USA: implications for provenance and metamorphic studies. Lithos 51, 181– 203.

David, K., Schiano, P., Alle`gre, C.J., 2000. Assessment of the Zr/Hf fractionation in oceanic basalts and continental materials during petrogenetic processes. Earth Planet. Sci. Lett. 178, 285– 301.

Deer, W.A., Howie, R.A., Zussman, J., 1992. An Introduction to the Rock-Forming Minerals, 2nd ed. Longman Group Limited, Essex, England. 696 pp.

Dickinson, W.R., Suczec, C.A., 1979. Plate tectonics and sandstone compositions. Am. Assoc. Pet. Geol. Bull. 63, 2171.

Duddy, I.R., 1980. Redistribution and fractionation of rare earth and other elements in a weathering profile. Chem. Geol. 30, 363– 381.

Dupre´, B., Gaillardet, J., Rousseau, D., Alle`gre, C.J., 1996. Major and trace elements of river-borne material: the Congo Basin. Geochim. Cosmochim. Acta 60, 1301– 1321.

DWA (Department of Water Affairs), 1997. Appendix B: geomorphology and sedimentology. Maun Groundwater Development Project Phase 1. Water Affairs Department, Gaborone, Botswana. prepared by Eastend Investments.

Elderfield, H., Upstill-Goddard, R., Sholkovitz, E.R., 1990. The rare earth element in rivers, estuaries, and coastal seas and their significance to the composition of ocean waters. Geochim Cosmochim. Acta 54, 971– 991.

Fedo, C.M., Eriksson, K.A., Krogstad, E.J., 1996. Geochemistry of shales from the Archaean (~3.0 Ga) Buhwa Greenstone Belt, Zimbabwe: implications for provenance and source-area weathering. Geochim. Cosmochim. Acta 60, 1751–1763.

Gao, S., Wedepohl, K.H., 1995. The negative Eu anomaly in Archean sedimentary rocks: implications for decomposition, age and importance of their granitic sources. Earth Planet. Sci. Lett. 133, 81– 94.

Garver, J.I., Royce, P.R., Smick, T.A., 1996. Chromium and nickel in shale of the Taconic foreland: a case study for the provenance of fine-grained sediments with an ultramafic source. J. Sediment. Res. 100, 100– 106.

Goldstein, S.J., Jacobsen, S.B., 1987. The Nd and Sr isotopic systematics of river-water dissolved material: implications for the sources of Nd and Sr in seawater. Chem. Geol. 66, 245–272.

Goldstein, S.J., Jacobsen, S.B., 1988. Rare earth elements in river waters. Earth Planet. Sci. Lett. 89, 35– 47.

Gromet, L.P., Dymek, R.F., Haskin, L.A., Korotev, R.L., 1984. The North American shale composite: its compilation, major and trace element characteristics. Geochim. Cosmochim. Acta 48, 2469– 2482.

Hassan, S., Ishiga, H., Roser, B.P., Dozen, K., Naka, T., 1999. Geochemistry of Permian–Triassic shales in the Salt Range, Pakistan: implications for provenance and tectonism at the Gondwana margin. Chem. Geol. 158, 293–314.

Ishiga, H., Dozen, K., 1997. Geochemical indications of provenance change as recorded in Miocene shales: opening of the Japan Sea, San'in region, southwest Japan. Mar. Geol. 144, 211 –228.

Jahn, B.M., Condie, K.C., 1995. Evolution of the Kaapvaal Craton as viewed from geochemical and Sm–Nd isotopic analyses of intracratonic pelites. Geochim. Cosmochim. Acta 59, 2239– 2258.

Kampunzu, A.B., Akanyang, P., Mapeo, R.B.M., Modie, B.N., Wendorff, M., 1998a. Geochemistry and tectonic significance of Mesoproterozoic Kgwebe metavolcanic rocks in northwest Botswana: implications for the evolution of the Kibaran Namaqua–Natal Belt. Geol. Mag. 133, 669– 683.

Kampunzu, A.B., Bonhomme, M.G., Kanika, M., 1998b. Geochronology of volcanic rocks and evolution of the Cenozoic Western branch of the East African rift system. J. Afr. Earth Sci. 26, 441–461.

Kampunzu, A.B., Armstrong, M.P., Modisi, M.P., Mapeo, R.B., 1999. The Kibaran belt in southwest Africa: ion microprobe U– Pb zircon data and definition of the Kibaran Ngami belt in Botswana, Namibia and Angola. Gondwana Res. 2, 571–572.

Kampunzu, A.B., Armstrong, R.A., Modisi, M.P., Mapeo, R.B.M., 2000. Ion microprobe U–Pb ages on single detrital zircon grains from Ghanzi Group: implications for the identification of a Kibaran-age crust in northwestern Botswana. J. Afr. Earth Sci. 30, 579–587.

Lahtinen, R., 2000. Archaean–proterozoic transition: geochemistry, provenance and tectonic setting of metasedimentary rocks in central Fennoscandian Shield, Finland. Precambrian Res. 104, 147–174.

Le Gall, B., Tshoso, G., Jourdan, F., Fe´raud, G., Bertrand, H., Tiercelin, J.J., Kampunzu, A.B., Modisi, M., Dyment, J., Maia, M., 2002. Ar–Ar geochronology and structural data from the Okavango giant mafic dike swarm, Karoo large igneous province, N Botswana. Earth Planet. Sci. Lett. 202, 595–606.

Mapeo, R.B.M., Armstrong, R.A., Kampunzu, A.B., 2000. Ages of detrital zircon grains from Neoproterozoic siliciclastic rocks in Shakawe area: implications for the evolution of the Proterozoic crust in northern Botswana. S. Afr. J. Geol. 103, 156–161.

Mapeo, R.B.M., Armstrong, R.A., Kampunzu, A.B., 2001. Ion microprobe U–Pb zircon geochronology of gneisses from the Gweta borehole, NE Botswana: implications for the Paleoproterozoic Magondi belt in southern Africa. Geol. Mag. 138, 299–308.

McCarthy, T.S., Ellery, W.N., 1995. Sedimentation on the distal reaches of the Okavango fan, Botswana, and its bearing on calcrete and silcrete (Ganister) formation. J. Sediment. Res., Sect. A Sediment. Pet. Proc. 65, 77– 90.

McCarthy, T.S., Metcalfe, J., 1990. Chemical sedimentation in the semi-arid environment of the Okavango Delta, Botswana. Chem. Geol. 89, 157–178.

McCarthy, T.S., Stanistreet, I.G., Cairncross, B., 1991. The sedimentary dynamics of active fluvial channels on the Okavango fan, Botswana. Sedimentology 38, 471– 487.

McCarthy, T.S., Green, R.W., Franey, N.J., 1993. The influence of neo-tectonics on water dispersal in the northeastern regions of the Okavango swamps, Botswana. J. Afr. Earth Sci. 17, 23– 32.

McCarthy, T.S., Cooper, G.R.J., Tyson, P.D., Ellery, W.N., 2000. Seasonal flooding in the Okavango Delta, Botswana—recent history and future prospects. S. Afr. J. Sci. 96, 25–33.

McLennan, S.M., Taylor, S.R., Eriksson, K.A., 1983. Geochemistry of Archean shales from the Pilbara Supergroup, Western Australia. Geochim. Cosmochim. Acta 47, 1211– 1222.

McLennan, S.M., Taylor, S.R., McCulloch, M.T., Maynard, J.B., 1990. Geochemistry and Nd–Sr isotopic composition of deep sea turbidites: crustal evolution and plate tectonic associations. Geochim. Cosmochim. Acta 54, 2015– 2050.

Modisi, M.P., 2000. Fault system of the southeastern boundary of the Okavango Rift, Botswana. J. Afr. Earth Sci. 30, 569– 578.

Modisi, M.P., Atekwana, E.A., Kampunzu, A.B., Ngwisanyi, T.H., 2000. Rift kinematics during the incipient stages of continental extension: evidence from nascent Okavango rift basin, northwest Botswana. Geology 28, 939– 942.

Nesbitt, H.W., Young, G.M., 1982. Early Proterozoic climates and plate motions inferred from major element chemistry of lutites. Nature 299, 715– 717.

Nesbitt, H.W., Young, G.M., 1984. Prediction of some weathering trends of plutonic and volcanic rocks based on thermodynamic and kinetic considerations. Geochim. Cosmochim. Acta 48, 1523– 1534.

Nesbitt, H.W., Young, G.M., 1989. Formation and diagenesis of weathering profiles. J. Geol. 97, 129– 147.

Nesbitt, H.W., Young, G.M., McLennan, S.M., Keays, R.R., 1996. Effect of chemical weathering and sorting on the petrogenesis of siliciclastic sediments, with implications for provenance studies. J. Geol. 104, 525– 542.

Plank, T., Langmuir, C.H., 1998. The chemical composition of subducting sediment and its consequences for the crust and mantle. Chem. Geol. 145, 325– 394.

Reeves, C.V., 1978. The gravity survey of Ngamiland: 1970–71. Geol. Surv. Botsw., Bull. 11, 84 pp.

Ringrose, S., Huntsman-Mapila, P., Kampunzu, A.B., Downey, W., Coetzee, S., Vink, B., Matheson, W., Vanderpost, C., 2005. Sedimentological and geochemical evidence for palaeo-environments in Makgadikgadi sub-basin, in relation to the MOZ rift depression, Botswana. Palaeogeogr. Palaeoclimatol. Palaeoecol. (in press).

Roser, B.P., Korsch, R.J., 1988. Provenance signatures of sandstone –mudstone suites determined using discriminant function analysis of major-element data. Chem. Geol. 67, 119–139.

Sawula, G., Martins, E., Nengu, J., Themner, K., 1992. Notes on trace metals in the Boro River, Okavango Delta. Botsw. Notes Rec. 24, 135– 149.

Taylor, S.R., McLennan, S.M., 1985. The Continental Crust: Its Composition and Evolution. Blackwell Scientific, Oxford. 312 pp.

Taylor, S.R., McLennan, S.M., 1995. The geochemical evolution of the continental crust. Rev. Geophys. 33, 241–265.

Thomas, D.S.G., Shaw, P.A., 1991. The Kalahari Environment. Cambridge University Press, Cambridge. 284 pp.

Toulkeridis, T., Clauer, N., Krfner, A., Reimer, T., Todt, W., 1999. Characterization, provenance, and tectonic setting of Fig Tree greywackes from the Archaean Barberton Greenstone Belt, South Africa. Sediment. Geol. 124, 113–129.

Trescases, J.-J., 1997. The lateritic nickel–ore deposits. In: Paquet, H., Clauer, N. (Eds.), Soils and Sediments. Mineralogy and Geochemistry. Springer Verlag, Berlin, pp. 125– 138.

Wronkiewicz, D.J., Condie, K.C., 1987. Geochemistry of Archean shales from the Witwatersrand Supergroup, South Africa: source-area weathering and provenance. Geochim. Cosmochim. Acta 51, 2401– 2416.

V. SEDIMENT GEOCHEMISTRY, PROVENANCE AND TECTONIC SETTING: APPLICATION OF DISCRIMINATION DIAGRAMS TO VERY EARLY STAGE OF INTRACONTINENTAL RIFT EVOLUTION, WITH EXAMPLES FROM THE OKAVANGO AND SOUTHERN TANGANYIKA RIFT BASINS

V.1. Géochimie et provenance des sédiments, contexte tectonique : application des diagrammes de discrimination aux sédiments des phases précoces d'un rift intracontinental, exemples des bassins de l'Okavango et du Sud Tanganyika.

Résumé de l'article

Dans ce papier, nous avons appliqués des diagrammes de variations et de discrimination tectonique aux données géochimiques acquises sur des sédiments Quaternaires de bassins de rift précoce du Rift Est Africain. Nous avons utilisé des échantillons de deux segments du rift correspondant à deux phases différentes d'évolution: le cône alluvial naissant de l'Okavango et le bassin lacustre mature du Lac Tanganyika. Nous avons définis deux nouveaux domaines dans le champ des marges passives du diagramme de discrimination tectonique préexistant. Nos échantillons sont en général, enrichis en SiO_2 et appauvris en Na_2O, CaO and TiO_2 ce qui reflète le fort degré de maturité de ces sédiments. La distinction entre le domaine des sédiments de l'Okavango et ceux du Tanganyika est évidente et se manifeste largement dans les concentrations de SiO_2 et d'Al_2O_3. La géochimie des sédiments du Lac Tanganyika de sous-bassin du Mpulungu indique que la source immédiate de matériel est une roche sédimentaire quartzeuse mais que la source ultime est felsique. Celle ci est représentée dans la région par les grès de la formation de Mbala et le socle granitique qui affleurent tous deux au sud du lac. Les sédiments de l'Okavango proviennent de roches sources felsiques et mafiques à ultramafiques avec probablement une source immédiate sédimentaire quartzeuse.

V.2 Sediment geochemistry, provenance and tectonic setting: Application of discrimination diagrams to very early stages of intracontinental rift evolution, with examples from the Okavango and Southern Tanganyika rift basins

P. Huntsman-Mapila[1,2,*], J-J. Tiercelin[2], M. Benoit[2], J. Cotten[2], C. Hémond[2]

[1] *Harry Oppenheimer Okavango Research Centre, University of Botswana, P/Bag 285, Maun, Botswana*
[2]*UBO-CNRS UMR 6538, Institut Universitaire Européen de la Mer, 29280 Plouzané, France*
**Author for correspondence (email*: pmapila@orc.ub.bw)*

Article to be submitted to the Journal of African Earth Sciences

V.2.1.Introduction

The significance of sedimentary geochemistry in determining the provenance of sedimentary suites, their evolution, and source weathering is well established in the literature (Bhatia, 1983; Condie et al., 1995; Cullers, 1994a and b; Cullers et al., 1987, 1988; McLennan et al., 1990, 1993; Roser and Korsch, 1986; Roser and Korsch, 1988; Wronkiewicz and Condie 1987). The relationship between the tectonic setting and variables such as provenance, relief, physical sorting and weathering control the composition of sediments. Immobile trace element compositions and rare earth element (REE) abundances of sediments are good indicators of source rock chemistry, since these elements are little-fractionated by sedimentary processes and low grade metamorphism (Taylor and McLennan, 1985; McLennan, 1989) whilst more mobile elements are helpful for understanding weathering regimes and palaeoenvironmental conditions (Nesbitt and Young, 1984; Fedo et al., 1996).

Tectonic processes give a distinctive geochemical signature to sediments in two ways: 1) tectonic settings have characteristic provenance signals and 2) they are characterized by their sedimentary processes (Rollinson, 1993). For sandstones, the relationship between the geochemical composition, the provenance of sediments and the tectonic setting can be a useful tool in elucidating information from ancient rocks. The use of major (Bhatia, 1983; Roser and Korsch, 1986; 1988). and trace element (Bhatia and Crook, 1986) compositions in diagnostic diagrams has been shown to be useful in determining tectonic settings.

In order to test the accuracy of various diagnostic diagrams for tectonic setting of ancient sediments, they should be tested against modern sediments of a known tectonic setting. This has been done in the past (Bhatia, 1983; Bhatia and Crook, 1986; Roser and Korsch, 1986; Roser, 1996) but more data are required on recent sediments of known tectonic setting to validate and refine these established discrimination criteria. In this paper, we use data from young (late Pleistocene to Holocene) sediments from a known tectonic setting, the East African Rift System (EARS), an early stage rifted basin, to establish how well discriminant diagrams and bivariate plots of tectonic settings categorize these sediments. Attention has been devoted to very early stages of rift creation, using examples of two rift segments at two different stages of evolution in the EARS for which we attempt to define new fields.

The aims of this study are therefore 1) to compare the tectonic fields defined for Lake Tanganyika and Okavango Delta sediments and establish how the results correspond with existing tectonic classifications; 2) to define fields for early stage rift sediments (both nascent alluvial fan (NAF) and mature lacustrine basin (MLB)) within the passive margin setting and 3) and finally we use our data to establish the provenance of the Lake Tanganyika sediments from the Mpulungu sub-basin.

V.2.2. Geological setting

V.2.2.1. Classification of tectonic settings

Bhatia (1983) describes a simplified tectonic classification of continental margins and oceanic basin based on geochemical composition. The author defines fields for four tectonic settings being Oceanic Island Arc (OIA), Continental Island Arc (CIA), Active Continental Margins (ACM) and Passive Margins (PM). The field defined for passive margins include a wide range of tectonic environments, from rifted continental margins of the Atlantic-ocean type, sedimentary basins near to collision orogens and inactive or extinct convergent margins (Bhatia, 1983; Bhatia and Crook, 1986). Passive margin settings have also been grouped into pre-rift, rift-valley or graben and Atlantic-type trailing edges. Passive margin sediments are highly mature and derived from recycling of older sedimentary or metamorphic rocks (Bhatia, 1983).

V.2.2.2. Description of rift settings

Rift basins, which develop in continental crust, will, if the rifting process continues, lead to the development of an ocean basin flanked by passive margins. They generally consist of a suite of individual half-grabens (50-100 km long and 20-80 km wide) bounded by major normal faults. They can be filled with both continental and marine deposits. Rift creation demonstrates several successive stages of structural and sedimentary evolution, according to pre-rift and syn-rift structural and magmatic conditions. Successive stages of rift evolution were proposed on the basis of the interpretation of seismic sequences identified in the Lake Tanganyika Trough (PROBE Project; Burgess, 1985). In this paper, attention has been devoted to very early stages of rift creation, using examples of two rift segments at two different stages of evolution in the EARS. Such early stages were tentatively illustrated by recent to modern tectonic and sedimentary environments observed in the Southern Complex of the EARS (Tiercelin and Mondeguer, 1991), and more particularly by the Okavango Basin and the southern end of the Lake Tanganyika Trough, that represent two successive phases in the very early stage of rift creation.

The early initiation stage in the development of a continental rift is characterized by the development of shallow half-graben basins where nascent faults exert a primary control in drainage evolution and the formation of catchments (Gawthorpe and Leeder, 2000). This stage is illustrated by the present Okavango alluvial fan located in a broad subsiding half-graben, strongly controlled by fault growth (Modisi, 2000). The immediate successive stage concerns the development of deeper basins where swamps and shallow lacustrine environments (<50 m water depth) occur, as the result of fault growth and propagation, and initiation of basin subsidence. A more mature stage concerns the development of well-defined, actively subsiding half-graben basins, where propagation and interaction between fault segments lead to basin linkage and strong control of drainage. Wider and deeper lacustrine environments characterize this stage, which is illustrated by the southern Mpulungu subbasin of Lake Tanganyika.

V.2.2.3. The East African Rift System

The East African Rift System is a vast Cenozoic structure with a length of more than 4500 km, extending from Afar in the north to the south of the African continent (Botswana, Mozambique) (Figure V-1). It is a major intracontinental extension zone, with two main branches characterized

by N-S to NNE-SSW oriented deep troughs, mainly half-grabens. The Eastern Branch with a length of 1800 km extends from the Afar Depression to the Kenya Rift and the North Tanzanian Divergence. The early phases of rifting characterizing this branch are dated from Eocene - Lower Oligocene and resulted in major fissural volcanic activity and half-graben development in northern Kenya and southern Ethiopia (Morley et al., 1992; Ebinger and Ibrahim, 1994; Ebinger et al., 2000; Tiercelin et al., 2004). Extensive volcanism is a main characteristic of this part of the rift, and is represented by volcanism which developed from the early Cenozoic and is active up to present (Morley, 1999; Chorowicz, 2005).

The Western Branch, with a length of 2500 km, is more complex in structure and includes the Lake Tanganyika and Lake Malawi Troughs, which are the two largest and deepest structures of the EARS. Compared to the Eastern Branch, the Western Branch is marked by having only a few volcanic provinces which are: Virunga, Kivu and Rungwe (Figure V-1). Initial volcanic activity occurred in these regions at about 8 Ma (Ebinger et al., 1989). Two major NW-SE-trending transcurrent fault zones, the Aswa Fault Zone and the TRM (Tanganyika-Rukwa-Malawi) Fault Zone, act as links between the Eastern and Western Branches, and between segments of the Western Branch, respectively. These transverse structures are recognized as Late Precambrian features reactivated during the Cenozoic rifting phases (McConnell, 1980).

To the southwest, a suite of half-graben basins extends from the southern Tanganyika-northern Malawi region in a NE-SW direction, forming the “Southern Complex” (Mondeguer et al., 1989; Tiercelin and Mondeguer, 1991) (Figure V-1). This Southern Complex, which includes the Okavango Basin, contrasts to the main directions of the other branches of the EARS as it is much younger than the other segments of EARS and has no record of volcanic activity during the Cenozoic.

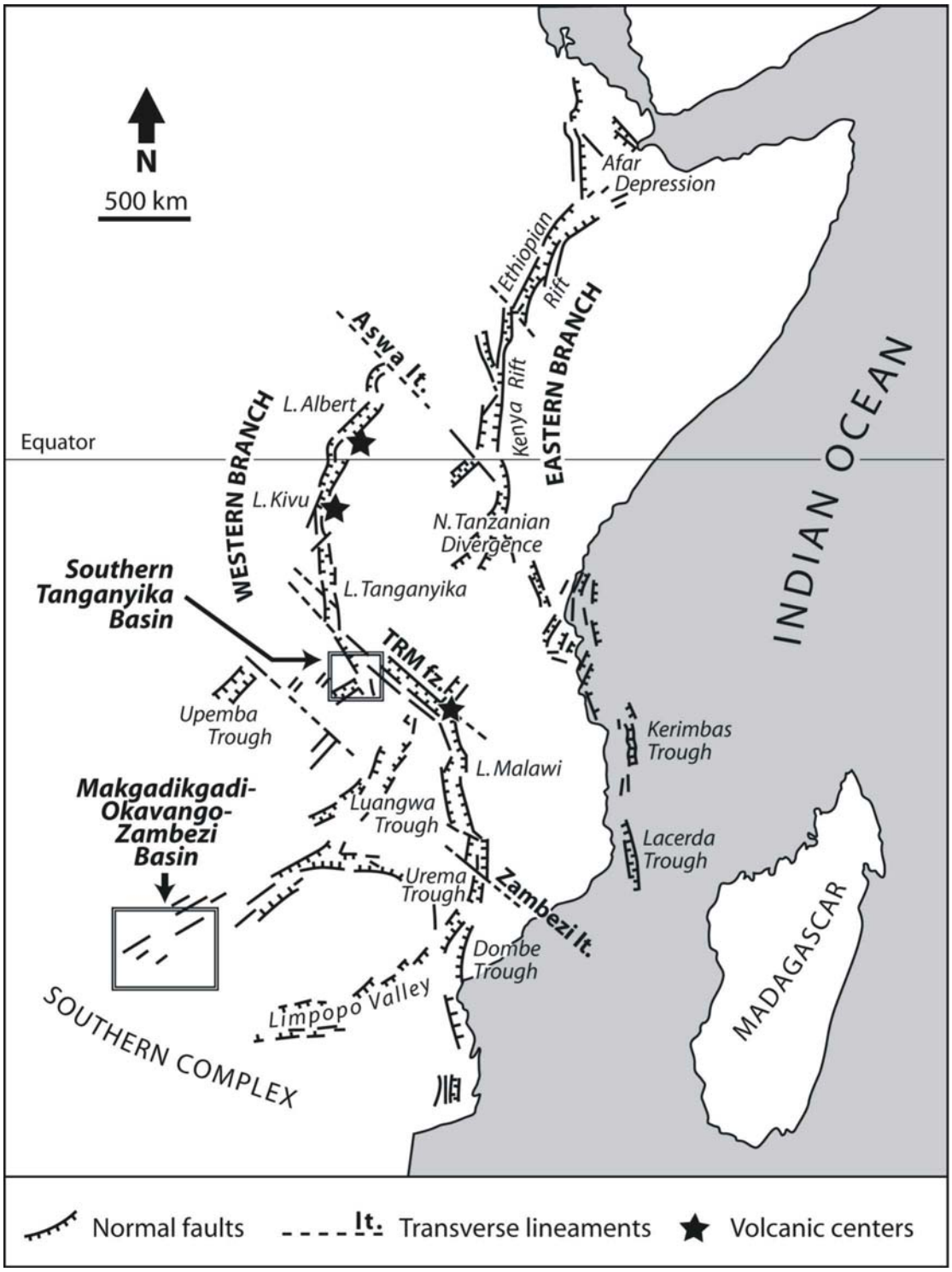

Figure V 1. Map of East African Rift System showing the Western and Eastern Branches and the Southern Complex. Boxes show location of study areas.

V.2.2.4. Okavango Delta setting

The Okavango Basin is a typical half-graben (McCarthy et al., 1993; Modisi, 2000; Modisi et al., 2000) which is considered as the extreme end of a suite of rift basins extending northeast-southwest from west of Lake Tanganyika and Malawi basins, known as the "Southern Complex" (Mondeguer et al., 1989) (Figure V-1). On the basis of geophysical characteristics (Reeves, 1972; Shudofsky, 1985; Ballard et al., 1987), this Southern Complex appears as a broad tectonically active zone that is interpreted as a nascent southwestern branch of the East African Rift System (Reeves, 1972). The Okavango Basin is located within the wider Kalahari Basin, which is a shallow intracontinental basin. This half-graben is today occupied by a large inland alluvial fan of extremely uniform gradient (Gumbrict et al., 2001) fed by the Okavango River which enters the Okavango Basin through a narrow NW–SE-trending swamp called the Panhandle (Figure V-2). Unlike Lake Tanganyika with its high escarpments, the NE-SW orientated Thamalakane and Kunyere Faults, which bound the basin to the south, are barely visible from the surface with the exception of the escarpment on the southern shore of Lake Ngami (Huntsman-Mapila et al., 2006).

The Okavango Delta overlies Precambrian igneous –metamorphic rocks that include the following main units (Figure V-2): (1) Paleoproterozoic ~2.05 Ga augen gneiss, granites and amphibolites exposed in the Qangwa area (Kampunzu and Mapeo, unpublished data) and 2.03 Ga granulites exposed in the Gweta area (Mapeo and Armstrong, 2001); (2) Mesoproterozoic 1.2–1.0 Ga gabbros, granites, metarhyolites and metabasalts (Kampunzu et al., 1998b, 1999); (3) Neoproterozoic siliciclastic and carbonate sedimentary rocks forming a blanket above older Proterozoic rocks (Kampunzu et al., 2000; Mapeo et al., 2000); (4) Karoo Supergroup, including mainly siliciclastic sedimentary rocks deposited during the Permo-Carboniferous and mafic lavas and dolerites emplaced between ca. 181–179 Ma (Carney et al., 1994; Le Gall et al., 2002).

Elemental compositions, binary diagrams, interelements ratios and source-rock discrimination diagrams supported by quantitative modeling, indicate that the Okavango sediments originate from the mixing of reworked aeolian quartz, diagenetic carbonates and a component derived from three distinct source rock groups, including ultramafic–mafic and felsic source rock association, with or without input of intermediate source rocks. Proterozoic granitoids and mafic–ultramafic

rocks exposed in NW Botswana and in adjacent countries (Angola and Namibia) represent source rocks for the Okavango sediments (Huntsman-Mapila et al., 2005).

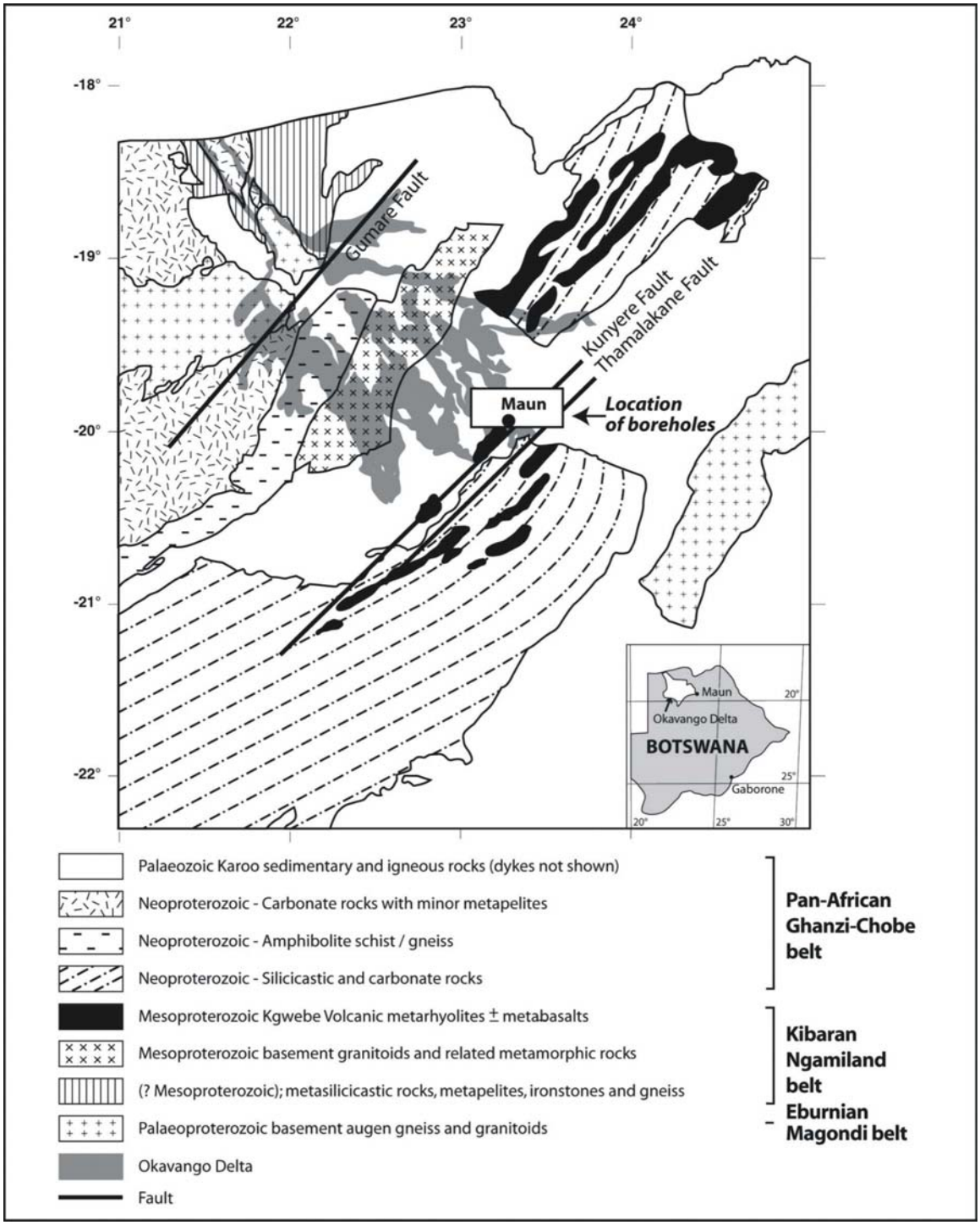

Figure V 2. Precambrian geology map of NW Botswana (Kampunzu et al., 2000). Box shows location of boreholes. Inset: location of the Okavango Delta in Botswana

V.2.2.5. Lake Tanganyika setting

The Lake Tanganyika Trough (3° 30'-8° 50' S, 29°-31°20' E) is the largest structure of the Western Branch of the EARS. It is structurally divided into two main basins, the northern basin orientated N0^{o,} and the southern basin oriented in the N150^{o} direction, separated by N130-150°-trending horst block called the Kalemie-Mahali shoal (Mondeguer, 1991) (Figure V-3 a and b). These two basins are occupied by Lake Tanganyika, which is 650 km long and the deepest of the African rift lakes at 1470 m. The basin geometry and stratigraphy of the Tanganyika Basin were documented by the seismic reflection studies of Projects PROBE and GEORIFT (Rosendahl et al., 1986, 1988; Tiercelin and Mondeguer, 1991; Lezzar et al., 1996). The central part of the basin is known to contain a >5-km thick sequence of rift-related sediments (Rosendahl et al., 1986; Morley, 1988). Age estimates by Cohen et al. (1993) suggest that the central segment of the Tanganyika Basin began to form between 9 and 12 Ma, whereas the northern basin, characterized by a 4-km-thick sequence of sediments (Rosendahl et al., 1986; Ebinger, 1989), formed more recently, at 7-8 Ma. The southern end of the basin, known as the Mpulungu sub-basin (Mondeguer, 1991), contains a 2.5 km thick pile of rift sediments with an estimated age of 4-2 Ma. The Mpulungu sub-basin is 100 km long, 25 km wide with up to 800 m water depth. (Figure V-3 b) The sub-basin is delineated by three groups of faults: a main group trending N150° forming the Mpulungu Border Fault characterized by important vertical throw of at least 2000 m, a second group of faults oriented N70 that develops on the western flank of the Mpulungu Basin, and a minor group of faults oriented N30°, respectively. The two main groups of faults deeply intersect the Upper Precambrian tabular terrains of the northern side of the Zambian craton (also known as Bangweulu Block) (Unrug, 1984).The craton is of Middle Proterozoic age (around 1820 Ma (Brewer et al., 1979)), and mainly composed of granites, granitoides and metavolcanites; 2) the Mporokoso Group formed of conglomerates, sandstones, quartzites and shales; and 3) the Katanga super-group, that include conglomeratic and quartzitic series overlain by carbonate series (Daly and Unrug, 1983) (Figure V-3 c). To the south-east of the Mpulungu sub-basin is the Rungwe volcanic province (Figure V-3 a), which is the most southern eruptive centre in the EARS western branch. Volcanic activity in the Rungwe started in the Late Miocene (~ 8 Ma) and remained active during the late Pleistocene and Holocene with major pyroclastics eruptions (Harkin, 1960; Ebinger et al., 1989; Williams et al., 1993).

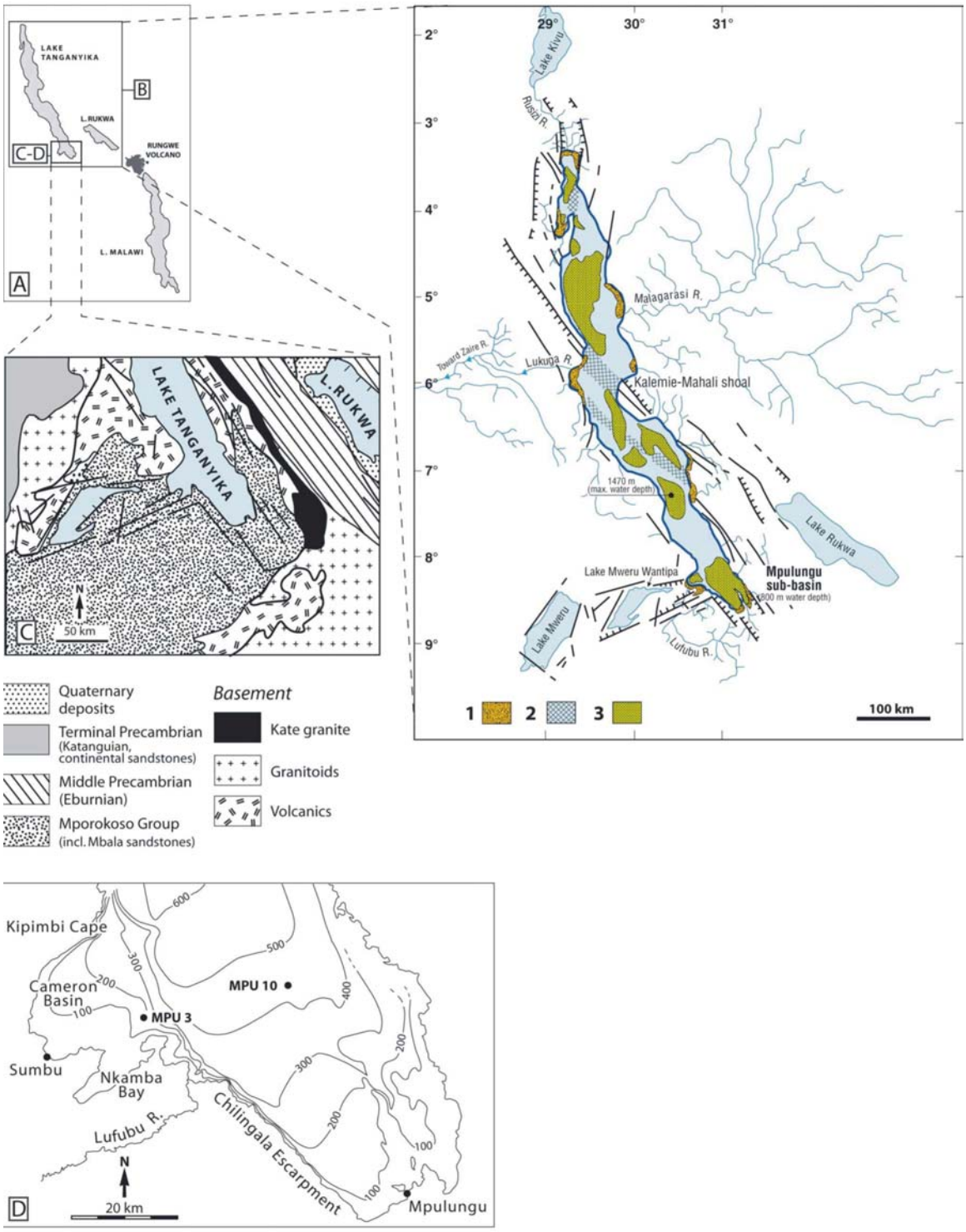

Figure V 3. A) showing location of Lake Tanganyika with respect to the Rungwe volcanic field and Lake Malawi: B) showing the structure and hydrology of Lake Tanganyika. Key 1-littoral platforms; 2-transverse shoals; 3-sub-basin deep zones (after Tiercelin and Mondeguer, 1991): C) geological map of the southern Lake Tanganyika basement (after Mondeguer, 1991); D) Mpulungu sub-basement showing bathymetry and location of MPU-10 and MPU-3 sites.

V.2.3 Description of samples and analysis

For the Okavango sediments, ninety samples were collected at 3-m intervals up to depths of between 69 – 147 m. from seven boreholes drilled during the Maun Groundwater Development Project (DWA, 1997). Details of the samples are given in Chapter IV (Huntsman-Mapila et al., 2005). The Okavango Delta sediments are well sorted fine to medium-grained sands, with variable amounts of carbonates and minor silt and clay (Huntsman-Mapila et al., 2005; DWA, 1997). Chemical analyses of the bulk Okavango sediments were performed at Chemex Laboratories in Canada. Major elements were determined using inductively coupled plasma-atomic emission spectrometry (ICP-AES). Trace and rare earth elements were analysed using inductively coupled plasma –mass spectrometry (ICP-MS) (detection limits generally between 0.1 and 0.5 ppm) with the exception of Li, Cr, Ni and Pb that were determined by flame AAS (detection limits 1 ppm). The precisions are <1% and <10% for major and trace elements, respectively.

Lake Tanganyika sediments were recovered from the Mpulungu sub-basin duirng the GEORIFT Project of Elf-Aquitaine. Several Kullenberg piston cores were collected in December 1985 in the central part of the Mpulungu sub-basin and on the platform/slope of the Cameron Bay (Figure V-3 d) (Mondeguer, 1991). Sediments from two cores have been considered for this study: the MPU-10 core, 8.09 m long, was collected from a water depth of 422 m in the central part of the basin, and the 11.19 m long MPU-3 core was collected from a water depth of 140 m at the limit of the slope between the Cameron Bay and the Mpulungu sub-basin (Figure V-3 d) The MPU-3 core is characterized in the lower part (11.19-7.80 m) by a clastic, quartz-rich, silt-sized facies locally interrupted by diatom-rich laminae. From 7.80 m to the top of the core, the sediments are laminated, diatom-rich, organic muds. MPU-10 core, from the deeper water site, is a dark grey vaguely laminated mud (Mondeguer, 1991). Biogenic sedimentation was occasionally interrupted by wind-blown volcanic ash, interpreted as related to explosive activity in the Rungwe volcanic centre, which resulted in the formation of thin pinkish yellow layers identified at different depth in the various cores collected from the Mpulungu sub-basin (Mondeguer, 1991). Transition between clastic and organic facies at 7.80 m on MPU 3 corresponds to a sedimentary discontinuity which was also identified on high–resolution seismic lines acquired in the Mpulungu sub-basin (Tiercelin et al., 1989). These two cores reflect a suite of climate-controlled lake level fluctuations that, at several times from at least 35000 yr B.P., brought down the level of

Lake Tanganyika to about the –300 m depth contour (Mondeguer et al., 1989; Tiercelin et al., 1989).

For the Lake Tanganyika sediments, analysis of the samples was done on approximately every 20 cm intervals for a total of 80 samples from two cores recovered from the southern part of the Lake Tanganyika basin. A detailed description of the cores and the sample analysis can be found in Chapter VIII. Analysis was done on the bulk samples which were all muds and < 0.63 μm in grain size with the exception of three samples from the MPU-3 core from below the discontinuity at 780 cm. These three samples were sieved using a 0.63 μm sieve. Sample analysis was conducted at IUEM-UBO. Major elements were measured by ICP-AES with an ISA Jobin-Yvon JY 70 Plus apparatus. Trace element and rare earth element (REE) measurements were conducted using ICP-MS using a Finnigan Element 2 ICP-MS.

V.2.4 Results

V.2.4.1 Discrimination diagrams using major elements

Results from the major element data from both the Okavango Delta sediments and the Lake Tanganyika sediments were plotted for tectonic setting discrimination. Plots of TiO_2, Al_2O_3/SiO_2, K_2O/Na_2O and $Al_2O_3/(CaO + Na_2O)$ versus Fe_2O_3 + MgO are shown in Figure V-4. The different fields represented in this diagram are Oceanic island arc (OIA), Continental island arc (CIA), Active continental margin (ACM) and Passive margin (PM) and were drawn from Bhatia, (1983). Values were recalculated on a volatile free basis. It should be noted that for the Okavango samples which have variable amounts of carbonates, only samples with CO_2 < 0.2 wt. % were plotted to avoid the diagenetic input of CaO and MgO. For the Tanganyika samples, diagenetic carbonates represent a negligible component and therefore all samples were used. In addition, volcanic ash samples were removed as they represent the input of unweathered material into the passive margin setting. Important also is that both the Okavango and the Tanganyika samples have an SiO_2 dilution factor – the Okavango sediments from Kalahari aeolian sand and the Lake Tanganyika samples from biogenic silica.

For the plot of TiO_2 wt. % versus Fe_2O_3 + MgO wt. % (Figure V-4 a), the samples from both the Okavango and Tanganyika fall predominantly in the PM field with some overlap into the ACM

field. Figure V-4 b shows the plot of Al_2O_3/SiO_2 versus Fe_2O_3 + MgO wt. %. Again, the Okavango and Tanganyika samples trend predominantly towards the PM field. However, the Tanganyika samples have higher Al_2O_3/SiO_2 ratios than the represented field. This is because the fields were drawn for sands and sandstones where as the Tanganyika samples, being muds, have a higher content of Al_2O_3. Figure V-4 c of K_2O/Na_2O versus Fe_2O_3 + MgO wt. % has a broad range of samples but with all samples falling within the PM field. The plot of $Al_2O_3/(CaO + Na_2O)$ again has a broad range, due to Al_2O_3 from the Tanganyika samples, but the samples from both Okavango and Tanganyika fall predominantly within the PM field with minor overlap with the ACM field.

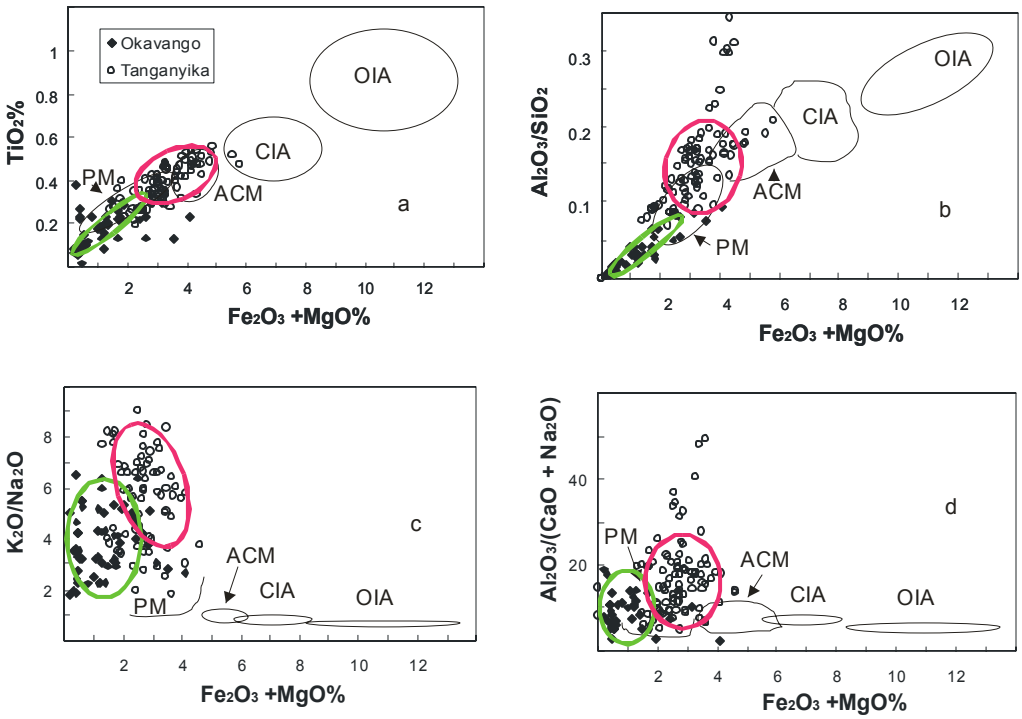

Figure V 4. Plots of TiO_2 (a), Al_2O_3/SiO_2 (b), K_2O/Na_2O (c) and $Al_2O_3/(CaO + Na_2O)$ (d) versus Fe_2O_3 + MgO. Tectonic fields are oceanic island arc (OIA), continental island arc (CIA), active continental margin (ACM) and passive margin (PM) Green field represents the Okavango alluvial fan (AF) and the pink field represents Tanganyika lacustrine basin (LB).

Three tectonic settings, PM, ACM and OIA are recognized in the K_2O/Na_2O versus SiO2 discrimination diagram of Roser and Korsch (1986) (Figure V-5). As grain size has an influence on the chemical composition of sediments, Roser and Korsch (1986) plotted sand-mud couplets for modern sediments to test the validity of their diagram for muds and sands. In general, sediments plot where expected except that fore-arc sands plot in the OIA field whilst the associated muds plot in the ACM field. Again, for the Okavango samples, carbonate free sediments were used and all samples were recalculated on a volatile free basis. Ash samples from Tanganyika were also excluded. On this diagram the samples fall within the PM field with minor overlap of both the Okavango and the Tanganyika sediments into the ACM field.

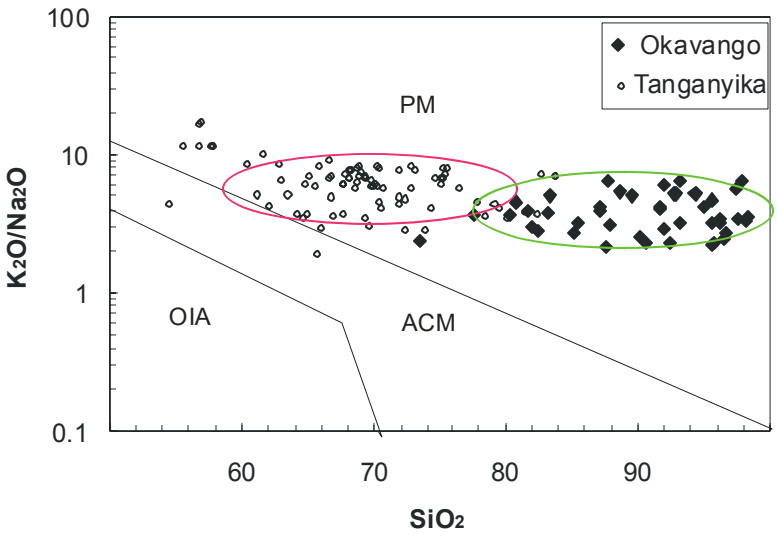

Figure V 5. K_2O/Na_2O versus SiO_2 discrimination diagram of Roser and Korsch (1986). Tectonic fields are oceanic island arc (OIA), active continental margin (ACM) and passive margin (PM) Green field represents the Okavango alluvial fan (AF) and pink field the Tanganyika lacustrine basin (LB).

The sandstone discriminant function diagram of Bhatia (1983) is based on a bivariate plot of first and second discriminant functions of major element analyses. The plot represents four different tectonic settings (OIA, CIA, ACM, PM). The functions and the plotting coordinates are from Bhatia, (1983). For the Okavango and Tanganyika sediments (Figure V-6), the samples from both suites all fall within the PM field with the exception of one sample, which is the ash layer from MPU-10 taken from a depth of 650 cm. This sample falls on the border between PM and CIA.

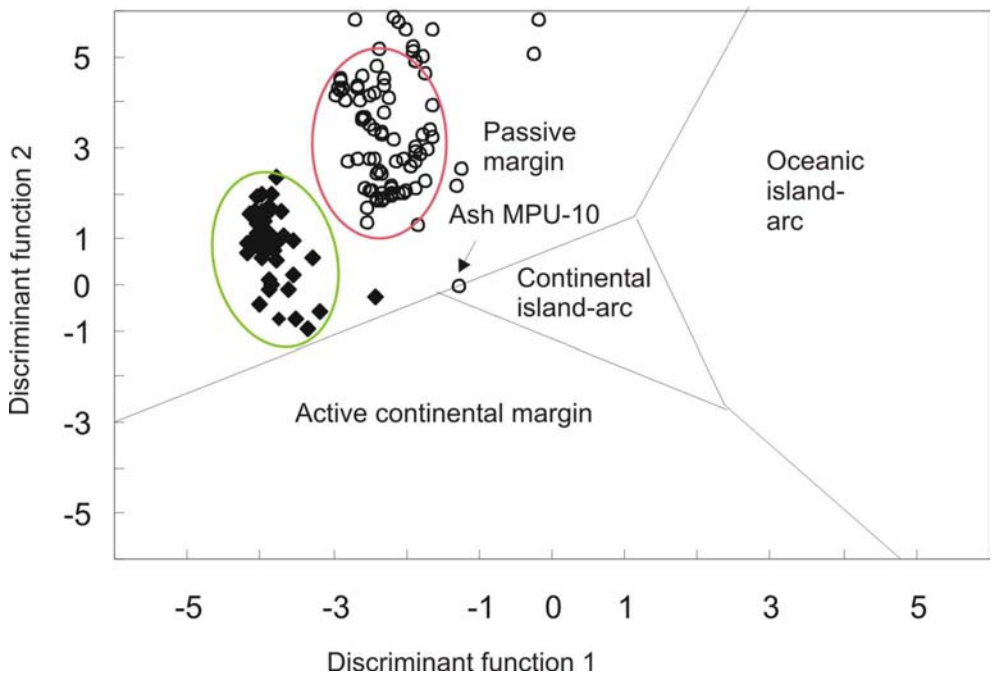

Figure V 6. Sandstone discriminant function diagram of Bhatia (1983). Green field represents the alluvial fan (AF) and the pink field the Tanganyika lacustrine basin (LB).

Figure V-7 shows the discriminant function diagram for the provenance signatures of sandstone-mudstone suites using major elements (after Roser and Korsch, 1988). Fields for dominantly mafic, intermediate and felsic igneous provenances are shown with the field for a quartzose sedimentary provenance. The plotting coordinates were extracted from Roser and Korsch, (1988).

For this diagram, the Okavango sediments plot in the field for a quartzose sedimentary provenance and the Tanganyika sediments also plot in this field but with a few samples in the intermediate igneous provenance field and the ash layer in the felsic field.

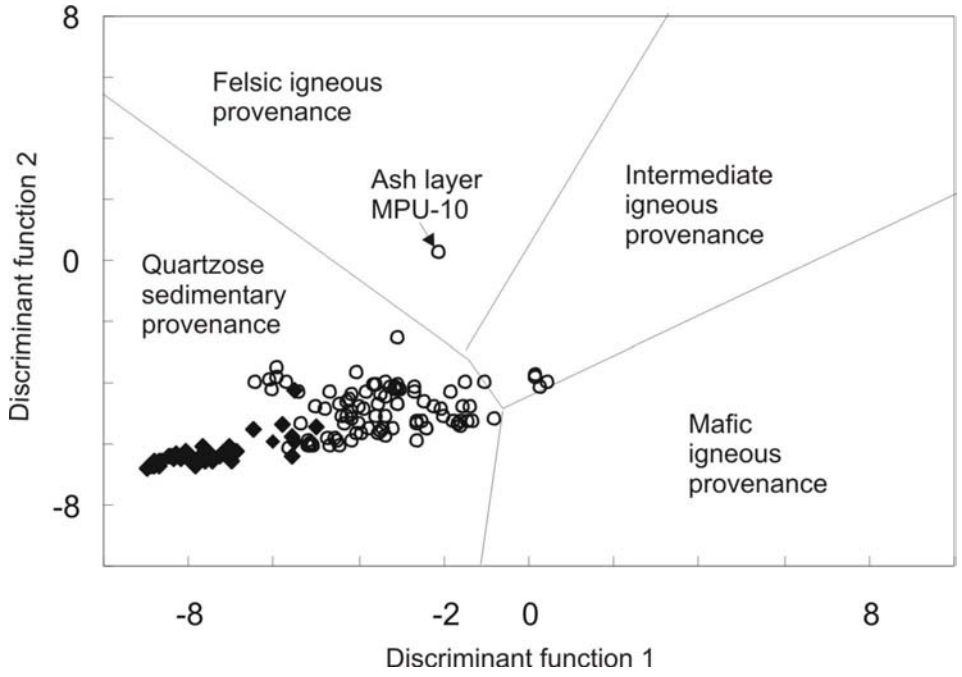

Figure V 7. Discriminant function diagram for the provenance signatures of sandstone-mudstone suites using major elements (after Roser and Korsch, 1988)

V.2.4.2 Discrimination diagrams and ratios of trace and rare earth elements

Cullers et al., (1988) showed that ratios such as La/Sc, Th/Sc Th/Co and La/Co in sediments could be used to distinguish between a felsic and a mafic source. The immobile elements La and Th are more abundant in felsic than in mafic rocks but the reverse is true for Sc and Co. Table V-1 shows the calculated ratios for both the Okavango sediments and the Tanganyika sediments. The Th/Cr ratios for the Okavango sediments overlap values recorded in sediments originating from both felsic and mafic sources whereas the Th/Cr ratios for the Tanganyika sediments encompass the range for fine grained sediments from felsic sources. For the Th/Sc ratios, the Okavango sediments overlap the range of ratios obtained for sediments from felsic and mafic source rocks and Tanganyika sediments fall within the range for fine grained sediments from felsic sources. The range of Eu/Eu* (Eu anomaly) for the Okavango sediments overlaps the ranges recorded in clastic sediments from felsic and mafic source rocks. For the Tanganyika sediments, the samples all fall within the range for a felsic source, however, there is some overlap between this range and the range for a mafic source. The La/Sc ratios of the Okavango sediments overlap the ratios recorded in sediments originating from felsic and mafic source rocks whereas the Tanganyika samples fall well within the range for a felsic source. La/Co ratios for the

Okavango sediments include low values similar to those recorded in sediments from mafic sources and higher values (up to 1.39) requiring either an intermediate composition source or a contribution from both mafic and felsic source rocks. Tanganyika samples all fall within the felsic source range.

Wronkiewicz and Condie (1987) indicated that the source rock lithology (mafic, intermediate or felsic) strongly influences the concentrations of Th, Sc, La, Zr, Hf and Co in the siliciclastic sedimentary rocks. The relationships between these elements were used to devise ternary diagrams for the identification of the nature of the source rocks of siliciclastic sedimentary rocks. In the diagram La–Th–Sc (Figure V-8) the Okavango sediments define evolutionary trends or a field extending from mafic to felsic source rock endmembers. Since these elements do not enter in the structure of quartz, these trends/fields exclude the quartz component of the sediments. The Tanganyika sediments are more tightly grouped together, around the field for a felsic source.

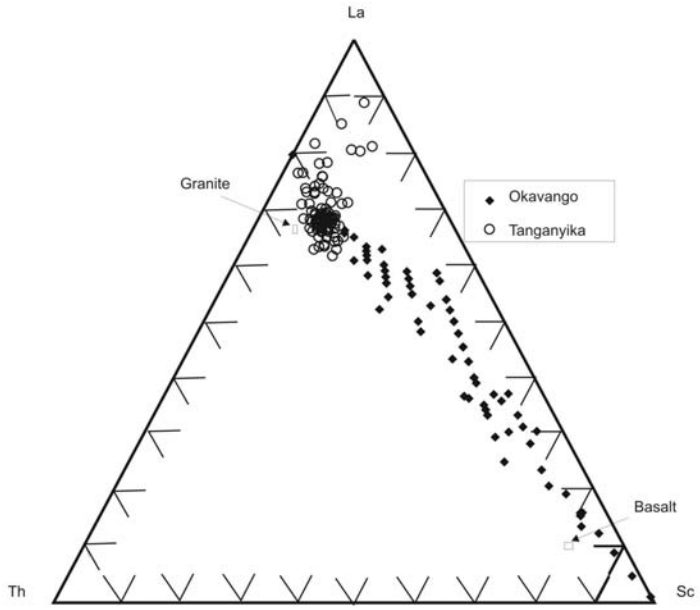

Figure V 8. La-Th-Sc ternary diagram. Data for Okavango sediments from Huntsman-Mapila et al., 2005.

Chondrite normalized diagrams (Figure V-9) both the Okavango and Tanganyika samples have similar REE patterns to the pattern of the Post Archean Australian shales (PAAS) (Taylor and McLennan, 1985). However, the Okavango sediments are less enriched in REE (∑REE range 7.9 – 152 (avg. = 46) ppm) than the Tanganyika samples (∑REE range 101 – 395 (avg. = 203) ppm). The volcanogenic horizons indicated on the REE diagram show an enrichment of both LREE and HREE relative to the surrounding matrix with ∑REE range 486 – 778 (avg. = 632) ppm). Similar enriched REE patterns were reported by Williams et al., (1993) who analyzed ash layers from the Rungwe volcanic field recorded in the lacustrine sediments of Lake Malawi.

Both suites exhibit light rare earth element (LREE) enrichment with respect to heavy rare earth elements (HREE). The La_N/Sm_N for the Okavango sediments is between 3 – 8.4 (avg. = 4.2). For the Tanganyika sediments, excluding the ash layers, the La_N/Sm_N ranged between 3.9 – 7.8 (avg. = 4.9). The ash layers had a La_N/Sm_N of 4.9 – 8.8 (avg. = 6.8) indicating the highest LREE enrichment. The REE patterns of both the Okavango and Tanganyika sediments are characterized by chondrite-normalized REE values (La_N up to Yb_N) greater than one. The average values for La_N/Yb_N for the Okavango samples is 10.3, for the Tanganyika muds is 12.4 and for the Tanganyika ash layers is 19.7.

Table V 1. The range of elemental ratios in shales and fine sandstones derived from felsic and mafic rocks (Pennsylvanian-Permian age, Colorado, USA) and comparison with the range for Okavango and Tanganyika sediments

Ratio	Shales		fine sandstone		Okavango sediments	Tanganyika sediments
	Range of sediment from felsic sources	range of sediment from mafic sources	range of sediment from felsic source	range of sediment from mafic sources	range[2]	Range
Th/Cr[1]	0.067-4.0	0.002-0.045	0.13-2.7	0.018-0.046	<0.001-0.75	0.29-3.24
Th/Sc[1]	0.64-18.1	0.05-0.4	0.84-20.5	0.05-0.22	<0.001-2	0.51-8.36
Eu/Eu*[1]	0.32-0.83	0.7-1.02	0.4-0.94	0.71-0.95	0.3-0.9	0.49-0.76
La/Sc[1]	0.7-27.7	0.4-1.1	2.5-16.3	0.43-0.86	0.01-6.7	3.96-30.19
La/Co[1]	1.4-22.4		1.8-13.8	0.14-0.38	0.03-1.39	3.77-42.65

1) Cullers, 2000

2) Huntsman-Mapila et al. (2005)

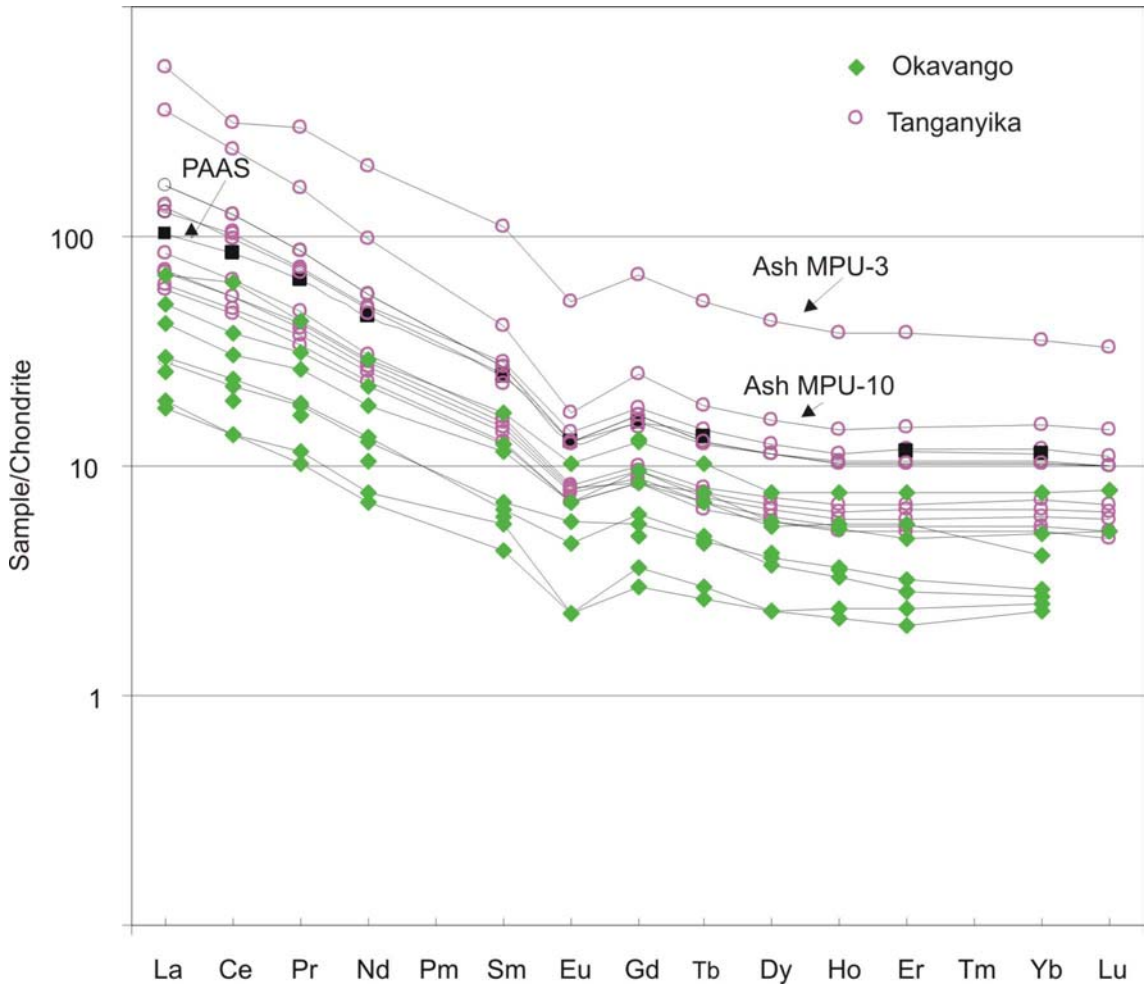

Figure V 9. Chondrite normalized REE diagram showing the Okavango and Tanganyika sediments. PAAS is shown for comparison (black squares). Data for Okavango sediments from Huntsman-Mapila et al., 2005.

VI.2.5 Discussion

V.2.5.1 Inferred tectonic setting of the depositional basin

Major elements undergo changes during sedimentary processes, for example, in most basins, SiO_2 becomes enriched, while Na_2O and CaO are depleted in sandstones compared with the source rock composition. Thus, the major element chemistry gives some clues as to the provenance type as well as the degree of reworking and weathering conditions, all of which are controlled by the tectonic setting of the basin (Bhatia, 1983).

Useful discriminating parameters of tectonic setting for major elements include Fe_2O_3 + MgO%, TiO_2% and the Al_2O_3/SiO_2, K_2O/Na_2O and $Al_2O_3/(CaO+Na_2O)$ ratios (Figure V-4). The ratio Al_2O_3/SiO_2 in sediments will give an indication of the quartz enrichment. The ratio of K_2O/Na_2O is a signal of the K-feldspar and mica content versus plagioclase content in the sediments, whilst the $Al_2O_3/(CaO+Na_2O)$ is a ratio of the relatively immobile to the more mobile elements. In general, as the tectonic setting changes from oceanic island arc to continental island arc to active continental margins to the passive margin type, there is a detectable decrease in Fe_2O_3+MgO, TiO_2, Al_2O_3/SiO_2 and an increase in K_2O/Na_2O and $Al_2O_3/(CaO+Na_2O)$ (Bhatia, 1983; Roser and Korsch, 1986; 1988).

Passive margin sandstones are generally enriched in SiO_2 and depleted in Na_2O, CaO and TiO_2. They also usually exhibit a large variation in their K_2O/Na_2O and $Al_2O_3/(CaO+Na_2O)$ compositions and have a low Fe_2O_3+MgO content. This is a reflection of the recycled nature of passive margin sediments with an enrichment of quartz and the depletion of chemically unstable grains, for example, feldspars (Bhatia, 1983; Roser and Korsch, 1986; 1988). Relative tectonic stability which results in enhanced weathering leads to the maturity of the sediments of this setting. Both the Okavango and Tanganyika sediments fall predominantly within the PM field for major element discriminant plots. There is a clear distinction between the fields for the Okavango sediments (nascent rift setting) and the Lake Tanganyika (mature rift setting) sediments in these figures (V-4, V-5 and V-6). This distinction is largely due to the higher quartz content of the Okavango nascent rift sediments, reflecting the different depositional environment, compared to the Tanganyika mature lacustrine basin sediments which have a higher Al_2O_3 content.

The early initiation stage in the development of a continental rift is characterized by the development of shallow half-graben basins where nascent faults exert a primary control in evolution of drainage and drainage catchments (Gawthorpe and Leeder, 2000). This stage is illustrated by the present Okavango alluvial fan which is a broad subsiding half-graben occupied by an alluvial fan. Quartz rich sediments (reworked aeolian sand) are deposited in a network of meandering channels in this low gradient alluvial fan. A more mature stage concerns the development of well-defined, actively subsiding half-graben basins, where propagation and interaction between fault segments lead to basin linkage and strong control of drainage. Wider and deeper lacustrine environments characterize this stage, which is illustrated by the southern Mpulungu subbasin of Lake Tanganyika.

The local climatic conditions of both Lake Tanganyika and the Okavango must also be considered, where more humid phases, for example the last deglacial, would result in enhanced weathering of the sediments compared to more arid phases such as the Last Glacial Maximum. The imprint of climate change on the sediments would occur over a much shorter time scale (10^1 – 10^4) than the tectonic signature (10^4 – 10^6) (le Turdu et al., 1999). Both the Okavango and the Lake Tanganyika sediments are fairly recently (Late Pleistocene to Holocene) recycled and deposited sediments of an older origin. Therefore, within each group (ie. Okavango and Tanganyika) the climatic signature is by far the stronger of the two for describing variability. However for this work, we use the bulk characteristics of each group and discount the variablilty within each group to define the tectonic fields.

REE concentrations in sediments is a useful indicator of crustal provenance because of the nearly quantitative transfer of these elements in sedimentary systems (Taylor and McLennan, 1985) In general, mud derived from continental crust is LREE enriched (McLennan, 1989). Both the Okavango and the Tanganyika sediments show REE patterns typical of continentally-derived sediments.

The samples from the volcanic ash layers in the Lake Tanganyika sediments, provide interesting results and the geochemistry reflects the different history of these samples. The ash layers would have been deposited as the result of a major ash fall from the Rungwe Massif to the south of Lake Tanganyika. The unweathered ash therefore would not have undergone the same mode of transport (including weathering, erosion and fluvial transport) as the matrix material from the cores. One ash samples in Figure V-6, plots on the margin of PM and CIA. Sediments from the CIA are mainly derived from felsic volcanic rocks (Bhatia, 1983). The unweathered silicic composition of this volcanic ash is reflected in this diagram.

V.2.5.2 Provenance

The majority of the sediments from the Okavango and Tanganyika fall within the quartzose sedimentary provenance field (Figure V-7). The dilution factor of SiO_2 from Kalahari aeolian quartz for the Okavango sediments may influence this result. In the diagrams La–Th–Sc (Figure V-8), the Okavango sediments define an evolutionary trend or a field extending from mafic to felsic source rock endmembers. Since these elements do not enter in the structure of quartz, these

trends/fields exclude the reworked aeolian sand component of the sediments. However, if there is an immediate source material of the Okavango sediments the quartzose sedimentary rock could be represented in the area by the Karoo Supergroup or by the Kalahri Group which forms the cover for a large part of the catchment. However, the trace and REE chemistry demonstrate that, for the non-aeolian quartz component, the ultimate sources require both felsic and ultramafic–mafic rocks (Huntsman-Mapila et al., 2005). Proterozoic granitoids and mafic–ultramafic rocks exposed in NW Botswana and in adjacent countries (Angola and Namibia) represent source rocks for the Okavango sediments. For the Mpulungu basin sediments from Lake Tanganyika, again the immediate source material is a quartzose sedimentary rocks, probably represented by the sandstones of the Mbala formation. The ultimate source material was a felsic source, possibly represented by the basement granites. Both of these possible sources outcrop along both sides of south Lake Tanganyika

V.2.6 Conclusions

Discriminant diagrams for tectonic setting used in this paper place the majority of these East African Rift sediments analysed in this work within the PM setting. Passive margin sandstones are generally enriched in SiO_2 and depleted in Na_2O, CaO and TiO_2 reflecting their highly recycled and matured nature. Based on our results, we have suggested two new fields (alluvial fan and lacustrine basin), within the previously defined passive margin field, to help discriminate sediments from an early stage rift setting. The REE patterns from both the Okavango and Lake Tanganyika exhibit patterns similar to PAAS, with the ash layers from the Rungwe volcanics in the Tanganyika samples exhibiting an enrichment in REE. The sediment samples from the Mpulungu sub-basin in Lake Tanganyika indicate that the immediate source material is a quartzose sedimentary rock but the ultimate source material was a felsic source. These are represented in the area by the sandstones of the Mbala formation and the granitic basement, both which outcrop to the south of the lake. The Okavango sediments require both felsic and ultramafic–mafic source rocks with possibly an immediate quartzose sedimentary source.

Acknowledgements

The Botswana Geological survey is acknowledged for permission to obtain samples from the Okavango boreholes and the University of Botswana for providing funds for this research project

(RP680-063). Susan Ringrose and Sidonie Revillon made improvements to an earlier version of the text.

References

Ballard, S., Pollack, H.N., Skinner, N.J., 1987. Terrestrial heat flow in Botswana and Namibia. Journal of Geophysical Research 92, 6291-6300.

Bhatia, M.R., 1983. Plate tectonics and geochemical composition of sandstones. Journal of Geology 91, 611-627.

Bhatia, M.R., Crook, K.A.W., 1986. Trace element characteristics of graywackes and tectonic setting discrimination of sedimentary basins. Contributions to Mineralogy and Petrology 92, 181-193.

Brewer, M.S., Halsam, H.W., Darbyshire, P.F.P., Davis, A.E., 1979. Rb/Sr age determinations in the Bangweulu Block, Luapula Provnice, Zambia. Inst. Geol. Sci. London 79 (5), 11 pp.

Burgess, C.F., 1985. The structural and stratigraphic evolution of Lake Tanganyika: a case study of continental rifting. Thesis, Duke University, Durham, 46 pp.

Carney, J.N., Aldiss, D.T., Lock, N.P., 1994. The geology of Botswana. Geological Survey Department, Lobatse, Botswana, pp. 113.

Chorowicz, J. 2005. The East African rift system. Journal of African Earth Sciences 43, 379–410.

Cohen, A.S., Soreghan, M.J., Scholz, C.A., 1993. Estimating the age of formation of lakes: an example from Lake Tanganyika, East African Rift system. Geology 21, 511-514.

Condie, K.C., Dengate, J., Cullers, R.L., 1995. Behaviour of rare earth elements in a paleoweathering profile on granodiorite in the Front Range, Colorado, USA. Geochimica Cosmochimica Acta 59, 279-294.

Coussement, C., 1995. Structures transverse et extension intracontinentale. Le rôle des zones de failles d'Assousa et Tanganyika-Rukwa-Malawi dans la cinématique néogène du système de Rift Est Africain. Thesis, Université de Bretagne Occidentale, Brest, 222 pp.

Cullers, R.L., 1994a. The controls on the major and trace element variations of shales, siltstones, and sandstones of Pennsylvanian-Permian age from uplifted continental blocks in Colorado to platform sediment in Kansas, USA. Geochimica Cosmochimica Acta 58, 4955-4972.

Cullers, R.L., 1994b. The chemical signature of source rocks in size fractions of Holocene stream sediment derived from metamorphic rocks in the Wet Mountains region, USA. Chemical Geology 113, 327-343.

Cullers, R.L., 2000. The geochemistry of shales, siltstones and sandstones of Pennsylvanian-Permian age, Colorado, USA: implications for provenance and metamorphic studies. Lithos 51, 181-203.

Cullers, R.L., Barrett, T., Carlson, R., Robinson, B., 1987. Rare earth element and mineralogical changes in Holocene soil and stream sediment: a case study in the Wet Mountains, Colorado, USA. Chemical Geology 63, 275-297.

Cullers, R.L., Basu, A., Suttner, L.J., 1988. Geochemical signatureof provenance in sand-size material in soils and stream sedimentsnear the Tobacco Root batholith, Montana, USA. Chemical Geology 70, 335-348.

Daly, M.C., Unrug, R. 1983. The Muva Supergroup of northern Zambia: a craton to mobile belt sedimentary sequence. Transaction of the Geological Society of South Africa 85, 155-165.

DWA (Department of Water Affairs), 1997. Appendix B: Geomorphology and Sedimentology. In: Maun Groundwater Development Project Phase 1. Water Affairs Department, Gaborone, Botswana, prepared by Eastend Investments.

Ebinger, C.J., 1989. Tectonic development of the western branch of the East African Rift system. Bulletin of the Geological Society of America 101, 885-903.
Ebinger, C.J., Deino, A.L., Drake, R.E., Tesha, A.L., 1989. Chronology of volcanism and rift basin propogation: Rungwe volcani province, East Africa. Journal of Geophysical Research 94, 15785-15803.
Ebinger, C.J., Ibrahim, A., 1994. Multiple episodes of rifting in Central and East Africa: A re-evaluation of gravity data. Geological Rundschau 83, 689-702.
Ebinger, C.J., Yemane, T., Harding, D.J., Tesfaye, S., Kelley, S., Rex, D.C., 2000. Rift deflection, migration, and propagation: Linkage of the Ethiopian and eastern rifts, Africa. Bulletin of the Geological Socciety of America 112, 163-176.
Fedo, C.M., Eriksson, K.A., Krogstad, E.J., 1996. Geochemistry of shales from the Archaean (~ 3.0 Ga) Buhwa Greenstone Belt, Zimbabwe: implications for provenance and source-area weathering. Geochimica Cosmochimica Acta 60, 1751-1763.
Gawthorpe, R.L., Leeder, R., 2000. Tectono-sedimentary evolution of active extensional basins. Basin Research 12, 195-218.
Gumbrict, T., McCarthy, T.S., Merry, C.L., 2001. The topography of the Okavango Delta, Botswana, and its tectonic and sedimentological implications. South African Journal of Geology 104, 243-264.
Haddon, I.G., 2000. Kalahari Group sediments. In: T.C. Partridge and R.R. Maud (eds).The Cenozoic of Southern Africa. Oxford University Press, pp. 173-181.
Huntsman-Mapila, P., Kampunzu, A.B., Vink, B. and Ringrose, S. (2005) Cryptic indicators of provenance from the geochemistry of the Okavango Delta sediments, Botswana. Sedimentary Geology, 174 (1-2), 123-148.
Huntsman-Mapila, P., Huntsman-Mapila, P., Ringrose, S., Mackay, A.W., Downey, W.S., Modisi, M., Coetzee, S.H., Tiercelin, J-J., Kampunzu, A.B., Vanderpost C., 2006. Use of the geochemical and biological sedimentary record in establishing palaeo-environments and climate change in the Lake Ngami basin, NW Botswana. Quaternary International 148, 51-64.
Kampunzu, A.B., Lubala, R.T. 1991. Magmatism in extensional structural settings: The phanerozic African Plate. Springer-Verlag berlin, 637 pp.
Kampunzu, A.B., Akanyang, P., Mapeo, R.B.M., Modie, B.N., Wendorff, M., 1998a. Geochemistry and tectonic significance of Mesoproterozoic Kgwebe metavolcanic rocks in northwest Botswana: implications for the evolution of the Kibaran Namaqua-Natal Belt. Geological Magazine 133, 669-683.
Kampunzu, A.B., Bonhomme, M.G., Kanika, M., 1998b. Geochronology of volcanic rocks and evolution of the Cenozoic Western branch of the East African rift system. Journal of African Earth Sciences 26, 441-461.
Kampunzu, A.B., Armstrong, M.P., Modisi, M.P., Mapeo, R.B., 1999. The Kibaran belt in southwest Africa: ion microprobe U-Pb zircon data and definition of the Kibaran Ngami belt in Botswana, Namibia and Angola. Gondwana Research 2, 571-572.
Kampunzu, A.B., Armstrong, R.A., Modisi, M.P. Mapeo, R.B.M., 2000. Ion microprobe U-Pb ages on single detrital zircon grains from Ghanzi Group: implications for the identification of a Kibaran-age crust in northwestern Botswana. Journal African Earth Sciences 30, 579-587.
Le Gall, B., Tshoso, G., Jourdan, F., Féraud, G., Bertrand, H., Tiercelin, J.J., Kampunzu, A.B., Modisi, M., Dyment, J., Maia, M., 2002. Ar-Ar geochronology and structural data from the Okavango Giant mafic dike swarm, Karoo large igneous province, N Botswana. Earth Planetary Science Letters 202, 595-606.
Le Turdu, C., Tiercelin, J-J., Gibert, E., Travi, Y., Lezzar, K.E., Richert, J.P., Massault, M., Gasse, F., Bonnefile, R., Decobert, M., Gensous, B., Jeudy, V., Tamrat, E., Mohammed, M.EU., Martens, K., Atnafu, B., Chernet, T., Williamson, D., Taieb, M., 1999. The

Ziway-SHala lake basin system, Main Ethiopian Rift: Influence of volcanism, tectonics, and climatic forcing on basin formation and sedimentation. Palaeogeography, Palaeoclimatology, Palaeoecology 150, 135-177.
Lezzar, K.E., Tiercelin, J.J., De Batist, M., Cohen, A.S., Bandora, T., van Rensbergen, P., Le Turdu, C., Wafula, M., Klerk, J., 1996. New seismic stratigraphy and Late Tertiary history of the North Tanganyika Basin, East African Rift system, deduced from multifold reflection and high resolution seismic data and piston core evidence: Basin Research 8, 1-28.
Mapeo, R.B.M., Armstrong, R.A., Kampunzu, A.B., 2000. Ages of detrital zircon grains from Neoproterozoic siliciclastic rocks in Shakawe area: implications for the evolution of the Proterozoic crust in northern Botswana. South African Journal of Geology 103, 156-161.
McCarthy, T.S., Green, R.W., Franey, N.J., 1993. The influence of neo-tectonics on water dispersal in the northeastern regions of the Okavango swamps, Botswana. Journal of African Earth Sciences 17, 23-32.
McLennan, S.M., Taylor, S.R., Eriksson, K.A., 1983. Geochemistry of Archean shales from the Pilbara Supergroup, Western Australia. Geochimica Cosmochimica Acta 47, 1211-1222.
McLennan, S.M., Taylor, S.R., McCulloch, M.T., Maynard, J.B., 1990. Geochemistry and Nd-Sr isotopic composition of deep sea turbidites: crustal evolution and plate tectonic associations. Geochimica Cosmochimica Acta 54, 2015-2050.
McLennan, S.M., Rare earth elements in sedimentary rocks: Influence of provenance and sedimentary processes: Mineralogical Society of America 21, 683-724.
McLennan, S.M., Hemming, S., McDaniel, D.K., Hanson, G.N., 1993. Geochemical approaches to sedimentation, provenance and tectonics. Geological Society of America 284, 21-40.
McConnell, R.B., 1980. A resurgent taphrogenic lineament of Precambrian origin in eastern Africa. Journal of the Geological Society of London 137, 483-489.
Modisi, M.P., 2000. Fault system of the southeastern boundary of the Okavango Rift, Botswana. Journal of African Earth Sciences 30, 569-578.
Modisi, M.P., Atekwana, E.A., Kampunzu, A.B., Ngwisanyi, T.H., 2000. Rift kinematics during the incipient stages of continental extension: evidence from nascent Okavango rift basin, northwest Botswana. Geology 28, 939-942.
Mondeguer, A., Ravenne, C., Masse, P., Tiercelin, J.J., 1989. Sedimentary basin in an extension and strike-slip background : the South Tanganyika troughs complex, East African Rift. Bull. Soc. Geol. Fr., 8 (3), 501-522.
Mondeguer, A., 1991. Bassins sédimentaires en contexte extensif et décrochant: l'exemple du "Complexe des fosses sud-Tanganyika", Rift Est- Africain. Morphostructures et sédimentation. PhD thesis. l'Université de Bretagne Occidentale.
Morley, C.K., 1988. Variable extension in Lake Tanganyika. Tectonics 7, 785-801.
Morley, C.K., Wescott, W.A., Stone, D.M., Harper, R.M., Wigger, S.T., Karanja, F.M., 1992. Tectonic evolution of the northern Kenyan Rift. Journal of the Geological Society of London 149, 333-348.
Morley, C.K., 1999 (Ed). Geoscience of rift systems- evolution of East Africa. American Association of Petroleum Geologists, Tulsa, 222 pp.
Nesbitt, H.W., Young, G.M., 1984. Prediction of some weathering trends of plutonic and volcanic rocks based on thermodynamic and kinetic considerations. Geochimica Cosmochimica Acta 48, 1523-1534.
Reeves, C.V., 1972. Rifting in the Kalahari? Nature 237, 95-96.
Rollinson, H., 1993. Using geochemical data: Evaluation, Presentation, Interpretation. Longman Scientific and Technical, New York, 352 pp.
Rosendahl, B.R., Reynolds, D.J., Lorber, P.M., Burgess, C.F., McGill, J., Scott, D., Lambiase, J.J., Derksen, S.J., 1986. Structural expression of rifting: lessons from Lake Tanganyika,

Africa. In: L.E., Frostick, R.W., Renault, I. Reid and J.J. Tiercelin (eds). Sedimentation in the African Rifts. Geological Society of London Special Publication 25, 29-43.
Rosendahl, B.R., Versfelt, J.W., Scholz, C.A., Buck, J.E., Woods, L.D., 1988. Seismic atlas of Lake Tanganyika, East Africa: Project PROBE Geophysical Atlas Series, Folio 1, Durham, Duke University.
Roser, B.P., Korsch, R.J., 1986. Determination of tectonic setting of sandstone-mudstone suites using SiO_2 content and K_2O/Na_2O ratio. Journal of Geology 94, 75-83.
Roser, B.P., Korsch, R.J., 1988. Provenance signatures of sandstone-mudstone suites determined using discriminant function analysis of major-element data. Chemical Geology 67, 119-139.
Shudofsky, G.N., 1985. Source mechanisms and focal depths of East African earthquakes using Rayleigh-wave inversion and body-wave modeling. Geophysical Journal of the Royal Astronomical Society 83, 563-614.
Taylor, S.R., McLennan, S.M., 1985. The continental crust: its composition and evolution. Oxford, Blackwell Scientific, 312 pp.
Taylor, S.R., McLennan, S.M., 1995. The geochemical evolution of the continental crust. Review of Geophysics 33, 241-265.
Tiercelin, J.-J., Thouin, C., Tshibangu, K., Mondeguer, A., 1989. Discovery of sublacustrine hydrothermal activity and associated massive sulphides and hydrocarbons in the north Tanganyika trough, East African Rift. Geology 17, 1053-1056.
Tiercelin, J-J, Mondeguer, A., 1991. The geology of the Tanganyika Trough. In: Coulter G.W. (ed). Lake Tanganyika and its life. Oxford University Press, Oxford, pp. 7-48.
Tiercelin, J-J., Potdevin, J-L., Morley, C.K., Talbot, M.R., Bellon, H., Rio, A., Le Gall, B., Vetel, W., 2004. Hydrocarbon potential of the Meso-Cenzoic Turkana Depression, northern Kenya. I. Reservoirs: depositional environments, diagenetic characteristics, and source rock-reservoir relationships. Marine and Petroleum Geology 21, 41-62.
Unrug, R., 1984. The mid-proterozoic Mporokoso group of northern Zambia: Stratigraphy, sedimentation and regional position. Precambrian Research 24, 99-121.
Williams, T.M., Henney, P.J., Owen, R.B., 1993. Recent eruptice episodes of the Rungwe Volcanic Field (Tanzania) recorded in the lacustrine sediments of the Northern Malawi Rift. Journal of African Earth Sciences, 17, 33-39.
Wronkiewicz, D.J., Condie, K.C., 1987. Geochemistry of Archean shales from the Witwatersrand Supergroup, South Africa: source–area weathering and provenance. Geochimica Cosmochimica Acta 51, 2401-2416.

VI. SEDIMENTOLOGICAL AND GEOCHEMICAL EVIDENCE FOR PALAEO-ENVIRONMENTAL CHANGE IN THE MAKGADIKGADI SUBBASIN IN RELATION TO THE MOZ RIFT DEPRESSION, BOTSWANA

VI.1. Changements paléo-environnementaux dans le sous-bassin de Makgadikgadi en relation avec la dépression du rift de MOZ (Botzwana): approche géochimique et sédimentologique

Résumé de l'article

Ce travail présente de nouvelles évidences pour les changements de paléo-environnement qui ont eu lieu pendant le Pléistocène dans le nord-ouest du Botswana. Des lignes de rivage encroûtées le long de la marge nord-est du sous-bassin de Makgadikgadi (MSB) nous donnent des informations paléo-environnementales dans le contexte de la dépression du rift Makgadikgadi-Okavango-Zambezi (MOZ). Les données de terrain, les analyses XRD et les mesures géochimiques montrent que les lignes de rivage de MSB sont composées de calcrète (type LU1), de calcrète riches en MgO avec de la silice (type LU2), de silice-calcrète (type LU3) et de silcrète (type LU4). Les épisodes d'eau douce ont été suivis par des épisodes secs ou la calcrète s'est formée, en alternance avec des silicifications répétitives. La formation des calcrètes dans les sédiments littoraux de la cuvette était peut être biologique ou fonction de l'environnement. La précipitation de calcrète étant en partie contrôlée par le rapport de Mg/Ca dans l'eau interstitielle des sédiments de la marge, cela suggère l'existence de conditions évaporatiques dans un bassin fermé. Les phases de silicification semblent être liées aux périodes où les conditions géochimiques sur le littoral de la cuvette ressemblaient aux conditions actuelles, avec de l'eau hyper-sodée type Na-CO_3-SO_4-Cl. L'eau souterraine, acide, avec une salinité moyenne et saturée en silice, a précedé la précipitation du Si au moment où le pH diminuait. La mobilisation du Si est le résultat de la dissolution du quartz, amplifié par les diatomiées, les bactéries et les algues dans la zone littorale humide de la cuvette. L'eau interstitielle riche en SiO_2 a migré à travers la calcrète desséchée et craquelée, vers des zones de moindre salinité et de moindre pH entraînant un déplacement préférentiel de la calcrète et la précipitation de silcrète. Les dates approximatives de TL suggèrent que le sable littoral a été calcrètisé pendant les périodes sèches des paléo-lacs qui ont eu lieu avant 110 ka, 80 – 90 ka et 41 – 43 ka. Ces périodes concordent bien avec la chronologie de la carotte de Vostok pour l'Afrique du sud.

VI.2. Sedimentological and geochemical evidence for palaeo-environmental change in the Makgadikgadi subbasin in relation to the MOZ rift depression, Botswana

Susan Ringrose[a,*], Philippa Huntsman-Mapila[a,b], Ali Basira Kampunzu[c], William Downey[d], Stephan Coetzee[d], Bernard Vink[c], Wilma Matheson[e], Cornelis Vanderpost[a]

aHarry Oppenheimer Okavango Research Centre, University of Botswana, Private Bag 285, Maun, Botswana
bUBO-CNRS UMR, 6538 Domaine Oceaniques IUEM, 29280 Plouzane, France
cDepartment of Geology, University of Botswana, Private Bag 0022, Gaborone, Botswana
dDepartment of Physics, University of Botswana, Private Bag 0022, Gaborone, Botswana
eEES (Pty) Ltd., P.O. Box 31024, Gaborone, Botswana

Article published in Palaeogeography, Palaeoclimatology, Palaeoecology 217 (2005) 265-287

Abstract

This work considers new evidence for palaeo-environmental change taking place during the Pleistocene in northern Botswana. Duricrusted strandlines along the northeastern margin of Sua Pan provide palaeo-environmental data pertaining to the Makgadikgadi subbasin (MSB) with inferences regarding the larger Makgadikgadi–Okavango–Zambezi (MOZ) rift depression. Field, XRD and geochemical data show that MSB strandlines comprise calcretes (LU1 type), MgO-rich calcretes with silica (LU2 type), sil-calcrete (LU3 type) and silcrete (LU4 type). Early freshwater episodes appear to have been followed by calcrete-dominated drying phases interspersed with repeated silcretisation. Calcretisation through pan littoral sediments may have been both biogenically and environmentally induced. Calcite precipitation was in part controlled by the Mg/Ca ratio of pore water in the pan littoral zone suggesting closed basin type evaporative conditions, which were followed by a major desiccation interval. Phases of silcrete precipitation appear to be related to periods when the geochemistry of the lake littoral more closely resembled present-day Na–CO_3–SO_4–Cl-type brines. Silica saturated acidic, moderately saline groundwater preceded Si precipitation which took place as the pH reduced. Si mobilisation occurred (inter alia) as a result of quartz grain dissolution enhanced by diatoms, bacteria and algal growth in the moist pan littoral. SiO_2-rich pore waters migrated through cracked and desiccated calcrete into areas of lower salinity and lower pH resulting in preferential calcite removal and silcrete precipitation. Approximate TL dates imply that exposed littoral sand underwent calcretisation

during the drying phases of extensive palaeo-lakes which occurred prior to 110 ka, 80–90 ka and 41–43 ka. These wet periods compare fairly well with Vostok core chronologies for southern Africa

VI.2.1. Introduction

Fluvio-lacustrine deposition in northern Botswana has mainly taken place within a large structural (mega) depression, a southwesterly propagating extension of the east African rift system, which was initiated approximately 2.4–5.0 Ma (Du Toit, 1933; Tiercelin and Lezzar, 2002). This rift depression was drained and filled by southeasterly flowing rivers on a number of occasions during the Tertiary and Pleistocene as the area was faulted and half grabens developed (Cooke, 1980; Mallick et al., 1981; Modisi et al., 2000). Deeper structural subbasins formed mainly on the southern margin of the rift forming loci for lacustrine deposition (Thomas and Shaw, 1991; Gumbricht et al., 2001; Ringrose et al., 2002a). The MOZ (Makgadikgadi–Okavango–Zambezi) depression is controlled by a series of NE–SW normal faults related to incipient rifting which reactivated Proterozoic and Karoo structures (Baillieul, 1979; Smith, 1984; Modisi et al., 2000). Tectonic activity along the same trend resulted in uplift along the Zimbabwe–Kalahari axis possibly during the late Pliocene (Partridge and Maud, 2000; Moore and Larkin, 2001) causing the impoundment of proto Okavango, Kwando and upper Zambezi drainage and the development of the Makgadikgadi (MSB), Ngami and Mababe subbasins (Cooke, 1980; Ringrose et al., 2002b). The MSB comprises two large salt pans referred to as Sua Pan in the east and Ntwetwe Pan in the west covering some 37000 km^2. This work considers new approaches to the interpretation of palaeo-lacustrine environments from the Makgadikgadi subbasin (MSB) in the context the MOZ rift depression based on morpho-stratigraphic evidence and thermoluminescence (TL) dates. To avoid confusion, the term Lake Palaeo-Makgadikgadi which was intended to encompass all fluvio-lacustrine events in the nascent rift in the older literature (e.g., Cooke, 1979; Cooke and Verstappen, 1984; Thomas and Shaw, 1991; Ringrose et al., 1999a) is being discontinued, as it suggests an enlarged version of the present Makgadikgadi Pan complex (cf. Moore and Larkin, 2001). Hence, the introduction of the term Makgadikgadi–Okavango–Zambezi (MOZ) rift depression wetlands to help clarify the regional context. The apparent semi-continuous development of palaeo-lakes in the MSB from possibly late Pliocene to Recent times has been subject to speculation especially with respect to the nature of feeder channels and links to the Okavango system. Results of previous work have mainly been based on height data from assumed strandlines with minimum age 14C dates (Cooke and Verstappen, 1984; Thomas and Shaw, 1991, 2002; Ringrose et al., 1999a). The present work emphasises

duricrust strandline morphogenesis from the northeastern MSB to help interpret depositional environments. This takes place in the context of new indicative thermoluminescence (TL) dates which are used to amplify geochronological events. Specific aims include the development of morpho-stratigraphic records and the establishment of geochemical units intended to develop innovative data for palaeoenvironmental change. Strandline evolution in terms of MSB and MOZ depression palaeo-environments is further elaborated.

VI.2.2. Study area

The study area forms part of the northeastern Makgadikgadi subbasin in north central Botswana between 19.80 S–21.60 S and 25.75 E–26.40 E covering approximately 3600 km2 (Figure VI-1). Background geology comprises Archean terrain covered by >250 m of Karoo sediment (Lebung and Ecca Groups) crossed by the Okavango dyke swarm including Proterozoic and Jurassic mafic dykes (Geological Survey of Botswana, 2000). These in turn are covered by Kalahari Group sediments (Mallick et al., 1981). The development and subsequent enlargement of the MSB appears to have resulted from downwarping at the intersection of NE–SW nascent rift structural trends with orthogonal NW–SE Karoo trends (Figure VI 1). A significant feature in the study area is Sua Spit, which in common with other remnant linear features in the MSB follows NW–SE trends. Sua Pan is infilled with clay, silt and fine sand currently saturated by a near surface brine aquifer of the Na–CO3–SO4–Cl type (Eugster and Hardie, 1978; Shaw et al., 1990). Sua Pan is the lowest member of the Pan sequence with a sump level of 890 m a.s.l. The area is sparsely vegetated with anomalously low rainfall at c. 400 mm/year (Ringrose et al., 1999b). The precipitation rate is exceeded by the evapotranspiration rate by a factor of three (Bhalotra, 1987).

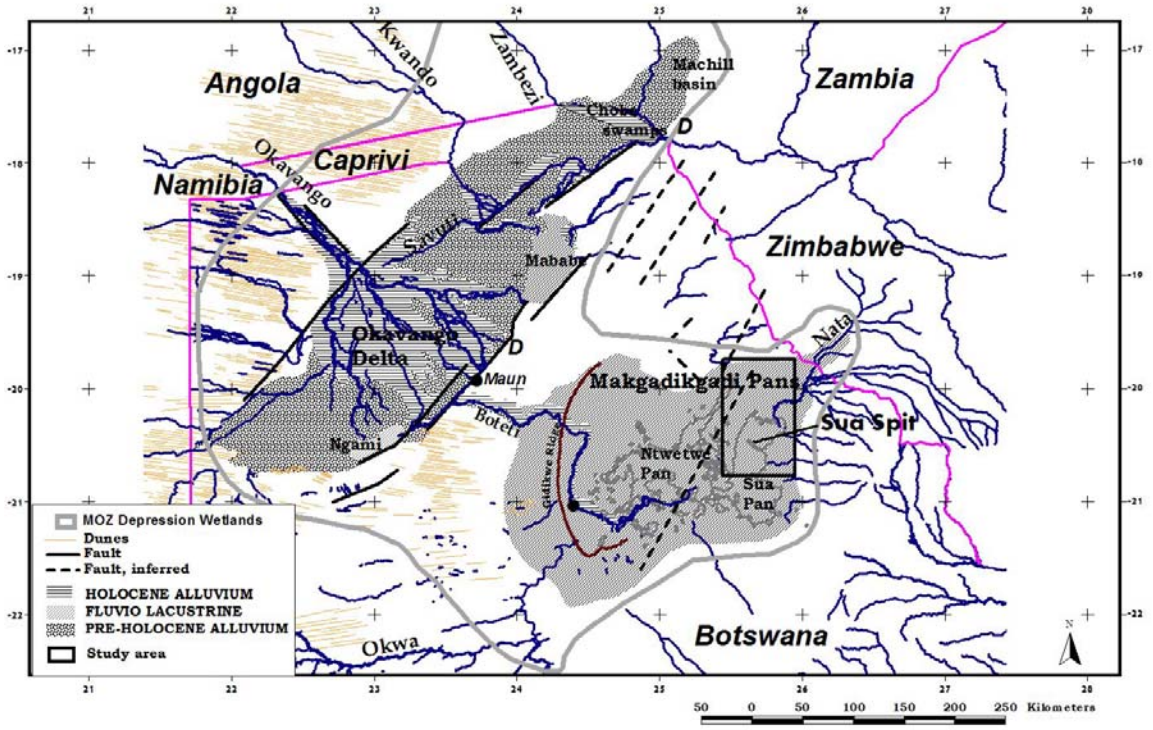

Figure VI 1. Location of the palaeo-Makgadikgadi sub-basin (MSB) in relation to the Makgadikgadi-Okavango-Zambezi (MOZ) rift depression (D=location of TL date sites)

VI.2.3. Analytical techniques

Field work at three locations took place between 1999 and 2002 and was aimed at characterizing duricrusts throughout the known range of strandline levels. Observational data and samples were taken from twenty gravel pits and road cuts in Location 1, ten hand dug pits in Location 2 and five gravel pits in Location 3 (Figure VI-2). Satellite images provided a basis for the selection of northwest–southeast and north–south transects which were used to establish topographic profiles and the locations for duricrust examination. Topographic profiling took place to fit the strandlines into the existing height-based geochronology. For this, a Trimble 4700 differential GPS was used in Location 1. Topographic data for Locations 2 and 3 were obtained from topographic maps and survey beacons the heights of which were available from the Botswana Department of Surveys and Mapping. Additional contour data were obtained from the Makgadikgadi Pans Development Plan (Republic of Botswana, 2000). Field methods included the clearing of pit faces, their differentiation into sedimentary units, the development of a systematic field description following terminology available in Wright and Tucker (1991) and the sampling of all major units and plant remains. Units intended for TL analysis were covered by a tarpaulin and sampled in the dark. Samples comprised large coherent megaaggregates which were dug from the interior of the pit wall, covered immediately in aluminium foil and placed in a lightproof plastic container. A series of samples were taken from each location intended to be representative of older litho-clasts, intermediate indurated and younger friable nodular horizons. Samples were taken from homogeneous horizons, representative of material supplying the environmental dose rate. Twenty duricrust samples were sent to the Council for Geoscience, Pretoria for thin sectioning. The thin sections were later investigated under plain and cross-polarised light using a Zeiss Axioplan microscope. A Philips XL30 environmental scanning electron microscope (ESEM) with an electron microprobe (EDAX) was used to obtain preliminary micro-textural information, to determine the nature of microorganisms and to provide localised qualitative elemental data. Naturally occurring surfaces were examined without preparatory polishing to preserve micro-textures.

Twenty bulk samples were subject to X-ray diffraction powder analysis using a Phillips PW 3710 XRD unit, operated at 45 kV and 40 mA, employing Cu-K alpha radiation and a graphite monochronomator. The samples were scanned from 3^{o} to 70^{o} 2θ and their diffractograms recorded. After initial scanning, the bulk samples were leached in a dilute 10% HCl solution. The

leached residues were scanned for minor and accessory insoluble silicate phases. Whole rock chemical analyses were performed on twenty-five samples at Chemex Laboratories (Canada). Major element compositions were determined using an ICP-AES with a detection limit of 0.01 wt.% and precision of ±1%. Inorganic CO2 and organic C were determined using a Leco-Gasometric and Leco-IR detector with detection limits of 0.2% and 0.01%, respectively. Eleven samples were dated using TL techniques (Aitken, 1985). This technique was used because it has provided reliable dates in the past (Blumel et al., 1998; Ringrose et al., 1999a, 2002a,b). Literature sources suggest a degree of comparability between TL and OSL (optical spin luminescence) (e.g., Radtke et al., 1999; Huaya et al., 2004). Quartz grains in the size range 90–125 μm, assumed to have undergone total bleaching in a shallow water environment before duricrust precipitation, were extracted from litho-clasts and nodules using a series of treatments. These included removal of carbonates and iron staining using hydrochloric acid and digestion of organic material using hydrogen peroxide. Fluorosilicic acid was used to dissolve feldspars while heavy minerals were separated using sodium polytungstate. Remaining magnetic minerals were removed using an electromagnetic separator. The purity of the final quartz extract was tested using Infrared Stimulated Luminescence to ensure that no feldspars were present. The clean sample was subjected to a hydrofluoric acid etch for 40 min at 24 ^{o}C to remove the outer a affected skin. The grains were mounted on 10-mm-diameter stainless steel discs and fixed using Silkospray silicone oil. Multiple aliquots were used for each additive dose step and regenerated bleached samples. The strontium 90 β source was calibrated against a known β source to deliver 1.9 Gy min^{-1}. Additive doses +β1, +β2 etc. in Gy were used for natural and bleached samples (Table VI-1). Following the appropriate irradiations, the sample was stored for 24 h and preheated at 220 ^{o}C for 300 s before TL measurement using a Riso D12 reader (Botter-Jensen and Duller, 1992). A second glow normalisation was performed on the glowed out samples using a dose of 6 Gy for each sample. The TL glow curves show convincing temperature plateaux over the temperature ranges (Table VI-1). Exponential regressions for TL in relation to Dose were performed for each sample and the equivalent dose (DE) obtained from which the residual TL was subtracted. The TL data were fitted by exponential regression over the best temperature plateau range for both the additive dose and bleached regenerated data and a comparison made of the respective curve forms. In this case, the R^2 regenerated TL growth curve coefficient was within an acceptable range. The environmental dose rate was determined by a low-level alpha counter (Elsec 7286) using a 42-mm ZnS screen (Zoller and Pernicka, 1989). The values shown assume secular equilibrium for both U and Th chains (Carl, 1987). Uncertainty levels on Table VI-1 represent one standard deviation. The potassium content (wt.%) was determined using a

Corning 410 flame photometer. The moisture value used in the age equation determination of these samples is ±5%. The cosmic dose was calculated taking into consideration depth of burial, overburden density and porosity, sample coordinates and altitude.

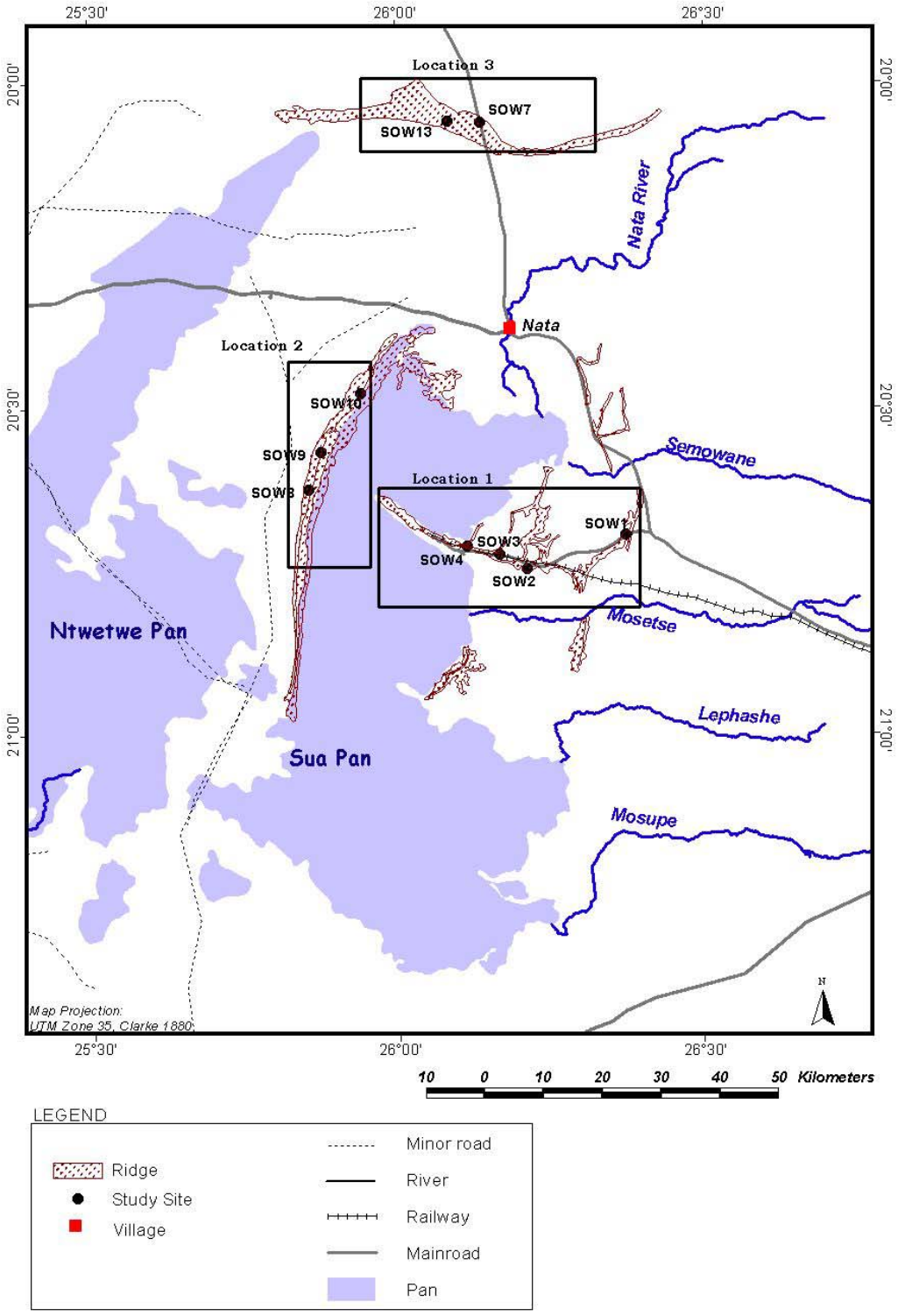

Figure VI 2. Study area and sample locations on the northeastern margin of the palaeo-Makgadikgadi sub-basin.

Table VI 1. Data inputs for thermoluminescence analysis (see text for explanation)

Sample	SOW13S2P	SOW13S1	SOW13S3	SOW13S2A	SOW7AS2	SOW13S2	SOW1 S6	SOW4 S4	SOW8A	MAUNSE12A	KVFS3
Sample (De)(Gy)	86.77±0.79	164.851±81	118.78±6.71	72.37±1.79	157.83±15.28	50.02±1.24	219.83±7.20	111.57±9.00	48.66±3.81	337.50±16.90	666.00±33.30
Sediment U ppm	0.92±0.09	1.92±0.19	1117±0.62	1.02±0.15	0.75±0.05	110±90.09	8112±0.26	0.80±0.09	15.73±0.61	1.33±0.18	0.93±0.09
Sediment Th ppm	1.73±0.30	4.14±0.62	4.60±0.62	2.57±0.48	1.14±0.18	1.37±0.28	1.47±0.86	0.92±0.28	16.18±2.03	6.00±0.58	1.47±0.28
K wt%	0.32±0.03	0.740±.03	0.58±0.03	0.30±0.03	1.58±0.03	0.74±0.03	0.28±0.03	2.28±0.33	0.54±0.03	2.00±0.03	1.00±0.03
Dose rate mGya-1	799±66	1613±119	1313±106	866±79	1956±118	1213±84	2423±174	2570±162	5560±401	2813±178	1350±93
Plateau (Temp. range oC)	319-354	316-411	296-365	303-354	328-399	331-435	307-345	334-376	314-377	-	-
Additive Dose +b1(Gy)	116.67	33.33	66.67	100	100	26.67	133.33	26.67	26.67	-	-
+b2	233.33	66.67	100	166.67	200	66.67	283.33	166.67	56.67	-	-
+b3	333.33	266.67	150	266.67	533.33	233.33	500	266.67	100	-	-
+b4	-	-	366.67	-	-	-	-	-	166.67	-	-

VI.2.4. Topographic, Stratigraphic and Petrographic Results

Location 1 ridges were examined at eleven locations and in detail at exposures SOW1 to SOW4 (Figure VI-2). The Pan floor immediately adjacent to Sua Spit lies at an elevation of 904 m and rises up through a series of minor sand and duricrust ridges, the most prominent of which lie at 906 m and 908 m. The exposures examined in detail occur immediately landward of the Spit such that SOW4 stands at 911 m, SOW3 at 924 m SOW2 at 926 m and SOW1 at 936 m. While the lowest unit in the upper SOW1 ridge is an indurated, calcareous lithoclastic bed showing desiccation cracking, the lowest units in the remaining profiles (SOW2-4) comprise well developed (3-5 cm) rhyzoliths in a green, granular calcareous matrix (Figure VI-3). The rhyzoliths appear to be root casts (*sensu* Klappa, 1980) in units which also contain small litho-clasts showing desiccation cracking and void formation. The rhyzoliths are large, up to 1-2 cm in diameter and 8-10 cm long, comprising a greenish-white calcareous exterior (1-2 mm) and grey-brown siliceous interior (Figure VI-4A). This unit grades upwards into moderately indurated nodular calcrete with cracked siliceous litho-clasts in a partially indurated sandy calcareous matrix. The nodules are small and composed of concentric shells of $CaCO_3$ accreted around quartz or calcite nuclei and occur more towards the top of the unit, while the litho-clasts are larger (1-3 cm) and more angular. In SOW2 and 3 the nodules grade upwards into a more friable, nodular calcrete. In SOW4 the nodular litho-clastic unit is replaced vertically by calcareous siltstone showing major desiccation cracking (Figure VI-4B) succeeded by honeycomb calcrete which in turn is capped by an indurated, calcareous hardpan comprising calcareous litho-clasts (Figure VI-3). SOW2, 3 and 4 are capped by indurated, calcrete hardpan with calcareous and siliceous litho-clasts. In contrast the higher SOW1 units comprise lower laminar calcrete which is rhyzolith free and succeeded by a calcareous siltstone showing major desiccation cracking. This is overlain by friable, nodular calcrete and capped by conglomeratic hardpan made up of indurated duricrust comprising either large (0.5-3.0 cm) quartz and calcrete clasts in a micritic, partially Fe stained matrix. The conglomeratic quartz clasts show evidence of vertical and peripheral cracking in addition to Fe staining.

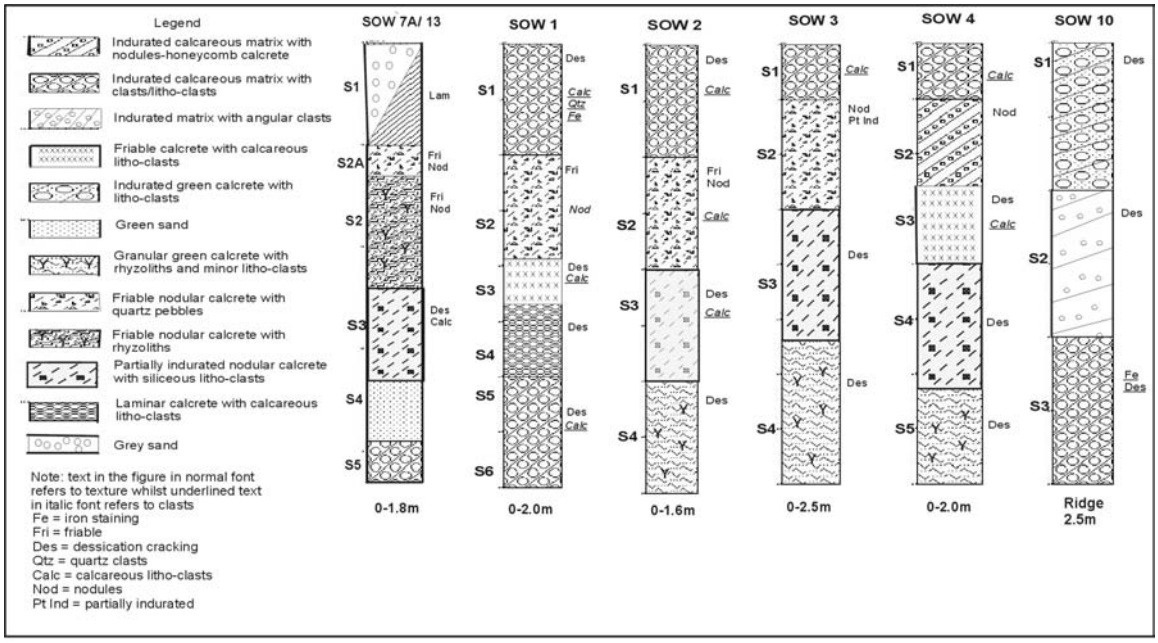

Figure VI 3. Stratigraphic profiles of duricrusts in the three sample locations (SOW1-4=Location 1, SOW 10=Location 2, SOW7A and SOW 13=Location 3)

A series of ridges were examined Location 2 adjacent to the west side of Sua Pan, in detail at the indurated SOW10 ridge. The Pan floor west of Sua Spit lies at an elevation of about 900 m and rises up through a series of lower sand ridges to more prominent duricrust ridges at 904 m and 906 m. The SOW10 906 m ridge is completely lithified and comprises three units (Figure VI-3). The lower unit is composed of recrystallised green calcrete with calcareous and siliceous litho-clasts showing extensive cracking. The siliceous litho-clasts are lensoid (terrazzo) in shape with notable Fe staining (Figure VI-4C). The intermediate unit is made up of brecciated sil-calcrete litho-clasts in an indurated calcareous matrix with voids and desiccation cracking throughout. The upper unit is composed of indurated calcareous sediment with severely cracked sub-rounded green litho-clasts showing laminar to massive infilling. Lower Location 2 sand ridges rise up 1-3 m from the western edge of Sua Pan. The sandy ridges, examined at SOW8B comprise 0.5 m uniform sand with disseminated calcareous particles and scattered rhyzoliths. A series of silica rich lensoid terrazo plates are present along the former shoreline. These plates vary in length from 2-10 cm and are 1-3 cm in thickness and lie on the present pan edge in random discontinuous sheets (Figure VI-4D).

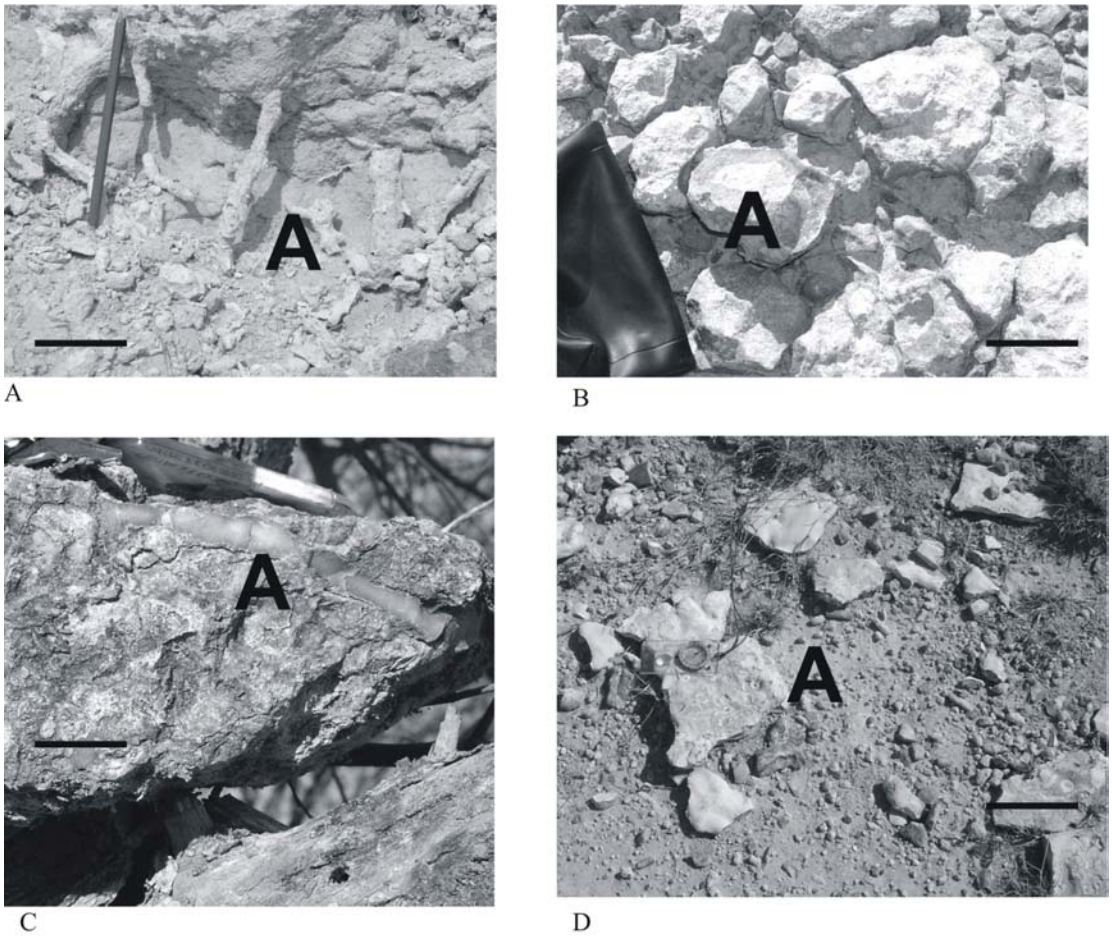

Figure VI 4. 4A-Numerous rhyzoliths (A) in green, granular calcareous matrix at SOW3 S4 (bar=6 cm); 4B-Dessication cracking showing alteration of $CaCO_3$ rich pebbles (A) by silica rich porewater SOW4 S3 (bar=10 cm); 4C-Lensoid terrazzo plates congealed in the SOW10 ridge (bar=5 cm); 4D-Lensoid terrazzo plates along the edge of Sua Pan near SOW10 (bar=8 cm)

SOW7A and 13 occur in Location 3 on the northeastern margin of the Makgadikgadi Basin at around 943-945 m (Figure VI-2). In terms of height and lateral continuity, ridges at this elevation have been described as representing the oldest strandline features in the PMSB (Thomas and Shaw, 1991). The basal bed of SOW7A comprises an indurated litho-clastic unit with sub-rounded quartz clasts in a hardened calcareous matrix (S5, Figure VI-3). In contrast, the basal unit of SOW13 (S4, Figure VI-3) is made up of semi-consolidated light green sand with calcareous fragments and fine quartz particles interspersed with rhyzoliths. Both lower units are replaced by partially indurated nodular calcrete with siliceous, angular, large (to 4 cm), litho-clasts showing evidence of desiccation cracking. This is succeeded in both profiles (SOW13 and 7A) by friable nodular calcrete with abundant rhyzoliths. The rhyzoliths are mostly large (up to 3.5 cm diameter and 2-6 cm long) comprising calcareous outer sheaths with a siliceous infilling. This unit grades upwards into a friable nodular bed with quartz clasts. The nodules are mainly composed of quartz nuclei with carbonate rich concentric outer shells. The profiles are capped by a massive calcareous hardpan in SOW13 and massive grey sand in SOW7. The hardpan comprises lenticular siliceous clasts in a calcareous matrix.

VI.2.5. X Ray Diffraction and Geochemical Results

XRD analyses of litho-clastic and nodular samples indicate that the MSB duricrusts may be subdivided into calcite or quartz dominated types (Table VI-2). In Location 1 SOW1, calcite (or calcite with dolomite) is dominant and varies from 66 vol% to 80 vol% calcite down profile. More quartz clasts are found in the upper units. The presence of feldspars is low at 1-2 vol% microcline and albite, despite the proximity of Karoo bedrock. The proportion of dolomite (3-4 vol%) and the presence of palygorskite (3-8 vol%) with sepiolite (2-8 vol%) confirm the prevalence of Mg in the strandline duricrusts. The presence of Mg rich clays and dolomites suggests formation in Mg-rich alkaline environments, normally associated with a closed basin depositional history (e.g. Watts, 1980; Eugster and Kelts, 1983; Alonso-Zarza et al., 2002). Results from SOW3 litho-clasts and nodules show a more even proportion of calcite (9-47 vol%) and quartz (30-45 vol%). Mg is abundant throughout with the S2 unit containing 42 vol% dolomite. The proportion of feldspars is slightly higher than that found in SOW1 at 4-6 vol% microcline and 3-6 vol% albite. The presence of illite (3-12 vol%) or possibly glauconite contrasts with the palygorskite and sepiolite found in SOW1 and may be detrital in origin.

On the western side of Sua Pan at Location 2, the ridge at SOW10 comprises an even proportion of calcite and quartz with minor dolomite (2 vol%) towards the top of the ridge, higher quartz (72 vol%) about half way down and higher calcite (74 vol%) towards the ridge base (Table VI-2). The feldspar proportion is low throughout. The percentage of illite (or glauconite) increases towards the base (from 2-7 vol%). Watts (1980) discusses how glauconite is lost during calcretisation as glauconite and calcite are incompatible (cf. Krumbein and Garrels, 1952). The pan edge duricrusts (SOW8A/8B) show relatively equal proportions of quartz (33-40 vol%) and calcite (24-40 vol%) with intermediate feldspars. Two samples contain relatively high proportions of magadiite and kenyaite whose presence implies that the pan littoral was exceptionally alkaline and saline during their formation. Both minerals are considered to have formed from a reaction between dissolved halite and silica (Vink et al., 2001).

Towards the northern edge of the basin at SOW7A, XRD analysis on litho-clasts and nodules shows that high calcite concentrations (64 vol%) towards the base become lower (to <1 vol%) towards the top of the profile while the reverse is true for quartz (89-22 vol%). An exceptional unit to this trend is SOW7A which shows high quartz and low calcite towards the base of the profile (Table VI-2). Most units contain 3-12 vol% clay which may be either detrital illite or glauconite and a low feldspar content. A relatively high dolomite percentage (15 vol%) occurs towards the top of the profile at SOW7A S2. SOW13 also comprises dolomite (38 vol%) towards the top of the profile in association with a variable quartz (20-66 vol%) and calcite (8-60 vol%) content. The SOW13 samples contain a high proportion of neoformed sepiolite (10-15 vol%). The Mg rich mineral suite implies neoformation of clays and dolomite likely under alkaline rich, closed basin conditions (Watts, 1980; Eugster and Kelts, 1983).

Table VI 2. Results of X-Ray diffraction analysis (vol%) on selected MSB strandline sediments.

SAMPLE	Cal	Dol	Qtz	Mcl	Alb	Mca	Pal	Sep	Ill	Cly	Mag	Ken	Hem	Hal
SOW 1-S1	66	3	23	2	<1	-	4	-	-	-	-	-	-	-
SOW 1-S2	72	4	18	1	2	<1	-	-	-	-	-	-	-	-
SOW 1-S3	74	5	13	1	1	-	3	2	-	-	-	-	<1	-
SOW 1-S4	65	5	18	2	1	-	8	-	-	-	-	-	-	-
SOW 1-S5	62	4	13	3	2	-	7	8	-	-	-	-	-	-
SOW 1-S6	80	-	14	<1	<1	-	5	-	-	-	-	-	-	-
SOW 3-S1	43	10	36	4	6	2	-	-	-	-	-	-	-	-
SOW 3-S2	9	42	36	5	3	-	-	-	-	4	-	-	-	-
SOW 3-S3	36	7	45	5	4	-	-	-	-	-	-	-	<1	-
SOW 3-S4	47	-	30	6	3	-	-	-	12	-	-	-	-	-
SOW 7A-S1	<1	-	88	5	1	-	-	-	5*	-	-	-	-	-
SOW 7A-S2	30	15	50	2	<1	-	-	-	3*	-	-	-	-	-
SOW 7A-S2A	18	2	70	5	1	-	-	-	-	4	-	-	-	-
SOW 7A-S3	2	-	82	5	1	-	-	-	10	-	-	-	-	-
SOW 7A-S4	64	-	22	2	1	-	-	-	12*	-	-	-	-	-
SOW 8A	40	-	33	3	4	-	-	-	-	-	10	10	-	-
SOW 8B	24	-	40	2	3	-	-	-	-	-	15	15	-	-
SOW 10-S1	44	2	45	1	1	-	-	-	2	6	-	-	-	-
SOW 10-S2	22	-	72	2	1	-	-	-	4	-	-	-	-	-
SOW 10-S3	74	-	18	1	<1	-	-	-	7	-	-	-	-	-
SOW 13-S1	30	-	52	4	3	-	-	10	-	-	-	-	-	-
SOW 13-S1A	60	-	20	<1	1	-	-	14	-	-	-	-	-	-
SOW 13-S2	8	-	65	5	5	-	-	15	-	-	-	-	-	2
SOW 13-S2A	10	38	42	3	1	-	-	-	3	-	-	-	-	-

Cal=Calcite, Dol=dolomite,.Qtz=quartz, Mcl=microline, Alb=albite, Mca=micas, Pal=palygorskite, Sep=sepiolite, Ill=Illite, Cly=clay minerals, Mag=magadiite, Ken=kenyaite,Hem=hematite,
Hal=halite
* Approximate
quantities

Geochemical results from twenty nodular and litho-clast samples indicate a high correlation between $CaCO_3$ and SiO_2 (R^2=0.985) suggesting inverse precipitation trends (cf. Gwosdz and Modisi 1983) and the incompatibility of precipitation environments of these two elements (Thomas and Shaw, 1991). AlO_2 and $Fe2O_3$ are also correlated (R^2=0.751) along with SiO_2 and TiO_2 at R^2=0.617 implying that most silicates are derived from Precambrian bedrock sources as a result of weathering and transportation. There is no correlation between $CaCO_3$ and MgO nor between SiO_2 and MgO. Results indicate high LOI values (>30 vol%) in the SOW1, SOW7A S4 and SOW10 S3 implying a high carbon content for these calcretes (Table VI-3). Geochemical results along with XRD data indicate that the MSB duricrusts may be sub-divided into four sub-groups broadly following classifications proposed by Walker (1960), Summerfield (1983a, 1983b) and Nash and Shaw (1998). Litho-unit $CaCO_3$ and SiO_2 proportions in relation to profile heights and duricrust type are shown on Table VI-4. Specifically, litho-unit 1 (LU1) is banded between 60-80 wt% calcite and 10-30 wt% SiO_2 and is referred to as calcrete (Figure VI-5). While examples of LU1 are present at all locations, the high calcite litho-unit is found mainly at 936 m in Location 1, SOW1. Litho-unit 2 (LU2) is banded between 35-50 wt% calcite and 35-52 wt% SiO_2, and composed of approximately equal proportions of calcite and siliceous sediment. This is referred to as calcrete with silica. LU2 duricrusts occur throughout the study area but are found mainly around 924 m (SOW3). Litho-unit 3 (LU3) is banded between 15-30 wt% calcite and 58-72 wt% SiO_2 and so has a higher proportion of silica rich sediment and occurs at Locations 2 and 3, but mainly in SOW13 between 943-945 m. This litho-unit is referred to as sil-calcrete based both on relative composition and matrix epigenesis (Nash and Shaw, 1998). Litho-unit 4 (LU4) is banded between <10 wt% calcite and 78-95 wt% SiO_2 and is therefore composed mainly of siliceous sediment, including silcrete and occurs entirely along the 943-945 m strandline at SOW7A and SOW13 (Table VI-4).

Average proportions of low quantity major elements per litho-unit are shown in Figure VI-6, from which minimal amounts of P_2O_5, MnO and Cr_2O_3 are omitted. Trends mainly show increasing MgO and an increase in the Mg/Ca ratio towards the calcite rich litho-units (i.e. towards LU1). The dominant major element after SiO_2/$CaCO_3$ is MgO which is particularly high in LU2 samples.These are relatively rich in dolomite while LU1 samples show relatively high proportions of sepiolite and palygorskite (cf. Table VI-2). This contrasts with the remaining low quantity major elements all of which increase towards the more silica rich litho-units (LU4). For instance, in LU1 the Al_2O_3 content is low between 0.67-1.77 wt% and increases through the

remaining litho-units to between 1.09-3.06 wt% in LU2, to between 1.84 to 2.07 wt% in LU3 and 1.72-3.35 wt% in LU4 (Table VI-3, Figure VI-5). K_2O, Na_2O and Fe_2O_3 increase with the proportion of clay minerals and feldspars towards LU4. TiO_2 also increases towards the more SiO_2 rich litho-units (Figure VI-6). These overall trends suggest that aggressive calcretisation/dolomitisation at high pH levels led to the almost complete replacement of most pre-existing silicates especially in LU1 and LU2 duricrists. The relatively high Mg/Ca ratios of these sediments suggests the prevalence of alkaline, highly evaporative conditions typified by closed basin environments. This contrasts with the apparently less intense process of silcretisation (in the LU4 and LU5 duricrusts) which in the MSB appears to take place under acidic, moderately saline conditions causing a number of the remaining silicates to survive intact. The lower than 1.2wt% TiO_2 content in all the litho-units infers that the mobilisation of pre-existing silicates may have been a dominant process in the pan littoral environments (Summerfield, 1982; Nash *et al*., 1994).

Table VI 3. Major element composition in wt. % in relation to morpho-stratigraphic sequence from MSB strandlines (missing are Cr_2O_3 at 0.01 wt.% for all samples and MnO ranging from 0.01-0.09 wt.% for all samples)

SAMPLE	SiO_2	K_2O	Al_2O_3	CaO	Fe_2O_3	MgO	Na2O	P2O5	TiO2	CO2inorg %	LOI
SOW 1-S1	25.6	0.33	1.5	37.74	0.66	1.96	0.15	0.01	0.09	29.6	32.73
SOW 1-S2	19.24	0.3	1.11	41.19	0.6	1.92	0.17	0.03	0.06	31.8	35.6
SOW 1-S3	14.09	0.2	0.67	42.96	0.31	3.21	0.17	0.05	0.05	33.6	38.65
SOW 1-S4	23.64	0.3	1.12	36.57	0.47	3.71	0.2	0.04	0.08	31	34.39
SOW 1-S5	24.34	0.38	1.42	35.62	0.49	4.72	0.23	0.01	0.08	28.8	33.55
SOW 1-S6	17.15	0.31	1.11	42.67	0.46	1.84	0.15	0.01	0.06	33.6	36.47
SOW 3-S1	42.47	0.78	2.03	25.16	0.62	4.08	0.4	0.01	0.08	22.8	25.05
SOW 3-S2	42.16	1.06	3.06	17.86	0.87	9.38	0.65	0.01	0.12	22.8	24.73
SOW 3-S3	48.88	1.02	2.68	19.95	0.66	4.87	0.52	0.01	0.1	17.8	21.75
SOW 3-S4	38	0.94	2.43	26.5	0.65	4.26	0.5	0.01	0.11	22.4	26.21
SOW 10-S1	47.16	0.76	1.29	25.92	0.5	0.82	0.23	0.27	0.09	20	23.11
SOW 10-S2	72.5	1.1	1.84	12.18	0.69	0.71	0.2	0.03	0.1	10	11.22
SOW 10-S3	20.83	0.65	1.03	41.29	0.42	0.98	0.14	0.03	0.05	32.6	34.37
SOW 8A	50.87	0.74	1.64	21.79	0.47	1.14	1.95	0.01	0.08	17	22.05
SOW 8B	62.03	0.7	1.78	13.35	0.53	1.53	2.68	0.01	0.08	9.6	17.92
SOW 7A-S1	93	0.92	2.18	0.24	0.68	0.43	0.16	0.01	0.14	0.2	2.09
SOW 7A-S2	50.9	0.94	1.94	21.33	0.68	3.55	0.18	0.01	0.09	18.6	20.95
SOW 7A-S2A	72.56	0.92	2.02	10.39	0.61	2.01	0.14	0.01	0.1	8.6	11.04
SOW 7A-S3	86.09	1.64	3.35	1.11	1.23	2.05	0.2	0.01	0.15	0.8	3.79
SOW 7A-S4	28.16	1.11	1.77	36.3	0.75	1.18	0.14	0.03	0.08	28.2	30.77
SOW 13-S1	58.68	0.85	2.07	16.94	0.72	3.09	0.26	0.01	0.15	13.2	17.79
SOW 13-S1A	29.03	0.54	1.26	33.87	0.47	3.53	0.21	0.03	0.08	26	31.5
SOW 13-S2	78.46	0.87	1.72	4.63	0.63	3.43	1.03	0.01	0.16	3.4	10.27
SOW 13-S2A	46.02	0.5	1.09	18.15	0.39	9.09	0.21	0.01	0.11	21.8	25.1
SOW 13-S3	67.03	0.87	1.85	13.43	0.68	2.19	0.14	0.01	0.16	9.6	13.64

Table VI 4. Duricrust type and calcite-silica composition (wt.%) in relation to morpho-stratigraphic sequence from MSB strandlines.

SAMPLE	Height m.asl	$CaCO_3$	SiO_2	Litho-unit	Duricrust type
SOW 1-S1	936	67.32	25.6	1	Calcrete
SOW 1-S2	936	72.32	19.24	1	Calcrete
SOW 1-S3	936	76.41	14.09	1	Calcrete
SOW 1-S4	936	70.5	23.64	1	Calcrete
SOW 1-S5	936	65.5	24.34	1	Calcrete
SOW 1-S6	936	76.41	17.15	1	Calcrete
SOW 3-S1	924	51.85	42.47	2	Calcrete with silica
SOW 3-S2	924	51.85	42.16	2	Calcrete with silica
SOW 3-S3	924	40.48	48.88	2	Calcrete with silica
SOW 3-S4	924	50.94	38	2	Calcrete with silica
SOW 7A-S1	943-945	0.45	93	4	Silcrete
SOW 7A-S2	943-945	42.3	50.9	2	Calcrete with silica
SOW 7A-S2A	943-945	19.56	72.56	3	Sil-calcrete
SOW 7A-S3	943-945	1.82	86.09	4	Silcrete
SOW 7A-S4	943-945	64.13	28.16	1	Calcrete
SOW 8A	905	38.66	50.87	2	Calcrete with silica
SOW 8B	908	21.83	62.03	3	Sil-calcrete
SOW 10-S1	910	45.48	47.16	2	Sil-calcrete
SOW 10-S2	910	22.74	72.5	3	Sil-calcrete
SOW 10-S3	910	74.14	20.83	1	Calcrete
SOW 13-S1	943-945	30.02	58.68	3	Sil-calcrete
SOW 13-S1A	943-945	59.13	29.03	2	Calcrete with silica
SOW 13-S2	943-945	7.73	78.46	3	Silcrete
SOW 13-S2A	943-945	49.58	46.02	3	Sil-calcrete
SOW 13-S3	943-945	21.83	67.03	4	Silcrete

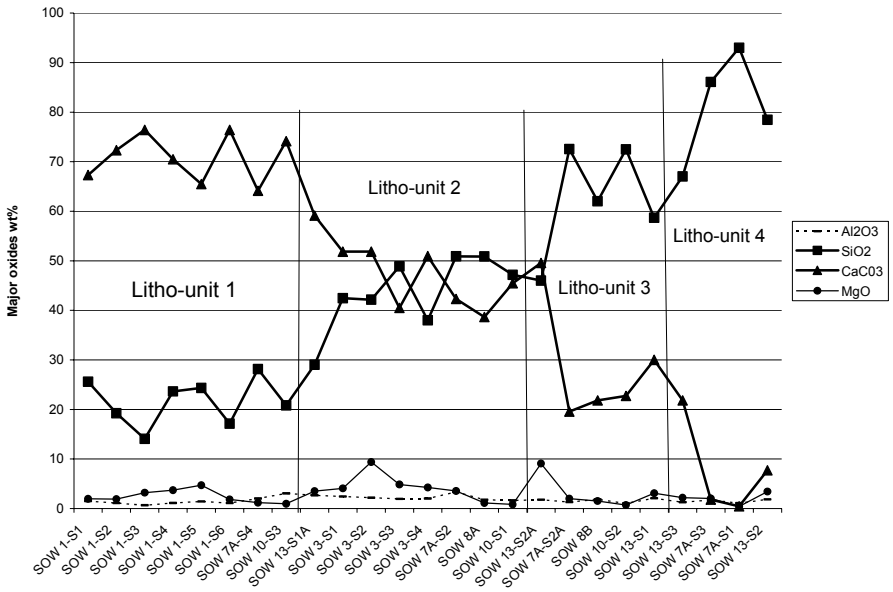

Figure VI 5. Results of bulk geochemical analysis showing the subdivision of samples into four litho-units based on relative percentages of SiO_2 and $CaCO_3$. Amounts of MgO and Al_2O_3 also shown.

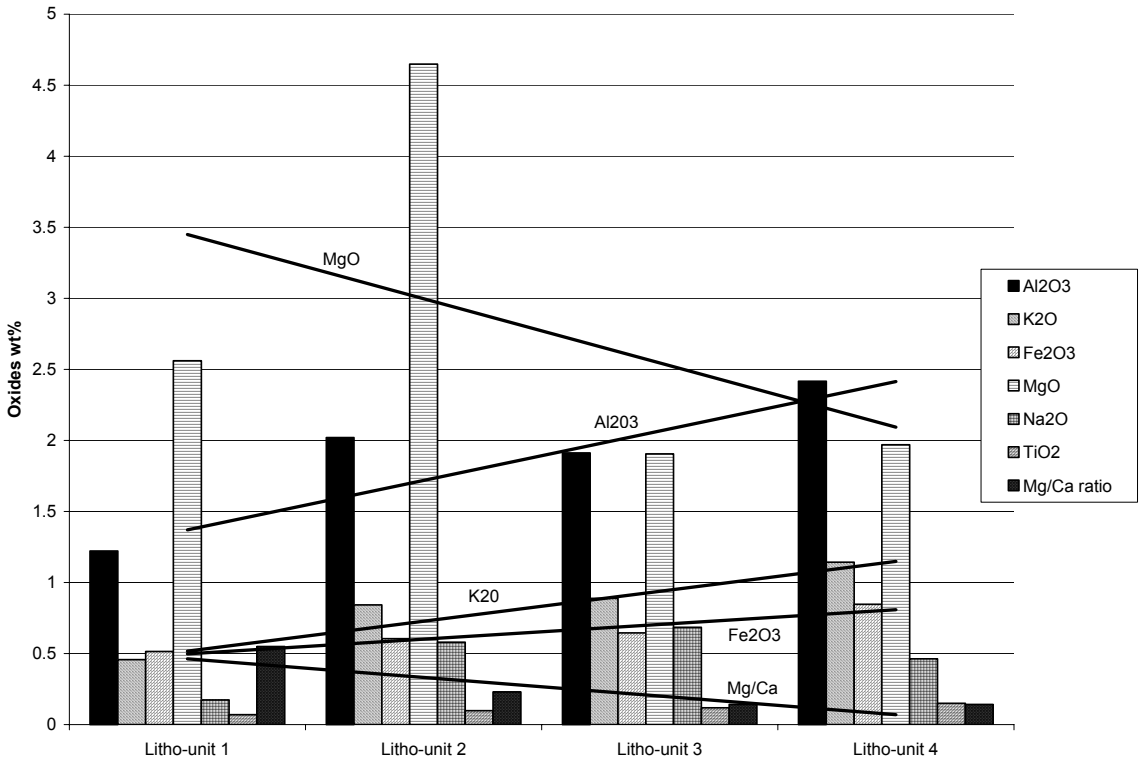

Figure VI 6. Trends in the lower quantity macro-elements relative to the four litho-units showing increasing MgO and Mg/Ca ratio with increasing $CaCO_3$ (to left) and increase in remaining elements with increasing SiO_2 (to right). Elements shown on histograms from left to right are Al_2O_3, K_2O, Fe_2O_3, MgO, Na_2O, TiO_2 and the Mg/Ca ratio.

VI.2.6 Thin section and ESEM results

Detailed thin section and ESEM analysis was undertaken to augment geochemical and XRD data and to provide insight into complex calcretisation and especially silicification processes. Litho-clast samples were selected for this work because these usually demonstrate several stages of silicification often of an originally calcareous deposit (cf. Ringrose et al., 1999a; Nash and Shaw, 1998). ESEM investigations in low vacuum mode on sub-samples from SOW1 S5 the indurated litho-clastic unit, show rounded quartz clasts with evidence of shallow etch marks closely associated with remobilised crypto-crystalline silica in addition to laminar calcrete fragments (Figure VI-7A). In this LU1 calcrete sample, EDAX results show equal proportions of Si and Ca on the remobilised surface indicating the close association of recrystallised quartz and calcite in the matrix (Table VI-5). The laminar calcrete appears to be relatively untouched and co-exists with remobilized amorphous silica. In a second slide (not shown) unmodified bedded Karoo sandstone clasts with circum-peripheral cracking are also evident in the mixed matrix. The SOW4 S4 sample reveals remobilised silica in the form of large and small interlayered Si plates which appear to be cracked suggesting a pressure solution mechanism (cf. Monger and Daugherty, 1991). Of particular interest are sub-samples which contain bacterial mat colonies either coating siliceous plates, within small voids or occupying pre-existing organically formed casings (Figure VI-7B). The casing analysed is more Si rich than the background silcrete plates implying that bacteria were sequestering Si initially from the void lining or casing (Table VI-5). The cocci infill and individual cocci are further enriched in Si relative to background and casing compositions while the cocci themselves also show traces of Ti not present in the background sample (Table VI-5). Once initiated, bacterial growth appears to be uniform with identifiable mound and chain patterns. Individual cocci are normally rounded and about 5-6 μm in diameter although some appear to be stunted or truncated (Figure VI-7C).

Thin section analysis of a lensoid shoreline sample from SOW 10 terrazzo plates show several stages of Si re-crystallisation (Figure VI-4B, Table VI-6). ESEM analysis of a SOW10 shoreline silica plate indicates that the sample is composed of rounded quartz and calcite pseudomorphs along with rounded 'onion ring' ghost structures in an amorphous silica rich matrix (Table VI-5, Figure VI-7D). The matrix contains between 42-76 wt% cryptocrystalline Si with discrete Ti rich minerals. Close examination of a Ca rich clast shows a transition of increasing silica content from the relatively Ca rich interior out towards the Si rich matrix (Table VI-6). The transition which is gradual shows a layered sequence of columnar calcite grains alternating with equiaxial calcite grains (Figure VI-8A).

The process seems to imply a systematic incursion (replacement) of Si rich pore fluids into a disintegrating calcrete clast. A quartz clast with accreted calcite layers also shows impregnation with Si rich pore fluids (Table VI-5). The calcite layers may have transformed into a porous columnar structure prior to silica mobilisation (Figure VI-8B). The 'onion ring' structures represent a more advanced stage in the process which terminates in the total replacement of clast-like shapes with matrix silica (Figure VI-7D). The fact that some of the original calcite remains in what appears as matrix material may account for the apparent co-existence and inverse relationship of Ca and Si in the matrices of MSB duricrusts.

Thin section data from Location 3 (SOW13 S2 S3 units) litho-clasts shows at least three stages of crystallisation in the matrix. The matrix comprises SiO_2 rich earlier microcrystalline and later cryptocrystalline phases with accompanying voids, some of which are filled by late stage authigenic silcrete (Table VI-6). ESEM analysis of a nodular sample (from SOW13 S2) shows high proportions of Mg and Ca in overgrowth structures (agglomerates) developed on quartz rich clastic sediment (Table VI-5). Further analysis revealed Si rich fungal hyphae and unidentified diatoms in a Si rich environment. Some of the hyphae occur as branching forms about 100 μm long, emplaced over inter-particle voids (Figure VI-8C). Others are smaller forming stub like growths 20 μm long or thin curvilinear forms around 30 μm in length (cf. Monger and Adams, 1996). The diatoms are also long (c. 30 μm) and fragmented in death assemblages adding silica to the littoral sediment. Both the diatoms and the hyphae suggest a wet (damp) environment during the time of deposition and both are involved in Si accumulation suggesting that biogenic sources were an important factor in silica accumulation and mobilisation.

VI.2.7 Thermoluminescence Dating

Samples for TL dating were obtained from Locations 1 and 3. Sand grains were dated from upper and lower units at SOW1, 3 and 4, SOW7A and SOW13 (Figure VI-3). Sand grains were also taken from a calcrete pit on an upper Thamalakane terrace near Maun (MaunSE12a) and from a lower terrace adjacent to the Zambezi river west of Kasane (KVFS3) to assist in providing a regional (MOZ) context (Figure VI-1). The sand was obtained from older litho-clasts or rhyzoliths.

The date KVF S3 was taken from the Chobe confluence with Zambezi river and is estimated at around 493 309 3 ± 3 985 years which is a minimum age as the sample is saturated. This date tends to suggest that a lower-mid Zambezi link was re-established during the mid-Pleistocene, inferring

that direct outward drainage from the northern margin of the MOZ depression took place around this time (cf. Thomas and Shaw, 1991). Meanwhile, the MSB may have been operating as a separate basin, being infilled during major wet periods throughout the mid-late Pleistocene from the northeast, south and west (Nash et al., 1994b; Ringrose et al., 1999a, 2002a).

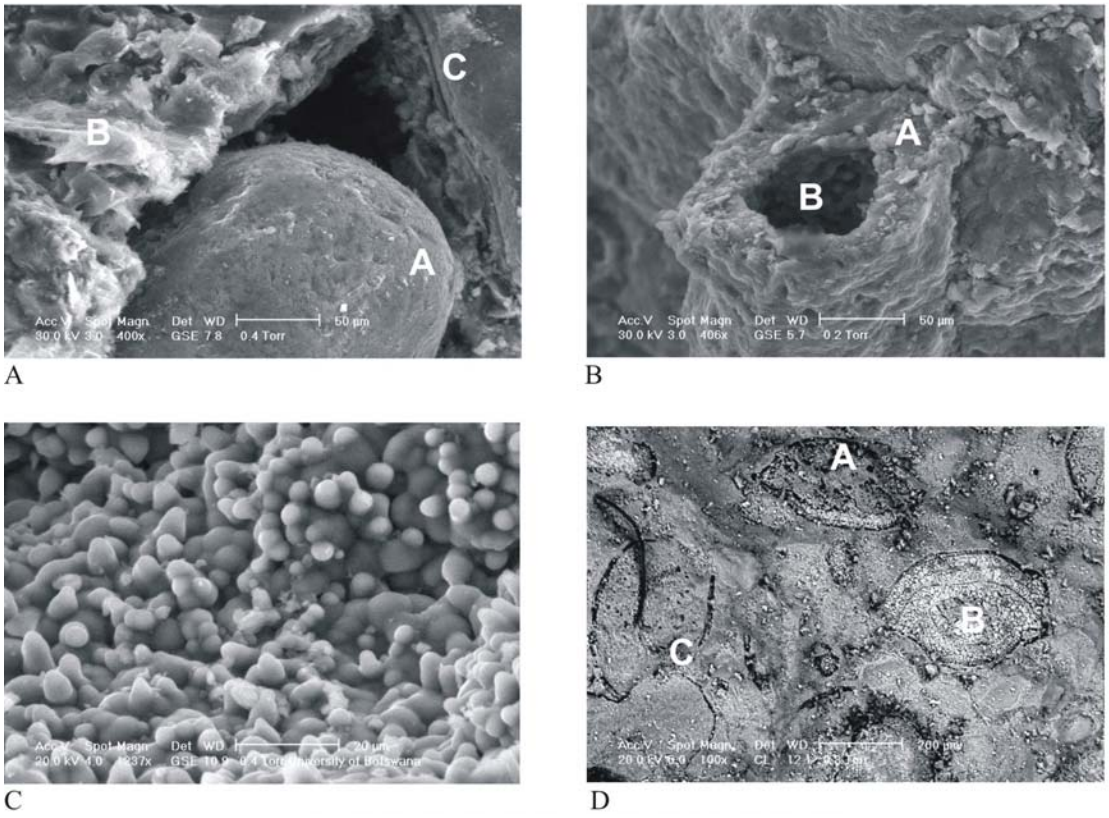

Figure VI 7. 7A-SEM photograph showing rounded quartz clast with evidence of shallow etch marks (A) and remobilised silica (B) with laminar calcrete (C) in SOW1 S5 sample. ;7B SEM photograph of silica rich organic casing (A) hosting bacterial cocci coating (B) (SOW4 S4); 7C SEM photograph detail of silica rich bacterial cocci showing developed and stunted growth forms (SOW4 S4); 7D SEM photograph showing Si rich (A) and Ca rich (B) pseudomorphs with 'onion ring' ghost structures (C) in an amorphous silica matrix (SOW10 shoreline SiO_2 plate).

TL dates were obtained from samples representing different diagenetic stages within the morpho-stratigraphic units from Location 3 on PMB strandlines. The oldest approximate date in the series is from the inner portion of a rhyzolith from the lower part of SOW13 S2 (P) from which an estimated age of post root calcification is given at 108 555 ± 9017 years ago. This earliest date is partially substantiated by a similar though slightly younger date from a siliceous clast within the hardpan of SOW13 S1 which is estimated as being formed around 102 194 ± 7621 years ago. These are the oldest recorded approximate dates on MSB upper strandlines (943-945 m) and appear to indicate the onset of a drying phase following an earlier late Pleistocene wet interval which occurred more than 110 000 years ago. Data from the Vostock core (Petit, 1999) and archeological data from Butzer (1984) and Brook et al., (1998) confirm wet conditions in the region around 120 000 years ago. Peaks in the Vostock data are constrained by ^{18}O data from drill holes off South Africa and Sea Surface Temperatures off Namibia, all of which appear to relate to Milankovitch precessional cycles (Partridge et al., 1999; Tyson et al., 2002). An estimated TL age from sand grains within a calcretised upper Thamalakane terrace north-east of Maun (MAUNSE12a) in the central MOZ (Okavango) basin gives a minimum sample age of 119 981 ± 9850 years but could be older as it is saturated. This early wet interval may have manifested as a series of wetland areas emerging from a "lake Okavango" extending southwards and eventually overspilling into the MSB over gaps in the Gidikwe ridge (cf. Cooke and Verstappen, 1984; Thomas and Shaw, 1991; Ringrose et al., 1999a,) more than 110 000 years ago.

Table VI 5. Duricrust composition (wt.%) from samples SOW4 (4), SOW 13 (13) and SOW1 (1) from ESEM EDAX microprobe measurements

Location	Na	Mg	Al	Si	S	Cl	K	Ca	Ti	Mn	Fe
SOW1calc		13.23	4.41	36.72			0.75	43.13			1.75
SOW1calc		17.34	2.92	38.76			0.72	38.59			1.66
SOW4S4bkgd	0.58	8.41	10.33	64.75		0.72	8.92				6.28
SOW4S4casing		9.65	5.27	78.04			4.27				2.77
SOW4S4infill		4.33	5.46	82.32			4.42				3.47
SOW4S4cocci		5.29	5.16	80.84			4.8		0.36		3.55
SOW10matrix1	1.27	0.69	1.01	41.21	0.08	0.12	0.54	1.86			0.85
SOW10matrix2	0.9	0.69	1.18	47.19	0.11	0.07	0.58	1.28			0.46
SOW10matrix3	2.18	1.95	2.2	76.47			1.35	3.32	0.48	0.36	1.68
SOW10Ti matrix	1.29	1.25	1.26	17.31			0.43	1.13	37.56	1.48	35.45
SOW10Sicentre	1.28	1.07	1.05	37.92	0.17	0.07	0.57	2.34	0.1		0.73
SOW10Sicol2	0.67	0.85	0.68	11.54	0.14	0.15	0.43	28.89	0.06		0.52
SOW10Sicol1	0.72	0.8	0.79	12.92	0.05	0	0.44	26.23	0.11		0.59
SOW10Simatrix	0.85	0.84	0.95	38.57	0.13	0.09	0.44	2.56			0.56
SOW10Cacol3	0.62	0.72	0.62	9.72			0.35	35.42			0.54
SOW10Cacol2	0.6	0.59	0.5	8.28			0.22	37.85			0.28
SOW10Caeqi-ax	0.68	0.95	0.78	11.62	0.05	0	0.41	27.32	0.12		0.69
SOW10Cacol1	0.6	0.72	0.68	14.12	0.12	0.11	0.35	31.46	0.2		0.55
SOW10Camatrix	0.85	0.87	0.95	36.25	0.1	0.07	0.55	3.87			0.42
SOW13agglom	1.37	14.41	4.42	57.59		3.77	2.9	12.54			
SOW13hyphae	1.66	15.85	5	50.81		4.45	3.08	16.25	0.38		5.52
SOW13ovrgrths	0.58	6.71	3.83	70.76		2.42	1.86	11.8			2.04

A second series of dates were obtained from sand grains in litho-clasts and nodules within the morpho-stratigraphic sequences at Locations 1 and 3. A siliceous litho-clast from SOW13 S3 was given an approximate TL date of 90 436 ± 8909 years. A nodule from within the overlying nodular rhyzolith unit from SOW7A S2 was given an approximate TL age of 80 678 ± 9202 years while a nodule from the rhyzolith free upper unit (SOW13 S2A) was dated at approximately 83 568 ± 7898 years. Interestingly an approximate age of 90 728 ± 7161 years was also obtained from a litho-clast from SOW1 S6. These dates may represent the drying phase of a second wet interval which appears to have attained a similar elevation in the MSB (943-945 m) to the earlier (>110 ka) interval but which shows evidence of a later decline to the 936 m level. These dates are again consistent with Milankovitch cycles which suggest that after the 120 ka. warm-wet period, less intense wet conditions recurred every 23 000 years such that a second warm, wet peak was evident around 97 ka, a third around 74 ka and a fourth around 51 ka in the southern African region (Tyson et al., 2002). As similar dates occur at both higher and lower strandline levels these are therefore considered to represent the close of a major infilling and evaporative event at >80-90 ka yrs. This extended over a range of heights (from 945 to 936 m) in the MSB with the later 936 m level being more indicative of strongly evaporative conditions.

Younger dates were obtained from a siliceous litho-clast from within the nodular unit (SOW13 S2) which resulted in an estimated TL age of 41 243 ± 3033. A litho-clastic sample from SOW4 S4 was also approximately dated at 43 408 ± 4443 years. These two dates imply a third Late Pleistocene wet interval which spanned an even wider range of heights (from 943-945 to 911 m) as it dried out in the MSB around 41 000 years ago. While higher palaeo-lake levels may have extended into MOZ depression, closed basin conditions may be inferred from the 924-911 m strandline duricrusts which fall within the LU2 high MgO type (Figure VI-5). The >41-43 ka. palaeo-lake event to some extent confirms earlier ^{14}C dating (c. 41 ka) previously described in the MSB by Cooke (1975); Cooke and Verstappen (1984); Shaw and Cooke (1986), Shaw and Thomas (1988), Thomas and Shaw (1993, 2002). The 41 ka wet interval is in general agreement with isotopic data from southern Botswana (e.g. Holmgren et al., 1995).

A sample from Location 2, SOW8A taken from a shoreline siliceous, lensoid nodule was TL dated at approximately 8753 ± 931 years. This date largely corresponds to the last major drying interval within the MSB, an episode which infers open basin conditions as fresh water from rivers to the west probably entered the lake during this episode, in a similar way to the ephemeral river inflow which

occurs today (Shaw et al., 1997). The post 40 ka period saw a continuation of the calcification processes in an evaporative transgressive-regressive environment to c. 8 ka with almost complete drying to the present day (cf. Rust et al., 1984; Scott, 1993). The date from the pan edge environment suggests that the ultimate drying phase of the Makgadikgadi complex commenced towards the close of the Holocene altithermal (Partridge et al., 1997).

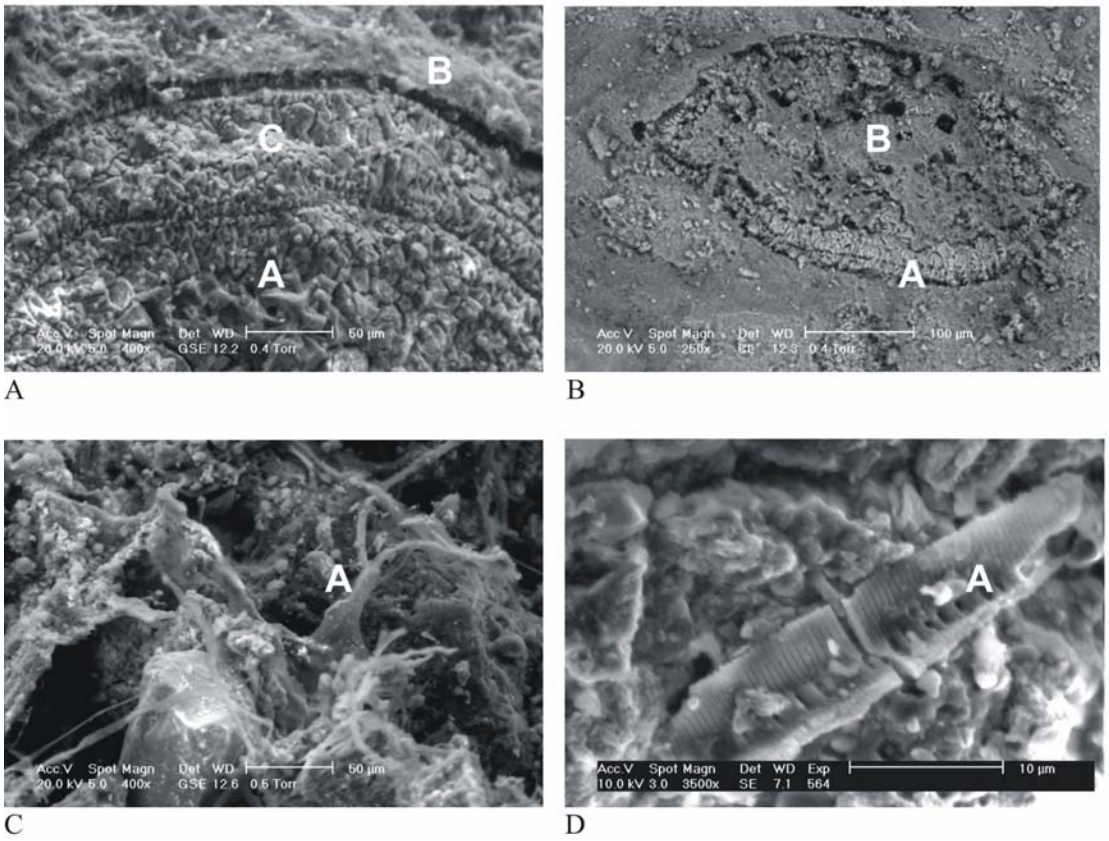

Figure VI 8. 8A SEM photograph of Ca rich clast showing transition stages from Ca rich interior (A) out towards the Si rich matrix (B) through a layered sequence of columnar and equiaxal calcite (C). (SOW10 shoreline SiO_2 plate); 8B SEM photograph of a Si rich clast (B) with accreted columnar calcite (A) inferring impregnation with Si rich matrix silica (SOW10 shoreline SiO_2 plate); 8C SEM photograph of Si rich fungal hyphae (A) emplaced over inter-particle voids (SOW13 S2); 8D SEM photograph of Si rich diatoms (A) about 30 µm from a fragmented death assemblage (SOW7A S2).

Table VI 6. Summary of depositional and diagenetic characteristics of major duricrust deposits of northern Sua Pan (MSB)

Duricrust type and type location	Fabric/texture	Composition	Structure	Late stage overprints
SOW 1 - Calcrete (LU1 type) S20.5249 E26.3740	Clast supported hardpan- Ca and Si lithoclasts-matrix supported Replacive/displaciv e calcrete matrix surface Fe mottling	Micritic low Mg calcite Microspar pore cement-secondary cements	Calcareous rhyzoliths, qtz clasts and calcareous lithoclasts, laminar and nodular-friable	Coated calcareous and quartz clasts. Secondary zonation and replacement by calcite. Void formation and infill Si cocci
SOW 2-4 Calcrete with silica (LU2 type) S20.5542 E26.1686	Matrix and host fabric supported, Laminar and massive void filling cement, Microcrystalline silica overgrowths	Cryptocrystalline green silica, microcrystalline pore lining cement high Mg calcite	Massive to blocky, friable, conglomeratic, abundant rhyzoliths (8-10cm)	Clast desiccation and cracking, coated buff silc-calc lithoclasts, concentric zonal replacement and void infilling
SOW 10 Sil-calcrete S20.3062 E25.9441	Matrix and host fabric supported, Laminar and massive void filling cement, Microcrystalline silica overgrowths	Dense cryptocrystalline (matrix and clasts)with lensoid microcrystalline crack and void infilling	Laminar massive, rounded silcrete clasts, peripherally layered with elongate silica nodules	Clast desiccation and cracking, coated silcrete lithoclasts, concentric zonal replacement, void infillings and large open voids
SOW 8A Sil-calcrete (LU2 type) S20.54361 E025.85368	Homogeneous cryptocrystalline silica	Cryptocrystalline silica with microcrystalline crack and void infilling	Massive buff siliceous lensoid pan edge nodules terrazzo type	Coated silcrete nodules, void infillings and large open voids
SOW 7A/13 (Silcrete) (LU4 type) S19.8916 E26.1390	Matrix and host fabric supported, Laminar and massive void filling cement, Microcrystalline silica overgrowths	Cryptocrystalline silica and quartz clasts with microcrystalline crack and void infilling	Massive to blocky, friable-partially consolidated abundant rhyzoliths - friable green sand	Clast desiccation and cracking, coated silcrete lithoclasts, nodular, Fe staining, void infillings and large open voids

VI.2.8 Discussion and Conclusions

Morpho-stratigraphic and geochemical evidence developed in this work imply that both open and closed basin conditions were prevalent in the MSB throughout the Late Pleistocene mainly as a result of alternating wet and dry climatic intervals. Events described above imply that early fresh water episodes which probably resulted from regional wet events were followed by extensive drying as indicated by freshwater followed by multiple Mg-calcrete dominated phases. Later and repeated silcretisation appears to have taken as a result of more localised increases in the groundwater table when the normally saline groundwater was diluted by rain or river inflow. New evidence suggests three palaeo-lake events in the MSB, two of which precede earlier recorded wet intervals in Botswana. While the three phases are represented by duricrusted strandlines at present heights above sea level of 943-945 m , 936 m and 924-910 m, evidence from TL dates suggests that more than one elevation was occupied at least during the two later palaeo-lake events. The last major palaeo-lake event recorded here is comparable to existing ^{14}C dates at c 41 000 BP mainly from the western margin of the MSB (Cooke, 1975; Cooke and Verstappen, 1984; Shaw and Cooke, 1986, Shaw and Thomas, 1988). The range of strandline heights with similar dates may result from palaeo-lake levels moving rapidly and frequently forming transgressive/regressive cycles (Eugster and Maglione, 1978) during sustained drying.

The Late Pleistocene lake margin littoral environment and associated pore water seepage resulted in morpho-stratigraphic evidence reflecting multi-cyclic geochemical overprinting at all strandline levels. Early biogenic related calcretisation in Locations 1 and 3 followed the development of freshwater rhyzoliths in an earlier, open lake system. Later calcretisation events appear to result from the effect of various controls on calcite dissolution and precipitation in littoral pore waters during drying phases leading to saturation with respect to calcium and magnesium ions in the presence of bicarbonate. The ionic content of the major palaeo-lakes is assumed to have been introduced in solution from the catchment area (cf. McCarthy and Ellery, 1995). Saturation may have been a local, littoral effect induced in part biogenically (by macrophyte photosynthesis) and probably also by the slow loss of CO_2 by degassing (Eugster and Kelts, 1983). Biogenically and/or climatically induced precipitation took place as pore waters attained a pH level of >9. Calcite precipitated along with some dolomite as the ultimate nature of the carbonate phase was controlled by the Mg/Ca ratio of the water (Muller et al., 1972; Folk, 1974; Goudie, 1983). This may have been synchronous with the formation of sepiolite and/or

palygorskite which Watts (1980) indicates occurs during or immediately after calcite or dolomite precipitation. Higher MgO levels were found both in the 943-945 m and lower sequence (936-911 m) strandlines suggesting that closed basin type evaporative conditions occurred several times. Calcretisation of littoral sands appears to have been effected as the replacement of pre-existing silicates such that very low quantities of major elements (relative to the more silicified units) remain in the calcareous units. The extensive nature of the early calcareous strandline remnants infers that closed basin conditions were prevalent over long time spans suggesting long term tectonic stability and consistent drying. At Locations 1 and 3 the biogenic phase appears to have been followed by nodular (littoral) calcrete formation and is succeeded by major desiccation intervals, indicated by calcareous silt units in SOW1 and SOW4. The desiccation intervals suggest extensive drying around the palaeo-lakes following calcretisation.

Intermittent silification of earlier calcrete phases is the most widespread event in the strandline duricrusts and varies from silicified litho-clasts and nodules in Location 1 to the complete silicification of already silicified litho-clasts and nodules in Locations 2 and 3. Silicified duricrust units appear to be related to relatively minor rainfall or inflow events which increased the level of the groundwater table, maybe forming localised shallow palaeo-lakes. The geochemistry of the groundwater more closely resembled present day Na-CO_3-SO_4-Cl type brines. Silification typically involves a number of mechanisms including mobilisation, transport and precipitation (Smale, 1973; Summerfield, 1982, 1983b; Chadwick et al., 1987a, 1987b; Thiry et al., 1988; Borger et al., 2003). Petrographic studies indicate that multiple episodes of silicification are relatively common in semi-arid areas, particularly in the Kalahari environment (e.g. Summerfield 1982, 1983c; Arakel et al., 1989; Nash et al., 1994a, 1994b). The inverse relationships of the major oxides (high $CaCO_3$/low SiO_2) normally infers a semi-continuous process whereby at > pH 9, calcite precipitation takes place thereby lowering the pH and enabling SiO_2 to go into solution in the pore water and begin to occupy interstitial voids and cracks in the pre-existing duricrust (Gwosdz and Modisi 1983; Ringrose 1996; Nash 1997; Nash and Shaw 1998). However this effect practically discounts the salinity factor which is particularly prevalent in the warm, shallow littoral zone of semi-arid lakes where declines in near shore lakewater are associated with groundwater seepage. Recent work Sauer and Straht (2004) shows that in semi-arid (wet) lacustrine environments enhanced evaporation leads to a lowering of the pH and the development of a geochemical barrier which leads to the polmerisation and precipitation of silica. This process also effects the reduction and depletion of the major elements due to intense leaching while facilitating the concentration of TiO_2 (Watts, 1977). Work in Australia shows that

most variation in silica concentration is explained by pH and EC values (Lee, 2003). Conclusions indicate that lower pH and less saline groundwater (pH 2.8-3.99) contains higher concentrations of dissolved silicon than relatively higher pH (6-7.18) more saline groundwater. Acidic, moderately saline groundwater is in near equilibrium with respect to amorphous silica whereas near neutral, saline groundwater corresponds to undersaturated conditions. Hence silica in various forms may precipitate whenever Si saturation is reached and the required changes in pH may be inherent in the littoral groundwater and may not necessarily occur as a direct result of calcite precipitation (cf. Williams et al., 1985; Monger and Adams, 1996). However the two oxides are co-variant in the MSB which implies that even under different lake water geochemical conditions the degree (or intensity) of silification varies proportionally with the $CaCO_3$ content implying preferential replacement of calcite with remobilised silica. Silica appears to enter the groundwater through the dissolution of quartz grains affected in part by a sloughing-off process. The sloughed-off silica appears to recrystallise close to the site of dissolution as cryptocrystalline silica while also forming matrix silica involved in the replacement of calcite clasts. Much of this process may be enhanced by (*inter-alia*) diatoms, bacteria and algal growth which are active in Si uptake in the moist pan littoral. Shaw et al. (1990) and Harrison and Shaw (1995) also describe almost pure silcrete forming contemporaneously in a hyper-saline pit near Sua Pan by silica fixing cyanobacteria. Evidence from this work suggests that the abundant silica, often in the form of silcrete in the MSB is also the result of *in situ* silica precipitation under acidic, moderately saline porewater conditions along the pan edges.

Given the evidence presented in this work it is likely that both exogenic (fresh water incurions) and biogenic agencies were responsible for the extensive silcretisation in the MSB littoral duricrusts. Silicification episodes appear to post-date early relatively freshwater palaeo-lake stages (with macrophyte growth) and subsequent calcretisation in multiple stages after palaeo-lake events as a result of watertable fluctuations in a semi-arid environment similar to that occurring in Botswana at present (Bhalotra, 1987). The repetition of silica mobilisation through time may be responsible for prevalent SiO_2 increases up-profile. The apparent lack of intense silica remobilisation at the SOW1 (936 m) level suggests that elevated water table levels remained for a shorter duration at this height. As generally the similar water table levels (945-943 m, 924 m, 910 m) were involved in repeated SiO_2 re-mobilisation events over the 110 ka record, it is possible that the MSB was tectonically stable during at least the Late Pleistocene after initial faulting in the Late Tertiary.

Acknowledgements

The authors wish to acknowledge financial assistance from the University of Botswana, Research and Publications Committee (Grant RPC 509). The assistance was given in response to a request from the local SAFARI2000 committee for funding to consider Botswana palaeo-environments in the context of global climatic change. Soda Ash Botswana are thanked for allowing access to Sua Spit.

References.

Aitken, M.J., 1985. Thermoluminescence Dating. Academic Press Publishers: London.

Alonso-Zarza, A.M., Sanchez-Moya, Y., Bustillo, M.A., Sopena, A., Delgado, A., 2002. Silification and dolomitization of anhydrite nodules in argillaceous terrestrial deposits: an example of meteoric-dominated diagenesis from the Triassic of central Spain. Sedimentology, 49, 303-317.

Arakel, A.U., Jacobson, G., Salehi, M., Hill, C.M., 1989. Silicification of calcrete in palaeodrainage basins in the Australian arid zone. Aust J. Earth Sci., 36, 73-89.

Baillieul, T.A., 1979. A reconnaisance survey of the cover sands in the Republic of Botswana. J. Sediment. Petrol., 45,494-503.

Bhalotra, Y.P.R., 1987. Climate of Botswana, Part II: elements of climate, rainfall. Department of Meteorological Services, Ministry of Works and Communication, Gaborone, Botswana, 21pp.

Blumel, W.D., Eitel, B., Lang, A., 1998. Dunes in southeastern Namibia: evidence for Holocene environmental changes in the southwestern Kalahari based on thermoluminesence data, Palaeogeogr:, Palaeoclimatol., Palaeoecol., 138, 139-149.

Borger, H., McFarlane, M.J. Ringrose, S., 2004. Processes of silicate karstification associated with pan formation in the Darwin-Koolpinya area of northern Australia. Earth Surf. Proc. Landf., 29,359:371.

Botter-Jensen L, Duller G.T., 1992. A New System for Measuring Optically Stimulated Luminescence from Quaternary Samples. Nucl. Tracks and Radiation Meas,. 20, 202-205.

Brook, G.A., Cowart, J.B, Brandt, S.A., 1998. Comparison of Quaternary environmental change in eastern and southern Africa using cave speleotherm, tufa and rock shelter sediment data. In:Alsharan, A, Glennie, K.W.Wintle, G.L.Kendall, G.C. (Eds) Quaternary Deserts and Climate Change,. Balkema, Rotterdam, pp.239-250.

Butzer, K.W., 1984. Archeogeology and Quaternary environment in the interior of southern Africa. In Southern African Prehistory and Paleoenvironments, Chapter 1, Klein R.G., Balkema, A.A. (eds). Rotterdam, pp. 1-64.

Carl, C., 1987. Investigations of U series disequilibria as a means to study the transport mechanism of uranium in sandstone samples during weathering. Uranium 3, 285-305.

Chadwick, O.A., Hendricks, D.M., Nettleton, W.D., 1987a. Silica in duric soils: I a depositional model. Soil Sci. Soc. Amer. J., 51, 975-982.

Chadwick, O.A., Hendricks, D.M., Nettleton, W.D., 1987b. Silica in duric soils: II Minerology. Soil Sci. Soc. Amer. J., 51, 982-985.

Cooke H.J., 1975. The paleoclimatic significance of caves and adjacent landforms in the Kalahari of western Ngamiland, Botswana. Geog. J., 141, 430-444.

Cooke H.J., 1979. The origin of the Makgadikgadi Pans. Bots. Notes Records 11, 37-42.

Cooke H.J., 1980. Landform evolution in the context of climatic changes and neotectonics in the middle Kalahari of north-central Botswana. Trans. Inst. Brit. Geog., NS 5, 80-99.

Cooke H.J., Verstappen H.Th., 1984. The landforms of the western Makgadikgadi basin in northern Botswana, with consideration of the chronology of the evolution of Lake Palaeo-Makgadikgadi. Zeit. Geomorph., N.F.Bd28, Heft 1, 1-19.

Du Toit, A.L., 1933. Crustal movements as a factor in the evolution of South Africa, South Afric., J. Sci., 24, 88-101.

Eugster, H.P., Hardie, L.A., 1978. Saline Lakes, In: Lerman (Ed.) Chemistry, Geology and Physics of Lakes, Springer-Verlag, New York, pp. 273-293.

Eugster, H.P., Maglione, G., 1979, Brines and evaporites of the Lake Chad basin, Africa. Geochim. Cosmochim. Acta, 43, 973-981.

Eugster, H.P., Kelts, K., 1983. Lacustrine chemical sediments In: Goudie, A.G. and Pye, K., Chemical sediments and geomorphology: precipitates and residua in the near surface environment. London, Academic Press, pp.321-368.

Folk, R.L., 1974. The natural history of crystalline calcium carbonate: effect of magnesium content and salinity. J. Sediment. Petrol., 44, 40-53.

Geological Survey of Botswana, 2000. Geological Map of the Republic of Botswana (digital edition). Geological Survey of Botswana, Lobatse, Botswana.

Goudie A.S., 1983. Calcrete, In Chemical Sediments and Geomorphology: Precipitates and Residua in the near-surface environment, Goudie AG, Pye, K (eds). Academic Press Inc. Publishers, London

Gumbricht, T., McCarthy, T.S. Merry, C.L. 2001. The topography of the Okavango Delta Botswana, and its tectonic and sedimentological implications, South Afric. J. Geol., 104, 243-264

Gwosdz W., Modisi, M.P., 1983. The Carbonate Resources of Botswana. Botswana Geological Survey Mineral Resources Report 6, Lobatse, Botswana, 48pp.

Harrison, C.C. Shaw, P.A., 1995. Bacterial involvement in the production of silcretes? Bulletin Institut Oceanographique, Monaco, 14, 291-295.

Holmgren K., Karlen, W, Shaw, P., 1995 Palaeoclimatic significance of the stable isotopic composition and petrology of a late Pleistocene stalagmite from Botswana, Quat. Res., 43, 320-328.

Huaya L., Xiaoyong, W., Haizhou, M., Hongbing, T., Vandenberghe, J., Xiaodong, M., Zhen, L., Youbin, S., Zhisheng, A., Guangchao, C., 2004. The plateau monsoon variation during the past 130 kyr revealed by loess deposit at northeast Qinghai-Tibet, Global and Planetary Change, 41, 207-214.

Klappa C.F., 1980. Rhzyoliths in terrestrial carbonates: classification, recognition, genesis and significance. Sedimentology, 27, 613-629.

Krumbein, W.C., Garrels, R.M., 1952. Origin and classification of chemical sediments in terms of pH and oxidation-reduction potentials. J. Geol., 60, 1-33.

Lancaster, N., 1981. Palaeoenvironmental implications of fixed dune systems in southern Africa, Palaeogeogr:, Palaeoclimatol., Palaeoecol., 33,327-346.

Lancaster, N., 2000. Aeolian deposits. In Partridge T.C. and Maud R.R., (eds) The Cenozoic of Southern Africa, New York, Oxford University Press, 73-84.

Lee, S. 2003. Groundwater geochemistry and associated hardpans in southwestern Australia, In: Roach I.C. (ed) Advances in Regolith, CRC LEME, Curtin University of Technology, Western Australia, pp. 254-258.

Mallick, D.I.J, Habgood F, Skinner AC. 1981. A geological interpretation of Landsat imagery and air photography of Botswana. Overseas Geological and Mineral Resources, London, 56, 1-36.

McCarthy, T.S., Ellery, W.N., 1995. Sedimentation on the distal reaches of the Okavango fan, Botswana, and its bearing on calcrete and silcrete (ganister) formation, J. Sediment. Res, A65(1), 77-90.

Modisi, M.P., Atekwana, E.A., Kampunzu, A.B. Ngwisanyi, T.H., 2000. Rift kinematics during the incipient stages of continental expansion: Evidence from the nascent Okavango rift basin, northwest Botswana, Geol., 28, 939-942.

Monger, H.C., Daugherty, L.A., 1991b. Pressure solution: Possible mechanism for silicate grain dissolution in a petrocalcic horizon, Soil Sci. Soc. Amer. J., 55, 1625-1629

Monger, H.C. Adams, H. P., 1996, Micromorphology of calcite-silica deposits. Soil Sci. Soc. Amer. J., 60:519-530.

Moore A. E., Larkin, P. 2001. Drainage evolution in south-central Africa since the breakup of Gondwana. South Afric. J. Geol., 104, 47-68.

Muller, G., Irion, G., Forstner, U., 1972. Formation and diagensis of inorganic Ca-Mg carbonates in a lacustrine environment. Naturwissenschaften, 59 Jg 4, 158-164.

Nash D. J., 1997. Groundwater as a geomorphic agent in drylands. In Arid Zone Geomorphology: Process, Form and Change in Drylands, Thomas, D.S.G (Ed.). John Wiley Publishers, Chichester.

Nash D.J., Thomas D.S.G. Shaw P.A., 1994a. Siliceous duricrusts as palaeoclimatic indicators: evidence from the Kalahari desert of Botswana. Palaeogeogr:, Palaeoclimatol., Palaeoecol., 112, 279-295.

Nash D.J., Shaw P.A., Thomas D.S.G., 1994b. Duricrust development and valley evolution: process-landform links in the Kalahari. Earth Surf. Proc.Landf., 19, 279-317.

Nash D. J., Shaw P.A., 1998. Silica and carbonate relationships in silcrete-calcrete intergrade duricrusts from the Kalahari desert of Botswana and Namibia. J. Afric. Earth Sci. 27, 11-25.

Partridge, T.C., Demenocal, P., Lorentz, S.A., Paiker, M. J., Vogel, J.C., 1997. Orbital forcing of climate over South Africa: a 200,000-year rainfall record from Pretoria Salt Pan. Quat. Sci. Rev., 16, 1125-1133.

Partridge, T.C., Scott, L., Hamilton, J.E., 1999. Synthetic reconstructions of southern African environments during the Last Glacial Maximum (21-28 kyr) and the Holocene Altithermal, (8-6 kyr). Quat. Inter., 57/58, 207-214.

Partridge, T.C., Maud, R.R., 2000. The Cenozoic of southern Africa. New York: Oxford University Press, 406 pp.

Petit, J.R. 1999. Climate and atmospheric history of the past 420 000 years from the Vostock ice core, Antarctica. Nature 399:429-436.

Radtke, U., Janotta, A., Hilgers, A., Murray, A., 1999. The potential of OSL and TL for dating late-glacial and Holocene dune sands tested with independent age controls of the Laacher See tephra (12, 880a) at the section Mainz-Gonsenheim, 9th International Conference on Luminescence and ESR dating (LED99), Rome.

Republic of Botswana, 2000. Makgadikgadi Pans Development Plan, National Conservation Strategy Implementing Agency, Gaborone, Botswana, 211pp.

Ringrose, S., 1996. The geomorphological context of calcrete depositions in the Dalmore Downs area, Northern Territory Australia, J. Arid Environ 33, 291-307.

Ringrose, S., Downey, B., Genecke, D., Sefe, F., Vink, B., 1999a. Nature of calcareous deposits in the western Makgadikgadi basin, Botswana, J. Arid Environ, 43, 375-397.

Ringrose, S, Lesolle, D, Botshoma, T., Gopolang, B, Vanderpost, C., Matheson, W., 1999b. An analysis of vegetation cover components in relation to climatic trends along the Botswana Kalahari Transect. Bots. Notes Records, 31, 33-52.

Ringrose, S, Kampunzu, A.B., Vink, B., Matheson, W., Downey, W., 2002a. Origin and palaeo-environments of calcareous sediments in the Moshaweng dry valley, southeast Botswana. Earth Surf. Proc. Landf., 27, 591-611.

Ringrose, S., Huntsman-Mapila, P., Kampunzu, A.R., Matheson, W., Downey, W.S., Vink, B., 2002b. Geomorphological evidence for MOZ palaeo-wetlands in northern Botswana; implications for wetland change. Presentation to Monitoring of Tropical and Sub-

tropical Wetlands Conference, December 2002, Maun, Botswana, Published by HOORC and the University of Florida, Centre for Wetlands.
Rust U., Schmidt H., Dietz K., 1984. Palaeoenvironments of the present day arid southwestern Africa 30 000-50 000BP: results and problems. Palaeoecol. Africa 16, 109-148.
Sauer D., Straht K., 2004 Formation of calcretes and silcretes in the Alentejo (Portugal) and consequences for the landscape, ecosystems and land use. http://www.bodenkunde.ini-freiburg.de/eurosoil/abstracts/id256_Sauer.pdf.
SAFARI2000 website. 2000. http://www.safari.gecp.virginia.edu
Scott L., 1993. Palynological evidence for late Quaternary warming episodes in Southern Africa. Palaeogeogr., Palaeoclimatol., Palaeoecol., 101, 229-235.
Shaw, P.A., 1985. Late Quaternary landforms and environmental change in northwest Botswana; the evidence of Lake Ngami and the Mababe Depression. Trans. Inst. Brit. Geog., NS10, 333-346.
Shaw P., Cooke, H.J., 1986. Geomorphic evidence for the late Quaternary palaeoclimates of the middle Kalahari of northern Botswana. Catena. 13, 349-359.
Shaw P.A., Thomas, D.S.G., 1988. Lake Caprivi: a late Quaternary link between the Zambezi and middle Kalahari drainage systems. Zeit. Geomorph., 32, 329-337.
Shaw, P.A., Cooke, H.J., Perry, C.C., 1990. Microbalitic silcretes in highly alkaline environments: some observations from Sua Pan, Botswana. South Afric. J. Geol., 93:5/6, 803-808.
Shaw P.A, Stokes S, Thomas D.S.G., Davies F., Holmgren K., 1997. Palaeoecology and age of a Quaternary high level lake in the Makgadikgadi basin of the middle Kalahari. South Afric. J. Sci., 93, 273-277.
Smale. D., 1973. Silcretes and associated silica diagenesis in southern Africa and Australia. J. Sediment. Petrol., 43, 1077-1089.
Smith, R.A., 1984, Lithostratigraphy of the Karoo stratigraphy in Botswana, Botswana Geological Survey Bulletin, Lobatse, Botswana, 26, 34pp.
Stokes, S., Thomas D.S.G., Washington R., 1997. Multiple episodes of aridity in southern Africa since the last interglacial period. Nature 388, 154-158.
Summerfield, M. A., 1982. Distribution, nature and probable genesis of silcrete in arid and semi-arid southern Africa. In Aridic Soils and Geomorphic Processes. Yalon, DH (Ed). Catena Supplement 1, 37-65.
Summerfield M. A., 1983a. Silcrete as a palaeoclimatic indicator: evidence from southern Africa. Palaeogeogr., Palaeoclimatol., Palaeoecol., 41, 65-79.
Summerfield M. A., 1983b. Silcrete. In: Chemical Sediments and Geomorphology. Goudie, AS, Pye K (eds). Academic Press Publishers: London, pp. 19-91.
Summerfield, M. A., 1983c. Petrography and diagenesis of silcrete from the Kalahari basin and Cape coastal zone, southern Africa, J. Sediment. Petrol., 53, 895-909.
Thomas D.S.G., Shaw, P.A., 1991. The Kalahari Environment. Cambridge University Press Publishers: Cambridge, 248pp.
Thomas D.S.G., Shaw P.A. 1993. The evolution and characteristics of the Kalahari, southern Africa. J. Arid Environ. 25, 97-108.
Thomas D.S.G., Shaw, P.A. 2002. Late Quaternary environmental change in central southern Africa: new data, synthesis, issues and prospects, Quat. Sci. Rev., 21, 783-797.
Tyson, P.D. Fuchs, R., Fu, C, Lebel, L., Mitra, A.P. Odada, E, Perry, J., Steffen, W., Virji, H., (Eds) 2002, Global-Regional Linkages in the Earth System, START, Springer-Verlag, New York, 198pp.
Thiry, M., Ayrault, M.B., Grisoni, J., 1988. Ground water silicification and leaching in sands, example of the Fontainebleau Sand in the Paris Basin, Bull. Geol. Soc. Amer., 100, 1283-1290.
Tiercelin, J.J., Lezzar, K.E, 2002. A 300 million year history of rift lakes in Central and east Africa: an updated broad review. In: The East African Great Lakes, Limnology,

Palaeolimnology, and Biodiversity, (eds) E.O. Odada and D.O. Olago, Kluwer Academic Publishers, Dordrecht, pp. 3-60.
Vink, B., Ringrose, S., Kampunzu, A.R., 2001. The presence of magadiite and kenyaite in Sua pan, Central Botswana. Bots. J. Earth Sci., 5, 32-34.
Walker T.R., 1960. Carbonate replacement of detrital crystalline silicate minerals as a source of authigenic minerals in sedimentary rocks. Bull. Geol. Soc. Amer., 71, 145-152.
Watts N.L., 1980. Quaternary pedogenic calcretes from the Kalahari (southern Africa): mineralogy, genesis and diagenesis. Sedimentology 27, 661-686.
Watts S.H. 1970. Major element geochemistry of silcrete from a portion of inland Australia. Geochim. Cosmochim. Acta, 41, 1164-1167.
Williams, L.A., Parks, G.A., Crear, D.A., 1985. Silica diagenesis 1. Solubility controls. Journ Sed. Petrol. 55,301-311.
Wright V.P., Tucker ME., 1991. (Eds) Calcretes, Reprint Series Volume 2 of the International Association of Sedimentologists. Blackwell Scientific Publications, London, 352 pp.
Zoller L, Pernicka E. 1989. A note on overcounting in alpha-counters and its elimination. Ancient TL 7, 11-14.

VII. USE OF THE GEOCHEMICAL AND BIOLOGICAL SEDIMENTARY RECORD IN ESTABLISHING PALAEO-ENVIRONMENTS AND CLIMATE CHANGE IN THE LAKE NGAMI BASIN, NW BOTSWANA

VII.1. Enregistrement sédimentaire des variations du niveau du lac Ngami au Pléistocène supérieur et à l'Holocène

Résumé de l'article

Les sediments d'un profil de 4.6 m dans le lac asséché de Ngami dans le Nord-ouest du Botswana ont été analysés: mesures géochimiques (elements majeurs et trace) et datations (^{14}C et TL). Certains niveaux du profil sont riches en diatomées et ont été utilisés comme indicateurs des hauts et bas niveaux du lac. Les sédiments du Lac Ngami ont une teneur élevée en SiO_2 (51 – 92.5 wt.%, avg. 72.4 wt.%) et des teneurs variables en Al_2O_3 (2.04 – 17.2 wt.%, avg. = 8.88 wt.%). Des concentrations élevées en Al_2O_3 et en matière organique (LOI_{orgC}) indiquent que les conditions physico-chimiques dans le lac étaient stables de 42 ka jusqu'à 40 ka. La presence de diatomées suggère un milieu peu profond et saumâtre. A 40 ka, l'enregistrement par les sédiments lacustres s'arrête, peut-être à cause de l'activité tectonique. A 19 ka des conditions aérobie et turbulentes dominaient et le niveau du lac était a son maximum jusqu'à 17 ka. Les résultats d'analyse des terres rares, indiquent que des conditions alcalines prévalaient à 12 ka. La presence de diatomées suggère également un niveau peu profond pour cette période. L'augmentation du rapport Sr/Ca, la diminution du LOI_{orgC} et de Al_2O_3 durant la periode de 16 ka à 5 ka suggèrent un écoulement moindre dans le bassin et une diminution du niveau de lacustre. Ces conditions ont été maintenues par les pluies locales car la région a connu une période plus humide entre 16 et 11 ka. Ensuite, le niveau du lac a crû rapidement en quatre mille ans, probablement en réponse à de plus fortes précipitations en Angola. Ces resultats indiquent que les niveaux du lac Ngami sont lies à des changements de regime de precipitation en Angola et localement. Ces résultats confirment que l'actuel déphasage entre l'Afrique du sud et les region équatoriale d'Afrique existait au cours du Quaternaire supérieur à la hauteur des hauts-plateaux de l'Angola et du nord-ouest du Botswana.

VII.2 Use of the geochemical and biological sedimentary record in establishing palaeo-environments and climate change in the Lake Ngami basin, NW Botswana

P. Huntsman-Mapila[a,b*], S. Ringrose[a], A.W. Mackay[c], W.S. Downey[d], M. Modisi[e], S. H. Coetzee[d], J-J Tiercelin[b], A.B. Kampunzu[e], C. Vanderpost[a]

[a]*Harry Oppenheimer Okavango Research Centre, University of Botswana, Private Bag 285, Maun, Botswana*
[b]*UMR-CNRS 6538, Institut Universitaire Européen de la Mer, 29280, Plouzané, France*
[c] *Environmental Change Research Centre, Department of Geography, University College London, 26 Bedford Way, London, WC1H 0AP, United Kingdom*
[d] *Physics Department, University of Botswana, Private Bag 0022 Gaborone, Botswana*
[e]*Geology Department, University of Botswana, Private Bag 0022, Gaborone, Botswana*

Article published by Quaternary International 148 (2006) 51-64

Abstract

Sediment samples from a 4.6 m profile in the dry bed of Lake Ngami in NW Botswana were analysed for geochemistry and dated using both ^{14}C and TL methods. Certain units in the profile were found to be diatom rich and these, with the geochemical results, were used as indicators of high and low lake levels within the basin. The Lake Ngami sediments contain a high proportion of SiO_2 (51-92.5 wt.%, avg. 72.4 wt.%) and variable levels of Al_2O_3 (2.04-17.2 wt.%, avg. 8.88 wt.%). Based on elevated Al_2O_3 and organic matter (LOI_{orgC}) results, lacustrine conditions occurred at c. 42 ka until 40 ka and diatom results suggest that relatively deep but brackish conditions prevailed. At 40 ka, the lacustrine sedimentary record was terminated abruptly, possibly by tectonic activity. At ca.19 ka, shallow, aerobic, turbulent conditions were prevalent, but lake levels were at this time increasing to deeper water conditions up until c. 17 ka. This period coincides with the Late Glacial Maximum, a period of increased aridity in the central southern Africa region. Generally, increasing Sr/Ca ratios and decreasing LOI_{orgC} and Al_2O_3, from c. 16 ka to 5 ka, suggest decreasing inflow into the basin and declining lake levels. Based on the enrichment of LREE results, slightly alkaline conditions prevailed at c. 12 ka. Diatom results also support shallow alkaline conditions around this time. These lake conditions were maintained primarily by local rainfall input as the region experienced a warmer, wetter phase between 16 –

11 ka. Lake levels rose rapidly by 4 ka, probably in response to enhanced rainfall in the Angolan catchment. These results indicate that lake levels in the Lake Ngami basin are responding to rainfall changes in the Angolan catchment area and local rainfall. The results confirm that the present day anti-phase rainfall relationship between southern Africa and regions of equatorial Africa was extant during the late Quaternary over the Angolan highlands and NW Botswana.

VII.2.1 Introduction

The geochemistry of sediments reflects a combination of provenance, chemical weathering, hydraulic sorting, abrasion, redox condition and diagenesis (Taylor and McLennan, 1985; Condie, 1993). Lake deposits provide a continuous record of environmental changes which record climatic, hydrologic, sedimentological, tectonic, geochemical, biological and biochemical conditions. The focus of this study is the currently dry Lake Ngami, a 3000 km2 basin at the distal reaches of the Okavango Delta (Shaw et al., 2003). The Okavango Delta in north-west Botswana is an unstable hydrological system and change to this system is assumed to take place along five major pathways. These are characterised in terms of their driving agents as, climatic (with inputs of rainfall and solar energy); geological (neotectonic inputs); hydrological (surface and sub-surface water inputs); vegetational-geomorphological (channel blockages, island-floodplain building inputs); zoological (wildlife inputs) and human induced (fire and land-use change inputs) (McCarthy and Ellery 1993, Gieske 1996, McCarthy *et al,* 1998a and 1998b, Government of Botswana 2002, Ringrose et al., 2003).

Nicholson and Entekhabi (1986) report an inverse correlation between annual rainfall over southern Africa and parts of equatorial Africa for the period of meteorological record. Tyson et al., (2002a) compare data from lake sediments in Lake Naivasha in Kenya and a stalagmite record from Cold Air cave in Makapansgat valley in South Africa over the past 1,100 years. They report that during drier, cool periods in Lake Naivasha, conditions were warmer and wetter at Makapansgat. Conversely, cool dry conditions at Makapansgat correspond to periods of high lake levels at Naivasha.

Given the contrasting controls of weather in the equatorial region and subtropical Africa, inverse links between climates of the Angolan Highland catchment and the Lake Ngami basin may be expected. With future climate change scenarios (in particular, rainfall), there is often a discrepancy between the models and how well the models represent the present day climate. However, the model of change in wet season (December- February) precipitation from 1960-1990

to 2070-2100 (HadCM2 IS92a) developed by the Hadley Centre (http://www.metoffice.com/research/hadleycentre/models) shows an anti-phase effect in precipitation where a net decrease in precipitation for this period is shown for central southern Africa and an increase for tropical Africa, including the Angolan highlands.

The goals of this paper are: 1) to describe and interpret the Quaternary sediments deposited in the Lake Ngami basin, 2) to document climate-related changes in the sediment and 3) to indicate tectonically induced shifts in sedimentation patterns.

VII.2.2. Local setting and climate

The Okavango River which drains from the Angolan highlands, enters the Makgadikgadi-Okavango-Zambezi (MOZ) rift depression (Ringrose et al., 2005), through a narrow NW-SE-trending swamp called the Panhandle before extending into a large inland alluvial fan (McCarthy et al., 2000). Lake Ngami (Figure VII-1) is a depression at the distal end of the Okavango Delta, laterally linked by a network of low gradient channels to the Makgadikgadi and Mababe depressions.

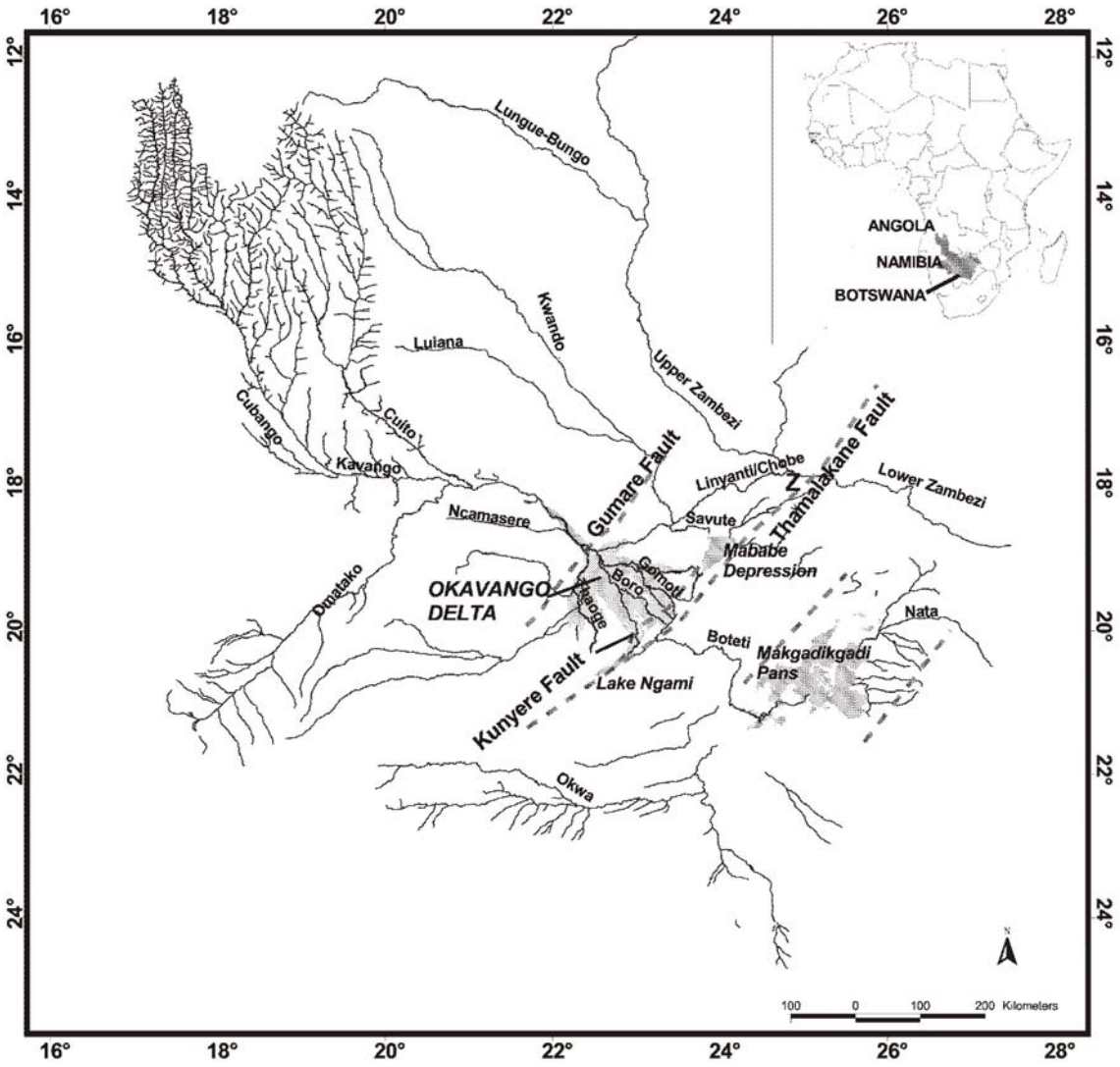

Figure VII 1. Okavango Delta in NW Botswana showing Lake Ngami to the south-west.

Flooding in the Okavango Delta is influenced by local rainfall and in-flow from the catchment in the Angolan highlands. Under the current climatic conditions, rainfall over the Okavango Delta is influenced by the anticyclonic conditions that dominate the interior of southern Africa and rainfall patterns are subject to an 18 year oscillation. The Angolan catchment climate is currently more strongly influenced by the Inter-Tropical Convergence Zone (ITCZ) and the Congo Air Boundary (CAB). The Okavango River derives its water from two major tributaries, the Cubango in the west and the Cuito in the east. The Cubango River responds to variability in the Atlantic equatorial westerlies and the Cuito River responds to tropical lows in the Indian Ocean easterlies. Rainfall over the Cubango catchment shows a quasi-18-year rainfall oscillation which is out of phase with that of central southern Africa (McCarthy et al., 2000).

Fluvio-lacustrine deposition in northern Botswana has predominantly occurred within a large structural depression formed by a southwesterly propagating extension of the East African rift system. This depression was drained and filled periodically by south easterly flowing rivers during the Tertiary and Pleistocene as the area was faulted and half grabens developed (Cooke, 1980; Mallick et al., 1981; Modisi et al., 2000). The MOZ depression is controlled by a series of NE-SW normal faults related to incipient rifting which reactivated Proterozoic and Karoo structures (Ballieul, 1979; Smith, 1984; Modisi et al., 2000). Tectonic activity along the same trend resulted in the uplift along the Zimbabwe-Kalahari axis possibly during the late Pliocene-early Pleistocene (Partridge and Maud, 2000, Moore and Larkin, 2001) causing the impoundment of proto Okavango, Kwando and upper Zambezi drainage and the development of the Makgadikgadi, Ngami and Mababe sub-basins (Cooke, 1980; Ringrose et al., 2005).

VII.2.3. Previous work on climate change and lake levels

VII.2.3 1. Regional palaeo-environmental studies

Climate forcing due to changes in the eccentricity of the earths orbit (Milankovitch cycles) and to the precession of the equinoxes have both been evident in southern Africa during the late Quaternary (Tyson and Preston-Whyte, 2000). Based on oxygen isotope temperatures from deep sea sediment cores, cycles with periods of about 100 000 years, 43 000 years, 24 000 years and 19 000 years have been identified (Imbrie et al., 1984). During perihelion conditions, wetter

summers prevail as the meridional temperature gradient between the equator and the South Pole strengthens as does the ITCZ (Tyson and Preston-Whyte, 2000). The 23 000 year cycles have been detected in the granulometric analysis of the sediments in a 90 m core taken from the Tswaing impact crater lake (formerly the Pretoria Saltpan) in the northern South Africa. The proxy rainfall series indicate five major rainfall intervals occurring between 100 ka and 200 ka with less well developed peaks occurring over the past 100 ka (Partridge et al., 1997).

Tyson and Preston-Whyte (2000) cite evidence for a warm period in southern Africa during the Last Interglacial at 125 ka and a short period of cooling during the Pleniglacial at about 75 ka. The Inter-Pleniglacial from 65 to 25 ka was a long period of cooler conditions that changed just before the start of the Last Glacial Maximum (LGM) at c. 21 ka. A minimum of less than 40% of present mean annual rainfall was experienced over the Kalahari during this time (Partridge et al., 1997). Between 16 ka and 11 ka a rapid increase of temperature occurred in southern Africa. Across much of the sub-continent the temperature rise seems to have been accompanied by increased moisture supply, as in the Kalahari (Shaw and Cooke, 1986).

During the Holocene Altithermal between 7 and 4.5 ka, the currently semi-arid western interior of southern Africa, which includes the Lake Ngami basin, received between 10-20 % more precipitation than the current mean annual precipitation for the region (Partridge et al., 1997). A regional high-resolution record from the middle Holocene (6.6 ka) to the present is the stable isotope record for the Cold Air Cave in the Makapangsgat Valley in northern South Africa (Repinski et al., 1999). A number of events are apparent in the $\delta^{18}O$ record. The first is the end of the warm Holocene altithermal until just after 6 ka BP. Warmer conditions occurred again at around 4 ka and 2.2 ka. Five centuries of cooling associated with the Little Ice Age from A.D. 1300 to 1800 were also recorded.

VII.2.3.2. Palaeo-environmental studies conducted in the MOZ Basin

Sedimentological and geochemical evidence suggests that the Okavango Delta has expanded and contracted over the past 400,000 years and the region may have been subject to extensive flooding prior to 110 ka, 80-90 ka and 41-43 ka (Ringrose et al., 2005). Past levels of palaeo-Lake Tsodilo, in northwestern Botswana are a reflection of direct local precipitation as channels do not drain into the basin (Thomas et al., 2002). Mollusc remains found in palaeo-Lake Tsodilo,

suggest that permanent deep water occurred from 40-32 ka and diatom evidence suggests that from 36-32 ka the lake became more eutrophic and seasonal. In addition, dune construction around Tsodilo, probably associated with drier and windier climatic conditions occurred at 36-28 ka. Lacustrine conditions occurred in palaeo-Lake Tsodilo from 27-22 and 19-12 ka (Thomas et al., 2002). It is possible that the period between 22 and 19 ka may indicate a drying period in the region which coincides with the LGM in southern Africa (Partridge et al., 1999; Thomas et al., 2002).

Diatomite beds in Lake Ngami were first reported in the Southern Okavango Intergrated Water Development Phase 1 final report (SMEC, 1987) covering an area of approximately 30km^2 over the eastern portion of the basin. A study of lake Ngami shorelines, diatoms and Holocene sediments conducted by Shaw et al. (2003) suggested an extensive and slightly alkaline lake at 11 ka. They suggest that lake levels rose between 4 and 3 ka and conclude that this increase in lake levels must represent increase flow from the Okavango Delta and a more humid climate at least in the region of the rivers headstreams in Angola. In addition, Shaw et al. (2003) investigate diatoms at six sites in Lake Ngami. They report that the diatom taxa in the lake contrast with the *Eunotia* dominated acid pH taxa of the present day Okavango system reported in Ellery (1987). Robbins et al., (1998) based on archaeological investigations near Toteng, further suggested that a deep lake existed around 4 ka after which lake levels fell slightly between 3.8 and 2.4 ka (Figure VII-2).

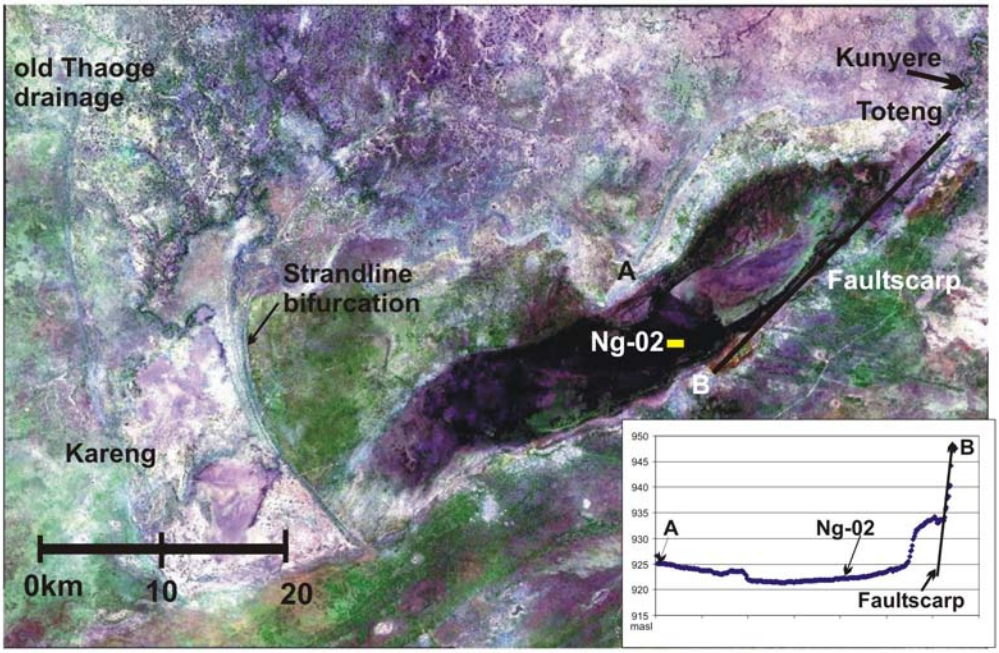

Figure VII 2. Satellite image of the Lake Ngami basin depicting the location of sampling site Ng-02, shoreline features and the faultscarp bounding the lake to the south.

Shaw (1985) reported that, based on documentary records, Lake Ngami was still a substantial lake in the 1850s but was becoming seasonal and by 1880 became a closed lake when inflow from the Thaoge channel ended. Inflow through the Kunyere was also significant, based on the presence of extensive diatom beds near Toteng (SMEC, 1987). Having been dry since 1989, Lake Ngami received water through the Kunyere in 2004. Prior to this, satellite imagery shows that 1984 and 1989 were the last two years with substantial water in the lake. These two years and 2004 correspond to the highest Okavango Delta inflow at Mohembo between 1981 and 2004 (P. Wolski, pers. comm.), suggesting that the lake is an integral part of the Okavango system.

VII.2.4. Sampling and analytical procedures

Field work took place between 2003 and 2004. A topographic profile across the lake bed was conducted using a Trimble 4700 Differential GPS to determine the elevation of the pit (Ng-02) and related lake basin and shoreline features. GPS points were corrected to benchmark BPS274 with an elevation of 926.550 masl. Sediments from a 4.6 m pit (Ng-02) dug into the lake bed (Figure VII-2) were collected at 10cm intervals to give 46 samples. Dried subsamples were used for the analysis of major, trace and rare earth elements (REE), loss on ignition (LOI) and S.

Major, trace and REE analyses were performed at Chemex Laboratories in Canada. Major elements were determined using ICP-AES. Trace and rare earth elements were analysed using ICP-MS (detection limits generally between 0.1 and 0.5 ppm) with the exception of Cr, Ni and Pb that were determined by flame AAS (detection limits 1 ppm). Total S was measured at the HOORC Environmental Laboratory on 300 mg samples by combustion and infrared absorption spectrometry using a Leco S-144DR sulphur analyser. The organic and carbonate contents were estimated from weight loss on ignition (LOI) at 550^{o}C (LOI_{orgC}) and 950^{o}C (LOI_{inorgC}) respectively. For all geochemical data, the significance of correlation was tested using the two sided test at a 95% confidence limit (Rollinson, 1993).

Three samples were dated at the University of Botswana using thermo-luminescence (TL) techniques (Aitken, 1985) after protecting the samples from exposure to sunlight. It was assumed that the samples had undergone total bleaching in a shallow water environment before deposition. TL was used because it provided reliable dates in the past (Blumel et al., 1998; Ringrose et al., 2002) and literature sources suggest a degree of comparability between TL and OSL (Optically Stimulated

Luminescence) (e.g. Radtke et al., 1999, Huaya et al., 2004). Alpha counting was carried out on a portion of the whole sample using an Elsec 7286 (Low Level Alpha Counter) to determine abundances of Uranium and Thorium (ppm) and a Corning 410 Flame Photometer to determine Potassium weight percentage (Table VII-1). Carbonates and iron staining was removed using hydrochloric acid and organic matter using hydrogen peroxide. TL values were determined using a Riso D12 reader. The environmental dose rate was determined by a low level alpha counter (Elsec 7286) using a 42 mm ZnS screen (Zoller and Pernicka, 1989). The values shown assume secular equilibrium for both U and Th chains (Carl, 1987). Uncertainty levels (Table VII-2) represent one standard deviation. The cosmic dose was calculated taking into consideration depth of burial, overburden density and porosity, sample co-ordinates and altitude.

AMS ^{14}C dating was conducted at Poznan Laboratory in Poland. The samples were mechanically cleaned under binocular microscope to remove root fragments. The datable pieces of sample were collected, rinsed with 4% HCl (room temperature), 0.5M NaOH (60°C) and again 4% HCl (room temperature) to remove all traces of carbonates in the samples. The combustion to CO_2 was performed in a closed quartz tube together with CuO and Ag wool to 900°C. The sample CO_2 was then reduced with H_2 over approximately 2 mg of Fe powder as a catalyst, and the resulting carbon/iron mixture is pressed into a pellet in the target holder (Czernik and Goslar, 2001). The ^{14}C concentration of the samples was measured with a National Electrostatics Corporation "Compact Carbon AMS" spectrometer by comparing the simultaneously collected ^{14}C, ^{13}C and ^{12}C beams of each sample with those of oxalic acid standard, CO_2 and coal background material (Goslar et al., 2004). Conventional 14C ages were calculated with a $\delta^{13}C$ correction for isotopic fractionation (Stuiver and Polach, 1977) based on the $^{13}C/^{12}C$ ratio measured by the AMS-system simultaneously with the $^{14}C/^{12}C$ ratio. As this $\delta^{13}C$ includes the effects of fractionation during graphitisation in the AMS-system and, therefore, cannot be compared with $\delta^{13}C$ values obtained per mass spectrometer on CO_2. For the determination of the measurement uncertainty (standard deviation) both the counting statistics of the ^{14}C measurement and the variability of the interval results that, together, make up one measurement were observed. The larger of the two was adopted as the measurement uncertainty. To this the uncertainty connected with the subtraction of the background was added. The quoted 1-sigma error is thus the best estimate for the full measurement and not just based on counting statistics.

ESEM analysis was undertaken at the University of Botswana using a Philips XL30 environmental scanning electron microscope to obtain micro-textural information and to make critical taxonomic identifications on some of the main diatom species found in the sediments. An in-depth quantitative investigation of diatom changes in the lake is currently being prepared, but here we report briefly on summary, qualitative diatom composition of several samples spanning the length of the stratigraphic sequence. This information is useful because species composition can further highlight relative changes in lake chemistry associated with prevailing climatic conditions (Mackay et al., 2003) and diatoms have shown to be particularly useful proxies in African lakes (Gasse et al., 1997; Stager et al., 1997). Sediment samples were prepared according to standard laboratory procedures (Battarbee et al., 2001) and examined at high magnification (x1000) using oil-immersion light microscopy with phase contrast. Taxa were identified using a range of diatom flora, especially those of African lakes (e.g. Gasse, 1986) and oligotrophic, temperate lakes (e.g. Krammer & Lange-Bertalot, 1986-1991).

Table VII 1. Data inputs for TL.

Sample	Ng-02 T220	Ng-02 T380	Ng-02 T440
Equivalent Dose (Gy)	32.59±0.48	33.57±1.64	73.89±2.29
Diameter of grains (um)	107±17	107±17	107±17
Density of quartz grains g.cm-3	2.65	2.65	2.65
Sediment U ppm	3.68±0.25	0.73±0.06	2.83±0.19
Sediment Th ppm	9.62±0.0.82	1.18±0.0..18	5.90±0.62
K wt%	1.22±.03	0.64±.03	0.86±0.03
Water content (Wt.%)	12 +-8	12 +-8	15+-5
Cosmic Dose rate uGya-1	170.00±17.00	150.00±15.00	140±14
Dose rate uGya-1	2,672±277	943±91	1824±132
Age (years BP)	12,197+-1,277	35,602 +-3,851	40,499+-3,187
Additive Dose +b1(Gy)	19.9	26.53	66.33
+b2	39.8	66.33	132.67
+b3	82.92	116.08	232.17
+b4	149.25	199	331.67
+b5		331.67	497.5

Table VII 2. Results from C14 and TL dating.

Sample	Description	Depth (cm)	Age estimate	Method
Ng-02 T90	Organic FeO rich fired clay	90	3.675 +-0.030 ka BP	C14
Ng-02 T220	Diatom rich organic silt	220	12.197 +-1.277 ka	TL
Ng-02 T220	Diatom rich organic silt	220	14.740 +- 0.080 ka BP	C14
Ng-02 T320	Organic rich lake sediment	320	17. 890 +- 0.080 ka BP	C14
Ng-02 T380	Fine pale yellow sand with minor diatoms	380	35.602 +- 3.851 ka	TL
Ng-02 T440	Diatom rich lake sediments	440	40.499+- 3.187 ka	TL

VII.2.5. Topographic and stratigraphic results

Ng-02 lies at an elevation of 922 m, close to the lake sump at 921 m. The lake bed rises gradually to 925 m in a southerly direction (B) with a terrace at 934 m and up to 948 m along the fault scarp (Figure VII-2). The lowest unit of Ng-02, UP460 (Figure VII-3) comprises an unconsolidated silty sand with minor calcrete. Freshwater diatoms are present in this unit as evidenced by the presence of valves of genus *Aulacoseira ambigua* (Fig 4a) and fragments of a periphyton taxon belonging to the genus *Surirella engleri* (Figure VII-4b). The unit directly above (UP440) consists of a compact fine grain pale yellow sand with minor diatom fragments and calcrete nodules (Figure VII-4c and d). Early stages of amorphous silica forming on the quartz grains is also evident in Figure VII-4d. The sand unit changes abruptly into a white diatomite (UP350) with a thickness of about 20 cm (Figure VII-4e). Diatoms in this bed include fragmented pieces of genus *Nitzschia* (e.g. *N. amphibia*) before changing abruptly into an organic rich silty sand of 30 cm thickness (UP330). This grades gradually into a gray laminar (cm scale) diatomaceous silt with FeO staining (UP300) and then a diatom rich silt of 80 cm thickness (UP240). Silt with minor calcrete nodules (UP160) is overlain by a dark gray laminar diatomite (UP120) of 20 cm thickness. Large intact valves of *S. engleri* from UP120 were found in the sample collected at 110 cm depth. Valves from *A. ambigua* and broken fragments of genus *Surirella* were found at 100 cm depth (Figure VII-4f, g and h). UP120 is overlain by organic rich clay with laminar (cm scale) and columnar structure (UP100) with evidence of burnt peat. The top 10 cm of the profile is an organic rich silt. More detailed diatom descriptions are given below.

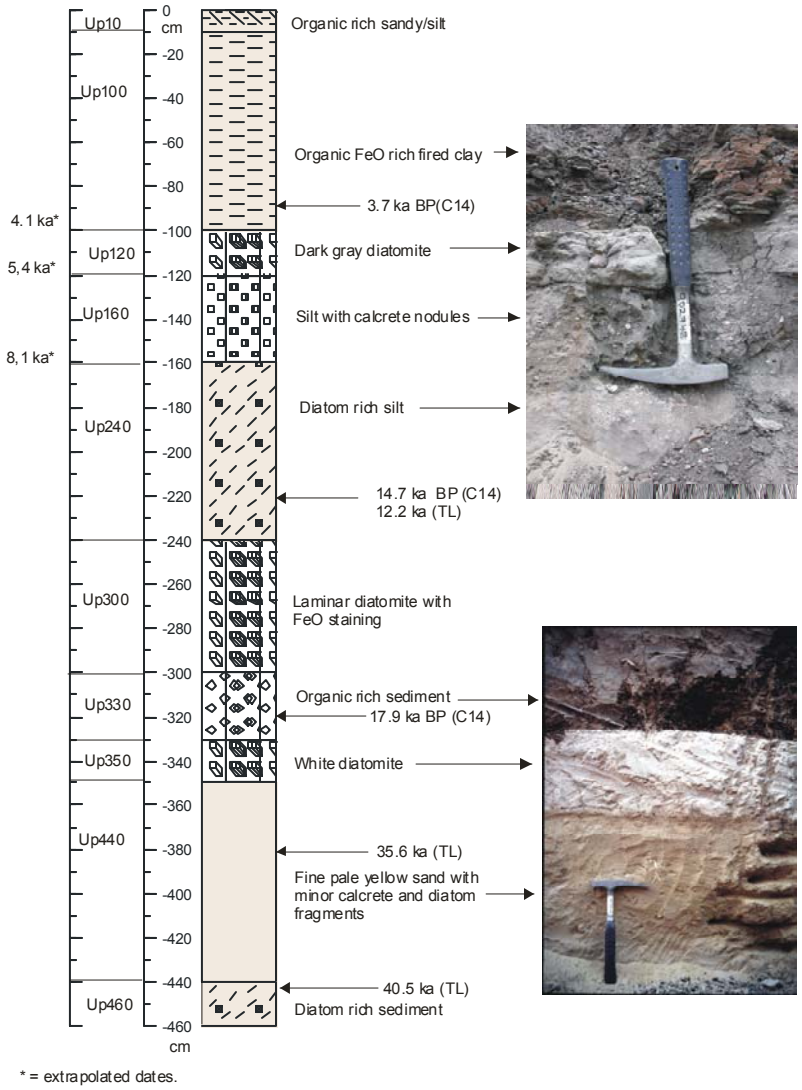

Figure VII 3. Stratigraphic log of Ng-02 depicting the units within the sampling pit

VII.2.6. Geochemical characteristics of the Ng-02 samples

The Lake Ngami sediments contain a high proportion of SiO_2 (51-92.5 wt.%, avg. 72.4 wt.%) and variable levels of Al_2O_3 (2.04-17.2 wt.%, avg. 8.88 wt.%) (Table VII-3). Al_2O_3 and SiO_2 are significantly negatively correlated (r = -0.94). TiO_2 varies between 0.23-0.77 wt. % with an average value of 0.51 wt. %. TiO_2 and SiO_2 are significantly negatively correlated (r = -0.94). TiO_2 and Al_2O_3 are positively correlated (r = 0.91) being both associated with the flux of fine sediment into the basin.

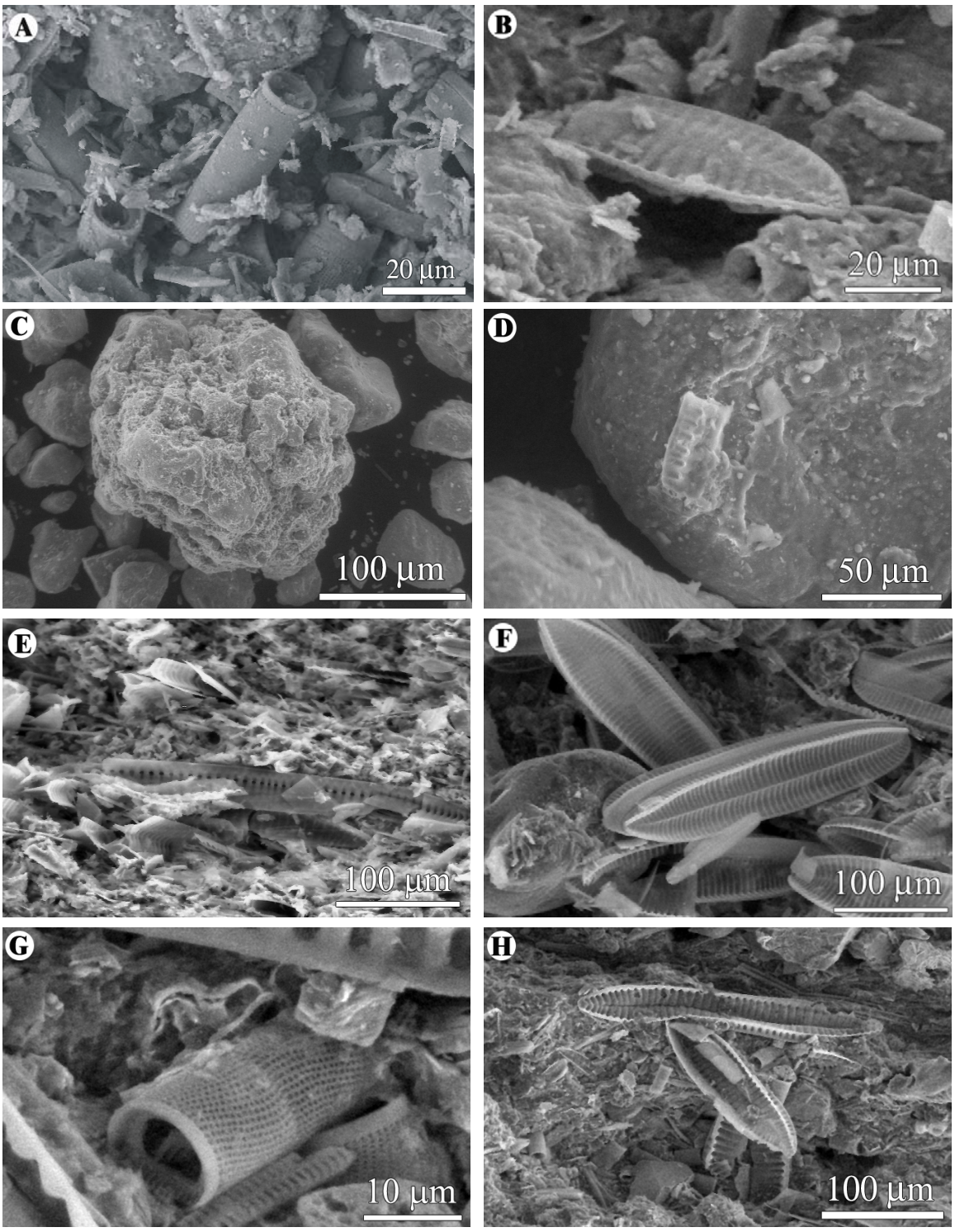

Figure VII 4. ESEM images of selected samples: a) centric valves of genus *Aulacoseira*; b) broken *Surirella* fragments from UP460 unit; c) calcrete nodule and quartz grains in UP440 unit; d) fragment of diatom on quartz grain from UP440 unit; e) broken diatom of genus *Nitzschia* from UP350 unit; f) large intact *Surirella* from UP120 sampled from a depth of 110 cm; g) genus *Aulacoseira* from UP120 sampled from 100 cm depth; h) broken fragments of genus *Surirella* taken from UP120 unit at 100 cm depth

Table VII 3. Geochemical results for selected samples.

Sample	Ng-02 T20	Ng-02 T80	Ng-02 T100	Ng-02 T110	Ng-02 T120	Ng-02 T190	Ng-02 T270	Ng-02 T320	Ng-02 T330	Ng-02 T380	Ng-02 T440	Ng-02 T460
Depth (cm)	20	80	100	110	120	190	270	320	330	380	440	460
SiO2 (%)	56.6	51	60.8	78.1	91.6	75.1	69.1	60.6	75.2	90.9	76.7	73
Al2O3	14.35	16.3	9.08	4.46	2.04	8.56	11.6	14.85	7.02	2.36	6.36	7.64
Fe2O3	5.51	6.16	4.6	2.09	1.1	3.48	4.66	6.44	3.3	0.99	3.07	4.12
CaO	0.44	0.16	0.28	0.41	0.11	0.29	0.56	0.85	1.92	0.39	2.66	1.42
MgO	0.83	0.99	0.92	0.41	0.14	0.67	0.89	1.03	0.76	0.17	0.67	1.02
TiO2	0.74	0.71	0.65	0.62	0.25	0.44	0.56	0.6	0.54	0.25	0.38	0.53
P2O5	0.05	0.07	0.07	0.02	<0.01	<0.01	0.01	0.01	0.01	<0.01	<0.01	0.03
LOI(orgC)	16.3	15.2	16.7	9.29	2.32	7.29	8.65	10.8	3.43	0.97	6.05	11.9
LOI(inorgC)	1.16	2.39	2.25	1.04	0.15	0.71	1.31	1.25	2.70	0.59	2.15	2.27
S	0.088	0.108	0.132	0.066	0.013	0.015	0.01	0.015	0.012	<0.005	0.012	0.01
Co (ppm)	19.7	20.7	15	7.6	3.2	14.2	10.8	13	7.2	2.4	8.7	11.7
Pb	20	15	12	9	5	14	15	19	12	<5	10	12
Cr	190	130	130	210	250	100	100	100	130	80	170	120
Ni	35	37	29	17	12	27	26	41	22	8	21	25
V	148	164	111	46	14	108	126	149	74	23	70	103
Sr	67	53.6	77	110	46.5	49.9	53.6	73.6	83.8	42.4	103	101.5
Th	12	11	7	3	1	6	9	11	6	2	5	6
Mo	3	2	3	4	3	<2	<2	<2	2	<2	2	2
Y	27.7	20.6	15	9.3	4.6	19.3	17	16.3	12.6	3.7	8.7	11.2
La	36.1	29.9	20.7	12.4	5.9	26.7	25.6	25.6	16.7	3.9	13.8	14.6
Ce	69.4	56.1	41.1	26.7	11.6	49.1	50.2	51.3	34	6.5	26.9	27.3
Nd	31.9	25.7	19.7	12.5	5.5	22.8	23.7	25.1	16.7	3.2	12.6	14.6
Sm	6	4.9	3.8	2.4	1	4.6	4.5	5	3.3	0.6	2.5	2.9
Gd	5.5	4.6	3.5	2.1	1	4.1	4.1	4.2	3	0.6	2.2	2.6
Yb	2.6	2.1	1.6	1.1	0.5	1.7	1.8	1.8	1.5	0.5	1	1.3

VII.2.6.1. Redox condtions

Al_2O_3 and LOI_{orgC} are significantly positively correlated (r = 0.75) and are both elevated in the UP460, UP330 and UP100 units (Figure VII-5a). LOI_{orgC} and Fe_2O_3 are also significantly positively correlated (r = 0.79). Elevated LOI_{orgC} is an indication of anaerobic conditions in the basin. Organic matter accumulates in wetland environments that are saturated with water thereby inhibiting decomposition (Collins and Kuehl, 2001). Elevated Al_2O_3 suggests clay minerals were either washed into the basin or weathered *in situ*, both indicating wet conditions. P_2O_5 values are generally low (<0.01 wt. %) with the exception of the UP100 upper unit suggesting higher nutrient levels in the water towards the final stages of the lake (Figure VII-5b).

The UP100 unit shows high levels of S (Figure VII-5b). LOI_{orgC} and S are significantly positively correlated (r = 0.87). Values of Fe_2O_3/Al_2O_3 and S are both elevated in the upper UP100 unit indicating that free dissolved sulphide was present in the bottom water or subsurface anoxic conditions (Figure VII-5c). The marked increase in LOI_{orgC}, S and Fe_2O_3/Al_2O_3 in the UP100 unit are significant suggesting a change from suboxic to anoxic. This occurs again in the UP330 unit, and to a lesser extent in the UP460 unit.

The degree of pyritization in the sedimentary record could also indicate anoxic conditions. The extent of correlation between the transition metals V, Cr, Ni, Co, and Pb to S was calculated resulting in r = 0.40, r = 0.26, r = 0.47, r = 0.68, r = 0.37 respectively. V, Ni, Co and Pb are significantly correlated suggesting that these elements concentrations are related to sulphide accumulation in the Lake Ngami sediments. These transition metals exhibit similar patterns when plotted versus depth of samples (Figure VII-5d). These in turn correlate closely to the patterns generated for LOI_{orgC} and Al_2O_3. Mo can also exhibit a large uptake on pyritization (Huerta-Diaz and Morse, 1992) and this appears to occur in the UP100 unit suggesting anoxic conditions (Figure VII-5c).

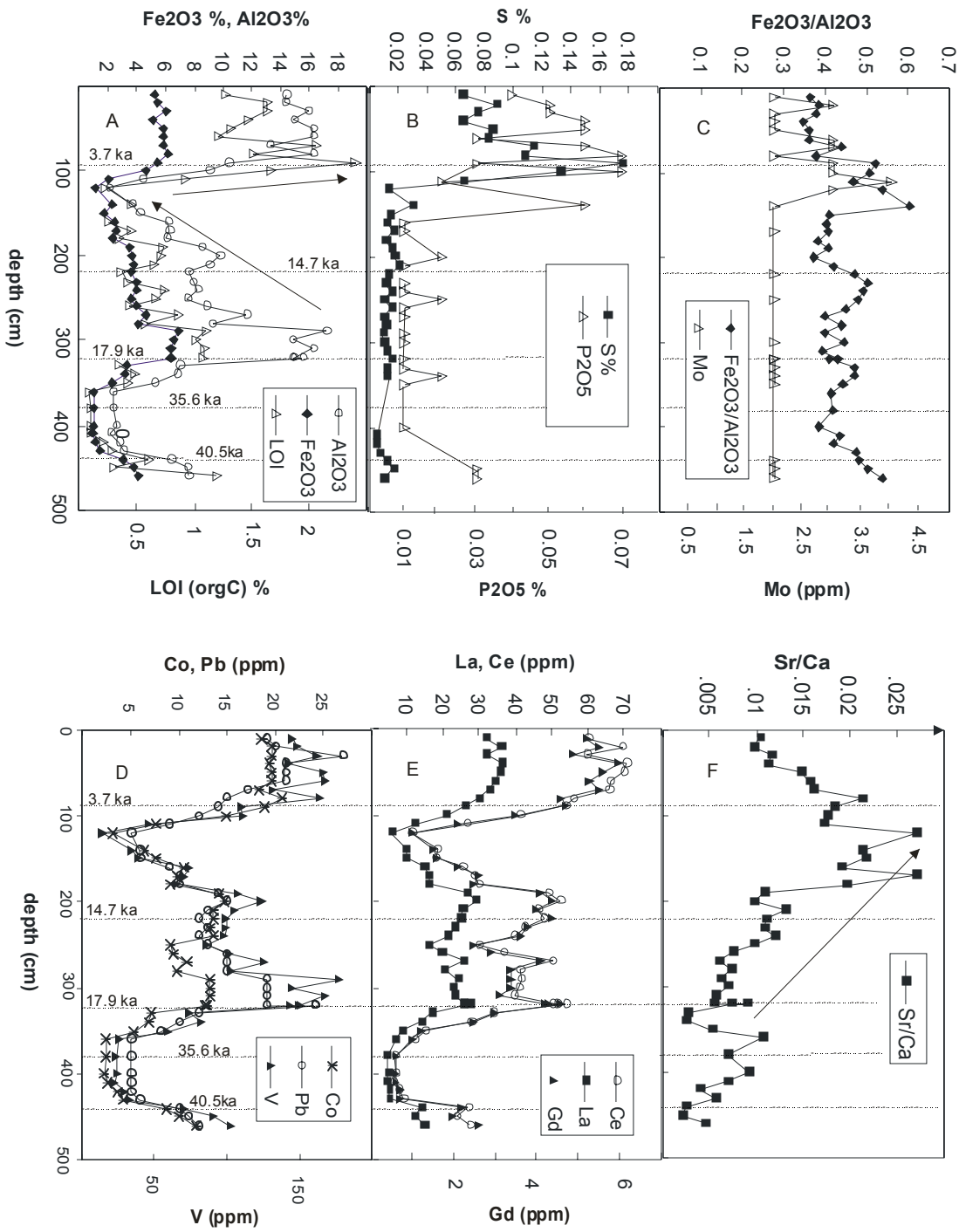

Figure VII 5. Selected elements and ratios plotted versus depth for profile Ng-02

REEs are used as chemical indicators of geologic processes, including assessment of crustal sources, the redox state of water and depositional environment. The REEs are relatively insoluble and are present in low concentrations in terrestrial waters; thus the REEs present in terrigenous sediment are chiefly transported as particulate matter and reflect mainly the chemistry of their source. Studies have indicated that high pH water show enrichments in heavy REEs (HREE) and the degree of enrichment appears to increase with increasing alkalinity (Moller and Bau, 1993; Johannesson et al., 1994). For the high pH alkaline waters, speciation modelling (Johannesson et al., 1994) indicates that REE dicarbonate complexes are the only important form of dissolved REE. The HREE are more strongly complexed in alkaline solution leading to enrichment of the HREEs over light REEs (LREE) in the water. This implies that certain sediments should be the site of preferential accumulation of LREE.

La_N/Yb_N ratios vary slightly between the different units with values ranging between 0.53 to 1.16 with an average value of 0.93. Values are lower (0.53-0.84, avg. 0.68) for the UP440 unit indicating a moderate depletion of LREE. Samples Ng-02 T190 and Ng-02 T200 taken from the UP240 unit show slight enrichment in LREE, indicating possible alkaline conditions.

Normalization of Ce abundances to those of its neighbouring REE, measured in various biogenic and authigenic components has been used to deduce redox conditions of the water column at the time of REE uptake by these phases. Unlike the other REE, cerium can undergo oxidation from soluble Ce(III) to highly insoluble Ce (IV). Its fixation in particulate matter, including organics is thought to be responsible for distinctive depletion of Ce in well oxygenated seawater (Wright et al., 1987; Liu et al., 1988; Bellanca et al., 1997).

Ce/Ce* variations can be explained by simple mixing of various components (essentially biogenic and authigenic) and of detrital materials (dominantly alumino-silicates) with crust-like Ce signatures. A positive correlation ($r = 0.88$) exists between Al_2O_3 and Ce concentrations for the Lake Ngami sediments (Figure VII-5e), and a comparison of Ce/Ce* values with concentrations of terrigenous indices SiO_2 and TiO_2 indicate that there are weak significant correlations ($r = -0.37$, $r = 0.34$ respectively) between these factors suggesting that fine sediment detrital flux does contribute to Ce/Ce* distribution. However, significant correlations exist between Ce/Ce* and S ($r = 0.59$) and Ce/Ce* and LOI_{orgC} ($r = 0.44$) indicating that redox conditions does play a role in the Ce/Ce* distribution in Lake Ngami sediments.

Samples from Ng-02 in general show a slight depletion in Ce/Ce* (0.84-1.02, avg. 0.93) indicating aerobic, alkaline conditions did not predominate in the basin. Only samples from UP120 show a slightly positive Ce/Ce* suggesting that at this stage the water was relatively more oxygenated and alkaline.

Liu et al. (1988) report an enrichment of middle REE (MREE) in fossil apatite. We interpret the lower La_N/Sm_N ratios (0.75- 1.08, avg. 0.87) as an expression of MREE enrichments, possibly due to diagenetic phosphates. The weak significant positive correlation between Sm and Nd and P_2O_5 (r = 0.46 for both) suggests that phosphate precipitation contributed to MREE distribution. It is also noteworthy that P_2O_5 values are also weakly correlated with Th and Y (r = 0.38 and 0.48 respectively) which is consistent with substitution of Th, Y and MREE in the lattice of Ca-phosphate.

VII.2.6.2. Salinity and alkalinity levels

In a closed lake, as the volume of the lake changes as a result of variations in the hydrological regime of the catchment, so the chemistry of the water evolves. As the water level drops during periods of decreased precipitation/ evaporation (P/E) ratio, the dissolved ions are concentrated until a point is reached where the least soluble minerals start to precipitate. Calcium carbonate ($CaCO_3$) is precipitated early in this process and is virtually insoluble except at low salinities (Eugster and Hardie, 1978). The trace element chemistry of Mg and Sr is an indicator of palaeosalinity as during evaporative concentration of lake water in closed basins, precipitation of $CaCO_3$ often gives rise to an increase in the Mg/Ca and Sr/Ca meq ratio of the water and consequently a positive correlation with salinity (Eugster and Kelts, 1983).

CaO values in the lake Ngami sediments are generally low (0.1-3.84 wt. %, avg. 0.62 wt. %) with higher values associated with the UP460 unit. MgO values range between 0.14-1.09 wt. % with an average value of 0.68 wt. %. Sr levels in the Lake Ngami sediments range between 41.1 to 132 ppm (avg. 64.4 ppm). The significant positive correlation between MgO and LOI_{inorgC} (r = 0.72) and Sr and LOI_{inorgC} (r = 0.57) is an indication that Mg and Sr in the sediments is partially controlled by chemical sedimentation of carbonates. However, unlike Sr and CaO, MgO values are also correlated with Al_2O_3 and TiO_2 (r = 0.77 and r = 0.90 respectively, which demonstrates that MgO concentrations are also controlled by the input of clay minerals into the basin.

Consequently, only Sr and CaO are used for palaeo-salinity reconstruction of the Ng-02 sediments.

There appears to be an overall increase in the Sr/Ca ratio between 320 cm and 120 cm suggesting a period of increased salinity. This corresponds to a period of decreasing LOI_{orgC} implying aerobic conditions and lower Al_2O_3, therefore less clastic input which again suggests a lowering of lake levels. At a depth of 120 cm (UP120), the 20 cm bed of diatomite indicates that diatoms were the dominant component in the lake, with very little clastic input.

VII.2.7. Diatom composition of Ng-02 samples

The lower section of the core (sample Ng-02 T440) taken from unit UP460 (c.40.5 ka) contains abundant diatom remains. The assemblage is dominated by *A. ambigua*, *Denticula kuetzingii* and *Fragilaria construens*, while other common taxa include *Fragilaria brevistriata*, *Nitzschia amphibia*, *Synedra ulna*, *Rhopolodia gibba* and *Cyclotella pseudostelligera*. This assemblage suggests that well-mixed conditions prevailed as *A. ambigua* is an obligate planktonic diatom that grows in open freshwaters (Gasse and van Campo, 2001). *D. kuetzingii* may also be found growing in open water, although it can be classified as epiphytic too, i.e. it grows attached to aquatic macrophytes growing in the littoral regions of the lake. However, it is usually classified as growing in waters with high electrolytic composition, suggesting that the lake at this time was relatively deep (compared with other sections of the core) but brackish. The presence of *R. gibba* confirms this interpretation.

Sample Ng-02 T410 from unit UP440 contains very few diatoms, but for those that are present, *Denticula kuetzingii* is the most common. This perhaps suggests a shallow water environment with abundant macrophytes in littoral regions.

Sample Ng-02 T320 occurs in the unit UP330 (c. 18 ka). In this section, there were rather fewer diatoms present than in Units UP460-440, and many valves were broken, making positive identifications of some of the smaller benthic taxa more difficult. Nevertheless, the assemblage was dominated by *F. construens*, while *D. kuetzingii*, *F. brevistriata* and *N. amphibia* were all common. *A. ambigua* was present too, although this species can grow in shallower waters, but still as a planktonic diatom (Gasse 1986; Kilham 1990). It is likely therefore that the lake was

deep enough to support populations of *A. ambigua*, although the distribution of this species is likely to have been restricted.

Samples Ng-02 240 & 180 between units UP300-240 (c. 15 ka – 10 ka) contains the largest number of different taxa (i.e. these units are characterised by a large alpha diversity) and diatom valves were relatively well preserved. The assemblage was dominated by the brackish species *D. kuetzingii* and *N. amphibia*, while other common taxa included the shallow water, epiphytic species *F. construens*, *F. pinnata*, *Achnanthes minutissima* and *Cymbella gracilis* and the alkalophilous species *Cyclotella meneghiniana*. The lake is likely to have been shallow at this time, and fairly alkaline with a basic pH, and with significant macrophyte growth in the extended littoral regions of the lake. Interestingly though, taxa such as *A. ambigua* was also found, suggesting that either pockets of deeper water remained, or lake levels were perhaps undergoing considerable fluctuations, between marshy to deeper water environments. The presence of *C. stelligera* also suggests fluctuating water levels, as this species can grow both in pelagic and littoral regions of a lake.

Samples Ng-02 110 & 100 in unit UP120 (c. 5 ka - 4 ka) are characterised mainly by shallow water taxa including the periphytic *A. minutissima*, *Cymbela silesiaca* (which grows mainly in shallow water, circumneutral waters, attached to plants), *D. kuetzingii*, *N. amphibia*, *R. gibba* (another epiphyte which grows in waters with moderate to fairly high conductivity) and the very large *S. engleri* (valves were over 200 μm long). The ecology of this latter taxon is not well known, although Gasse (1986) has found it both in the plankton and living on the bottom sediments of freshwater lakes often in slightly alkaline waters.

The final two samples in this qualitative assessment were Ng-02 T80 & T40, from unit UP100 (c. 3 ka – 2 ka). In both these samples, very few diatoms were present, with considerable numbers of broken valves, making positive identifications of small benthic taxa difficult. Sample Ng02-T80 contained very few taxa (e.g. *N. amphibia* and low numbers of *F. construens* and an unidentified *Eunotia* spp.). Palaeoenvironmental reconstructions are therefore difficult, except to say perhaps that very shallow water conditions prevailed. Sample Ng-02 T40 was dominated by *F. pinnata* and *N. amphibia*, but also abundant were the taxa *A. ambigua* and *C. stelligera*, suggesting lake water conditions perhaps becoming deeper, with increased mixing of the water column.

VII.2.8. Palaeo-environmental interpretation

Based on slightly elevated but declining Al_2O_3 and LOI_{orgC} results, lacustrine conditions occurred in Lake Ngami at c. 42 ka until c. 40 ka. Diatom results indicate that relatively deep but brackish conditions prevailed. The higher CaO values of the UP460 unit might suggest more saline conditions however, Sr/Ca ratios are relatively low in this unit. Work conducted on stalagmites in the Gcwhiaba Caves, approximately 70 km from Lake Ngami, reported enhanced local rainfall between 45 and 37 ka (Cooke, 1984). Lake Tsodilo had lacustrine conditions between 40 – 32 ka. This suggests that enhanced local rainfall in addition to in-flow through the Okavango River system contributed to lacustrine conditions in the Lake Ngami basin.

The lacustrine conditions in the basin appear to have been terminated rapidly at ca. 40 ka. Within the margins of error, the sample dated at 40 ka (UP460) and the sand unit (UP440) sample dated at 36 ka, are identical, suggesting that these events could be co-incidental events. This would suggest that the lower sand unit was deposited rapidly implying fluvial sedimentation. Shaw et al., (2003) also report compact yellow sand at the bottom of one of their profiles in the lake bed on the northern edge of the lake. We believe that the sand unit occurs as a result of shallow flow-through conditions in the basin, and this is supported by grain size data. Samples from this unit show a distinct 3 Φ peak. Ringrose et al., (submitted paper) report an increase in the 3 Φ peak in fluvial environments as opposed to the 2 Φ 'dune' peak. The onset of this sedimentary environment may have resulted from tectonic tilting of the basin. Strandline bifurcation (Figure VII-2) is evidence that tilting has occurred in the basin. Gumbricht et al., (2001) describe tilting of palaeo-shorelines in the Mababe Depression and relate this to neo-tectonic activity in the Okavango Delta.

The sharp transition between the sandy UP440 unit and the overlying diatom unit (UP350) and the large gap between the dates of UP440 and UP330 suggests a depositional hiatus and possible erosion. This could reflect a possible seismic and/or fluvial event in the basin, or just non-deposition due to dessication of the lake.

At 19 ka, shallow, aerobic, turbulent lake conditions were prevalent, but lake levels were at this time increasing to deeper water conditions up until c. 17 ka. This period coincides with the Late

Glacial Maximum (LGM), a period of increased aridity and cooler conditions in the region (Partridge et al., 1999). The fact that the Lake Ngami Basin appears to have been filling during this time of regional aridity appears to result from increased flow from the Okavango River and a more humid climate in the region of the rivers headwaters in Angola, suggesting an anti-phase climate between the two regions.

Increasing Sr/Ca ratio and decreasing LOI_{orgC} and Al_2O_3, from c. 16 ka, suggest decreased inflow into the basin and a lowering of lake levels. Lacustrine conditions were probably maintained primarily by local rainfall input as the region experienced a warmer, wetter phase between 16 – 11 ka (Shaw and Cooke, 1986). Based on the enrichment of LREE in the UP240 unit, slightly alkaline conditions may have prevailed at c. 12 ka and again in the UP120 unit (c. 5 ka). Diatom results from Ng-02 T240 and T180 also support shallow alkaline conditions at this time. Shaw et al. (2003) suggested an extensive and slightly alkaline lake at 11 ka.

Fairly shallow lake levels prevailed at UP120 but the lake was filling rapidly by 4 ka. Shaw et al., (2003) proposed that lake levels rose between 4 and 3 ka. Talma and Vogel (1992) report a cooling event in southern Africa at 4.7 to 4.2 ka (post Holocene Altithermal) recorded in the Cango Cave isotope record. Based on our results, the basin continued to fill until 3.7 ka BP and from then, it appears to have fluctuated and eventually gone into decline as indicated by decreasing S and LOI_{orgC} values until 2.4 ka. Based on LOI_{orgC} values, the lake levels began to rise again until ca. 0.8 ka, when it fell again. This corresponds well with findings of Robbins et al. (1998) who suggested a deep lake around 4 ka and a slightly lower lake between 3.8 and 2.4 ka.

VII.2.9. Conclusions

Inorganic and organic carbon content, S, Al_2O_3 and various REE have been used in conjunction with diatoms to distinguish between high and low lake levels in the Lake Ngami basin.

Lacustrine conditions in the Lake Ngami basin are suggested 42 ka - 40 ka consistent with events in palaeo-Lake Makgadikgadi (Ringrose et al., 2005) and Milankovitch cycles. The sedimentary record at 40 ka appears to have been influenced by tectonic activity, as lacustrine sediments are abruptly replaced with fine grained yellow sands. Deeper lake levels are reported for the period 19 ka -17 ka (LGM) followed by predominantly shallower alkaline conditions between 16 ka -5

ka. Lake levels were high at c. 4 ka and continued to fill until 3.7 ka, declined until 2.4 ka, increased until 0.8 ka and from then, lake levels declined.

During the LGM of southern Africa, a period of cooling and drying in the region, Lake Ngami levels were rising. Conversely, when the southern African region started to become warmer and wetter following the LGM, Lake Ngami was going through a phase of reduced inflow. The results indicate that the present day dipole effect in precipitation between central southern Africa and regions of equatorial Africa, was extant during the late Quaternary over NW Botswana and the Angolan highlands.

Acknowledgements

University of Botswana Research and Publication Fund is acknowledged for the grant (RP116) to conduct this research. This is an IUEM contribution no. 959. Piotr Wolski is acknowledged for assistance with the topographic survey and Figure 1. Thebe Kemosodile and Dikitso Kolokose are thanked for assistance with field work and sampling. Martin Todd is acknowledged for discussions on climate models. We gratefully acknowledge the constructive comments Tine Laerdal and one anonymous reviewer.

References

Aitken, M.J., 1985. Thermoluminescence Dating. Academic Press Publishers: London.

Baillieul, T.A., 1979. A reconnaisance survey of the cover sands in the Republic of Botswana. Journal of Sedimentary Petrology 45,494-503.

Battarbee R.W., Jones V.J., Flower R.J., Cameron N.G., Bennion, H., Carvalho L. and Juggins S. 2001. Diatom analysis. In: Last W.M. and Smol J.P. (eds), Tracking Environmental Change Using Lake Sediments, Vol. 3: Terrestrial, Algal and Siliceous Indicators. Kluwer Academic Publishers, Dordrecht, The Netherlands, pp. 171–205.

Bellanca, A., Masetti, D., Neri, R., 1997. Rare earth elements in limestone/marlstone couplets from the Albian-Cenomanian Cismon section (Venetian region, northern Italy): assessing REE sensitivity to environmental changes. Chemical Geology 141, 141-152.

Blumel, W.D., Eitel, B., Lang, A., 1998. Dunes in southeastern Namibia: evidence for Holocene environmental changes in the southwestern Kalahari based on thermoluminesence data. Palaeogeography, Palaeoclimatology, Palaeoecology 138, 139-149.

Botter-Jensen L, Duller G.T., 1992. A New System for Measuring Optically Stimulated Luminescence from Quaternary Samples. Nucl. Tracks and Radiation Measures 20, 202-205.

Carl, C., 1987. Investigations of U series disequilibria as a means to study the transport mechanism of uranium in sandstone samples during weathering. Uranium 3, 285-305.

Condie, K.C., 1993. Chemical composition and evolution of the upper continental crust: contrasting results from surface samples and shales. Chemical Geology 104, 1-37.
Collins, M.E., Kuehl, R.J., 2001. Organic matter accumulation and organic soils. In: Richardson, J.L., Vepraskas, M.J., (Eds) Wetland soils. Lewis Publishers, USA, pp. 13-162.
Cooke H.J., 1980. Landform evolution in the context of climatic changes and neotectonics in the middle Kalahari of north-central Botswana. Trans. Inst. Brit. Geog., NS 5, 80-99.
Cooke, H.J., 1984. The evidence from northern Botswana of climatic change. In: J. Vogel (ed.), Late Cenozoic palaeoclimates of the Southern hemisphere. Balkema, Rotterdam, pp. 265-278.
Czernik J., Goslar T., 2001. Preparation of graphite targets in the Gliwice Radiocarbon Laboratory for AMS 14C dating. Radiocarbon, 43, 283-291.
Ellery, K., 1987. Wetland plant community composition and successional processes in the Maunachira River system of the Okavango Delta. Unpublished MSc thesis. Johannesburg.
Eugster, H.P., Hardie, L.A., 1978. Saline Lakes, In: Lerman (Ed.) Chemistry, Geology and Physics of Lakes, Springer-Verlag, New York, pp. 273-293.
Eugster, H.P., Kelts, K., 1983. Lacustrine chemical sediments In: Goudie, A.G. and Pye, K., Chemical sediments and geomorphology: precipitates and residua in the near surface environment. London, Academic Press, pp.321-368.
Gasse, F. 1986. East African diatoms: taxonomy, ecological distribution. Bibliotheca Diatomologica, J. Cramer, Berlin. 201 pp + 44 plates.
Gasse, F., Barker, P., Gell, P.A., Fritz, S.C., Chalie, F. 1997. Diatom-inferred salinity in palaeolakes: an indirect tracer of climatic change. Quaternary Science Reviews, 16, 547-563.
Gasse, F. & Van Campo, E. 2001. Late Quaternary environmental changes from a pollen and diatom record in the southern tropics (Lake Tritrivakely, Madagascar). Palaeogeography, Palaeoclimatology and Palaeoecology, 167, 287-308.
Gieske, A., 1996. Vegetation driven groundwater recharge below the Okavango delta, (Botswana) as a solute sink mechanism - an indicative model. Botswana Journal of Earth Sciences 3, 33-44.
Goslar T**.,** Czernik J., Goslar E., 2004. Low-energy ^{14}C AMS in Poznań Radiocarbon Laboratory, Nuclear Instruments and Methods B, 223-224, 5-11.
Government of Botswana, 2002. Okavango Delta Management Plan, National Conservation Strategy Implementing Agency, Gaborone, Botswana, 156pp.
Gumbricht, T., McCarthy, T.S., Merry, C.L., 2001. The topography of the Okavango Delta, Botswana, and its tectonic and sedimentological implications. South African Journal of Geology 104, 243-264.
Huaya L., Xiaoyong, W., Haizhou, M., Hongbing, T., Vandenberghe, J., Xiaodong, M., Zhen, L., Youbin, S., Zhisheng, A., Guangchao, C., 2004. The plateau monsoon variation during the past 130 kyr revealed by loess deposit at northeast Qinghai-Tibet, Global and Planetary Change, 41, 207-214.
Huerta-Diaz, M.A., Morse, J.W., 1992. Pyritization of trace metals in anoxic marine sediments. Geochimica Cosmochimica Acta 56, 2681-2702.
Imbrie, J. et al., 1984. The orbital theory of Pleistocene climate: support from a revised chronology of the marine δO18 record. In Berger, A.L., Imbire, J., Hays, J., Kukla, G., and Saltzman, B., (eds.). milankovitch and climate, Part 1. Dordrecht: D. Reidel. 269-305.
Johannesson, K.H., Lyons, W.B., Bird, D.A., 1994. Rare earth element concentration and speciation in alkaline lakes from the western USA. Geophysical Research Letters 21, 773-776.

Kilham, P. (1990). Ecology of *Melosira* species in the Great Lakes of Africa. *In* Tilzer, M.M. & Serruya, C. (Eds): Large lakes, ecological structure and function. Springer-Verlag Berlin, pp 414-427.

Krammer K. and Lange-Bertalot H. 1986–1991. Bacillariophyceae. Gustav Fisher Verlag, Stuttgart

Liu, Y.G., Miah, M.R.U., Schmitt, R.A., 1988. Cerium: a chemical tracer for paleo-oceanic redox conditions. Geochimica Cosmochimica Acta 52, 1361-1371.

Mackay, A.W., Jones, V.J. & Battarbee, R.W. (2003) Approaches to Holocene climate reconstruction using diatoms. In *Global change in the Holocene*; eds: Mackay, A.W., Battarbee, R.W., Birks, H.J.B. & Oldfield, F. Published by Arnold. (Chapter 20) pp 294-309.

Mallick, D.I.J, Habgood F, Skinner AC. 1981. A geological interpretation of Landsat imagery and air photography of Botswana. Overseas Geological and Mineral Resources, London, 56, 1-36.

McCarthy, T.S., Ellery, W.N., 1993, The Okavango Delta, Geobulletin 36(2):5-8.

McCarthy, T.S., Ellery, W.N., Bloem, A., 1998a. Some observations on the geomorphological impact of hippopotamus *(Hippopotamus amphibius* L.) in the Okavango Delta, Botswana. African Journal of Ecology, 36, 44-56.

McCarthy, T.S., Ellery, W.N., Dangerfield, J.M., 1998b. The role of biota in the initiation and growth of islands on the floodplains of the Okavango alluvial fan, Botswana. Earth Surface Processes and Landforms, 23, 291-316.

McCarthy, T.S., Cooper, G.R.J., Tyson, P.D., Ellery, W.N., 2000. Seasonal flooding in the Okavango Delta, Botswana – recent history and future prospects. South African Journal of Science 96, 25-33.

Modisi, M.P., Atekwana, E.A., Kampunzu, A.B. Ngwisanyi, T.H., 2000. Rift kinematics during the incipient stages of continental expansion: Evidence from the nascent Okavango rift basin, northwest Botswana, Geology, 28, 939-942.

Moller, P., Bau, M., 1993. Rare earth patterns with positive cerium anomaly in alkaline waters from Lake Van Turkey. Earth Planetary Science Letters 117, 671-676.

Moore A. E., Larkin, P. 2001. Drainage evolution in south-central Africa since the breakup of Gondwana. South African Journal of Geology 104, 47-68.

Nicholson S.E., Entekhabi, D., 1986. The quasi-periodic behaviour of rainfall variability in Africa and its relationship to the Southern Oscillation. Archives for Meteorology, Geophysics and Bioclimatology 34, 311-348.

Partridge, T.C., Demenocal, P., Lorentz, S.A., Paiker, M. J., Vogel, J.C., 1997. Orbital forcing of climate over South Africa: a 200,000-year rainfall record from Pretoria Salt Pan. Quaternary Science Review 16, 1125-1133.

Partridge, T.C., Scott, L., Hamilton, J.E., 1999. Synthetic reconstructions of southern African environments during the Last Glacial Maximum (21-28 kyr) and the Holocene Altithermal, (8-6 kyr). Quaternary International 57/58, 207-214.

Partridge, T.C., Maud, R.R., 2000. The Cenozoic of southern Africa. New York: Oxford University Press, 406 pp.

Petit, J.R. 1999. Climate and atmospheric history of the past 420 000 years from the Vostock ice core, Antarctica. Nature 399:429-436.

Radtke, U., Janotta, A., Hilgers, A., Murray, A., 1999. The potential of OSL and TL for dating late-glacial and Holocene dune sands tested with independent age controls of the Laacher See tephra (12, 880a) at the section Mainz-Gonsenheim, 9th International Conference on Luminescence and ESR dating (LED99), Rome.

Repinski, P., Holmgren, K., Lauritzen, S.E., Lee-Thorp, J.A., 1999. A late Holocene climate record from a stalagmite, Cold Air Cave, Northern Province, South Africa. Palaeogeography, Palaeoclimatology, Palaeoecology 150, 269-277.

Ringrose, S., Vanderpost, C. and Matheson, W., 2003. Mapping ecological conditions in the Okavango delta Botswana using fine and coarse resolution systems including simulated SPOT VEGETATION imagery, International Journal of Remote Sensing, 24(5): 1029-1052.

Ringrose, S., Huntsman-Mapila, P., Kampunzu, A. B., Matheson, W., Downey, W., Vink, B., Coetzee, C., and Vanderpost, C., 2005. Sedimentological and geochemical evidence for palaeo-environmental change in the Makgadikgadi subbasin, in relation to the MOZ rift depression, Botswana. Palaeogeography, Palaeloclimatology, Palaeoecology, V. 217 (3-4) pp. 265-287.

Ringrose, S., Huntsman-Mapila, P., Downey, W., Coetzee, S., Vink, B., Kemosidile, T., Vanderpost, C., Kolokose, D., (submitted paper) Impact of poast and present sedimentary processes on morpho-unit development in the distal okavango alluvial fan, Botswana. Earth Surface Processes and Landforms.

Robbins, L., Murphy, A., Campbell, A., brook, G., Reid, D., Haberyan, K., Downey, W., 1998. Test excavations and reconnaissance palaeoenvironmental work at Toteng, Botswana. South African Archaeological Bulletin 53, 125-132.

Rollinson, H., 1993. Using geochemical data: evaluation, presentation, interpretation. Longman, Singapore.

Shaw, P.A., 1985. Late Quaternary landforms and environmental change in northwest Botswana; the evidence of Lake Ngami and the Mababe Depression. Trans. Inst. Brit. Geog., NS10, 333-346.

Shaw P., Cooke, H.J., 1986. Geomorphic evidence for the late Quaternary palaeoclimates of the middle Kalahari of northern Botswana. Catena. 13, 349-359.

Shaw P.A, Stokes S, Thomas D.S.G., Bateman, M., Davies F., 2003. Holocene fluctuations of Lake Ngami, Middle Kalahari: chronology and responses to climatic change. Quaternary International, 111, 23-35.

Smith, R.A., 1984, Lithostratigraphy of the Karoo stratigraphy in Botswana, Botswana Geological Survey Bulletin, Lobatse, Botswana, 26, 34pp.

Snowy Mountain Engineering Corporation (SMEC), 1987. Southern Okavango Integrated Water Development Phase 1: Final Report, Technical Study, Vol 11. Irrigated Agricultural Development Potential. Government of Botswana, Department of Water Affairs, Gaborone.

Stager, J.C., Cumming, B. & Meeker, L.D. 1997. An 11,400-year high resolution diatom record from Lake Victoria, East Africa. Quaternary Research, 47, 81-89.

Stuiver, M., Polach, H.A., 1977. Discussion: Reporting of 14C Data. Radiocarbon 19 (3), 355-363.

Talma, A. S. and J. C. Vogel. 1992. Late Quaternary paleotemperatures derived from a speleothem from Cango Caves, Cape Province, South Africa. Quaternary Research, 37, 203-213.

Taylor, S.R., McLennan, S.M., 1985. The Continental Crust: its composition and evolution. Blackwell, Oxford, 312pp.

Thomas D.S.G., Shaw, P.A. 2002. Late Quaternary environmental change in central southern Africa: new data, synthesis, issues and prospects, Quaternary Science Reviews 21, 783-797.

Thomas, D.S.G., Brook, G., Shaw, P., Bateman, M., Haberyan, K., Appleton, C., Nash, D., McLaren, S., Davies, F., 2002. Late Pleistocene wetting and drying in the NW Kalahari: an interated study from the Tsodilo Hills, Botswana. Quaternary International.

Tyson, P.D., Preston-Whyte, R.A., 2000. The weather and climate of Southern Africa. Oxford University Press, Cape Town, 396pp.

Tyson, P.D., Lee-Thorp, J., Holmgren, K., Thackeray, J.F., 2002a. Changing gradients of climate change in southern Africa during the past millennium: implications for population movements. Climate Change 52, 129-135.
Tyson, P.D. Fuchs, R., Fu, C, Lebel, L., Mitra, A.P. Odada, E, Perry, J., Steffen, W., Virji, H., (Eds) 2002b, Global-Regional Linkages in the Earth System, START, Springer-Verlag, New York, 198pp.
Wright, J., Schrader, H., Holser, W.T., 1987. Paleoredox variations in ancient oceans recorded by rare earth elements in fossil apatite. Geochimica Cosmochimica Acta 51, 631-644.
Zoller L, Pernicka E. 1989. A Note on Overcounting in Alpha-Counters and its Elimination. Ancient TL 7, 11-14.

VIII. MAJOR AND TRACE ELEMENT GEOCHEMISTRY OF LAKE TANGANYIKA SEDIMENTS: IMPLICATIONS FOR LATE QUATERNARY CLIMATIC VARIABILITY

VIII.1. Changements paléo-environnementaux dans le bassin du Tanganyika au Quaternaire : approche géochimique des éléments traces et majeurs

Résumé de l'article

Au cours de ce travail, nous avons étudiés les changements paléo-environnementaux du bassin du Tanganyika pendant la fin du Pléistocène et durant Holocène à l'aide d'outils géochimiques (mesure des éléments majeurs et traces). Les sédiments des deux sondages étudiés (MPU-3 et MPU-10) proviennent du sous bassin de Mpulungu. Ils sont essentiellement laminés, constitués de boues organiques riches en diatomées et sont occasionnellement interrompus par des niveaux de cendres volcaniques aériennes. Ces cendres viennent du système volcanique de Rungwe, situé au sud-est du bassin du Tanganyika. Les sédiments du sous-bassin Mpulungu proviennent d'un matériel modérément à fortement altéré, typique de la zone climatique tropicale. Les variations du rapport Ti/Al sont, selon notre interprétation, liées aux variations de flux de kaolinite et de feldspath et non aux variations de taille de grains des apports détritiques. Durant le Dryas récent (12.5 – 11.5 ka BP) les rapports Ti/Al et K/Al des sédiments diminuent fortement, indiquant que les sédiments proviennent d'une source altérée. A partir de 11.2 ka, les rapports Ti/Al et K/Al augmentent et atteignent un plateau à ca. 6.5 ka. Ces résultats indiquent que pendant les périodes humides, l'augmentation du couvert végétal limite l'érosion des sols, favorisant leur stabilité. Il en résulte une érosion mécanique moindre, mais une érosion chimique accrue. Pendant les périodes plus sèches, la végétation est plus clairsemée ce qui favorise la désagrégation mécanique. Ceci entraîne l'érosion et le transport, dans le bassin, du matériel fortement altéré au cours des épisodes humides précédents. Les éléments traces, sensibles aux changements de conditions d'oxydoréduction, ont été utilisés pour reconstruire les variations du niveau du lac. Les concentrations en éléments traces du site en eaux peu profondes MPU-3 sont plutôt contrôlés par le flux détritique et sont donc peu représentatives pour reconstruire les variations du niveau du lac. En revanche, les résultats pour le site en eaux profondes MPU-10 suggèrent que même pendant le dernier maximum glaciaire (LGM), les conditions sont restées euxiniques. Ainsi, le

niveau du lac n'est pas descendu à moins de 200 – 300 m durant cette période. Les variations du rapport Nb/Ti sont utilisées comme indicateur du transport des cendres volcaniques. Ces variations indiquent des conditions relativement instables entre la fin du Pleistocène jusqu'à ca. 15.4 ka. Les directions de vent étaient variables avec une dominante au Nord, principalement pendant le dernier maximum glaciaire (21.5 – 18.3 ka). Entre 13.2 ka et 11 ka, ce qui couvre le Dryas récent, les rapports Nb/Ti sont élevés, ce qui reflète des épisodes majeurs de retombées de cendres volcaniques. Ces rapports diminuent ensuite au cours du temps. Le pic en Nb/Ti, observé à 13.2 ka et représentatif de l'éruption majeure, pourrait aussi refléter l'érosion et le transport des cendres volcaniques déposées sur l'ensemble de la zone entre le sud du lac Tanganyika et le nord du lac Malawi. Les rapports Nb/Ti des sédiments Holocène sont généralement plus faibles et plus stables que ceux des sédiments de la fin du Pléistocène. Cette régularité pourrait indiquer un retour à des conditions plus stables avec des vents de Nord dominant pendant cette période humide.

VIII.2. Major and trace element geochemistry of Lake Tanganyika sediments: implications for late Quaternary climatic variability

P. Huntsman-Mapila[1,2,*], J-J. Tiercelin[2], M. Benoit[2], J. Cotten[2], M. Talbot[3], C. Hémond[2], D. Hureau-Mazundier[2]

[1] *Harry Oppenheimer Okavango Research Centre, University of Botswana, P/Bag 285, Maun, Botswana*
[2] *UMR-CNRS 6538, Institut Universitaire Européen de la Mer, 29280 Plouzané, France*
[3] *Department of Earth Sciences, University of Bergen, Allegt. 41, 5007 Bergen, Norway*
* *Author for correspondence (email : pmapila@orc.ub.bw)*

Article to be submitted to: *Palaeogeography, Palaeoclimatology, Palaeoecology*

Abstract

In this study, geochemical proxies for climate change were employed on samples from two cores from the Mpulungu sub-basin, southern Lake Tanganyika. The sedimentation in these cores, which are predominantly laminated, diatom-rich organic muds, was occasionally interrupted by wind-blown volcanic ash, interpreted as related to volcanic activity in the Rungwe volcanic province to the south-east of the Tanganyika basin. The Lake Tanganyika sediments from the MPU-3 and MPU-10 core represent sediments originating from moderate to strongly weathered source material typical of a tropical climate zone. The Ti/Al flux has been interpreted as variations due to the kaolinite and feldspar flux rather than grain size variations in the terrestrial input. During the Younger Dryas (YD) event, both Ti/Al and K/Al fall drastically, indicating the input of more weathered source material. By 11.2 ka, both Ti/Al and K/Al rise rapidly, reaching a plateau at ca. 6.5 ka. These results reflect the fact that during more humid periods, the increased tree cover would limit soil erosion through enhanced soil stability, resulting in less physical weathering but more pronounced chemical weathering. The sparser vegetation of drier periods would enhance physical weathering leading to the erosion and transport into the basin of material chemically weathered during the previous wet phase. Redox sensitive trace elements used as geochemical proxies for past climate induced lake levels fluctuations indicate that at the shallow MPU-3 site, these elements are ultimately controlled by detrital flux and therefore have limited use in palaeoredox reconstruction. The MPU-10 deeper water site suggests that even during the

Last Glacial Maximum (LGM), euxinic conditions were maintained. This suggests that the water did not fall much below 200 – 300 m during this time. Nb/Ti results suggest that in the late Pleistocene, until ca 15.4 ka, fairly unstable conditions, with changing wind directions but more frequent north winds particularly between 21.5 – 18.3 ka (LGM). From the time of the major ash fall at 13.2 ka to ca 11 ka, which covers the YD event, our records show Nb/Ti ratios that are diminishing with time. The very high peak at 13.2 ka representing the major ash fall followed by diminishing values could in fact be reflecting erosion and river transport of ash falls deposited on land as the whole area between southern Lake Tanganyika and northern Lake Malawi would have been covered in ash from this eruption. The Holocene sediments show a generally more stable and relatively low pattern for Nb/Ti value than for the late Pleistocene. This stable pattern could reflect a general return to predominantly north winds during this humid period.

VIII.2.1. Introduction

Lake sediments are highly sensitive indicators of climate variability and environmental change. A number of proxies exist for tracking environmental dynamics, including geochemistry which can provide valuable information on changes in weathering profiles and depositional environments. During more humid periods, chemical weathering may be enhanced (White et al., 1999; Ding et al., 2001; Singh and Rajamanni, 2001) while the thicker vegetation cover and more stable soils typical of wetter environments may reduce physical weathering (Kauppila and Salonen, 1997). Concentrations of the redox-sensitive elements in sediments can reflect water levels and allow us to reconstruct palaeodepositional conditions in the sedimentary basin (Werne et al., 2002; Lyons et al., 2003; Sageman et al., 2003; Tribovillard et al., 2006).

Studies on lake cores from Tropical Africa have focussed more on using biofactors such as pollen, (e.g. Bonnefille et al., 1991; Vincens, 1991; Vincens et al., 1993; Vincens et al., 2005) and diatoms (e.g. Barker et al., 2002; Gasse et al., 1989; Gasse and Van Campo, 1998; Gasse et al., 2002) to detect palaeoclimate variations. Geochemical methods have not been extensively used in this region with the exception of organic geochemistry and stable isotopes (e.g. Beuning et al., 1997; Russell and Johnson, 2005; 2006; Talbot and Livingstone, 1989; Talbot and Laerdal., 2000; Talbot et al., 2006) and magnetic susceptibility (e.g. Williamson et al., 1991; Garcin et al., 2006a). By approaching this study of climate variability and past environmental dynamics in the Lake Tanganyika Basin from a geochemical perspective (major and trace element), we attempt to present a new perspective on previous climate change work done on cores from the Mpulungu Basin. The objectives of this paper are therefore: 1) to present new geochemical data from Lake

Tanganyika sediments; 2) to determine climate induced changes in the sedimentary geochemistry and 3) to compare the geochemically based climate proxies with existing diatom, pollen and organic geochemistry data from the same cores and regional work.

VIII.2.2. Geological and limnological setting

Lake Tanganyika is part of the western branch of the East African Rift System and lies at an altitude of 773m. It is 650 km long and up-to 70 km wide (Scholz and Rosendahl, 1988) and at 1470 m is the deepest of the African rift lakes (Figure VIII-1 a and b). Lake Tanganyika occupies a series of linked, axial-rift, half-graben basins (Figure VIII-1 c). The southern end of Lake Tanganyika basin, known as the Mpulungu sub-basin (Mondeguer, 1991), contains a 2.5 km thick pile of rift sediments with an estimated age of 4-2 Ma. The Mpulungu sub-basin is 100 km long, 25 km wide with up to 800 m water depth (Figure VIII-1 d). To the south-east of the Mpulungu sub-basin is the Rungwe volcanic massif, which is the southernmost eruptive centre in the EARS western branch. Volcanic activity in the Rungwe started in the Late Miocene (~ 8 Ma) and remained active during the late Pleistocene and Holocene with major pyroclastics eruptions (Harkin, 1960; Ebinger et al., 1989; Williams et al., 1993). Thin tephras have been identified in a number of cores from southern Lake Tanganyika (Livingstone, 1975 (T2 core); Haberyan and Hecky, 1987; Tiercelin and Mondeguer, 1991). The Holocene sediments of Lake Tanganyika are predominantly laminated, organic-rich diatomaceous silts (Degens et al., 1971) with minor clays (primarily kaolinite, with lesser amounts of chlorite and illite) (Cohen, 1989).

Hydrogen sulphide, carbon dioxide and methane are present in the deeper lake where below 240 m conditions are permanently anoxic (Coulter and Spigel, 1991; Barrat et al., 2000). Most of the river discharge into the lake is from the Malagarasi River from the east and Ruzizi Rivers from the north. The Lufubu river (Figure VIII-1 c) drains into the basin from the south, traversing the sandstones of the Mbala formation and the granitic basement. The Ruzizi is reported to be the major source of water and salts for Lake Tanganyika (Hecky, 1978). The steep escarpments of the rift basin have streams which also contribute to the water budget. Because of high evaporation rates, under modern conditions, closure of Lake Kivu would result in closure of Lake Tanganyika, as the Ruzizi inflow is greater (3.2 km^3/yr) than the Lukuga discharge (2.7 km^3/yr) (Casanova and Hillaire-Marcel, 1992). The lake was divided into two or more separate basins during major lowstands (Tiercelin and Mondeguer, 1991).

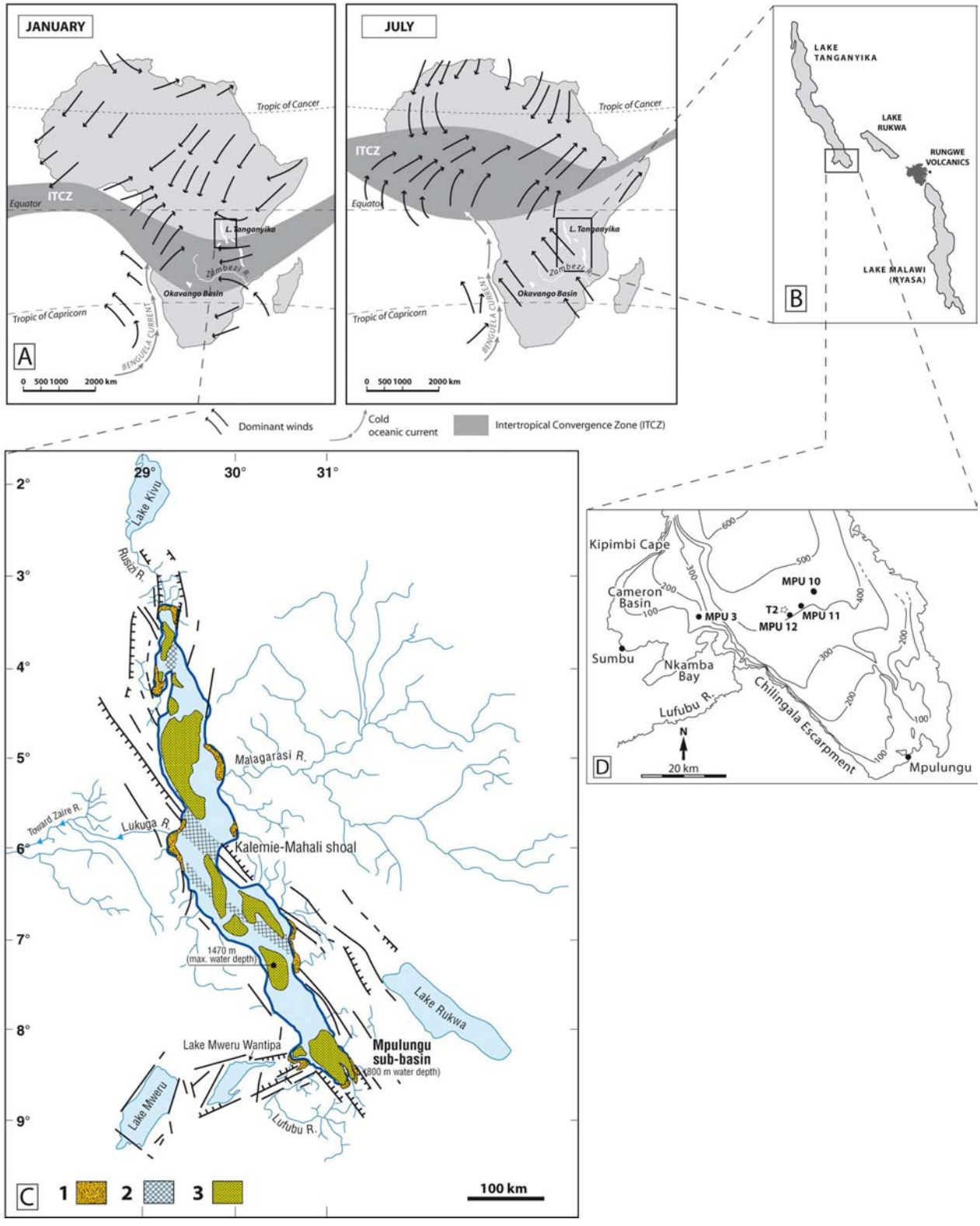

Figure VIII 1. A) Present ITCZ seasonal migration over Africa shown as dark grey band. Predominant wind directions are represented as black arrows. Figure from Grand Atlas du Continent Africain (1973): B) location of Lake Tanganyika with respect to the Rungwe volcanic field and Lake Malawi: C) the structure and hydrology of Lake Tanganyika. Key 1-littoral platforms; 2-transverse shoals; 3-sub-basin deep zones (after Tiercelin and Mondeguer, 1991): D) Mpulungu sub-basin showing bathymetry and location of MPU-10 and MPU-3 sites in addition to MPU-11 and MPU-12 (Mondeguer, 1991) and the T2 core (Livingstone, 1975).

There is a single rainy season in the 231,000 km^2 catchment area from November to April with a mean annual rainfall of 1000-1100mm (Coulter and Spigel, 1991). In this tropical summer rainfall zone, the northeast and southeast trade winds converge in a low pressure zone known as the Intertropical Convergence Zone (ITCZ). Rainfall in the region is strongly influenced by the seasonal migration of the ITCZ to the north and south of the equator (Figure VI-1 a). When the ITCZ migrates northwards during winter, southern Africa is dominated by a high pressure cell that surpresses convection of moisture off the Indian Ocean (Lindesay, 1998). South easterly winds predominate during the dry season, resulting in seasonal upwelling of deep water at the southern end of Lake Tanganyika (Coulter and Spigel, 1991). During the rainy season, solar heating forces air to rise through convection, resulting in the African monsoon. The strength of African monsoon and variations of the mean ITCZ position over tropical Africa were mainly driven by the earths 23 kyr precessional cycle which results in changes in the amount of solar radiation received at low latitudes (deMenocal et al., 2000; Tyson and Preston-Whyte, 2000; Baker et al., 2001; Barker et al., 2004)

VIII.2.3. Previous work on climate change and lake levels

A greater understanding of climate variability in the African tropics is needed as the area is a centre of atmospheric convection which forces regional atmospheric circulation patterns (Barker, et al., 2004). Major climate forcing factors influencing the region at the glacial-interglacial time-scale include orbital configurations, the volume of high latitude ice sheets, and atmosphere, ocean and land surface conditions (Street-Perrott and Perrott., 1990; Kutzbach and Liu, 1997; Barker et al., 2004).

VIII.2.3.1 Last Glacial Maximum

The hydrological record reconstructed from sediments from tropical African lakes have shown that most of the East African lakes from the ITCZ region were at a low level (Beuning et al., 1997; Gasse et al., 1989; Gasse et al., 2002; Barker and Gasse, 2003, Scholz et al., 2003; Talbot et al., 2006) during the cooler and drier Last Glacial Maximum (LGM). During the LGM (23-18 ka BP) generally dry conditions prevailed in both hemispheres associated with lower tropical land and sea surface temperatures. Sedimentological studies from Tswaing Crater (Pretoria Salt Pan) indicate that whilst enhanced summer rainfall is predicted due to orbital forcing during the LGM, the grain-size (Partridge et al., 1997) and diatom data (Metcalfe, 1999) indicate increased aridity. High resolution seismic profiles in Lake

Tanganyika indicate a LGM low stand ca. 250-300m below current lake levels (Tiercelin and Mondeguer, 1991). This is supported by a multi-proxy study of a core from central Lake Tanganyika where Scholz et al. (2003), from abundances of benthic diatoms, infer that the lake was about 350 m lower than present during the LGM. South east African lakes Malawi and Rukwa indicate from diatom records, a negative water balance during the LGM (Johnson et al., 2004; Barker et al., 2002). Pollen records from Lake Rukwa spanning the last 23 kyr indicate that between 23 and 20 kyr cal BP vegetation indicates cooler and probably drier climatic conditions than today (Vincens et al., 2005). Pollen records from cores in the Mpulungu sub-basin suggest a mean temperature decrease of about 4.2^{o}C and mean annual precipitation decrease of about 180 mm/yr (Vincens et al., 1993).

However, during the LGM, summer insolation, which is under the control of orbital precession (Berger, 1978), was at a maximum in the southern tropics, and might normally have been expected to strengthen the summer African monsoon (Kutzbach and Liu., 1997), resulting in higher rainfall inland. Recent studies from Lake Masoko have suggested water levels in this crater basin were higher, reflecting a moister climate locally at this time (Garcin et al., 2006b). In addition, work conducted at Lake Ngami, situated in NW Botswana has suggested that this basin, which receives inflow from Angola, was at a highstand during the LGM (Huntsman-Mapila et al., 2006). Reconstructions of the equatorial river discharge, on the other hand, indicate significantly lower discharge and dry conditions in the Congo basin during the LGM (Adegbie et al., 2003; Schefuss et al., 2005).

VIII.2.3.2 Deglacial period

Lake Tanganyika diatom records (Gasse et al., 1989) of MPU 3 and MPU 12 (location shown in Figure VIII-1 d) suggest that the lake was between 350 – 400 m lower than today at ca. 21 ka and an initial P-E increase between 21 and 15 ka followed by a substantial rise at 15 ka during the African humid period. These results agree with those of Talbot et al., (2006) who report marked increase in TOC between 19 and 16.5 ka and 15.5 and 14.5 in the Mpulungu basin cores MPU-3 and MPU-10. Pollen evidence from two other cores (MPU 11 and MPU 12) from the Mpulungu Basin (Vincens, 1991) suggest a cold episode between 22 and 15 ka with a woodland vegetation that was limited in distribution and not very diverse. The woodland cover was scattered and had herbaceous vegetation groundcover. This was followed by a transitional period until 12 ka. The development of woodland vegetation, implying an increase in rainfall occurred after 12 ka.

In equatorial Africa, significantly wetter conditions followed the LGM which leading to a rise in water levels in many of the lakes. Most equatorial lakes rose substantially at ca. 15 ka although in some lakes an earlier humid phase is apparent. Rapid refilling of Lake Victoria commenced at ca. 15 ka BP (Talbot and Laerdal, 2000) and flow from Lake Victoria via Lake Albert into the Nile was re-established no later than 14.5 ka (Williams et al., 2006). Talbot et al., 2006 report major changes in organic matter (OM) composition in Mpulungu cores (Lake Tanganyika) during and following the period of lake level change. Diatom records from Lake Rukwa indicate that deep water conditions were reached by 13.5 ka BP (Barker et al., 2002).

VIII.2.3.3 The Younger Dryas cold event (ca. 12.5 – 11.5 kyr)

During the Younger Dryas (YD), event, dry climatic conditions with increased northerly trade winds prevailed over much of Africa. This resulted in the failure of the African monsoon which in turn led to lower lake levels in a number of East African lakes at ca. 12.5 – 11.5 ka cal BP) (Street-Perrott and Perrott, 1990: deMenocal et al., 2000; Gasse, 2000; Peck et al., 2004). The failure of the African monsoon during the Younger Dryas, was then followed by a return to more humid climatic conditions leading into the generally more humid Holocene period (Barker et al., 2004; Johnson et al., 2004; Schefuss et al., 2005).

VIII.2.3.4 The Holocene

Diatom records from Lake Rukwa show that between 11.8 and 6.7 ka cal BP the lake was deep and fresh (Barker et al., 2002) and may have overflowed into Lake Tanganyika (Haberyan, 1987). Based on sedimentologic and geochemical analyses of cores from Lake Edward, Russell et al. (2003) propose a well-mixed, deep waterbody between 11 and approximately 9 ka BP and increased wetness from approximately 9 to 7.5 ka BP. From 12.1 to 5.5 ka cal BP more humid conditions in Lake Rukwa are confirmed from the pollen record (Vincens et al., 2005). Barker et al. (2002) report saline conditions from the diatom record of Lake Rukwa after 5.5 ka cal BP and Russell et al. (2003) report the onset of drier conditions in Lake Edward from about 5.2 ka BP based on the occurrence of authigenic calcite. From 5.5 ka cal BP drier conditions are also indicated from the pollen record of Lake Rukwa, which intensify ca. 3.5 ka cal BP towards modern conditions (Barker et al., 2002).

VIII.2.4. Description of cores

The two Kullenberg piston cores (MPU-3, 11.19 m and MPU-10, 8.09 m) were collected from the Mpulungu sub-basin at the southern end of Lake Tanganyika (Figure VI-1 d) in 1985 as part of the Georift project. MPU-3 was retrieved from a water depth of 130 m and MPU-10 from a water depth of 422 m. The MPU-3 core is characterized in the lower part (11.19-7.80 m) by a clastic, quartz-rich, silt-sized facies locally interrupted by diatom-rich laminae (Figure VIII-2). Transition between clastic and organic facies at 7.80 m on MPU 3 corresponds to a sedimentary discontinuity which was also identified on high–resolution seismic lines acquired in the Mpulungu sub-basin (Tiercelin et al., 1989). From 7.80 m to the top of the core, the sediments are laminated, diatom-rich, organic muds. In this paper, we discuss results from 7.80 m to the top of the core. MPU-10 core, from the deeper water site, is a dark grey vaguely laminated mud (Mondeguer, 1991) (Figure VIII-2). There are no apparent discontinuities in the core which spans the period 30 – 7 ka (Talbot et al., 2006). The uppermost part of the core was lost during coring. For this paper we present results from 23.3 ka to 7 ka which spans the period of transition from the LGM to the Holocene.

Sedimentation in the Lake Tanganyika basin was occasionally interrupted by wind-blown volcanic ash, interpreted as related to explosive activity in the Rungwe volcanic centre, which resulted in the formation of thin pinkish yellow layers identified at different depth in the various cores collected from the Mpulungu sub-basin (Mondeguer, 1991). One particularly prominent tephra with an age of ca. 13.2 ka is present in all the cores from the Mpulungu sub-basin (Livingstone, 1975; Tiercelin and Mondeguer, 1991; Talbot et al., 2006).

VIII.2.5. Sampling and analysis

Analyses was performed on bulk mud samples which all had a grain size of < 0.63 μm. Approximately 1.00000 g of finely ground sample was weighed in a crucible and heated for 2 hours at 1000^{o}C for the determination of loss of ignition (LOI). Major elements were then measured by inductively coupled plasma-atomic emission spectrometry (ICP-AES) with an ISA Jobin-Yvon JY 70 Plus apparatus. 230 mg of the sample was digested in 3 ml of concentrated acid mixture (1:7 HNO_3-HF) at 90^{o}C for 2 hours and at 110^{o}C for ¼ hours. All reagents used were analytical grade. 96 ml of H_3BO_3 aqueous solution (20g/l H_3BO_3 and 0.5g/l CsCl) were added to neutralize the excess HF and dissolve the precipitated fluoride, CsCl acting as a buffer of the ionization phenomena in the flame and the argon plasma. After a two day complexation process where fluoride complexes as HBF_4 a clear solution is

obtained. The major elements were determined from the final solution without selective extraction, with boron being used as an internal standard. Calibrations were performed using the international standard JB2. Sediment standard LKSD-1 was also analysed to determine the recovery.

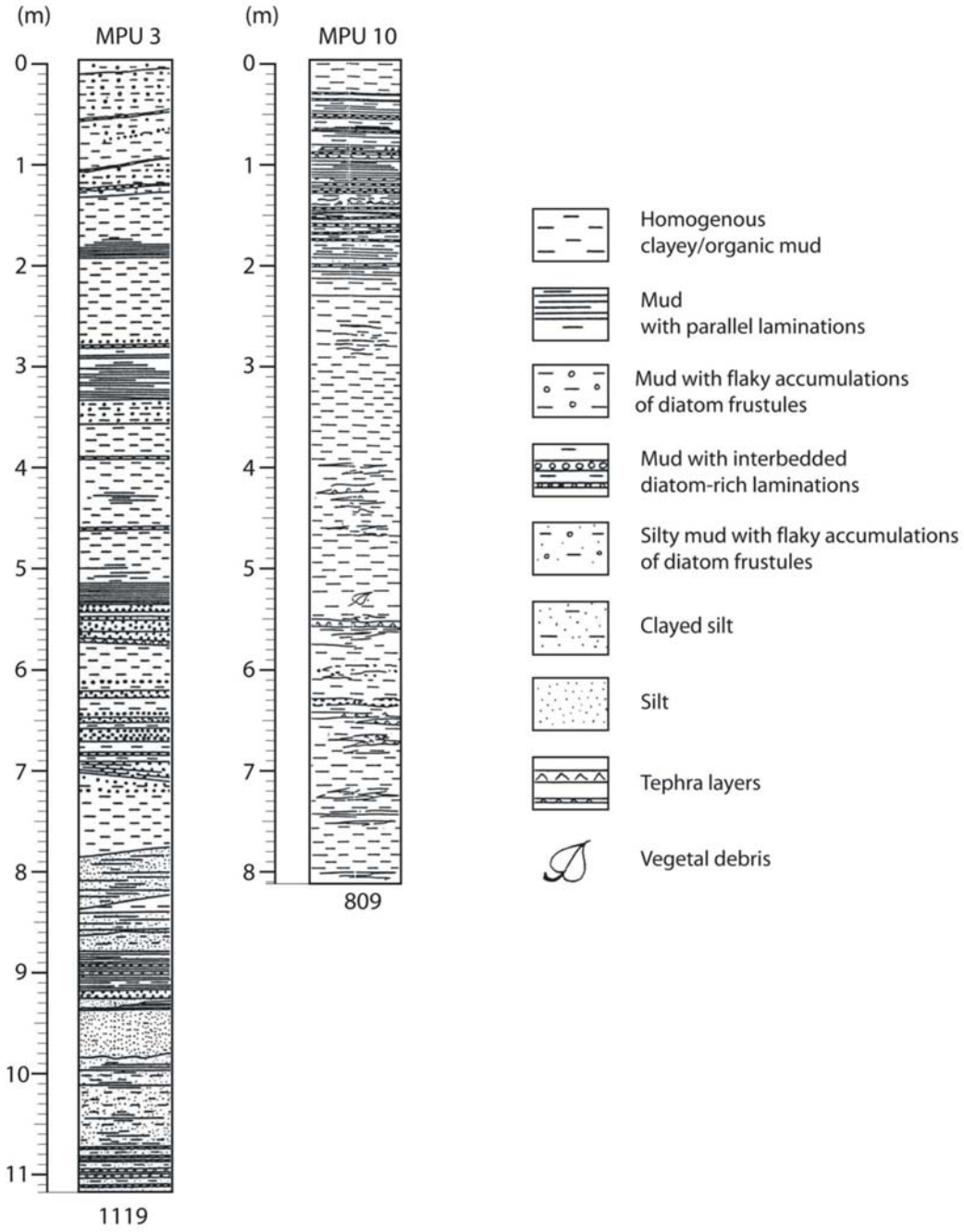

Figure VIII 2. MPU-3 and MPU-10 lithology: stratigraphic distribution of the main facies (after Mondeguer, 1991)

Trace element measurements were conducted using inductively coupled plasma-mass spectrometry (ICP-MS). Approximately 0.10000 g of finely ground sample was weighed into a clean Teflon beaker. 4 ml of H_2O_2 was added to each beaker and reacted for 2 hrs without heating and then at 60°C overnight to breakdown the organic matter. 1ml of HNO_3 and 3 ml of HF was added to each beaker and digested overnight at 110°C. Then the acid was allowed to evaporate. 2 ml of 3N HCl was added to the evaporate and left for approximately 1hr at 80°C with the lid on to re-dissolve all the sample. The solution was transferred to a bottle and diluted to 40 ml with 3N HCl and 4 drops of HF. The weight of the solution was recorded in order to be able to calculate dilution factors. Approximately 0.90000 g of the solution was weighed into a clean Teflon beaker and then 0.07000 g of pure Tm solution was added except to the blank and the internal standard (BHVO-2 or BEN). This was evaporated at 135°C and then 5 drops of HNO_3 was added followed by 14 ml of H_20. The samples were then analysed using a on a Finnigan Element 2 ICP-MS. Analyses were done at IUEM-UBO.

The chronologies were determined using AMS ^{14}C dating and the age model described in Talbot et al. (2006).

VIII.2.6. Results

A summary of results for major and trace elements for from MPU-3 and MPU-10 are presented in Table VIII-1 along with results for LKSD-1. The results indicate poor recovery of Zr and Hf in LKSD-1, which is attributed to incomplete digestion of Zr and Hf bearing minerals so these results have been discarded. The value we obtained for Nb on the ICP-MS differs from the reported value for LKSD-1 (Nb = 7 ppm) although our results were reproducible (avg = 3.69 ppm , sd = 0.53, n = 6). The standard was then re-analysed by XRF at IFREMER, Brest and a value of 3.85 ppm was obtained. We believe therefore that our Nb results are reliable and that the reported value for the standard may be overestimated. Poor or incomplete mixing of the LKSD-1 powder, especially where Nb-enriched phases occur as sparse sulphides minerals could be the cause of this (M. Benoit, pers. comm.).

Table VIII 1. Geochemical compositional ranges of Lake Tanganyika sediments for selected elements

Sample	LKSD-1 avg results	std dev	LKSD-1 reference	MPU -3 (n = 36)	range	average	MPU-10 (n = 23)	Range	average
SiO2 (%)	39.7	0.02	40.1		54.68 - 72.80	65.22		59.31 - 77.86	66.70
TiO2	0.5	0.00	0.5		0.20 - 0.55	0.40		0.19 - 0.43	0.32
Al2O3	7.6	0.16	7.8		6.42 - 19.55	11.66		5.44 - 12.42	9.54
Fe2O3	4.1	0.04	4.1		1.54 - 3.17	2.38		1.63 - 4.14	2.73
MnO	0.1	0.00	0.1		0.01 - 0.11	0.02		0.01 - 0.06	0.02
MgO	1.8	0.04	1.7		0.23 - 0.48	0.38		0.30 - 0.57	0.40
CaO	11.1	0.04	10.8		0.19 - 1.64	0.48		0.29 - 1.13	0.48
Na2O	1.9	0.04	2		0.09 - 0.99	0.20		0.10 - 0.57	0.24
K2O	1.1	0.03	1.1		0.47 - 1.88	1.36		0.47 - 1.23	0.84
P2O5	0.2	0.01	0.2		0.09 - 0.54	0.18		0.04 - 0.14	0.09
LOI	29.1	0.40	29.9		12.28 - 19.62	15.53		12.92 - 20.36	17.17
Total	96.9	0.10	99.9		82.85 - 100.06	97.82		97.49 - 99.75	98.54
Rb (ppm)	22.3	2.17	24		65.1 - 166.2	108.9		40.9 - 115.0	66.4
U	8.4	0.45	9.7		1.4 - 4.4	2.4		1.5 - 7.0	3.6
Nb	3.7	0.53	7		12.8 - 151.7	51.1		10.6 - 141.6	34.0
Cu	43.8	4.53	44		7.6 - 34.6	19.2		10.8 - 43.0	26.5
Pb	81.3	11.14	82		11.9 - 37.5	19.3		7.3 - 23.2	14.1
Co	10.89	0.75	11		2.4 - 9.0	5.8		3.4 - 12.2	6.6
Zn	376.57	14.45	331		24.6 - 103.6	50.3		38.0 - 122.9	66.5
Ni	16.79	1.23	16		7.2 - 27.7	15.4		8.8 - 51.6	18.4
V	48.42	3.94	50		12.6 - 47.7	27.6		6.6 - 61.9	31.0
Cr	24.91	1.53	31		8.8 - 45.6	25.4		4.6 -31.9	21.2

VIII.2.6.1 Major elements

VIII.2.6.1.1 Elements affected by weathering processes

The SiO_2 content in the MPU-3 core ranges between 54.68 - 72.80 wt. % (avg. = 65.22 wt. %) and between 59.31 - 77.86 wt. % (avg. = 66.7 wt. %) in the MPU-10 core. Al_2O_3 varies between 6.42 - 19.55 wt. % (avg = 11.22 wt. %) and 5.44 -12.42 wt. % (avg. = 9.54 wt. %) in MPU-3 and MPU-10 respectively and is negatively correlated with SiO_2 ($r^2 = .69$). In plots against Al_2O_3 (not shown), the oxides TiO_2, Fe_2O_3, MgO and K_2O and to a lesser extent, P_2O_5 and MnO show a correlation, indicating that they are associated with micaceous/clay minerals in the sediments. The samples from both cores are all enriched in SiO_2 with respect to the upper continental crust (UCC) and post-Archaean Australian shales (PAAS) (Taylor and McLennan, 1985; 1995; Plank and Langmuir, 1998). All samples are depleted in MgO, K_2O, Na_2O and CaO (with the exception of a sample at the top of the MPU-3 core). This is an indication of sediment from weathered source areas.

Ti is often contributed by heavy minerals such as rutile and anatase and the ratio of Ti/Al has been used to reflect grain size and consequently the strength of transport processes (Zabel et al., 1999; Meyers et al., 2001). K is usually associated with potassium feldspar or illite and the presence of either is representative of lower rates of chemical weathering suggesting arid conditions where physical weathering predominates. Feldspar and illite are relatively reduced in sediments from humid periods as the formation of kaolinite occurs. A depletion of potassium in sediments can be used therefore as an index of the chemical maturity of sediments and consequently a proxy for the intensity of chemical weathering (Schneider et al., 1997; Zabel et al., 2001).

Ti/Al and K/Al show strikingly similar distributions (Figure VIII-3 a and b). Similar patterns were reported by Schneider et al. (1997) in a study on Zaire (Congo) sediment load and by Zabel et al. (2001) in a study on sediment input to the Niger Fan. The ratio of Ti/Al of the Lake Tanganyika sediments ranges between 0.027 - 0.049 (avg. = 0.039) for MPU-3 and 0.031 - 0.045 (avg. = 0.039) for MPU-10. Results for both cores are in good agreement. Results indicate fairly elevated but unstable Ti/Al for the late Pleistocene in Lake Tanganyika up until ca. 18 ka where values become more stable. Values decline rapidly at 13.0 ka above the ash layer, until 12.1 ka

where both cores show a steady rise until ca. 6.5 ka. Values stabilize after 5.7 ka, and then decline. For K/Al again both MPU-3 and MPU-10 are in good agreement with ranges between 0.07 – 0.18 (avg. = 0.12) for MPU-3 and 0.07 – 0.13 (avg. = 0.09) for MPU-10. Both Ti/Al and K/Al, but particularly the former, show a prominent negative excursion which coincides with the Younger Dryas event (12.5 -11.5 ka BP). The input of unweathered ash is evident from the positive excursion at 13.2 ka for K/Al.

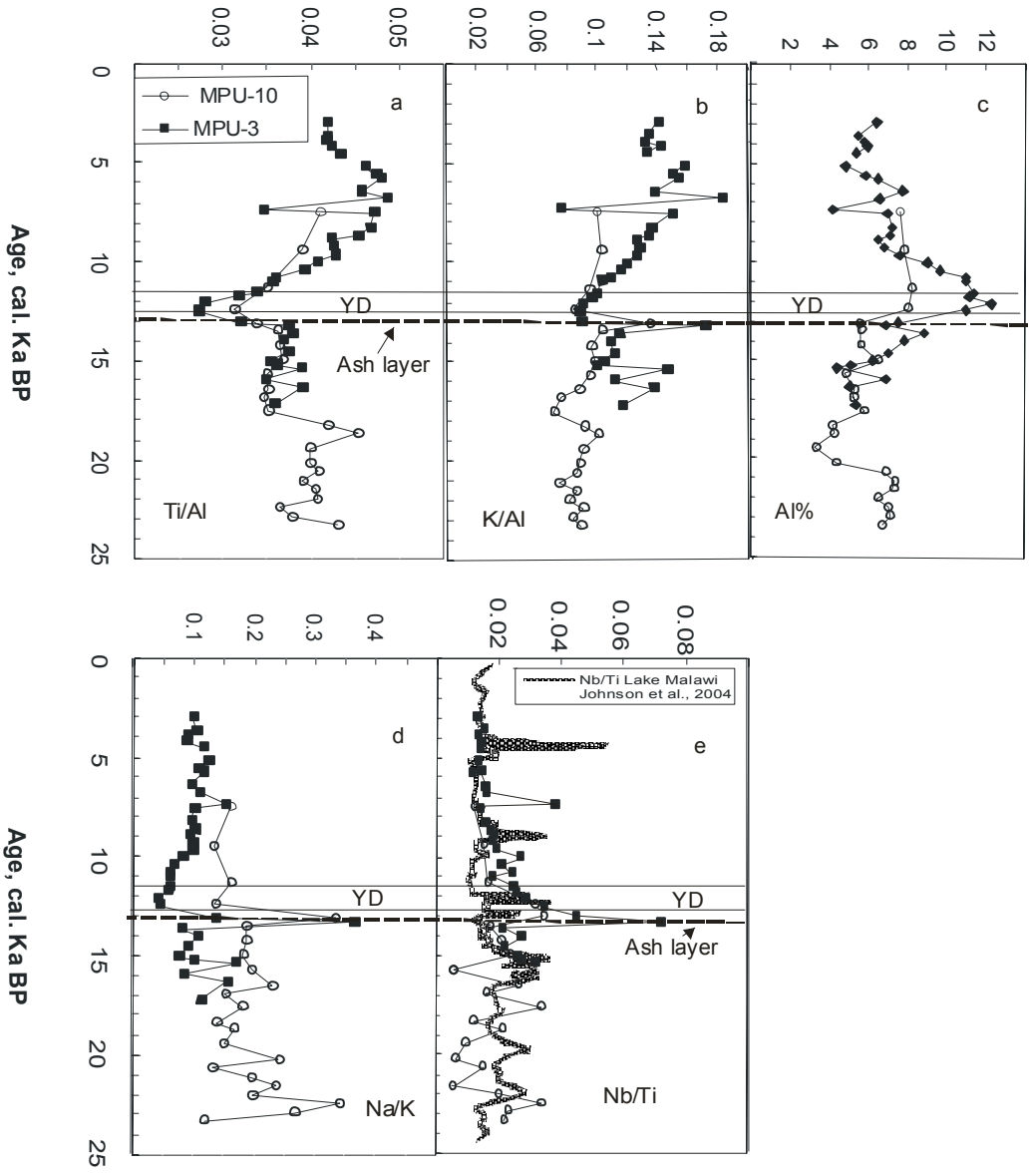

Figure VIII 3. Elemental ratios and concentrations plotted with age for both the MPU-3 and MPU-10 cores.

VIII.2.6.1.2 Indicators of relative abundance of volcaniclastic debris in sediments

Ratios of Na/K given an indication of changes of input of volcanic ash, (sodium) – which reflects aeolian delivery relative to detrital flux such as potassium input as illite (Dean and Arthur, 1998). Na/K ratios for the MPU-3 core range between 0.04 – 0.37 (avg. = 0.11) and for MPU-10 between 0.09 – 0.52 (avg. = 0.17). The positive excursions for the Na/K ratio agree well with the ash layer at 13.2 ka (Figure VIII-3 d). It is interesting to note that positive excursion of Na/K at 22.4 ka, 16.5 ka and 7.4 ka correspond exactly with negative excursions in the Ti/Al ratio which supports the idea that Na/K reflects windblown ash and Ti/Al reflecting sediment transported by a hydrogenous source. In addition, the marked steady rise in Ti/Al after 12.1 ka is reflected by generally low Na/K values.

VIII.2.6.2 Trace elements

VIII.2.6.2.1. Indicators of relative abundance of volcaniclastic debris in sediments

Niobium is an incompatible element which becomes concentrated in magma and not in silicate minerals. Elevated Nb concentrations are found in the volcanic ash from eruptions and within weathered ash. Nb/Ti ratios for both cores are in good agreement, with Nb/Ti between 0.01 – 0.07 (avg. = 0.02) for MPU-3 and between 0.005 – 0.08 (avg. = 0.02) for MPU-10. Results indicate clear positive excursions corresponding to the ash layer at 13.2 ka with additional positive excursion at ca. 22.4, 17.6, 16.5, 10.0 and 7.4 ka. Values are noisy for the late Pleistocene with low values (0.005) interspersed with positive excursions. After the ash layer at 13.2 ka, values drop off slowly and stabilize during the Holocene at 6.7 ka to average values of 0.014. The values show a roughly anti-phase relationship between Nb/Ti data from Lake Malawi (Johnson et al., 2004) (Figure VI- 4 e) more apparent in the record between 23 – 13.5 ka. It should be noted however that the Lake Malawi record has a much higher resolution and that some of our peaks are based on a single point.

VIII.2.6.2.2. Indicators of redox conditions

Reconstructing palaeoredox conditions is an attempt to determine whether conditions in the depositional sedimentary basin were oxidizing or reducing. Reducing conditions in a water column arise from one or more of the following 1) minimal lateral circulation in a deep water column; 2) thermohaline stratification and 3) levels of primary production that result in an oxygen

demand that exceeds renewal (Cruse and Lyons, 2004). Well-oxygenated surface waters are separated from anoxic or anoxic-sulfidic (euxinic) deeper waters by a transition zone called the chemocline. Oxic conditions were defined by Tyson and Pearson (1991) as having > 2 ml O_2/l H_2O in the bottom waters. Suboxic is defined as having $2 > O_2 > 0.2$. In anoxic conditions, O_2 is < 0.2 and no free H_2S is present. In euxinic conditions, free H_2S is present in the water column and O_2 = 0 ml O_2/l H_2O (Tyson and Pearson, 1991).

Metals that occur as minor and trace elements in clastic sediments may become concentrated by precipitation under appropriate redox conditions and thus have redox-proxy potential. These include Cu, Fe, Mo, U, Pb, Co, Zn, Ni, V and Cr (Sageman et al., 2003). Trace element ranges and averages are higher in the MPU-10 core with the exception of Pb and Cr. The Cu values range between 7.6 – 34.6 ppm (avg. = 19.2 ppm) for MPU-3 and between 10.8 – 43.0 (avg. = 26.5) for MPU-10. For Fe, values range between 1.85 – 3.94 wt. % (avg. – 2.9 wt. %) for MPU-3 and 1.88 – 5.21 wt. % (avg. = 3.06 for MPU-10). For Mo, the range of values for MPU-10 are 0.13 – 2.1 ppm (avg. = 0.74 ppm). For U, values are 1.4 – 4.4 ppm (avg. = 2.4 ppm) for MPU-3 and 1.5 – 7.0 ppm (avg. 3.8 ppm) for MPU-10. For Pb, in MPU-3 values range between 11.9 – 37.5 ppm (avg. = 19.3 ppm) and between 7.3 – 23.2 ppm (avg. = 14.1 ppm) for MPU-10. Co values range between 2.4 – 9.0 ppm (avg. = 5.8 ppm) in MPU-3 and between 3.4 – 12.2 ppm (avg. = 6.6 in MPU-10). Zn concentrations in MPU-3 range between 24.6 – 103.6 ppm (avg. = 50.3 ppm) and 38.0 -122.9 ppm (avg. = 66.5 ppm) for MPU-10. Ni values for MPU-3 are between 7.2 – 27.7 ppm (avg. = 15.4 ppm) for MPU-3 and between 8.8 – 51.6 ppm (avg. = 18.4 ppm) for MPU-10. V ranges between 12.6 – 47.7 ppm (avg. = 27.6 ppm) for MPU-3 and between 6.6 – 61.9 ppm (avg. = 31.0 ppm) for MPU-10. Cr ranges between 8.7 – 45.6 ppm (avg. = 25.5 ppm) for MPU-3 and between 4.6 – 39.1 ppm (avg. = 19.8 ppm) for MPU-10.

In order to look at the palaeoredox potential of the trace metals in the Mpulungu sub-basin sediments, it was necessary to eliminate those metals which had an over-riding non-hydrogenous source. For the Mpulungu sub-basin that would mean primarily the detrital and volcanoclasitc flux. A fraction of the trace-metal content of most sediments is of detrital origin. To determine which trace elements are predominantly controlled by detrital flux, we tested the correlation of these elements (at a 5 % confidence limit) versus aluminium and titanium, both of which are usually strongly detrital and immobile during diagenesis. In addition, to test the control by volcaniclasitc debris, we tested the correlation of these elements versus the Nb/Ti ratio.

In the MPU-3 core, the overwhelming majority of the elements tested (U, V, Cr, Co, Ni, Cu, and Pb) showed a significant correlation with Ti (U r^2 = 0.56, V r^2 = 0.66, Cr r^2 = 0.65, Co r^2 = 0.49, Ni r^2 = 0.68, Pb r^2 = 0.53 (n = 36)) and Al (U r^2 = 0.51, V r^2 = 62, Cr r^2 = 0.57, Co r^2 = 0.44, Ni r^2 = 0.63, Cu r^2 = 0.54, Pb r^2 == 0.50 (n = 36)) which suggests that detrital flux controls the concentration of these elements at the shallow water site. In addition, Pb, U, Zn and Mn showed significant correlation with the Nb/Ti ratio (Pb r^2 = 0.38, U r^2 = 0.53, Zn r^2 = 0.47, Mn r^2 = 0.74 (n = 36)) indicating that the input of volcanoclastic material controls the concentrations of these elements. The only element to show a significant correlation with (total organic carbon) TOC at this shallow water site is Zn (r^2 = 0.33, n = 36). Therefore, one must conclude that the MPU-3 record has limited use in palaeoredox reconstructions.

In the MPU-10 core, the only element to show a significant correlation with TOC and a non-significant correlation with Ti, Al and Nb/Ti is V (TOC r^2 = 0.53). The elements U and Mo show a significant positive correlation with TOC (U r^2 = 0.49, Mo r^2 = 0.46, n = 23) in addition to significance to Ti and Al for U and Nb/Ti for Mo. All these elements have been plotted on Figure VIII-4. There is a mild significant correlation between Mo and V (r^2 = 0.46, n = 23) and positive excursion of V are generally accompanied by an excursion in Mo. This has implications on the redox conditions as discussed later.

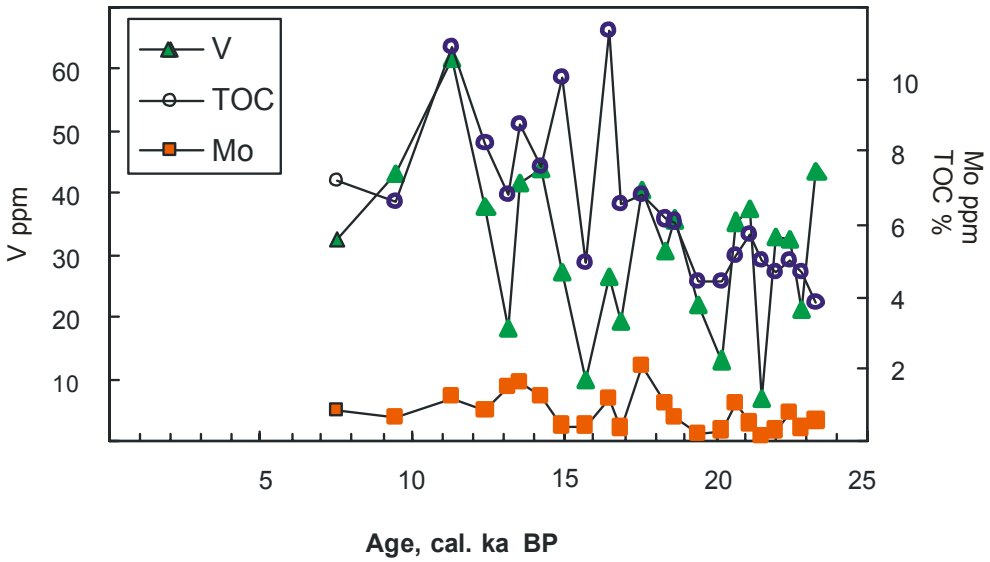

Figure VIII 4. Selected redox- sensitive metals plotted against age for MPU-10 core. TOC data from Talbot et al. (2006)

VIII.2.7. Discussion

Several factors control the chemical composition of elements in siliciclastic sedimentary rocks. These include diagenesis, metamorphism, composition of the source rocks, degree of weathering of the source area and the tectonic setting (e.g., Nesbitt and Young, 1982; McLennan et al., 1983; Wronkiewicz and Condie, 1987; Roser and Korsch, 1988). Wronkiewicz and Condie (1987) indicated that the source rock lithology (mafic, intermediate or felsic) strongly influences the concentrations of certain elements, including Th, and Co in the siliciclcastic sedimentary rocks. The Mpulungu sub-basin were plotted on ternary diagrams devised for the identification of the nature of the source rocks (Chapter VI) and results indicate that the sediments all plot close to the granite end member, suggesting a fairly uniform source rock lithology. Metamorphic remobilisation is excluded for the studied samples because the Mpulungu sediments are unconsolidated. The Mpulungu sediments contain only very minor carbonates and therefore diagenesis is not a main factor influencing chemical variation of the Lake Tanganyika sediment composition.

VIII.2.7.1 Source area weathering

The Ti/Al and K/Al profiles for both cores show interesting results. Most dramatic is the substantial decline in Ti/Al at 13.0 ka which post dates the major ash fall at 13.2 ka and therefore is not likely to be due to this. This corresponds well in timing to the Younger Dryas event and

shows that in terms of palaeoclimate, the YD event was the most prominent event between 23 ka to 3 ka BP. Both the Ti/Al and K/Al show very similar time distributions and we interpret the trends in element/Al ratios as do Schneider et al. (1997) where variations are due to the kaolinite and feldspar flux rather than grain size variations in the terrestrial input. One must note that during the YD event, both Ti/Al and K/Al fall drastically, indicating the input of more weathered source material. By 11.2 ka, both Ti/Al and K/Al rise rapidly, reaching a plateau at ca. 6.5 ka. These results suggest that during the dry Younger Dryas event the material being delivered to the basin is from a more weathered source and during the more humid Holocene up until 6.5 ka, the material is derived from a less weathered source. In order to attempt to interpret these results, one must not only consider detrial fluvial input into the basin but also vegetation cover and erosion processes in the basin. Vincens (1991) from a study on the MPU-11 and MPU-12 core describes the period between 15 and 12 ka BP as a period of expansion of wooded communities around Lake Tanganyika which reach their maximum expansion only after 12 ka BP. Garcin et al. (2006a) describes that from 15 ka BP to between 13.4 and 12 ka BP, arboreal cover developed in the Masoko catchment ($9^{o}20.0$'S, $33^{o}45.3$'E) possibly suggesting a shorter or less severe dry season during this phase. At ca. 11.7 ka BP, Garcin et al. (2006a) report an abrupt change in vegetation cover to a semi-deciduous more sparse vegetation cover indicating the establishment of a more pronounced seasonality at this time which remained throughout the early Holocene. Our data may well be reflecting the fact that during more humid periods, the increased tree cover would limit soil erosion through enhanced soil stability, resulting in less physical weathering but more pronounced chemical weathering (Kauppila and Salonen, 1997; White et al., 1999; Ding et al., 2001; Singh and Rajamanni, 2001). The sparser vegetation of drier periods would enhance physical weathering leading to the erosion and transport into the basin of material chemically weathered during the previous wet phase.

VIII.2.7.2 Palaeoclimatic conditions determined from volcanic ash in sediment

Elevated Nb/Ti levels in the Lake Tanganyika sediments are interpreted to reflect stronger south-east winds as volcanic ash or its weathered residue is transported from the Rungwe volcanics into the lake basin. Similar work has been conducted in Lake Malawi (Johnson et al., 2004), with elevated Nb/Ti in this case interpreted to reflect more frequent or stronger northerly winds. Lake Tanganyika is exposed to northerly winds in austral summer, when the ITCZ has migrated to its southern position and southerly winds in austral winter when the ITCZ migrates northwards. The results from Lake Tanganyika and Lake Malawi, when plotted together (Figure VIII-3 e) show a

rough antiphase relationship which is used in our interpretation. Our results suggest that in the late Pleistocene, until ca 15.4 ka, fairly unstable conditions prevailed, with changing wind directions but more frequent north winds particularly between 21.5 – 18.3 ka (LGM). This is supported by results from Johnson et al., 2004 who also report a predominance of north winds suggesting the migration of the ITCZ further southward or that it remained in the southern terminus longer, during the late Pleistocene. This would mean that a southward excursion of the ITCZ occurred during past northern hemisphere cold periods (Johnson et al., 2004). This southward excursion should imply that Tanganyika would experience longer summer rains and therefore have been at a highstand during the LGM. Johnson et al., 2004 suggest that the vertical convection associated with the ITCZ could be weakened during these periods, leading to less rainfall. During the humid deglacial period, both north and south winds blew over the basin, as suggested by the fluctuating Nb/Ti ratios which would have brought, the north winds in particular, more rain to the catchment area. From the time of the major ash fall at 13.2 ka to ca 11 ka, which covers the Younger Dryas event, our records show Nb/Ti ratios that are diminishing with time. During the Younger Dryas event, low lake levels have been observed in a number of African lakes which has been interpreted as resulting from dry climatic conditions with increased north tradewinds (Street-Perrott and Perrott, 1990; deMenocal et al., 2000; Gasse, 2000). The very high peak at 13.2 ka representing the major ash fall followed by diminishing values could in fact be reflecting erosion and river transport of ash falls deposited on land as the whole area between southern Lake Tanganyika and northern Lake Malawi were covered in ash from this eruption. The Holocene sediments show a more stable and relatively low pattern for Nb/Ti value than for the late Pleistocene with the exception of an input of volcanic ash at 7.4 ka. This stable pattern could reflect a general return to predominantly north winds during this humid period.

VIII.2.7.3 Redox conditions

Of the trace elements, Cr, U and V can be reduced and precipitate under anoxic conditions and the other elements Ni, Co, Cu, Zn, Cd and Mo accumulate predominantly under sulphate-reducing conditions (Tribovillard et al., 2006). In this work, we only use trace metal data from the MPU-10 core as the other core had an overwhelming influence of detrital flux on trace element composition. The fact that V enrichments are generally accompanied by Mo enrichment would suggest that euxinic conditions have prevailed in Mpulungu sub-basin at the sediment-water interface throughout the Late Pleistocene and Holocene. This has particular implications for the LGM, as even points at ca. 23 ka show this trend. This would suggest that water levels in Lake

Tanganyika did not drop sufficiently to develop oxic-anoxic conditions at this deeper water site. If water in Lake Tanganyika is reported to be permanently anoxic at depths of greater than 240 m and the MPU-10 site has a present day depth of 422 m, this would suggest that the water level would have dropped closer to 200 - 300 m during the LGM in order to maintain euxinic conditions even at this time, although during the LGM, the cooler climate and stronger winds may have led to decreased stability of the water column. A drop of closer to 350 - 400 m as suggested by from diatom records of Gasse et al. (1989) may lead to oxic conditions developing. The MPU-3 site, at a current water depth of 130 m, is not sufficiently deep for the accumulation of redox sensitive metals.

VIII.2.8. Conclusions

Geochemical proxies of lake sediments are shown here to provide convincing evidence for past climate-induced environmental changes in the southern Tanganyika basin. In particular that:

1) the Lake Tanganyika sediments from the MPU-3 and MPU-10 core represent sediments originating from moderate to strongly weathered source material typical of a tropical climate zone. The input of unweathered volcanic ash comes from air-borne volcanic ash linked to explosive activity in the Rungwe volcanic centre;

2) the Ti/Al flux has been interpreted as variations due to the kaolinite and feldspar flux rather than grain size variations in the terrestrial input. During the YD event, both Ti/Al and K/Al fall drastically, indicating the input of more weathered source material. By 11.2 ka, both Ti/Al and K/Al rise rapidly, reaching a plateau at ca. 6.5 ka. These results reflect the fact that during more humid periods, the increased tree cover would limit soil erosion through enhanced soil stability, resulting in less physical weathering but more pronounced chemical weathering. The sparser vegetation of drier periods would enhance physical weathering leading to the erosion and transport into the basin of material chemically weathered during the previous wet phase.

3) redox sensitive trace elements at the shallow MPU-3 site are ultimately controlled by detrital flux and therefore have limited use in palaeoredox reconstruction. The MPU-10 deeper water site suggests that even during the LGM, euxinic conditions were maintained. This suggests that the water did not fall much below 200 – 300 m during this time

4) Nb/Ti results suggest that in the late Pleistocene, until ca 15.4 ka, fairly unstable conditions prevailed, with changing wind directions but more frequent north winds particularly between 21.5 – 18.3 ka (LGM). From the time of the major ash fall at 13.2 ka to ca 11 ka, which covers the Younger Dryas event, our records show Nb/Ti ratios that are diminishing with time. The very high peak at 13.2 ka representing the major ash fall followed by diminishing values could in fact be reflecting erosion and river transport of ash falls deposited on land as the whole area between southern Lake Tanganyika and northern Lake Malawi would have been covered in ash from this eruption. The Holocene sediments show a more stable and relatively low pattern for Nb/Ti value than for the late Pleistocene with the exception of an input of volcanic ash at 7.4 ka. This stable pattern could reflect a general return to predominantly north winds during this humid period.

Acknowledgements

PH-M would like to acknowledge the University of Botswana for financial support and Claire Bassoullet for guidance in the laboratory and for insightful discussions on the Nb data. Joël Etoubleau is acknowledged for conducting the Nb analysis at IFREMER.

References

Adegbie, A.T., Schneider, R.R., Röhl, U., Wefer, G., 2003. Glacial millennial-scale fluctuations in central African precipitation recorded in terrigenous sediment supply and freshwater signals offshore Cameroon. Palaeogeography, Palaeoclimatology Palaeoecology 197, 323-333.

Baker, P.A., Rigsby, C.A., Seltzer, G.O., Fritz, S.C., Lowenstein, T.K., Bacher, N.P., Veliz, C., 2001. Tropical climate changes at millennial and orbital timescales on the Bolivian Altiplano. Nature 409, 698-701.

Barker, P., Telford, R., Gasse, F., Thevenon, F., 2002. Late Pleistocene and Holocene palaeohydrology of lake Rukwa, Tanzania, inferred from diatom analysis. Palaeogeography, Palaeoclimatology, Palaeoecology 187, 295-305.

Barker, P., Gasse, F., 2003. New evidence for a reduced water balance in East Africa during the Last Glacial Maximum; implication for model-data comparison. Quaternary Science Reviews 22, 823-837.

Barker, P.A., Talbot, M.R., Street-Perrott, F.A., Marret, F., Scourse, J., Odada, E.O., 2004. Late Quaternary climatic variability in intertropical Africa. In: R.W. Battarbee, F. Gasse and C.E. Stickley (eds). Past climate variability through Europe and Africa. Springer, Dordrecht.pp. 117-137.

Barrat, J.A., Boulègue, J., Tiercelin, J-J., Lesourd, M., 2000. Strontium isotopes and rare earth element geochemistry of hydrothermal carboante deposits from lake Tanganyika, East Africa. Geochimica et Cosmochimica Acta 64, 2, 287-298.

Berger, A., 1978. Long-term variations of caloric insolation resulting from the earth's orbital elements. Quaternary Research 9, 139-167.

Beuning, K.R.M., Talbot, M.R., Kelts, K., 1997. A revised 30,000-year paleoclimatic and paleohydrologic history of Lake Albert, East Africa. Palaeogeography, Palaeoclimatolgy, Palaeoecology 136, 259-279.

Bonnefille, R., Riollet, G., Buchet, G., 1991. Nouvelle séquence pollinique d'une tourbière de la crête Zaire-Nil (Burundi). Review of Palaeobotany and Palynology 67, 315-330.

Casanova, J., Hillaire-Marcel, C., 1992. Late Holocene hydrological history of Lake Tanganyika, east Africa, from isotopic data on fossil stromatolites. Palaeogeography, Palaeoclimatology, Palaeoecology 91, 35-48.

Cohen, 1989. Facies relationships and sedimentation in large rift lakes and implications for hydrocarbon exploration: Examples from Lakes Turkana and Tanganyika. Palaeogeography, Palaeoclimatology, Palaeoecology 70, 65-80.

Coulter, G.W., Spigel, R.H., 1991. Hydrodynamics. . In: Coulter G.W. (ed), Lake Tanganyika and its life. Oxford University Press, Oxford, pp. 49-75.

Cruse, A.M., Lyons, T., 2004. Trace metal records of regional paleoenvironmental variability in Pennsylvanian (Upper Carboniferous) black shales. Chemical Geology 206, 319-345.

Degens, E., Von Herzen, R., Wong, H.K., 1971. Lake Tanganyika: Water Chemistry, sediments, geological structure. Naturwissenschaften 58, 229-241.

deMenocal, P., Ortiz, J., Guilderson, T., Adkins, J., Sarnthein, M., Baker, L., Yarusinsky, M., 2000. Abrupt onset and termination of the African humid Period: rapid climate responses to gradual insolation forcing. Quaternary Science Reviews 19, 347-361.

Ding, Z.L., Sun, J.M., Yang, S.L., Liu, T.S., 2001. Geochemistry of the Pliocene red clay formation in the Chinese Loess Plateau and implications for its origin, source provenance and paleoclimate change. Geochimica Cosmochimica Acta 65 (6), 901-913.

Ebinger, C.J., Deino, A.L., Drake, R.E., Tesha, A.L., 1989. Chronology of volcanism and rift basin propogation: Rungwe volcanic province, East Africa. Journal of Geophysical Research 94, 15785-15803.

Garcin, Y., Vincens, A., Williamson, D., Buchet, G., Guiot, J., 2006a. Abrupt resumption of the African Monsoon at the Younger Dryas-Holocene climatic transition. Quaternary Science Reviews (submitted article).

Garcin, Y., Williamson, D., Taieb, M., Vincens, A., Mathe, P., Majule, A., 2006b. Centennial to millennial changes in lake deposition during the last 45,000 years in Tropical Southern Africa (Lake Masoko, Tanzania). Palaeogeography, Palaeoclimatology, Palaeoecology 239 (3-4), 334-354.

Gasse, F., Lédée, V., Massault, M., Fontes, J.Ch., 1989. Water-level fluctuations of Lake Tanganyika in phase with oceanic changes during the last glaciation and deglaciation. Nature 342, 57-69.

Gasse, F., Van Campo, E., 1998. A 40,000 yrs pollen and diatom record from southern tropics Lake Tritrivakely, Madagascar Plateaux). Quaternary Research 49, 299-311.

Gasse, F., 2000. Hydrological changes in the African tropics since the Last Glacial Maximum. Quaternary Science Reviews 19, 189-211.

Gasse , F., Barker, P., Johnson,T.C., 2002. A 24,000 yr diatom record from the northern basin of Lake Malawi. In: Odada E.O., and Olago, D.O. (eds), The East African Great lakes: Limnology, Palaeolimnology and Biodiversity. Dordrecht, Kluwer, pp. 393-414.

Grand atlas du continent Africain 1973. Première éditions. Editions Jeune Afrique.

Haberyan, K.A., 1987. Fossil diatoms and the history of Lake Rukwa, Tanzania. Freshwater Biology 17, 429-436.

Haberyan, K.A., Hecky, R.E., 1987. The late Pleistocene and Holocene stratigraphy and paleolimnology of lakes Kivu and Tanganyika. Palaeogeography, Palaeoclimatology, Palaeoecology 61, 169-197.

Harkin, D.A., 1960. The Rungwe volcanics at the northern end of Lake Nyasa. Mem. Geol. Surv. Tanganyika, II: 172pp.

Hecky, R.E., 1978. The Kivu-Tanganyika basin: the last 14,000 years. Pol. Arch. Hydrobiol., 25: 159-165.

Huntsman-Mapila, P., Huntsman-Mapila, P., Ringrose, S., Mackay, A.W., Downey, W.S., Modisi, M., Coetzee, S.H., Tiercelin, J-J., Kampunzu, A.B., Vanderpost C., 2006. Use of the geochemical and biological sedimentary record in establishing palaeo-environments and climate change in the Lake Ngami basin, NW Botswana. Quaternary International 148, 51-64.

Johnson, T.C., Brown, E.T., McManus, J., 2004. Diatom productivity in northern Lake Malawi during the past 25,000 years: implications for the position of the intertropical convergence zone at millennial and shorter time scales. In: R.W. Battarbee, F. Gasse and C.E. Stickley (eds). Past climate variability through Europe and Africa. Springer, Dordrecht. pp. 93-115.

Kauppila, T., and Salonen, V.-P. 1997. The effect of Holocene treeline fluctuations on the sediment chemistry of Lake Kilpisjarvi, Finland. Journal of Paleolimnology 30: 291-296.

Kutzbach, J.E., Street-Perrott, F.A., 1985. Milankovitch forcing of fluctuations in the level of tropical lakes from 18 to 0 kyr BP. Nature 317, 130-134.

Kutzbach, J.E. , Liu, Z., 1997. Response of the African monsoon to orbital forcing and ocean feedbacks in the middle Holocene. Science 278: 440-443.

Livingstone, D.A., 1975. Late Quaternary climatic change in Africa. Review of Ecology and Systematics 6, 249-280.

Lindesay, J.A., 1998. Present climates of Southern Africa. In: Hobbs, J.E., Lindesay, J.A., and Bridgeman, H.A., (eds), Climates of the Southern Continents: Present, Past and Future. John Wiley and Sons, New York, pp. 5-62.

Lyons, T.W., Werne, J.P., Hollander, D.J., Murray, R.W., 2003. Contrasting sulphur geochemistry and Fe/Al and Mo/Al ratios across the last oxic-to-anoxic transition in the Cariaco Basin, Venezuela. Chemical Geology 195, 131-157.

McLennan, S.M., Taylor, S.R., Eriksson, K.A., 1983. Geochemistry of Archean shales from the Pilbara Supergroup, Western Australia. Geochimica Cosmochimica Acta 47, 1211-1222.

Metcalfe, S.E., 1999. Diatoms from the Pretoria Salt Pan- a record of lake evolution and environmental change. In: Partridge, T.C. (ed.), Investigations into the origin, age and palaeoenvrionments of the Pretoria Saltpan. Geological Survey of South Africa. pp. 192-192.

Meyers, S., Sageman, B., Hinnov, L., 2001. Integrated quantitative stratigraphy of Cenomanian-Turonian Bridge Creek Limestone Member using evolutive harmonic analysis and stratigraphic modelling. Journal of Sedimentary Research 71, 628-644.

Mondeguer, A., Ravenne, C., Masse, P., Tiercelin, J.J., 1989. Sedimentary basin in an extension and strike-slip background : the South Tanganyika troughs complex, East African Rift. Bull. Soc. Geol. Fr., 8 (3), 501-522.

Mondeguer, A., 1991. Bassin sedimentaires en contexte extensive et decrochant: L'example du "Complexe des fosses sud-Tanganyika", Rift Est- Africain. Morphostructure et sedimentation. PhD thesis. L'Universite de Bretagne Occidentale.

Nesbitt, H.W., Young, G.M., 1982. Early Proterozoic climates and plate motions inferred from major element chemistry of lutites. Nature 299, 715-717.

Nesbitt, H.W., Young, G.M., 1984. Prediction of some weathering trends of plutonic and volcanic rocks based on thermodynamic and kinetic considerations. Geochimica Cosmochimica Acta 48, 1523-1534.

Nesbitt, H.W., Young, G.M., 1989. Formation and diagenesis of weathering profiles. Journal of Geology 97, 129-147.

Nesbitt, H.W., Young, G.M., McLennan, S.M., Keays, R.R., 1996. Effect of chemical weathering and sorting on the petrogenesis of siliciclastic sediments, with implications for provenance studies. Journal of Geology 104, 525-542.

Partridge, T.C., de Menocal, P.B., Lorentz, S.A., Paiker, M.J., and Vogel, J.C., 1997. Orbital forcing of climate over South Africa : A 200,000 year rainfall record from the Pretoria Saltpan. Quaternary Science Reviews 16, 1125-1133.

Peck, J.A., Green, R.R., Shanahan, T., King, J.W., Overpeck, J.T., Scholz, C.A., 2004. A magnetic mineral record of Late Quaternary tropical climate variability from Lake Bosumtwi, Ghana. Palaeogeography, Palaeoclimatology, Palaeoecology 215, 37-57.

Plank, T., Langmuir, C.H., 1998. The chemical composition of subducting sediment and its consequences for the crust and mantle. Chemical Geology 145, 325-394.

Roser, B.P., Korsch, R.J., 1988. Provenance signatures of sandstone-mudstone suites determined using discriminant function analysis of major-element data. Chemical Geology 67, 119-139.

Russell, J.M., Johnson, T.C., Kelts, K., Laerdal, T., Talbot, M.R., 2003. An 11000-year lithostratigraphic and paleohydrologic record from Equatorial Africa: Lake Edward, Uganda-Congo. Palaeogeography, Palaeoclimatology, Palaeoecology 193, 25-49.

Russell, J.M., Johnson, T.C., 2005. A high resolution geochemical record from Lake Edward, Uganda, Congo and the timing and causes of tropical African drought during the late Holocene. Quaternary Science Reviews 24, 1375-1389.

Russell, J.M., Johnson, T.C., 2006. The water balance and stable isotope hydrology of lake Edward, Uganda-Congo. Journal of Great Lakes Research 32 (1), 77-90.

Sageman, B.B., Murphy, A.E., Werne, J.P., Ver Straeten, C.A., Hollander, D.J., Lyons, T.W., 2003. A tale of shales: the relative role of production, decomposition, and dilution in the accumulation of organic-rich strata, Middle-Upper Devonian, Appalachian Basin. Chemical Geology 195, 229-273.

Schefuss, E., Schouten, S., Schneider, R.R., 2005. Climatic controls on central African hydrology during the past 20, 000 years. Nature 437, 1003-1006.

Schneider, R.R., Price, B., Muller, P.J., Kroon, D., Alexander, I., 1997. Monsoon related variations in Zaire (Congo) sediment load and influence of fluvial silicate supply on marine productivity in the east equatorial Atlantic during the last 200,000 years. Paleoceanography 12 (3) 463-481.

Scholz, C.A., Rosendahl, B.R., 1988. Low lake stands in lakes Malawi and Tanganyika, East Africa, delineated with multifold seismic data. Science 240, 1645-1648.

Scholz, C.A., King, J.W., Ellis, G.S., Swart, P.K., Stager, J.C., Colman, S.M., 2003. Paleolimnology of Lake Tanganyika, East Africa over the past 100 k yr. Jounral of Paleolimnology 30, 139-150.

Singh, P., Rajamani, V., 2001. REE geochemistry of recent clastic sediments from the Kaveri floodplains, southern India: Implication to source area weathering and sedimentary processes. Geochim. Cosmochim. Acta 65 (18), 3093-3108.

Street-Perrott, F.A., Perrott, R.A., 1990. Abrupt climate fluctuations in the tropics-the influence of Atlantic Ocean circulation. Nature 343, 607-612.

Talbot, M.R., Livingstone, D.A., 1989. Hydrogen index and carbon isotopes of lacustrine organic matter as lake level indicators. Palaeogeography, Palaeoclimatology, Palaeoecology 70, 121-137.

Talbot, M.R., Williams, M.A.J., Adamson, D.A., 2000. Strontium isotope evidence for late Pleistocene reestablishment of an intergrated Nile drainage network. Geology 28, 343-346.

Talbot, M.R., Laerdal, T., 2000. The Late Pleistocene-Holocene palaeolimnology of Lake Victoria, East Africa, based upon elemental and isotopic analyses of sedimentary organic matter. Journal of Paleolimnology 23, 141-164.

Talbot, M.R., Jensen, N.B., Laerdal, T., Filippi, M.L., 2006. Geochemical responses to a major transgression in giant African lakes. Journal of Paleolimnology. 35 (3), 467-489.

Taylor, S.R., McLennan, S.M., 1985. The continental crust: its composition and evolution. Oxford, Blackwell Scientific, 312 pp.
Taylor, S.R., McLennan, S.M., 1995. The geochemical evolution of the continental crust. Review of Geophysics 33, 241-265.
Tiercelin, J.-J., Thouin, C., Tshibangu, K., Mondeguer, A., 1989. Discovery of sublacustrine hydrothermal activity and associated massive sulphides and hydrocarbons in the north Tanganyika trough, East African Rift. Geology 17, 1053-1056.
Tiercelin, J-J, Mondeguer, A., 1991. The geology of the Tanganyika Trough. In: Coulter G.W. (ed), Lake Tanganyika and its life. Oxford University Press, Oxford, pp. 7-48.
Tribovillard, N., Algeo, T.J., Lyons, T., Riboulleau, A., 2006. Trace metals as paleoredox and paleoproductivity proxies: an update. Chemical Geology 232, 12-32.
Tyson, P.D., Preston-Whyte, R.A., 2000. The weather and climate of Southern Africa. Oxford University Press, Cape Town, 396pp.
Tyson, R.V., Pearson, T.H., 1991. Modern and ancient continental shelf anoxia: an overview. In: Tyson, R.V., Pearson, T.H., (Eds.), Modern and Ancient Continental Shelf Anoxia. Geological Society Special Publication 58, 1-26.
Vincens, A., 1991. Late Quaternary vegetation history of the South-Tanganyika Basin. Climatic implications in South Central Africa. Palaeogeography, Palaeoclimatology, Palaeoecology 86, 207-226.
Vincens, A., Chalié, F., Bonnefille, R., Guiot, Tiercelin, J-J., 1993. Pollen-derived rainfall and temperature estimates from lake Tanganyika and their implications for late Pleistocene water levels. Quaternary Research 40, 343-350.
Vincens, A., Buchet, G., Williamson, D., Taieb, M., 2005. A 23,000 yr pollen record from Lake Rukwa (8°S, SW Tanzania): New data on vegetation dynamics and climate in Central Eastern Africa. Review of Palaeobotany and Palynology 137, 147-162.
Werne, J.P., Sageman, B.B., Lyons, T., Hollander, D.J., 2002. An intergrated assessment of a "type euxinic" deposit: evidence for multiple controls on black shale deposition in the Middle Devonian Oatka Creek Formation. American Journal of Science 302, 110-143.
White, A.F., Blum, A.E., Bullen, T.D., Vivit, D.V., Schulz, M., and Fitzpatrick J., 1999. The effect of temperature on experimental and natural chemical weathering rates of granitoid rocks. Geochimica Cosmochimica Acta 63, 3277-3291.
Williams, M., Talbot, M., Aharon, P., Salaam, Y.A., Williams, F., Brendeland, K.I., 2006. Abrupt return of the summer monsoon 15,000 years ago: new supporting evidence from the lower White Nile valley and Lake Albert. Quaternary Science Reviews 25 (19-20) 2651-2665.
Williams, T.M., Henney, P.J., Owen, R.B., 1993. Recent eruptice episodes of the Rungwe Volcanic Field (Tanzania) recorded in the lacustrine sediments of the Northern Malawi Rift. Journal of African Earth Sciences, 17, 33-39.
Williamson, D., Thouveny, N., Hillaire-Marcel, C., Mondeguer, A., Taieb, M., Tiercelin, J.J., Vincens, A., 1991. Chronological potential of palaeomagnetic oscillations recorded in late Quaternary sediments from Lake Tanganyika. Quaternary Science Reviews 10, 351-361.
Wronkiewicz, D.J., Condie, K.C., 1987. Geochemistry of Archean shales from the Witwatersrand Supergroup, South Africa: source–area weathering and provenance. Geochimica Cosmochimica Acta 51, 2401-2416.
Zabel, M., Bickert, T., Dittert, L., Haese, R.R., 1999. Significance of the sedimentary Al:Ti ratio as an indicator for variations in the circulation patterns of the equatorial North Atlantic. Paleoceanography 14, 789-799.
Zabel, M., Schneider, R.R., Wagner, T., Adegbie, A.T., de Vries, U., Kolonic, S., 2001. Late Quaternary climate changes in central Africa as inferred from terrigenous input to the Niger Fan. Quaternary Research 56, 207-217.

IX. CONCLUSIONS

IX.1. Conclusions (Version française)

Cette thèse présente les résultats d'une étude géochimique des sédiments de deux bassins du Rift Est-africain à des stades précoces de leur développement, le Bassin de Makgadikgadi-Okavango-Zambezi (MOZ) situé au Botswana, et le Bassin de Mpulungu, qui constitue la terminaison sud du fossé du lac Tanganyika. Les bassins de rift qui se développent dans la croûte continentale vont, si le processus du rifting se poursuit, évoluer en un bassin océanique bordé par des marges passives. Le stade le plus avancé de rifting précoce concerne le développement de demi-grabens bien individualisés et subsidents, où la propagation des failles et leurs interactions vont conduire à des connections entre les bassins et un fort contrôle du drainage. Les environnements lacustres francs caractérisent ce stade qui est illustré par le Bassin de Mpulungu dans le fossé du lac Tanganyika. Le stade précédent concerne le développement d'environnements palustres et lacustres peu profonds (<50 m) qui se forment à la suite de la croissance et de la propagation des failles et de l'initialisation de la subsidence du bassin. Ce stade est représenté dans cette étude par le grand bassin de Makgadikgadi-Okavango-Zambezi. Le stade initial du développement d'un rift continental est caractérisé par la formation d'un hémi-graben peu profond, où les failles naissantes exercent un contrôle primaire sur l'évolution du drainage et sur la formation du bassin versant (Gawthorpe and Leeder, 2000). Ce stade est illustré par le cône alluvial actuel de l'Okavango qui occupe un hémi-graben subsident, fortement contrôlé par la réactivation de failles à l'intérieur du Bassin de Makgadikgadi-Okavango-Zambezi (Modisi, 2000; Ringrose et al., 2005).

Dans un premier temps, nous avons appliqué la technique des diagrammes de variations et de discrimination des environnements tectoniques aux données géochimiques obtenues acquises sur des échantillons de deux segments du rift correspondant à deux phases différentes d'évolution: le cône alluvial naissant de l'Okavango et le bassin lacustre mature de Mpulungu, Sud-Tanganyika. Nous avons utilisé le domaine tectonique défini pour les marges passives, lequel inclut une large gamme d'environnements tectoniques, pré-rift, rift, marges de rift, bassins sédimentaires d'avant-pays et marges convergentes inactives ou abandonnées (Bhatia, 1983; Bhatia and Crook, 1986). Nous avons ainsi pu définir deux nouveaux domaines d'environnement tectonique dans le champ « marges passives » du diagramme de discrimination tectonique préexistant, celui d'un bassin naissant caractérisé par le développement d'un delta continental (« alluvial fan », AF), et celui d'un bassin lacustre mature (« lacustrine basin », LB). Les nouveaux champs ainsi définis dans ce

travail pourront aider les chercheurs travaillant sur les sédiments anciens à définir les conditions tectoniques dont ces sédiments dérivent.

La provenance des sédiments de l'Okavango et de Mpulungu a également été identifiée dans cette étude. Cette notion de provenance des sédiments dans un bassin peut être un excellent indicateur des changements climatiques et /ou tectoniques dans un bassin (Leeder et al., 1998). Pour le Bassin de Mpulungu, nos résultats indiquent que la source immédiate de matériel est une roche sédimentaire quartzeuse mais que la source ultime est une roche felsique. Ces deux roches sont respectivement représentées dans la région par les grès de la Formation de Mbala et par le socle granitique que les grès de Mbala surmontent et qui constitue le craton zambien. Ces deux formations affleurent tous les deux dans le proche bassin-versant au sud du Bassin de Mpulungu. Ces résultats sont conformes au réseau hydrologique actuel de la rivière Lufubu, principal affluent du Bassin de Mpulungu, dont le bassin-versant est entièrement installé dans ces deux lithologies. Cela suggère que, pour la période de temps représentée par les sédiments du Bassin de Mpulungu concernés par cette étude (23 à 3 ka BP), le réseau hydrologique de la rivière Lufubu a été le pourvoyeur principal de sédiment dans le Bassin de Mpulungu.

Un des objectifs majeurs de cette thèse a été la compréhension des processus bio-géochimiques qui ont eu lieu dans ces bassins de rift à la suite des changements environnementaux. Ce travail contribue à une meilleure compréhension du processus de formation de calcrètes ou silcrètes en relation avec les changements climatiques dans des bassins lacustres de faible profondeur, où les épisodes d'eau douce sont suivis de phases arides dominées par la formation de calcrètes alternant avec des phases répétitives de formation de silcrètes. La précipitation de calcrètes est en partie contrôlée par le rapport Mg/Ca dans l'eau interstitielle de la zone littorale. La valeur de ce rapport peut permettre d'identifier des périodes de fermeture du bassin. Le développement des silcrètes est à relier à des épisodes de faibles précipitations ou d'écoulements ayant conduit à une remontée du niveau de la nappe d'eau souterraine, résultant en la formation de paléolacs peu profonds et localisés.

Les données géochimiques ont également été utilisées comme marqueur des changements du climat dans les bassins de Ngami et de Mpulungu. Les résultats obtenus pour le bassin du lac Ngami indiquent que les précipitations dans le bassin de l'Okavango au cours du Dernier Maximum Glaciaire étaient contrôlées par l'insolation aux basses latitudes (ie. forçage de la précession des équinoxes) par rapport au forçage glaciaire des hautes latitudes. Des résultats

similaires ont été obtenus par Garcin et al. (2006) pour le lac Masoko en Tanzanie. Les données des éléments traces des sédiments carottés dans le Bassin de Mpulungu suggèrent que le niveau du lac Tanganyika a subi une chute de l'ordre de 200–300 m durant le Dernier Maximum Glaciaire, bien plus faible que celle indiquée par des paramètres biologiques dans d'autres travaux. Ces sédiments révèlent aussi une excursion remarquable qui coïncide avec le Younger Dryas. Cet événement environnemental apparaît comme le plus important dans la région sud du lac Tanganyika pour la période 23 – 3 ka, caractérisé par un apport de matériel altéré dans le bassin suite à une modification importante du couvert végétal.

L'utilisation de la composition géochimique d'un sédiment se révèle être un outil particulièrement utile pour la reconstruction des conditions de dépôt dans un bassin sédimentaire, depuis l'identification des sources des différents éléments minéraux du sédiment, leur degré d'évolution en fonction de leur transport et également des conditions d'altération (liées à la fois au climat et au couvert végétal), et les conditions de transformation post-dépôt, en particulier au contact des eaux souterraines. Les conditions climatiques dans une région peuvent ainsi être déduites directement ou indirectement des associations d'éléments chimiques issues du bassin versant ou résultant de modifications pendant et après leur dépôt.

Certains forages réalisés dans le Delta de l'Okavango ont révélé la présence de fortes concentrations d'arsenic dans les eaux souterraines, résultat de la dissolution sous conditions réductrices des oxydes et des hydroxydes dans les sédiments avec le carbone organique. Les sédiments à forte teneur en arsenic sont des argiles riches en matière organique se présentant sous la forme de fines lentilles dans les dépôts sableux de la partie distale du Delta de l'Okavango. Ces lentilles se sont déposées dans des conditions lacustres résultant de périodes de pluviosité plus forte qu'aujourd'hui et du barrage des écoulements de la rivière Okavango par la faille de Thamalakane (Shaw, 1988). La teneur élevée en arsenic dans les eaux souterraines de l'Okavango pose désormais un problème pour la gestion de la demande en eau de bonne qualité dans cette région aride. Plus de travail est nécessaire pour une bonne compréhension de ce problème. Une étude systématique de tous les puits qui sont utilisés couramment pour l'eau potable dans la région est en cours. En raison de l'impact majeur de certains éléments chimiques sur la santé humaine, il est très pertinent que nous déterminions l'extension de la distribution en arsenic dans les eaux souterraines dans l'intégralité du Bassin de Makgadikgadi-Okavango-Zambezi, étant donné que l'ensemble de cette zone présente des dépôts d'environnements lacustres d'âges variés. Les eaux souterraines sont la source majeure de l'eau potable au Botswana.

En ce qui concerne les études paléoclimatiques, il serait extrêmement instructif de réaliser un sondage carotté dans une cuvette alimentée par l'eau de pluie au voisinage du bassin de MOZ, afin de pouvoir distinguer les apports des précipitations locales et les apports provenant du bassin angolais dans ce bassin. En plus, il serait extrêmement instructif de repeter le travail fait dans le bassin Lac Ngami mais en plus de detaile pour voir si les conditions climatiques peuvent etre deduites pendant le Younger Dryas et aussi pendant le Holocene.

IX.2 Conclusions (English version)

This thesis presents the results of a geochemical study of sediments from two rift basins in the East African Rift, the Makgadikgadi-Okavango-Zambezi (MOZ) basin and the Mpulungu sub-basin of Lake Tanganyika. Rift basins, which develop in continental crust, will, if the rifting process continues, lead to the development of an ocean basin flanked by passive margins. Rift basins consist of a suite of individual half-grabens bounded by major normal faults. The more mature stage of early rifting concerns the development of well-defined, actively subsiding half-graben basins, where propagation and interaction between fault segments lead to basin linkage and strong control of drainage. Wider and deeper lacustrine environments characterize this stage, which is illustrated by the southern Mpulungu subbasin of Lake Tanganyika. The immediate earlier stage concerns the development of basins where swamps and shallow lacustrine environments (<50 m water depth) occur, as the result of fault growth and propagation, and initiation of basin subsidence which is represented by the larger Makgadikgadi-Okavango-Zambezi basin. The early initiation stage in the development of a continental rift is characterized by the development of shallow half-graben basins where nascent faults exert a primary control in drainage evolution and the formation of catchments (Gawthorpe and Leeder, 2000). This stage is illustrated by the present Okavango alluvial fan which is a broad subsiding half-graben occupied by an alluvial fan, strongly controlled by the reactivation of faults within the larger Makgadikgadi-Okavango-Zambezi basin (Modisi, 2000; Ringrose et al., 2005).

The use of geochemical compositions of sediments in diagnostic diagrams has been shown to be useful in determining tectonic settings (Bhatia, 1983; Roser and Korsch, 1986; 1988). The field defined for passive margins include a wide range of tectonic environments, from rifted continental margins of the Atlantic-ocean type, sedimentary basins near to collision orogens and inactive or extinct convergent margins (Bhatia, 1983; Bhatia and Crook, 1986). Passive margin

settings have also been grouped into pre-rift, rift-valley or graben and Atlantic-type trailing edges. In this work we define two new fields for an alluvial fan (AF) and lacustrine basin (LB) tectonic environment within the passive margin field. We believe that these results will assist researchers working on ancient sedimentary rocks in classifying the tectonic environment of their samples.

The provenance of the sediments of both the Okavango Delta and Mpulungu sub-basin sediments was determined in this study. The provenance of sediments in a depositional basin can be a useful indicator of the past climatic and tectonic record (Leeder et al., 1998) in the catchment area. For the Mpulungu sub-basin, our results indicate that the immediate source material is a quartoze sedimentary rock represented by the sandstones of the Mbala formation. The ultimate source material was a felsic source represented by the basement granites. These results agree very well with the current hydrological conditions in the basin, where the Lufubu River traverses these two source rocks. This suggests that at least for the time period for the age of the Mpulungu sediments from this study (23 ka to 3 ka BP) that this has been the predominant hydrological link to the Mpulungu sub-basin. For the Okavango Delta sediments, the interpretation is more complex as the sediments the source of the sediments include a felsic rock source and a pyroxene and olivine rich mafic-ultramafic rock complexes which are mixed with sand and diagenetic carbonates to produce the Okavango sediments.

A major aim of this thesis was to improve our understanding of the biogeochemical processes occurring within these rift basins as a result of environmental changes. As a result of this work, we have improved our understanding of calcrete-silcrete formation in relation to climate change events in shallow lacustrine basins/ pans where freshwater episodes are followed by calcrete dominated drying phases interspersed with repeated silcretisation. Calcrete precipitation is in part controlled by the Mg/Ca ratio of pore water in the pan littoral zone and thus can be used to identify closed basin type conditions in the pan. Silicified duricrust units appear to be related to relatively minor rainfall or inflow events which increased the level of the groundwater table, maybe forming localised shallow palaeo-lakes.

Geochemical data was used as proxies for climate change in both the Lake Ngami (SW Okavango) and Mpulungu sub-basin of Lake Tanganyika. Results for Lake Ngami indicate that rainfall in the Okavango catchment area during the Last Glacial Maximum was controlled by low-latitude insolation (ie. precessional forcing) over high latitude glacial forcing. Garcin et al.,

(2006) report similar results for Lake Masoko, Tanzania. Trace element data of redox-sensitve metals from Mpulungu sediments suggests that the drop in lake level for Lake Tanganyika was closer to 200 – 300 m than the 350 – 400 m suggested from earlier work based on biological indicators. The Lake Tanganyika data shows a remarkable excursion coinciding with the Younger Dryas (YD) event, reflecting the input of previously chemically weathered material into the basin due to a change of vegetation cover. This illustrates that YD event brought about significant environmental in southern Lake Tanganyika.

The occurrence of elevated arsenic in groundwater of the Okavango Delta system is the result of a biogeochemical process whereby under reducing conditions, oxides and hydroxides from the sediments are dissolved thereby releasing arsenic into the system. The sediments with elevated arsenic are organic rich clays which occur as thin lenses in the sandy sediments of the lower Okavango Delta. These lenses were thought to have been deposited under lacustrine conditions, when water ponded up against the Thamalakane Fault during periods of higher rainfall than today (Shaw, 1988). The occurrence of arsenic in the groundwater will put a further strain on water demand managers who struggle to provide sufficient good quality groundwater in this arid country. Further work is needed in this area and we are currently undertaking a survey of existing wells in use for water supply in the region.

The use of the geochemical composition of sediments has been shown in this work to be a very useful tool for the reconstruction of the depositional conditions in a sedimentary basin, from the identification of source rocks, their degree of weathering (linked to climate and vegetation cover) and alteration due to transport and the post-depositional transformations, in particular those due to contact with groundwater. The climatic conditions of a region can be directly or indirectly deduced from the elemental composition of the sediments issued from the catchemnt or as a result of modifications both during and after deposition. A geochemical analysis of sediments for past climate reconstruction should be considered by researchers, in particular in situations where the pollen and diatom record are not well preserved.

Further work is needed in the use of geochemical tracers in climate change and tectonic evolution. With rest to past climates, it would be very informative to conduct a study in the MOZ basin where one collects a core from a rain-fed pan and another core from a basin which is fed by rivers originating in Angola. In this way it may be possible to distinguish between higher lake levels due to local rainfall as opposed to higher lake levels due to increased precipitation in the

Angolan highlands. In addition, it would be very informative to be able to repeat work carried out in the Lake Ngami Basin but on a much finer scale. In the work reported in this thesis, samples were collected over every 10 cm in the 4.6 m pit. Each 10 cm represents approximately 1000 yrs. Because of this we were not able to capture some of the interesting climate events such as how the lake basin responded during the Younger Dryas event or during climate events during the Early and Late Holocene. With respect to arsenic and human health, it is crucial that we determine the extent of arsenic distribution in groundwater in the entire Makgadikgadi-Okavango-Zambezi basin, as the whole area has, at different stages, had a lacustrine depositional environment. Groundwater is the major source of potable water in this region.

References

Bhatia, M.R., 1983. Plate tectonics and geochemical composition of sandstones. J. Geol. 91, 611-627.

Bhatia, M.R., Crook, K.A.W., 1986. Trace element characteristics of graywackes and tectonic setting discrimination of sedimentary basins. Contr. Mineral. Petrol. 92, 181-193.

Garcin, Y., Williamson, D., Taieb, M., Vincens, A., Mathe, P., Majule, A., 2006b. Centennial to millennial changes in lake deposition during the last 45,000 years in Tropical Southern Africa (Lake Masoko, Tanzania). Palaeogeography, Palaeoclimatology, Palaeoecology 239 (3-4), 334-354.

Gawthorpe, R.L., Leeder, R., 2000. Tectono-sedimentary evolution of active extensional basins. Basin Research 12, 195-218.

Leeder, M.R., Harris, T., Kirkby, M.J., 1998. Sediment supply and climate change: implications for basin stratigraphy. Basin Research 10, 7-18.

Modisi, M.P., 2000. Fault system of the southeastern boundary of the Okavango Rift, Botswana. J. Afr. Earth Sci. 30, 569-578.

Ringrose, S., Huntsman-Mapila, P., Kampunzu, A. B., Matheson, W., Downey, W., Vink, B., Coetzee, C., and Vanderpost, C., 2005. Sedimentological and geochemical evidence for palaeo-environmental change in the Makgadikgadi subbasin, in relation to the MOZ rift depression, Botswana. Palaeogeography, Palaeloclimatology, Palaeoecology 217 (3-4), 265-287.

Roser, B.P., Korsch, R.J., 1986. Determination of tectonic setting of sandstone-mudstone suites using SiO2 content and K2O/Na2O ratio. J. of Geol. 94, 75-83.

Roser, B.P., Korsch, R.J., 1988. Provenance signatures of sandstone-mudstone suites determined using discriminant function analysis of major-element data. Chem. Geol. 67, 119-139.

Shaw, P., 1988. After the floods: The fluvio-lacustrine landforms of northern Botswana. Earth Sci. Rev. 25, 449-456.

APPENDIX 1. CHARACTERIZATION OF ARSENIC OCCURRENCE IN THE WATER AND SEDIMENTS OF THE OKAVANGO DELTA, BOTSWANA

A1.1 Caractérisation de la distribution de l'Arsenic dans l'eau et les sédiments du Delta de l'Okavango, Botswana.

Résumé de l'article

Les analyses géochimiques ont été faites sur les eaux de surface, les eaux souterraines et les sédiments de l'Okavango en 2003 afin d'examiner la distribution et la géochimie de l'arsenic dans la région. L'eau de surface de l'Okavango, qui a un pH neutre - acide et un niveau de carbone organique dissout (COD) élevé présente des teneurs en arsenic un peu élevées par rapport à une valeur moyenne mondiale pour les fleuves. Dans vingt puits mesurés dans le cadre de ce projet, nous avons trouvé six niveaux d'arsenic dont la valeur dépasse 10 μg/l. Cette valeur est celle admise provisoirement par l'Organisation Mondiale de la Santé pour l'arsenic dans l'eau potable. Les résultats de spéciation suggèrent que As (III) est plus prédominant que As (V). Il existe une corrélation positive entre l'As et le pH et entre l'As et le COD dans l'eau souterraine. Pour les sédiments, il existe un corrélation positive entre l'As et le Co, l'As et le Fe, l'As et la perte au feu (LOI) et l'As et le pourcentage de la fraction fine. La dissolution sous condition réductrice des oxydes et des hydroxydes dans les sédiments avec le carbone organique comme accepteur d'électron est le mécanisme probable pour le dégagement de l'As des sédiments dans les eaux souterraines.

A1.2. Characterization of Arsenic occurrence in the water and sediments of the Okavango Delta, NW Botswana

P. Huntsman-Mapila*[a,b], T. Mapila[c], M. Letshwenyo[a] , P. Wolski[a] , C. Hemond[b]

a Harry Oppenheimer Okavango Research Centre, University of Botswana, P/Bag 285, Maun, Botswana
b UMR-CNRS 6538, Institut Universitaire Européen de la Mer, 29280 Plouzané, France
c Pangolin Enterprises, P/Bag BR 159, Gaborone, Botswana

Article published in Applied Geochemistry 21 (2006) 1376-1391

* Corresponding author: E-mail: pmapila@orc.ub.bw

Abstract

Detailed chemical analyses were performed on surface water, groundwater and sediment samples collected from the Okavango Delta between February and November, 2003 in order to examine the distribution and geochemistry of naturally occurring arsenic in the area. Surface water in the Okavango Delta, which is neutral to slightly acidic and has a high dissolved organic carbon (DOC), was found to be slightly enriched in As when compared to a global value for stream water. Of the 20 new borehole analyses from this project, six were found to have values exceeding 10 μg/l, the current World Health organization provisional guideline value for arsenic. The results from field speciation indicate that As (III) is slightly more predominant than As (V). There exists a positive correlation between As and pH and between As and DOC in the groundwater samples. For the sediment samples, there exists a positive correlation between As and Co, As and Fe, As and loss on ignition (LOI) and between As and the percent fines in the sample. Reductive dissolution of oxides and hydroxides in the sediments with organic carbon as an electron acceptor is the likely mechanism for the release of As from the sediments into the groundwater.

A1.2.1. Introduction

Botswana is a relatively large (582,000 sq. km) flat country with mean annual rainfall varying from 650 mm/a in the north to 250 mm/a in the south. Mean annual potential evapo-transpiration is estimated to be 4 to 5 times higher than the average mean annual rainfall (450 mm/a). Although groundwater recharge rates are generally low in Botswana, averaging 2.7 mm/a (Snowy Mountains Engineering Corporation (SMEC) et al., 1991), groundwater has been the main source

of potable water supply. Figures released in the National Water Master Plan (SMEC et al., 1991), indicate that groundwater accounted for 67% of the 1990 total water consumption in Botswana. The Okavango Delta (Figure A1-1) is part of a large alluvial fan complex in north-western Botswana. Flow into the Delta system through the Okavango River, which originates in Angola, peaks after the rainy season in Angola. Only 2% of the mean annual inflow leaves the system as surface water outflow through the Thamalakane and Boteti Rivers.

Arsenic in the environment has received renewed attention due to the recent studies of elevated arsenic in Bangladesh and neighbouring West Bengal, India (Chatterjee et al, 1995; Das et al., 1995; Nickson et al., 1998; BGS and DPHE, 2001; Welch and Stollenwerk, 2003), and the debates in the United States over the maximum contaminant level (MCL) for drinking water (US Environmental Protection Agency (US EPA), 2001a; SenGupta and Greenleaf, 2002).

Evidence shows that high-As groundwater can be associated with reducing conditions prevalent in alluvial and deltaic environments (Sengupta et al., 2004). Occurrence of As-enrichment in Bangladesh groundwater shows a close relationship with the geomorphological units. Quaternary sediments provide good aquifers in Bangladesh and As-enrichment is mainly resticted to the Holocene alluvial aquifers at shallow and intermediate depths (BGS and DPHE, 2001). The sediments are dominantly composed of sands, silts and clays (Ahmed, 2004).

The issue of potentially elevated arsenic in groundwater of the Okavango Delta was first raised during the second phase of the Maun Groundwater Development Project (MGDP) (Department of Water Affairs (DWA), 2003). Based on those preliminary results, it was decided to conduct a more comprehensive study. The objectives of this paper are therefore: (1) to present new chemical analyses of groundwater and surface water samples and Quaternary sediments from the Okavango Delta; (2) to relate the presence of arsenic in the Okavango Delta environment to the hydrogeological setting and geochemical processes; and (3) to determine the speciation of arsenic in the groundwater of the Okavango Delta.

A1.2.2. Hydrological setting

In semi-arid NW Botswana, the development potential of the Okavango Delta has included plans for agriculture and water for mining, whilst more recent interest in development has focused on water supply for human consumption (UNDP, 1977; DWA, 2003). Maun, with a population of

49,822 in 2001 (Central Statistics Office, 2001), is the main source of demand for potable water in the region. The rapid growth of Maun, estimated at 3.5% per annum, has necessitated exploration of groundwater resources.

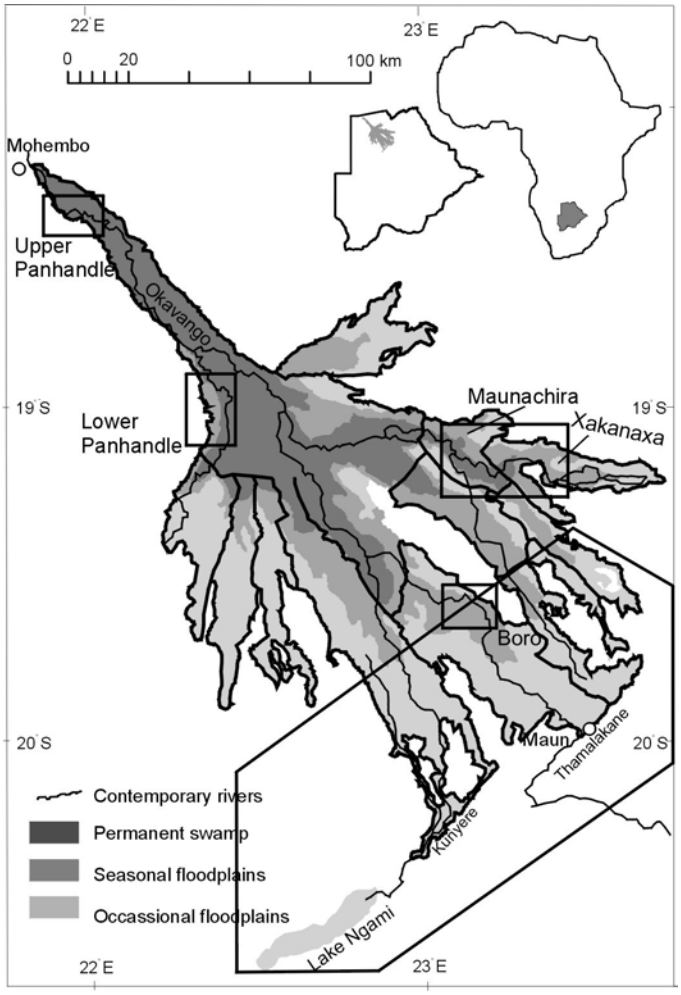

Figure A1 1. Location map of the Okavango Delta in NW Botswana with rectangles showing the location of the surface water sampling.

The construction of the Shashe wellfield (Figure A1-2) began in 1986 and has subsequently been expanded by three groups of boreholes between the 1980's and 1990's. The main source of recharge to the lower Okavango Delta is river recharge with localised rainfall providing minimal groundwater recharge (DWA, 2003) With no river flow in the Shashe river since 1989 and increasing extraction, the Shashe wellfield was becoming stressed and the shallow unconfined aquifer dewatered. Recent groundwater development strategies (MGDP) have focussed on assessing the Matsibe, Xudum, Kunyere and Gomoti areas (Figure A1-2) (DWA, 2003).

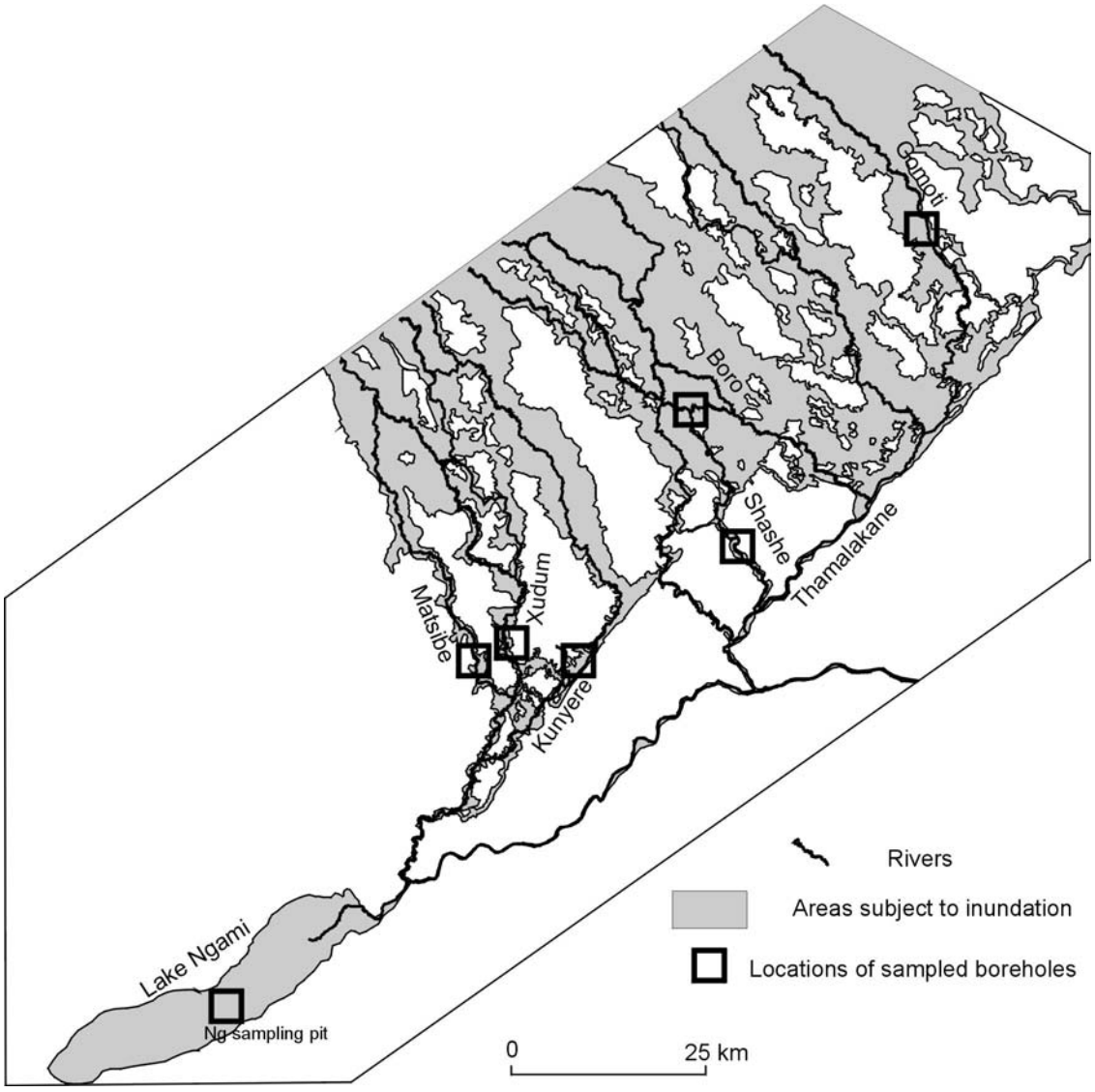

Figure A1 2. Detailed map of the southern Okavango region showing the location of borehole sampling points.

The Okavango Basin is a Quaternary half-graben (McCarthy et al., 1993a; Modisi, 2000; Modisi et al., 2000) inferred to represent the south-western tip of the East African rift system (Kampunzu et al., 1998). It is located within the Kalahari Basin which is a shallow intracontinental basin covered by sand dunes, minor lacustrine deposits and precipitates (e.g. Thomas and Shaw, 2002). The Okavango River enters the Middle Kalahari, through the Panhandle (Figure A1-1 and 2) before extending into an inland alluvial fan. The Okavango River drains from the central highlands of Angola where annual inflow is estimated at 1.01 x $10^{10}m^3$ measured at the apex of the Panhandle (McCarthy et al., 2000). The Okavango Delta shows progressive degrees of inundation throughout its length and is subdivided into distinct geomorphic regions: (1) the Panhandle where the Okavango River is constrained; (2) the permanent swamps (3) the seasonal floodplains and (4) occasional (or intermittent) floodplains (Gumbricht and McCarthy, 2003).

In the Upper Panhandle zone at Mohembo, the bulk of the water is confined to the main channel but immediately downstream, the Panhandle zone broadens and the main channel is flanked by areas of permanent swamp fringed by seasonal swamp. Guma Lagoon, located in the Lower Panhandle, is in the form of an old ox-bow. Narrow channels still link the lagoon to the main channel, however it now receives water primarily from the fringing swamp. In the Maunachira channel portion of the Okavango Delta, the water spreads out into numerous smaller channels with flow-through lagoons, such as Gadikwe and Xakanaxa. The Boro River on the south-western tip of Chief's Island is a major tributary of the Okavango Delta and has active flow throughout most of the year.

The sediments building up the Okavango Delta show a stratified profile and are predominantly sands with minor silts and clays that support both shallow unconfined and deeper semi-confined aquifers (DWA, 2003) which are hydraulically interconnected at a sub-regional scale. Groundwater recharge in the Okavango Delta is dominated by flood water infiltration whilst the role of rainfall recharge is rather limited. Wolski and Savenije (2006), during 7 years of observation of floodplain and island groundwater, recognized only 2 diffuse recharge events. In contrast, the arrival of the annual flood to the distal parts of the Delta caused recharge of the shallow phreatic aquifer raising the groundwater table by 1-3 m within one month. The shallow groundwater was, however, subject to evaporation and transpiration after flood recession, and thus only some part of the infiltration flux contributed to the net annual groundwater recharge. Groundwater flows in the Okavango Delta are dominated by local flow systems developed

between the floodplains where recharge occurs and islands, which are the discharge zones due to evapo-transpiration. The typical groundwater table gradients observed in these flow systems suggest that 95% of groundwater flow takes place in the top 60 m of the aquifer. The effect of groundwater discharge taking place through evapo-transpiration in islands, is that the island groundwater is enriched in dissolved salts (McCarthy and Ellery, 1994). That enrichment can reach the level where the shallow island groundwater is of much higher density than the underlying fresh groundwater, and can be subject to density-driven fingering and sinking to the bottom of the aquifer (Bauer et al., 2005).

A1.2.3. Sampling and analytical procedures

A1.2.3.1 Water sampling

Nine surface water samples were collected in February 2003 as part of the Conservation International AquaRAP project (Huntsman-Mapila et al., 2005a). Surface water samples were collected from 4 different areas of the Okavango Delta: (1) the Upper Panhandle; (2) Guma Lagoon in the Lower Panhandle; (3) Maunachira Channel and eastern portion of the Okavango Delta and (4) the Boro River on the south-western tip of Chief's Island (Figure V-2). Readings of pH, temperature, dissolved oxygen (DO) and electrical conductivity (EC) were taken in situ using a Hanna 991001 pH and temperature meter, a YSI 85 DO meter and a Hanna HI 9033 conductivity meter. Samples for metal analysis were filtered on site through a 0.45µm cellulose nitrate filter and acidified to pH < 2 with HNO_3. Samples for dissolved organic carbon were filtered through a Whatman glass fibre filter (GFF) and acidified with HNO_3. Anion samples were not filtered. Alkalinity titrations were conducted on site. Field blanks were filtered and acidified as the samples to ensure no contamination from this process each time the acid was renewed. All samples were stored in acid precleaned bottles (rinsed with 1% HNO3 followed by thorough rinsing with water). Samples were stored in a cooler box until transport to the laboratory where they were stored in a refrigerator until analysis.

Twenty groundwater samples were collected between June and November 2003 from boreholes in the occasional floodplain region of the Okavango Delta (Figure A1-2). pH , temperature, DO, EC and alkalinity measurements were taken immediately. In the field, a 250 ml sample was filtered through a 0.45 µm filter and acidified with H_2SO4 to pH < 2. Field blanks were filtered and acidified as the samples to ensure no contamination from this process each time the acid was

renewed. Anion samples were filtered but not acidified. All water samples were collected in HDPE bottles and refrigerated until analysis. Anion exchange columns for the speciation work were prepared in the laboratory using Bio-Rad econo-pac disposable 20 ml columns and the acetate form of Bio-Rad AG 1-X8 resin (100 – 200 mesh). Calibration of the packed columns using a spiked groundwater was conducted to ensure that the correct fractions were collected. 25 ml of the acidified filtered sample was passed through the column followed by 5 ml of 0.12N HCl. This fraction was labelled as As (III). The column was then eluted with 20 ml of the same acid to collect the As (V) fraction. According to Ficklin (1990), the volume of eluent required for the removal of As(V) can be variable but has occurred when the dark yellow colour of the acetate form of the resin has been entirely converted to the light yellow chloride form.

A1.2.3.2 Sediment sampling and pre-treatment

Sediments were collected at 1m intervals as boreholes were being drilled in the occasional floodplains of the distal reaches of the Okavango Delta. A shallow core (1 m) was also collected using an Eijkelkamp Beeker sampler for undisturbed sediments from a shallow backwater lagoon near Xakanaxa Lagoon (FigureA1-1). Samples from the core were collected from every cm and pore water was extracted, using a Buchner funnel, before storing the samples in plastic containers. An additional set of sediment samples was obtained from Lake Ngami, a drainage basin in the western portion of the Okavango Delta, where shallow (4 m) holes have been dug into the dry lake bed. All these sites are part of the Okavango Delta basin and receive water from the same source, the Okavango River.

Sediment samples were digested at 95 ^{o}C in 1:1 HNO_3 and 1:4 HCl according to the US EPA method 200.9 (US EPA, 2001b). A total of 29 sediment samples were digested at the Harry Oppenheimer Okavango Research Centre (HOORC) Environmental Laboratory. In addition a sample of STSD-4, a stream sediment composite sample from the Geological Survey of Canada was digested in triplicate to determine recovery as well as three blanks to ensure that contamination did not occur. A sample of the lubricant used during drilling was also digested to ensure no contamination of the sediments from the drilling process had occurred. The samples from Lake Ngami (NG) for As analysis were digested in aqua regia at Chemex Laboratories in Canada.

A1.2.3.3 Sample analysis

For the water samples, Ca, Mg, Fe and Mn were analysed on the flame atomic absorption spectrophotometer (Varian Spectra 220). Na and K were analysed on a Sherwood 410 flame photometer. Anion samples were analysed on a Dionex DX-120 ion chromatograph. All analyses were conducted at the HOORC Environmental Laboratory. Water samples for As analysis were analysed on a Varian SpectrAA 220 atomic absorption spectrophotometer equipped with a Varian GTA 110 graphite furnace (GFA), a deuterium arc background correction system, and pyrolytically coated graphite tubes. A nickel nitrate solution in nitric acid was used to stabilize the solution. The detection limit was 0.5 µg/l. An external reference was run every tenth sample. For surface water analyses, SLRS-4, a river water sample from the National Research Council of Canada was used (As concentration of 0.68 µg/l). Multiple injections were required for the surface water samples. For groundwater, two samples from the South African Bureau of Standards were used (As concentration of 15 and 33 µg/l) as external references. A blank and standard were run for resloping every twenty samples. An approximation of DOC was obtained by measuring the absorbance of the water samples at 280 nm using a Perkin Elmer Lamda 20 UV/Vis spectrophotometer (American Public Health Association (APHA) et al., 1995). Some organic compounds found in water such as lignin, tannin, humic substances and some aromatic compounds absorb ultraviolet radiation. The UV absorption is a useful approximate measure of DOC in the water of the Okavango Delta and absorbance at 280 nm in surface water has been found to give the best correlation (r=0.97) (Mladenov et al., 2005) for water samples from the Okavango Delta.

For the analysis of As, Ni, Co and Fe in the sediments, samples were run using the GFA and STSD-4 was used as an external reference. For the samples from Lake Ngami (NG) analysed at Chemex, Co and Ni were analysed on ICP-MS, As on GFA and Fe on ICP-AES. Loss on ignition (LOI) was determined on the sediments by combustion of the sample at 500^{o}C for 2 hours. Particle size analysis of the sediments was conducted using sieving techniques (Smith and Atkinson, 1975).

A1.2.4. Results

A1.2.4.1 Water samples

For all geochemical data, the significance of correlation was tested at 95% confidence limit (Rollinson, 1993).

Results of the nine surface water analyses are presented in Table V-1. Surface water samples presented in this paper have a low conductivity (35.9 – 75.2 µS/cm) and a near neutral to slightly acidic pH (5.53 – 7.24) typical of surface water from the Okavango Delta. DO values are variable (0.70 – 5.70 mg/l) as can be expected given the different habitats sampled (lagoons and channels). DOC in the surface water samples range between 5.5 – 16.6 mg/l. The predominant ions in the Okavango Delta water are Ca-HCO_3 and Ca-Na-HCO_3 as can be seen from the Piper Diagram (FigureV-3). As concentrations and precisions (% RSD) in these samples range from 1.1 – 3.1 ug/l and 4.0 – 11.7 % with an average concentration and precision of 2.3 µg/l and 6.2 % respectively. Recovery of As in the SLRS-4 reference material averaged at 107 %.

Table A1 1. Results from water quality analyses of the Okavango Delta samples

Sample	UPO1*	UP02*	LP03*	LP04*	LP05*	MC06*	MC07*	MC08*	B09*
type***	sw	sw	sw	sw	sw	sw	sw	sw	sw
date sampled	2-Feb-03	3-Feb-03	7-Feb-03	6-Feb-03	7-Feb-03	11-Feb-03	12-Feb-03	11-Feb-03	14-Feb-03
PH	6.55	6.45	6.5	6.62	5.53	7.09	7.2	7.24	6.67
temperature C	28.5	29.1	27.3	28.7	27.2	29	28.8	28.9	27.9
conductivity (uS/cm)	35.9	39	63	49.2	51.2	51.5	51.7	49.7	75.2
DO (mg/L)	5.7	0.79	2.3	2.58	0.70	5.16	5.28	5.52	1.13
Location	U. Panhandle	U. Panhandle	L. Panhandle	L. Panhandle	L. Panhandle	Maunachira	Maunachira	Maunachira	Boro
Habitat	lagoon	channel	channel	lagoon	channel	channel	lagoon	lagoon	channel
Ca mg/l	4.1	4.3	5.9	6.5	5.9	5.8	5.9	5.7	8.4
Mg	0.9	0.9	1.5	1.5	1.4	1.2	1.2	1.1	1.7
Na	2	2	3	2	3	3	3	3	5
K	2	2	3	1	3	2	2	2	3
Mn	<0.03	<0.03	<0.03	<0.03	0.03	<0.03	<0.03	<0.03	0.14
Fe	0.48	0.29	1.89	0.11	0.84	0.24	0.25	0.46	0.1
Alkalinity as CaCO3	25.6	26.8	27.7	35.4	31.7	34.2	34.2	31.7	50
Cl	0.28	0.48	0.88	0.24	0.24	0.61	0.29	0.35	0.31
SO4	0.23	0.20	0.26	0.07	0.25	0.30			0.09
NO3		0.45	0.20		0.03	0.60	0.04	0.01	0.84
DOC	5.6	5.5	14.1	6.5	7.7	8.4	11.1	16.6	13.3
As (ug/l)	2.1	2.1	2.5	1.1	2.1	2.6	2.7	2.6	3.1
% As (III)									
% As (V)									
% recovery									
As(III) / As (v)									

* field data from Huntsman-Mapila et al., 2005a

** borehole data from MGDP (DWA, 2003)

*** sw = surface water, gw = groundwater

**** result from unfiltered sample

Table A1-1. Results from water quality analyses of Okavango Delta samples continued

Sample	SHM01	SHM02	SHM03	SHM04	MAM05	MAM06	MAM07	KUM08	KUM09	KUM10	KUM11	KUM12	KUM13
type***	gw	gw	gw	gw	gw	gw	gw	gw	gw	gw	gw	gw	gw
date sampled	3-Oct-03	17-Oct-03	30-Nov-03	30-Nov-03	12-Aug-03	1-Jun-03	16-Jun-03	19-Aug-03	23-Jun-03	19-Jun-03	3-Jul-03	27-Jun-03	29-Aug-03
PH	7.94	8.45	7.18	7.22	7.5	8.19	8.46	8.06	8.07	8.53	8.21	7.64	7.04
temperature C	29.8	27.6	26.6	27	27.3	26.9	27.2	26.1	25.7	25.1	24.8	23.9	24.7
cond. (uS/cm)	2230	1747	1740	3770	686	1046	948	810	13830	728	1296	471	1420
DO (mg/L)	4.91	2.38	2.45	2.95	1.85	1.96	2.01	2.85	2.14	1.95	1.54	1.88	1.84
Location	Shashe	Shashe	Shashe	Shashe	Xudum	Xudum	Xudum	Matsibe	Matsibe	Matsibe	Matsibe	Kunyere	Kunyere
Habitat													
Ca mg/l	36.6	5.0	22.0	84.5	0.6		3	1.4	83.6	2.3	1.6	16.3	56.6
Mg	12.1	0.8	8.0	63.3	0.1		0.3	0.3	75.8	0.2	0.2	5.7	19.1
Na	440	390	350	720	190		270	230	1680	220	310	100	230
K	14	15	14	20	4		9	9	48	5	6	10	30
Mn	<0.03	<0.03	<0.03	<0.03	<0.03		<0.03	<0.03	0.17	<0.03	<0.03	<0.03	0.27
Fe	0.14				0.94		1.16	1.1		1.49	0.38	0.7	
Alk	503	516	488	486	417		425	430	1026	437	543	264	632
Cl	380.1	158.4	224.5	419.0	1.2		11.0	4.5	1596.7	9.9	56.9	165.3	85.9
SO4	411.5	345.7	203.9	1162.0	4.6		38.0	24.2	666.4	31.3	138.8	318.8	59.4
NO3			0.4		0.5			0.2	4.7	0.3	0.1		
DOC	3.2	2.8	3.6	2.6	5.5		19.1	4.3	8.6	13.8	5.6	5.3	5.7
As (ug/l)	4.2	4.0	5.2	14.6	8.3	97.5****	116.6	2.7	58.3	112.0	9.1	6.6	3.9
% As (III)			50.8	57.3									
% As (V)			44.1	29.3									
% recovery			94.8	86.7									
As(III) / As (v)			1.2	1.95									

Table A1-1. Results from water quality analyses of Okavango Delta samples continued

Sample	KUM14	KUM15	GOM16	GOM17	GOM18	GOM19	GOM20	9830**	9834**	9837**	9904**	9906**
type***	gw	gw	gw	gw	gw	gw	gw	gw	gw	gw	gw	gw
date sampled	3-Jul-03	3-Sep-03	4-Nov-03	20-Nov-03	12-Nov-03	12-Nov-03	30-Nov-03	15-Feb-03	8/27/2002	9/2/2002	12/18/2002	1/26/2003
PH	7.44	6.78	6.29	7.49	7.39	7.51	6.81	8.1	8.5	8.6	7.5	8.1
temperature C	24.4	26.5	33.8	28.3	29.5	27.9	26.7	25.3	24.3	25.4	26.5	28
conductivity (uS/cm)	725	809	398	1394	483	1025	542	1560	1457	1668	1340	1930
DO (mg/L)	2.43	1.67	0.81	1.22	1.02	1.59	1.57	1.7			1.25	3.5
Location	Kunyere	Kunyere	Gomoti	Gomoti	Gomoti	Gomoti	Gomoti	Boro	Boro	Boro	Gomoti	Gomoti
Habitat												
Ca mg/l	17.7	7.5	33.9	2.7	1.1	3.4	9.5	2.8	2.9	7.6	1.9	3.3
Mg	4.4	1.0	9.0	0.3	0.2	0.3	1.0	0.72	0.75	1.7	0.37	0.71
Na	150	170	28	300	170	260	130	454	392	390	370	404
K	10	10	8	3	2	10	12	6.6	14	9.3	5.2	4.2
Mn	<0.03	<0.03	0.19	<0.03	<0.03	<0.03	<0.03	<0.05	<0.05	<0.05	<0.05	<0.05
Fe	0.32	0.39	13.22		1.32	1.83		0.07	0.22	0.19	0.08	0.75
Alk	212	210	217	353	219	518	297	693	711	607	624	375
Cl	19.4	98.6	2.4	175.7	19.8	7.9	2.5	137.0	80.0	139.0	64.0	238.0
SO4	11.0	67.7	19.1	191.6	24.2	50.1	10.5	94.0	50.0	73.0	85.0	196.0
NO3	0.1	0.2	0.3	0.2	0.1	0.1	0.1	<0.1	<0.1	<0.1	<0.1	<0.1
DOC	3.5	3.6	10.4	3.1	4.4	4.6	2.2					
As (ug/l)	1.8	2.4	7.0	10.1	8.0	6.1	4.7	30	35.0	29.0	90	60
% As (III)			53.5	74.0	57.3	50.0						
% As (V)			56.7	48.3	79.0	58.6						
% recovery			110.3	122.4	136.3	108.6						
As(III) / As (v)			0.94	1.53	0.73	0.85						

The results of the twenty boreholes sampled during this study are presented in Table V-1. In addition, results of five boreholes sampled during MGDP have been included. Analysis of the MDGP samples were conducted at CSIR in South Africa. Conductivity values of all samples range between 398 – 13 830 μS/cm with an average of 1762 μS/cm. pH values range between 6.29 – 8.60 with an average value of 7.72. DO values range between 0.81 – 4.91 with an average value of 2.06 mg/l. Na is the predominant cation in all groundwater samples with the exception of sample GOM16 where Ca is the predominant ion (Figure A1-3). Thirteen of the boreholes have HCO_3 as the predominant anion (> 50 % meq) The remainder of the samples have variable proportions of HCO_3, SO_4 and Cl. Samples SHM04 is Na-SO_4-Cl type waters.

As values for all field blanks were less than the detection limit of 0.5 μg/l. All As values for the groundwater samples have precisions (% RSD) of less than 10 % with the exception of one sample (SHM04) with a RSD of 15 % which had a high background reading.

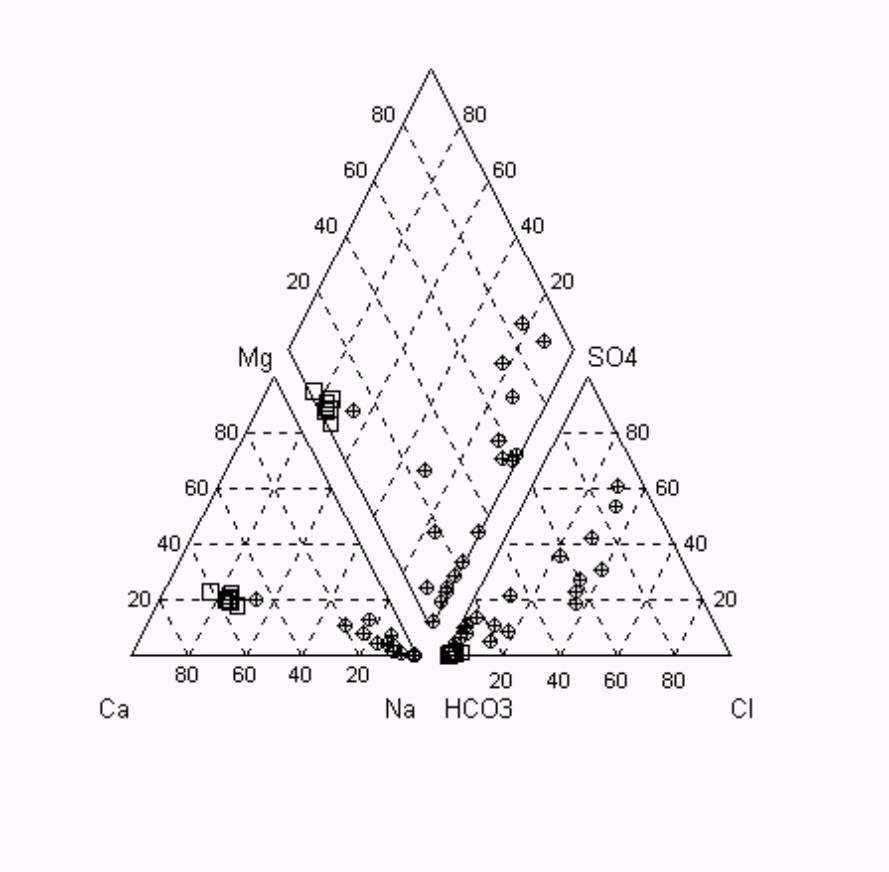

Figure A1 3. Piper diagram for surface and groundwater samples. Surface water samples are represented by squares and groundwater samples by spheres.

In the 20 new borehole analyses assessed in this study, As in groundwater ranges between 3.2 µg/l to 116.6 µg/l. Sample MAM06 with an As concentration of 97.5 is only available as an unfiltered As sample. Of the 20 boreholes, six have As concentrations higher than 10 µg/l, four have concentrations higher than 50 µg/l and two are higher than 100 µg/l.

For the speciation work, reliable results were only obtained for six of the boreholes tested due to difficulties experienced with calibration of the columns. Recovery of the As in the sample passed through the columns ranged between 86.7 – 136.3 % with an average of 109.8 %. As (III) in the sample ranged between 50.0 – 74.0 % of the total As with an average of 57.1 %. As (V) in the sample ranged between 29.3 – 79.0 % with an average value of 52.7 % of the total As in the sample.

The data indicates a relationship between As and pH in groundwater where As occurs at concentrations greater than 50 µg/l only in water at pH greater than 8.0 with the exception of sample 9904 with an As concentration of 90 µg/l and a pH of 7.5 (Figure A1-4a). This is also indicated by a significant positive correlation of As and pH in groundwater where r = 0.50 (n = 25) for groundwater. There exists a relatively strong positive correlation between As and DOC (Figure A1-4b) with r = 0.64 (n = 9) for surface water and r = 0.89 (n = 19) for groundwater. There is no significant correlation between As and EC (Figure A1-4c) and no significant correlation between As and alkalinity (Figure A1-4d), although pH and alkalinity are significantly correlated in groundwater. No correlation exists between Fe and As for surface water and groundwater samples.

A1.2.4.2 Sediment samples

In this study, the fraction of sediments between 0.5mm – 0.25 mm (2 Φ) has been classified as medium grain sand whilst the fraction between 0.25 – 0.125 mm (3 Φ) has been termed fine grain sand. The fraction that is < 0.06 mm has been classified as "fines" (ie silts and clays). The samples analysed are predominantly fine to medium grain sands with the exception of KUM10-28 which has a high (> 70 %) amount of fines and the lake sediment samples from Lake Ngami, which also have a higher percentage of fines than the samples from the Okavango Delta proper. There was insufficient sample from the Xak core to conduct particle size analyses.

The sediment sample STSD-4 that was analysed in triplicate for As had an average recovery of 100.7 %. The precision of the sediment sample data is < 13 % RSD for all samples with an average of 6.5 %. As concentrations in the sediments analysed range between 0.2 – 7.0 mg/kg with an average value of 2.2 mg/kg (Table A1-2). Values are highest in the samples from KUM10 which also had elevated As in the water sample. There exists a significant positive correlation between As and Co and between As and Fe (Figure A1-5a and b) in the sediment samples (both r = 0.54, n = 35). However, the samples from the shallow core, Xak, do not plot with the other samples. With Ni, there is no clear relationship with As. There exists a relatively strong correlation between As and the % fines in the samples (r = 0.64, n = 25) and between Fe and the % fines (r = 0.65, n= 18) and to a lesser extent between Co and the % fines (r = 0.30, n = 25) (Figure A1-5c, d and e).

A strong positive correlation exists between LOI and As (Figure A1-5f) for the samples from KUM10 and MAM05 ($r = 0.96$, $n = 21$) and Xak, although plotting separately from the other data points has $r = 0.78$ ($n = 8$). There is no correlation between As and LOI for the NG samples.

Table A1 2. Results of sediment sample analysis of the Okavango Delta sediments.

Sample	Sample depth (m)	As (mg/kg)	Co (mg/kg)	Ni (mg/kg)	Fe (%)	LOIorgC %	% medium sand	% fine sand	% fines
MAM05-2	2	2.6	8.2	39.5	0.40	4.9	27.4	12.3	4.6
MAM05-7	7	1.5	5.0	38.8	0.45	1.7	21.9	14.2	1.3
MAM05-13	13	2.6	7.1	92.4	0.53	4.5	23.3	8.2	9.9
MAM05-22	22	0.8	2.0	43.4	0.19	1.4	12.5	6.7	2.2
MAM05-33	33	1.2	5.8	42.8	0.26	1.5	41.0	20.6	6.6
MAM05-42	42	2.4	4.9	37.3	0.49	2.8	21.1	13.1	15.9
MAM05-63	63	0.4	3.9	50.4	0.24	0.1	51.1	38.1	0.2
KUM10-5	5	0.4	4.2	42.8	<0.05	0.3	51.6	29.3	0.2
KUM10-13	13	3.3	9.2	40.2	0.49	4.4	31.2	33.9	10.4
KUM10-17	17	3.7	7.6	40.0	0.57	5.2	21.6	20.1	32.3
KUM10-28	28	6.2	6.0	38.4	0.71	8.6	1.3	1.7	70.5
KUM10-29	29	3.6	5.8	32.1	0.44	5.0	17.6	5.7	16.1
KUM10-30	30	1.8	6.4	42.5	0.43	1.9	26.0	18.8	2.2
KUM10-32	32	2.3	6.6	44.4	0.39	2.0	24.3	14.9	4.9
KUM10-34	34	2.1	4.8	39.1	0.34	1.7	38.5	11.6	34.5
KUM10-47	47	1.4	5.6	36.1	0.44	2.3	30.7	10.8	10.7
KUM10-48	48	1.1	3.8	35.0	0.44	1.7	32.6	8.7	4.8
KUM10-49	49	0.9	2.6	32.6	0.37	1.3	15.0	21.1	10.5
KUM10-62	62	1.3	6.5	39.6	<0.05	1.7	51.9	15.0	3.7
KUM10-64	64	1.0	3.8	36.2	0.54	1.2	29.5	9.0	17.0
10-65	65	0.9	2.8	62.3	0.42	1.3			
XAK-2	0.02	1.3	6.7	90.5	0.35	45.0			
XAK-7	0.07	1.2	6.7	83.5	0.72	30.0			
XAK-11	0.11	0.7	6.1	75.2	0.67	26.8			
XAK-18	0.18	0.9	3.2	64.3	0.53	14.2			
XAK-21	0.21	0.9	3.8	71.7	0.42	23.1			
XAK-24	0.24	0.8	1.8	80.6	0.52	21.8			
XAK-30	0.3	0.9	0.3	56.9	0.54	6.9			
XAK-49	0.49	0.2	0.4	58.4	0.35	0.5			
NG210*	2.1	4	13.5	29	1.32	11.3	6.5	7.8	20.1
NG260	2.6	4	9.5	22	1.39	10.3	5.9	22.5	31.2
NG430	4.3	7	4.2	12	0.52	2.8	32.8	10.5	14.0
NG440	4.4	6	8.7	21	1.07	7.5	35.0	13.1	26.9
NG450	4.5	7	10.1	23	1.33	10.5			
NG460	4.6	2	11.7	25	1.44	10.8	28.0	25.8	27.9

*Co, Ni and Fe values for NG samples from Huntsman-Mapila et al., (2006)

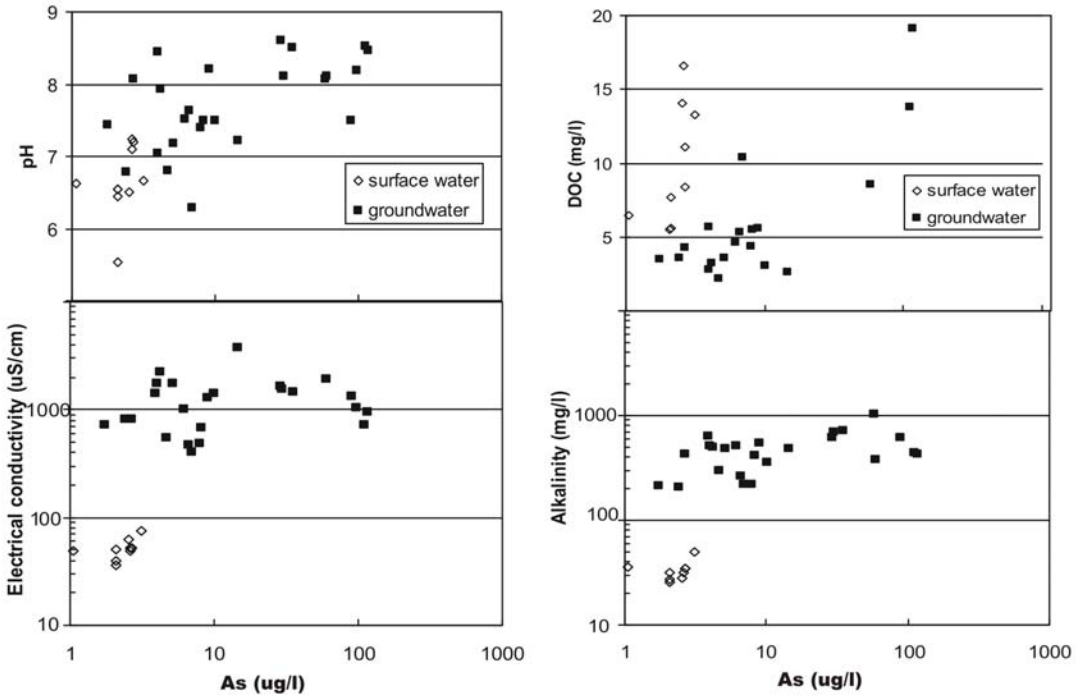

Figure A1 4. Binary diagrams for Okavango Delta surface and groundwater compositions.

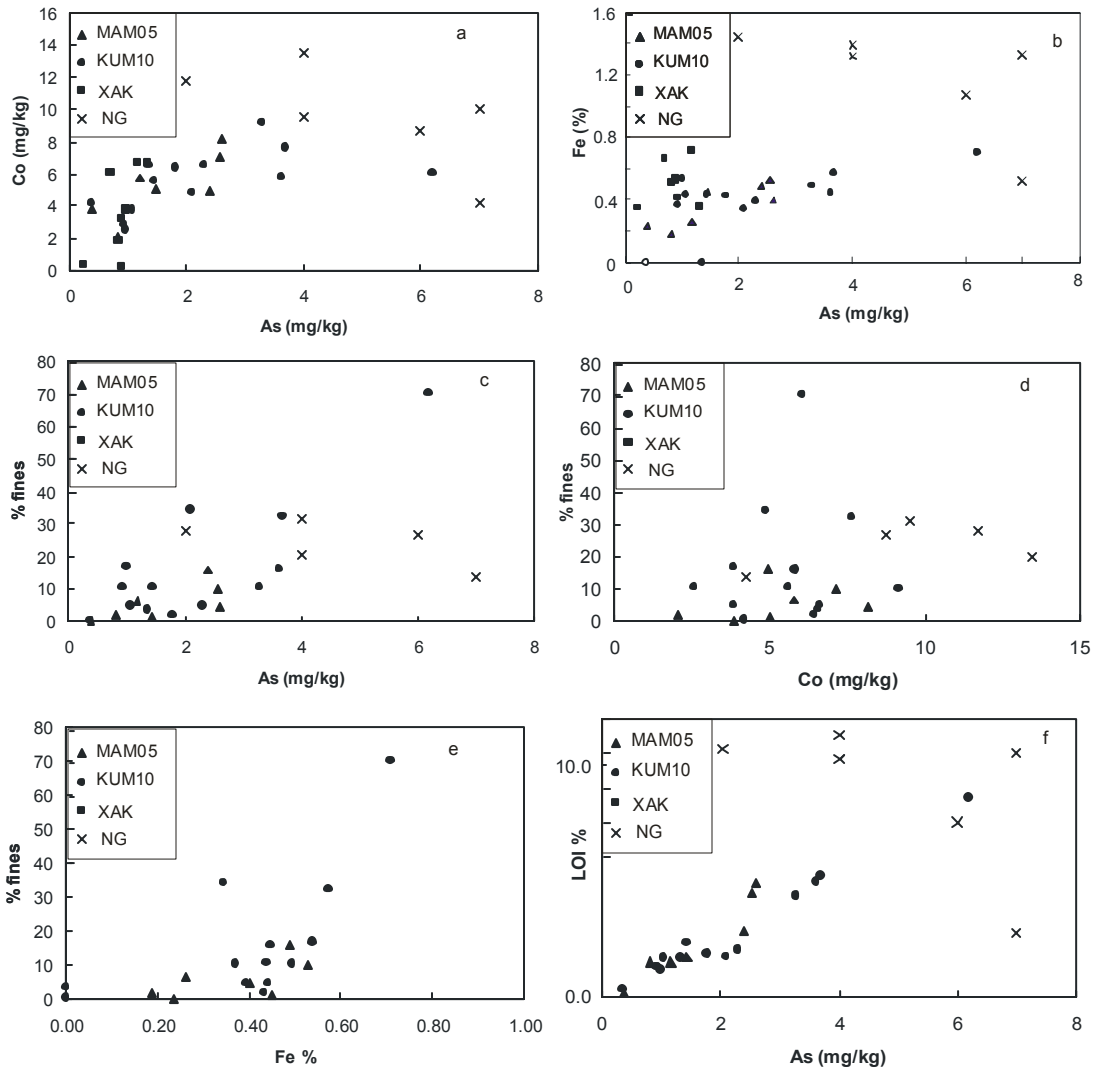

Figure A1 5. Binary diagrams for the Okavango Delta sediment compositions.

A1.2.5. Discussion

A1.2.5.1 General hydrochemistry

The Okavango Delta surface water has a low conductivity with the major cation being Ca and the major anion being HCO_3 (Hutton and Dincer, 1976; Sawula and Martins, 1991; Cronberg et al., 1995) with exceptions occurring in small saline pans on islands where the groundwater has come to the surface during the seasonal flood and experienced evaporative concentration. The surface water of the Delta has a typical tea colour from dissolved organic compounds, in particular fulvic

acids which are present in the water (Mladenov et al., 2005). The conductivity of the outflow of the Delta in Maun is typically double that of the inflow in the Panhandle caused by evaporative concentration. This bicarbonate dominant fresh surface water dominates the ground-water recharge during the advance of the seasonal flood. McCarty et al., 1998 plotted groundwater chemistry of 251 boreholes and found that bicarbonate dominated water is confined to the area of the Delta proper whilst chloride dominated water predominates in the region outside of the Delta. Three apparently isolated pockets of sulphate dominated water occur in the western fringe of the Delta. These authors concluded that neither the chloride nor the sulphate dominated water could have originated from recharge from the Okavango Delta surface water. Several studies have shown that lower salinity water frequently overlies water of higher salinity (Aquatec, 1982; BRGM, 1986; DWA, 2003; Bauer et al., 2005). In addition, salinity is spatially very variable, and that salinity can change by up to three orders of magnitude over a horizontal distance of a few tens of meters (McCarthy et al., 1993b).

A1.2.5.2 Nature and source of surface water arsenic

The As concentrations in the surface water of the Okavango Delta exceed the global average value of 1.7 µg/l for dissolved As in stream water (Martin and Whitfield, 1983) in all but one sample. The neutral to slightly acidic pH of the Delta water would suggest that the $H_2AsO_4^-$ inorganic species predominates. The relatively high DOC of the surface water would also suggest the presence of the methylated form of As.

Dowling et al., 2002 suggest that dissolved arsenic in the Bengal Basin is carried by the rivers and then removed by either flocculation of fine grained particles or bacterially reduced and precipitated to be stored in deltaic sediments. The suspended sediment component in the Okavango Delta needs also to be assessed. The particulate load in the Okavango Delta is however very low compared to the chemical precipitates. McCarthy et al., 2002 estimated that, under present conditions, 381,000 t of chemical sediment are accumulating on the fan each year compared to approximately 209,000 t of clastic load consisting of 170,000 t of bedload and 39,000 t of suspended load.

Slightly elevated As levels, compared to the global average, are occurring in the Okavango Delta surface water and possibly originate from the weathering of the bedrock in the region which comprises Proterozoic granitoids and mafic-ultramafic rocks (Huntsman-Mapila et al., 2005b).

No As values are available for these source rocks. Koljonen (1992) in Matschullat, 2000 reports that gabbros and basalts have an average concentration of 0.7 mg/kg and granites and granodiorites have an average As concentration of 3 mg/kg. Sulphide minerals in mineralised bedrock are vunerable to attack in humid environments rich in O_2 despite being relatively insoluble in pure water. The free O_2 in the water causes the oxidation of pyrite and arsenopyrite and liberates H_2SO_4. Under these acid conditions, As is highly mobile.

The transport of arsenic from source rocks in the Okavango Delta probably involves arsenic being stored in various geochemical environments while in transit. This may include the short-lived iron-monosulphide rich sediment which could accumulate in the system during wet periods.

A1.2.5.3 Nature and source of sediment arsenic

Sediment extraction work in this study reveals As concentrations of 0.2 – 7 mg/kg. The Delta sediments are predominantly fine to medium grain sands and the average As concentration for sandstones is given as 0.5 mg/kg (Onishi, 1969). Sediment samples from the Ganges-Brahmaputra-Meghna (GBM) Delta range between 0.5 – 17.7 mg/kg (Ahmed at al., 2004). Sengupta et al. 2004, in their study on arsenic in clay and sand sediments in the Bengal Delta, recorded 10 mg/kg and 4 mg/kg respectively.

The collection of the shallow core in Xakanaxa Lagoon was of interest as the core was taken in an active backwater swamp, where a vigorous release of gas was observed when the corer was placed in the organic rich sediments. This suggested a reducing environment perhaps comparable to the environment where the layers of the more fine grained/ organic rich sediments of the occasional floodplain were deposited in the past when this region was inundated with water (Huntsman-Mapila, 2006). It is thought that in the past, during periods of higher rainfall than today, water would pond up against the Thamalakane fault, resulting in the formation of what is referred to as Lake Thamalakane (Shaw, 1988).

It was hypothesized that the Xakanaxa lagoon site might represent a typical environment for active As deposition. In reducing environments, arsenite in the form of $H_3AsO_3^O$ is present at pH values less than 9.2 (Sracek et al., 2004) and a pH of about 7.0 is the adsorption optimum for arsenite. In these conditions, As can diffuse to adsorption sites on $Fe(OH)_3$ surfaces. In a reducing

environment, the electron donor for the reduction of Fe (III) oxides and hydroxides can be organic matter in sediments.

Other potential adsorbents of As include Al oxides and hydroxides (Stollenwerk, 2003) with halloysite and chlorite found to adsorb As (V) to a much greater extent than kaolinite, illite and montmorillonite (Lin and Puls, 2000). XRD work on the Okavango sediments (Huntsman-Mapila et al., 2005b) have shown that kaolinite is the predominant clay mineral in the Okavango sediments present at no more than 3 % for the samples analysed. It is therefore suggested that adsorption on Al oxides and hydroxides does not play a major role in fixing As in the sediments.
An earlier study of the sediments of the Okavango Delta revealed that of 90 samples analysed, the average S concentration was 0.04 % with a range of <0.01 – 0.52 %. The same samples had and average organic C content of 0.40 % with a range of <0.01 – 1.64 % (Huntsman-Mapila, unpublished data). This would suggest that organic C contributes to a much greater extent than S to the LOI of the sediments in the Delta. The strong positive correlation between As and LOI in this study suggests that the combustible elements of the sample play an important role in the adsorption of As in the Okavango Delta sediments.

A1.2.5.4 Nature and source of groundwater arsenic

The occurrence of elevated As in the groundwater of the Okavango Delta is not attributed to any anthropogenic activities as minimal agricultural activities occur in the region. The current study suggests a natural source and the release in groundwater through natural processes. Oxidation of arsenopyrite due to a lowering of the groundwater table was postulated as the dominant process for As mobilisation in the Ganges-Brahmaputra-Meghna (GBM) Delta (Bhattacharya et al., 1997; Nickson et al, 2000) However, recent studies (McArthur et al., 2001; Dowling et al., 2002; Anawar et al, 2003; Ahmed et al., 2004) have indicated that the reduction and dissolution of iron oxy-hydroxide coating on sand grains is another likely release mechanism. This is coupled to the degradation of organic matter in sediments whereby organic matter facilitates the transformation of Fe (III) to Fe (II) and As (V) to As (III). Because dissolved As, Fe and HCO_3 are positively correlated in some GBM groundwaters and because organic carbon is abundant in the GBM sediments, reduction of Fe oxides and release of As may be coupled with organic carbon oxidation (Nickson et al., 2000).

Results from the MGDP (DWA, 2003) indicate that there is a higher occurrence of elevated arsenic in boreholes screened below 72.6 mbgl than boreholes screened between 27.7 – 50.3 mbgl suggesting that elevated As levels are predominantly occurring in the deeper aquifers. This would suggest that the oxidation of sulphide minerals due to lowering of the groundwater table is not a probable mechanism in this case.

Recent studies have shown that certain Fe reducing bacteria can use humic substances as electron acceptors and reduce amorphous ferric oxide and crystalline iron oxides with a resulting product of siderite, in bicarbonate buffered solution (Little et al., 1997; Dong et al., 2000; Sengupta et al., 2004). There is a significant correlation between As and Fe in the Okavango sediments and between As and organic matter in both the sediments and groundwater. The oxidative degradation of DOC in the groundwater can produce high HCO_3 and create a favourable environment for the reduction of Fe and As. This hypothesis would suggest that the mechanism for the mobilisation of As into the Okavango Delta groundwater is similar to the processes occurring in the GBM Delta.
However, no correlation exists between As and Fe in the Okavango Delta groundwater. Zheng et al., 2004 had similar results in Bangladesh, where not all As-rich waters had elevated dissolved Fe. They suggest a "re-oxidation scenario" whereby the introduction of O_2 to SO_4 reducing groundwater can induce the oxidation of Fe (II) and As (III). This re-oxidation can lead to As and PO_4 co-precipitation or sorption onto newly formed Fe-oxyhydroxide. PO4 analyses were not conducted on the Okavango Delta samples so it is not possible to determine if a correlation exists between As and PO_4. This requires further investigation.

A1.2.6. Conclusions

From this preliminary study of the occurrence of naturally occurring arsenic in the sediments and water of the Okavango Delta, it has been found that:

Surface water in the Okavango Delta is slightly enriched in As when compared to a global value for stream water. The water is neutral to slightly acidic with a high DOC.
Of the 20 new borehole analyses from this study, six were found to have values exceeding 10 µg/l, the current World Health organization provisional guideline value for Arsenic (WHO, 2001).

There is an indication that As (III) is slightly more predominant than As (V) in groundwater. Reductive dissolution of Fe oxides and hydroxides in the sediments using organic carbon as an electron acceptor is a likely mechanism for the release of As from the sediments into the groundwater. Further work is required in order to understand the mechanisms involved in the release of As into the groundwater of the Okavango Delta.

The quantity of available water for supply to Maun was significantly increased through the drilling of the MGDP boreholes. It is evident that to address water shortages and associated problems, significant emphasis has to be given to water quality. Non-selective continual incrementing of quantity could lead to increased deterioration of water quality in Maun's water supply

Acknowledgements

The Director of the Department of Water Affairs, Botswana is acknowledged for granting permission to publish this work. This investigation was supported by a research grant (R050) from the University of Botswana Research and Publication Fund. Water Resources Consultants, in particular V. Masedi, are acknowledged for assistance in sample collection. H.A.B. Kampunzu, H. Jamieson, A. Charbonneau, B. Acheson and S. Ringrose are gratefully acknowledged for guidance, comments and support. This paper was significantly improved by comments from reviewers T.S. McCarthy and S. Appleyard. This is an IUEM contribution no. 984.

References

Ahmed, K.M, Bhattacharya, P., Aziz Hasan, M., Humayun Akhter, S., Mahbub Alam, S.M., Hossain Bhuyian, M.A., Badrul Iman, M., Khan, A.A., Sracek, O., 2004. Arsenic enrichment in groundwater of the alluvial aquifers in Bangladesh: an overview. Appl. Geochem. 19, 181-200.

Anawar, H.M., Akai, J., Komaki, K., Terao, H., Yoshioka, T., Ishizuka, T., Safiullah, S., Kato, K., 2003. Geochemical occurrence of arsenic in groundwater of Bangladesh: sources and mobilization processes. J. Geochem. Explor. 77, 109-131.

Aquatec, 1982. Watering point survey: Ngamiland cattle trek route. Aqua Tech Groundwater Consultants, Gaborone, pp.132.

APHA, AWWA, WFA, 1995. Standard Methods for the Examination of Water and Wastewater (19th Edition). APHA, Washington, pp. 5/60-5/62.

Bauer, P., Zimmermann, S., Held, R., T., G. and Kinzelbach, W., 2002. Is density fingering balancing the salt budget of the Okavango Delta? Evidence from field and modelling studies, 17th Salt Water Intrusion Meeting, Delft.

Bhattacharya, P., Chatterjee, D., Jacks, G., 1997. occurrence of arsenic-contaminated groundwater in alluvial aquifers from delta plains, eastern India: options for safe drinking water supply. J. Water Resour. Dev. 13, 79-92.

BGS, DPHE, 2001. Arsenic contamination of groundwater in Bangladesh, Vol. 2. Final Report, BGS Technical Report WC/00/19.

BRGM, 1986. Maun water supply hydrogeological survey. Bur. Rech. Geol. Mineres, Orleans, France, Vol 1 and 2, pp.99.

Central Statistics Office, 2001. Population of Towns, Villages and associated localities. Government Printer, Gaborone, pp.297.

Chatterjee, A., Das, D., Mandal, B.K., Chowdhury, T.R., Samanta, G., Chakraborti, D., 1995. Arsenic in groundwater in six districts of West Bengal, India: the biggest arsenic calamity in the world. Part 1: arsenic species in drinking water and urine of affected people. Analyst 120, 643-650.

Cronberg, G., Gieske, A., Martins, E., Nengu, J., Stenstrom, I.M., 1995. Hydrobiological studies of the Okavango Delta and Kwando/Linyanti/Chobe River, Botswana. Botsw. Notes Rec. 27, 151-225.

Das, D., Chatterjee, A., Mandal, B.K., Samanta, G., Chakraborti, D., 1995. Arsenic in groundwater in six districts of West Bengal, India: the biggest arsenic calamity in the world. Part 2: arsenic concentration in drinking water, hair, nails, urine, skin-scale and liver tissue (biopsy) of affected people. Analyst 120, 917-924.

Dong, H., Fredrickson, J.K., Kennedy, D.W., Zachara, J.M., kukadapu, R.K., Onstott, T.C. 2000. Mineral transformation associated with the microbial reduction of magnetite. Chem. Geol. 169, 299-318.

Dowling, C.B., Poreda, R.J., Basu, A.R., Peters, S.L., 2002. Geochemical study of arsenic release mechanisms in the Bengal Basin groundwater. Water Resour. Res. 38, 1173-1190.

DWA (Department of Water Affairs), 2003. Maun Groundwater Development Project Phase 2, Project Review Report. Department of Water Affairs, Gaborone, Botswana, prepared by Water Resources Consultants.

Ficklin, W., 1990. Extraction and speciation of arsenic in lacustrine sediments. Talanta 37, 831-834.

Gumbricht, T., McCarthy, T.S., 2003. Spatial patterns of islands and salt crusts in the Okavango Delta, Botswana. S. Afr. Geographic. J., 85, 164-169.

Huntsman-Mapila, P., Ringrose, S., Mackay, A.W., Downey, W.S., Modisi, M., Coetzee, S.H., Tiercelin, J-J., Kampunzu, A.B., Vanderpost, C., (2006) Use of the geochemical and biological sedimentary record in establishing palaeo-environments in the Lake Ngami Basin, NW Botswana. Quat. Int. 148, 51-64.

Huntsman-Mapila, P., Masamba, W.R.L., Masundire, H., and Nyateka, N., (2005a) Surface water quality of the Okavango Delta, Botswana: AquaRAP II – Low water survey. Final report for Conservation International.

Huntsman-Mapila, P., Kampunzu, A.B., Vink, B. and Ringrose, S. (2005b) Cryptic indicators of provenance from the geochemistry of the Okavango Delta sediments, Botswana. Sed. Geol. 174 (1-2), 123 -148.

Hutton, L.G., Dincer, T., 1976. Chemical and stable isotope composition of Okavango Delta waters. Tech. Note 23, UNDP/FAO, BOT/71/706, pp.18.

Kampunzu, A.B., Bonhomme, M.G., Kanika, M., 1998. Geochronology of volcanic rocks and evolution of the Cenozoic Western branch of the East African rift system. J.Afr. Earth Sci. 26, 441-461.

Koljonen, T., 1992. Geochemical Atlas of Finland, Part 2: Till. Espoo, Finland: Geological Survey of Finland.

Lin, Z., Puls, R.W., 2000. Adsorption, desorption and oxidation of arsenic affected by clay minerals and aging process. Environ. Geol. 39, 753-759.

Little, B., Wagner, P., Ray, R., Hart, K., Lavoie, D., Nealson, K., Aguilar, C., 1997. The role of biomineralisation in microbiologically influenced corrosion. Biodegradation 9, 1-10.
Martin, J.M., Whitfield, M., 1983. The significance of the river input of chemical elements to the ocean. In: Wong, C.S., Boyle, E., Bruland, K.W., Burtons, J.D., Goldberg, E.D., (Editors), Trace metals in sea water. Plenum, New York, pp. 265-296.
Matschullat, J., 2000. Arsenic in the geosphere – a review. Sci. Total Environ. 249, 297-312.
McArthur, J.M., Ravenscroft, P., Safiullah, S., Thirlwall, M.F., 2001. arsenic in groundwater :testing pollution mechanisms for sedimentary aquifer in Bangladesh. Water Resour. Res. 37, 109-117.
McCarthy, T.S., Green, R.W., Franey, N.J., 1993a. The influence of neo-tectonics on water dispersal in the northeastern regions of the Okavango swamps, Botswana. J. Afr. Earth Sci. 17, 23-32.
McCarthy, T.S., Ellery, W.N., Alar, K., 1993b. Vegetation induced subsurface precipitation of carbonate as an aggradational process in the permanent swamps of the Okavango (Delta) fan, Botswana. Chem. Geol. 107, 111-131.
McCarthy, T.S. and Ellery, W.N., 1994. The effect of vegetation on soil and groundwater chemistry and hydrology of islands in the seasonal swamps of the Okavango Fan, Botswana. J.Hydrol. 154(1-4), 169-193.
McCarthy, T.S., Bloem, A., Larkin, P., 1998. Observations on the hydrology and geohydrology of the Okavango Delta. S. Afr. J. Geol. 101(2), 101-117.
McCarthy, T.S., Cooper, G.R.J., Tyson, P.D., Ellery, W.N., 2000. Seasonal flooding in the Okavango Delta, Botswana – recent history and future prospects. S. Afr. J. Sci. 96, 25-33.
McCarthy, T.S., Smith, N.D., Ellery, W.N., Gumbricht, T., 2002. The Okavango Delta- Semiarid alluvial fan sedimentation related to incipient rifting. In: Renault, R.W., and Ashley, G.M. (editors) Sedimentation in Continental Rifts, SEPM Special Publication No. 73, 179-193.
Mladenov, N., McKnight, D.M., Wolski, P., Ramberg L., 2005. Effects of the annual flood on dissolved organic carbon dynamics in the Okavango Delta, Botswana. Wetlands, 25 (3), 622-638.
Modisi, M.P., 2000. Fault system of the southeastern boundary of the Okavango Rift, Botswana. J. Afr. Earth Sci. 30, 569-578.
Modisi, M.P., Atekwana, E.A., Kampunzu, A.B., Ngwisanyi, T.H., 2000. Rift kinematics during the incipient stages of continental extension: evidence from nascent Okavango rift basin, northwest Botswana. Geol. 28, 939-942.
Nickson, R., McArthur, J., Burgess, W., Ahmed, K.M., Ravenscroft, P., Rahman, M., 1998. Arsenic poisoning of Bangladesh groundwater. Nature, 395, 338.
Nickson, R., McArthur, J.M., Ravenscroft, P., Burgess, W.G., Ahmed, K.M., 2000. Mechanisms of As release to groundwater, Bangladesh and West-Bengal. Appl. Geochem. 15, 403-413.
Onishi, H., 1969. Arsenic. In: Wedepohl, K.H., (Editor), Handbook of geochemistry. Springer, Berlin.
Ringrose, S., Huntsman-Mapila, P., Kampunzu, A. B., Matheson, W., Downey, W., Vink, B., Coetzee, C., and Vanderpost, C., 2005. Sedimentological and geochemical evidence for palaeo-environmental change in the Makgadikgadi subbasin, in relation to the MOZ rift depression, Botswana. Palaeogeogr., Palaeoclimatol., Palaeoecol., 217 (3-4), 265-287.
Rollinson, H., 1993. Using geochemical data: evaluation, presentation, interpretation. Longman, Singapore.
Sawula, G., Martins, E., 1991. Major ion chemistry of the Lower Boro River, Okavango Delta, Botswana. Freshwater Biology 26, 481-493.

SenGupta, A.K., Greenleaf, J., 2002. Arsenic in subsurface water: Its chemistry and removal by engineered process. In: SenGupta , A.K. (Editor), Environmental separation of heavy metals. CRC Press, USA, pp. 265-305.
Sengupta, S., Mukherjee, P.K., Pal, T., Shome, S., 2004. Nature and origin of arsenic carriers in shallow aquifer sediments of Bengal Delta, India. Environ. Geol. 45, 1071-1081.
Schwartz, E.H.L. 1919. The Kalahari or thirstland redemption. Maskew Miller, Cape Town.
Shaw, P., 1988. After the floods: The fluvio-lacustrine landforms of northern Botswana. Earth Sci. Rev. 25, 449-456.
Smith, R.T., Atkinson, K., 1975. Techniques in pedology. Paul Elek Scientific Books, London, pp.113-121.
Snowy Mountain Engineering Corporation Ltd (SMEC), WLPU Consultants, Swedish Geological International AB, 1991. Botswana National Water Master Plan. Prepared for Department of Water Affairs, Botswana.
Sracek, O., Bhattacharya, P., Jacks, G., Gustafsson, J., von Bromssen, M., 2004. Behaviour of arsenic and geochemical modelling of arsnic enrichment in aqueous environments. Appl. Geochem. 19, 169-180.
Stollenwerk, K.G., 2003. Geochemical processes controlling transport of arsenic in groundwater: a review of adsorption. In: Welch, A.H., Stollenwerk, K.G. (Eds.), Arsenic in Groundwater: Geochemistry and Occurrence. Kluwer Academic Publishers, Boston, MA, pp. 67-100.
Thomas, D.S.G., Shaw, P.A., 2002. Late Quaternary environmental change in central southern Africa: new data, synthesis, issues and prospects. Quat. Sci. Rev. 21, 783-797.
UNDP, 1977. Investigation of the Okavango Delta as a primary source of water for Botswana. UN/ FAO DP/BOT/71/506. Report for the Department of water Affairs, Botswana.
US EPA, 2001a. Drinking water standard for arsenic. On line at http://www.epa.gov/safewaters/ars/ars_rule_factsheet.html
US EPA, 2001b. Method 200.9: Trace elements in water, solids and biosolids by stabilized temperature graphite furnace atomic absorption spectrometry. EPA-821-R-01-011.
Welch, A.H., Stollenwerk, K.G., 2003. Arsenic in groundwater: geochemistry and occurrence. Kluwer academic Publishers, Norwell, MA.
Wellington, J.H., 1948. The food-producing possibilities of the Okavango Delta. S. Afr. Sci., 11, 65-67.
World Health Organization (WHO), 2001. Arsenic in drinking water. http://www.who.int/inf-fs/en/fact210.html
Wolski, P., Savenije, H., 2006. Dynamics of surface and groundwater interactions in the floodplain system of the Okavango Delta, Botswana. J. Hydrol. 320, 283-301.
Zheng, Y., Stute, M., van Geen, A., Gavrieli, I., Dhar, R., Simpson, H.J., Schlossser, P., Ahmed, K.M., 2004. Redox control of arsenic mobilization in Bangladesh groundwater. Appl. Geochem. 19, 201-214.

LISTE DES FIGURES

LISTE DES TABLEAUX